THE UNIVERSITY of ADELAIDE

Preparation and Characterization of β-Galactosidase Nanobiocatalysts and Its Application for Galacto-Oligosaccharides Production

Mailin Misson

B. Sc. (Hons), M. Eng.

School of Chemical Engineering

Faculty of Engineering, Computer & Mathematical Sciences

The University of Adelaide

Submitted for the Degree of Doctor of Philosophy

March 2016

For my husband,

Johnes Julait

And precious daughter,

Michelle Andrea Joanne Johnes

Panel of Supervisors

Principal Supervisor

Dr. Hu Zhang (PhD)
School of Chemical Engineering
Faculty of Engineering, Computer and Mathematical Sciences
The University of Adelaide
Email: hu.zhang@adelaide.edu.au
Phone: +61 8 831 33810

Co-Supervisor

Associate Professor Bo Jin (PhD)
School of Chemical Engineering
Faculty of Engineering, Computer and Mathematical Sciences
The University of Adelaide
Email: bo.jin@adelaide.edu.au
Phone: +61 8 831 37056

Declaration

I certify that this work contains no material which has been accepted for the award of any other degree or diploma in my name, in any university or other tertiary institution and, to the best of my knowledge and belief, contains no material previously published or written by another person, except where due reference has been made in the text. In addition, I certify that no part of this work will, in the future, be used in a submission in my name, for any other degree or diploma in any university or other tertiary institution without the prior approval of the University of Adelaide and where applicable, any partner institution responsible for the joint-award of this degree.

I give consent to this copy of my thesis when deposited in the University Library, being made available for loan and photocopying, subject to the provisions of the Copyright Act 1968.

The author acknowledges that copyright of published works contained within this thesis resides with the copyright holder(s) of those works.

I also give permission for the digital version of my thesis to be made available on the web, via the University's digital research repository, the Library Search and also through web search engines, unless permission has been granted by the University to restrict access for a period of time.

Name : Mailin Misson

Signature : _____ Date: 04.03.2016

Preface

The doctoral thesis is prepared in "Publication" style according to the "specifications for Thesis (2015)" of the University of Adelaide. It includes publications that have been published or readyto be submitted for publication:

1. Misson, M., Zhang, H., Jin, B. (2015). Nanobiocatalyst Advancements and Bioprocessing Applications. Journal of the Royal Society Interface. 12 (102): 1-20.

2. Misson, M., Du, X., Jin, B., Zhang, H. (2016). Dendrimer-Like Nanoparticles Immobilized β -Galactosidase For Enhancing Galacto-Oligosaccharide Production. Enzyme and Microbial Technology. 84: 68-77.

3. Misson, M., Dai, S., Jin, B., Chen, B., Zhang, H. (2016). Manipulation of Nanofiber-Based β -Galactosidase Nanoenvironment for Enhancement of Galacto-Oligosaccharide Production. Journal of Biotechnology. 222: 56-64.

4. Misson, M., Jin, B., Chen, B., Zhang, H. (2015). Enhancing Enzyme Stability and Metabolic Functional Ability of β-Galactosidase through Functionalized Polymer Nanofiber Immobilization. Bioprocess and Biosystems Engineering. 38(10):1915-23.

5. Misson, M., Jin, B., Zhang, H. (2016). Characterization of β-Galactosidase/Polymer-Nanofibers Nanobiocatalysts and Application for Galactooligosaccharides Production. In preparation for submission.

6. Misson, M., Jin, B., Zhang, H. (2016). Recirculating Spiral Reactor for Galactooligosaccharide Production from Nanofiber-supported Nanobiocatalysts. In preparation for submission.

Some relevant components of the work that have been presented in conferences and symposiums:

1. Misson, M., Jin, B., Zhang, H. (2015). Immobilized β-Galactosidase on Functionalized Nanoparticles and Nanofibers: A Comparative Study. International Proceedings of Chemical, Biological and Environmental Engineering. DOI 10.7763/IPCBEE. 90: 1-7. (In 4th International Conference on Environment, Chemistry and Biology 2015, Auckland, New Zealand, 19th-21st November 2015) – Oral Presentation.

2. Misson, M., Jin, B., Dai, S., Zhang, H. (2014). Enzyme Immobilization of Functionalized Polystyrene Nanofibers for Bioprocessing Applications. International Journal of Bioengineering and Life Sciences. 1(12): 680. (In 16th International Conference on Biological and Bioprocess Engineering 2014, Sydney, Australia, 15th-16th December 2014) – Oral Presentation.

3. Misson, M., Jin, B., Zhang, H. (2015). Nano-Biocatalyst for Conversion of Dairy Industry Waste into Valuable Product. Spring Symposium MyPSA. Pp 11. Adelaide, Australia. (17th October 2015) – Oral Presentation.

4. Misson, M., Jin, B., Dai, S., Zhang, H. (2014). Enzyme Immobilization onto Acid-treated Electrospun Polystyrene Nanofibers. RACI SA Student Polymer & Bionanotechnology Symposium 2014. Pp 21. Adelaide, Australia. (28th July 2014) – Oral Presentation.

5. Misson, M., Jin, B., Zhang, H. (2014). Nanobiocatalysts for Bioconversion of Dairy Industry Wastes into Functional Products. Bioprocess Network Conference 2014. Melbourne, Australia (21st-23rd October 2014) – Oral Presentation.

6. Misson, M., Jin, B., Dai, S., Zhang, H. (2013). Optimization of Electrospun Polystyrene Nanofibers Synthesis for Enzyme Immobilization. RACI SA Student Polymer & Bionanotechnology Symposium 2013. Pp 11. Adelaide, Australia. (4th October 2013) – Poster Presentation.

In addition, some awards were achieved during PhD candidature:

1. Best Presentation in 4th International Conference on Environment, Chemistry and Biology (ICECB 2015), Auckland, New Zealand.

2. Best Presentation in Postgraduate Research Seminar in 2014, School of Chemical Engineering, The University of Adelaide, Adelaide, Australia.

3. Malaysian Government Scholarship (*Hadiah Latihan Di Bawah Skim Latihan Akademik IPTA* (SLAI) 2012-2016.

Acknowledgement

"The works of the Lord are great, studied by all who have pleasure in them"

(*Psalm 111:2*)

The creation of God in the universe are intriguing and astonishing, from the magnificent intricacy of a living cell to the complexity of life on earth. To God be the Glory! Knowing my incapability, weaknesses and level of knowledge, I therefore give my special gratitude beyond words to the Almighty God for giving me a continuous wisdom and courage to encounter this challenging PhD journey.

My utmost grateful goes to my research mentor and advisor, Dr Hu Zhang, for his academic guidance and technical supportsduring my experimental works and thesis writing, in which without his supervision I would not be able to generate this work as an accomplish thesis. I also feel indebted to the endless support from my co-supervisor, Associate Professor Bo Jin, in keeping my research at the right track and also creating positive vibes in my research environment and equipping me the important qualitiesfor life and career. Similar merits also dedicated to Associate Professor Sheng Dai for his scientific knowledge in polymer nanofibers and the fruitful research collaboration with Dr Xin Du in nanoparticles field.

A warm appreciation goes to my research group members: Masi, Amanda, Yusak, Huzairy, Cornelius, Ophelia, Jack, Aabhash, Amir, Umar, Steven, Bingyang, Penny and Giuseppe for their hands assistance, knowledge exchanges and friendship, as well as to my officemates in N247 and HDR students in school who had directly or indirectly contributed in my studies.

I also would like to convey my countless thanks to the School of Chemical Engineering for the HDR fund, the enormous supports from school top management and school administration team: Monica, Sue, Gemma, Michelle, Debra, and Pauline, Dr Sanaz for the lab safety, Dr Qiuhong for the assistance in Analytical Lab, and the technical supports by Jason Peak, Jeffrey Hiorns and Michael Jung from Workshop Department. Not forget to mention the HPLC facility support from Dr. Paul Grbin's research group in Waite Campus and the remarkable assistance for sugar analysis by Nick Van Holst.

My deep gratitude is also extended to the government of Malaysia for funding my study through *Biasiswa Skim Latihan Akademik IPTA*, the Universiti Malaysia Sabah (UMS) forthestudy leave and supporting my family, the *Unit Pengajian Lanjutan* team in UMS for the management support, and also to my academic and non-academic colleagues in Biotechnology Research Institute.

For the unconditional love and prayers from my family, I would like to express my sincere thankfulness especially to my dearest mom, dad, sisters, twin brothers, extended family members and family-in-laws. Their unfailing support and prayers were the greatest booster to my success crossing the finishing line. To my big family in Bethel International Church Adelaide, million thanks for the constant prayers and encouragement. Not forgetting to say thank you to my close friends in Adelaide; Christina, Sharon, Pei Yee, Daisy, Zarina, Asfizah, Nadiya, Faizah, Melati, Aida, and the rests that are not stated here, and all my supportive friends back home.

Last but not least, my heartfelt gratefulness to my other half, beloved husband and soul mate, Johnes, for his understanding and compromise to place me in the position where I am now. His sacrifice and dedication are beyond words. To my little precious, Michelle, thank you for always being my source of joy and strength that never fails to create smile on my face.

Abstract

Enzyme immobilization has been recognized as a promising technique to enhance enzyme stability, activity and reusability for the development of cost-effective, green and sustainable biotechnological processes. Recent development in nanotechnology has opened a new frontier for diverse nano-scale enzyme carriers. The immobilization of enzyme onto nanomaterials produces a nanobiocatalyst assembly, which maximizes reaction efficiencies by favoring desirable chemical reaction kinetics and selectivity for substrates, while the unique properties of nanocarriers offer a revolution of biocatalyst applications in the bioprocessing field. Nevertheless, the issues of enzyme leakage and conformational changes make the translation of the biocatalyst technology into commercial practices technically challenging and economically infeasible. Hence, investigating new technologies for fabricating the nanobiocatalyst with promising biocatalytic activities and functionalities is of great importance.

In this PhD research, nanoparticle- and nanofiber-based enzyme carriers were developed and explored to immobilize β-galactosidase for conversion of lactose from dairy industry wastes into galacto-oligosaccharide (GOS) as a high value product. The structure-function relationship for the nanocarrier, the enzyme-nanocarrier microenvironment and the enzyme-nanocarrier nanobiocatalyst structure were extensively evaluated, aiming to enhance the bioengineering performance of the nanobiocatalysts.

Dendrimer-like silica nanoparticles (HPSNs) with hierarchical pores were synthesized, characterized and functionalized with amino (NH_2) and carboxyl group (COOH) to facilitate enzyme binding. Our findings revealed that surface functionalization can promote enzyme affinity towards the nanomaterial interface and selectively enhance enzyme reusability and its catalytic activity for improving the GOS production yield.

A systematic synthesis of polystyrene nanofibers (PSNFs) was executed by optimizing key fabrication parameters using the electrospinning technique, including polymer concentration, electric voltage and distance between discharge needle tips and the collector. Surface modification of the PSNF was found to improve enzyme loading and activity. In addition, the local microenvironment of the nanobiocatalysts was able to

optimize the enzyme selectivity and specificity, resulting in favouring transgalactosylation over hydrolysis for the lactose bioconversion.

Further investigation to enhance the enzyme stability and catalytic activity at various operating conditions was conducted. PSNFs were chosen as the enzyme carrier owing to their scaling up potential in a manufacturing reactor system with their excellent mechanical and structural properties. Immobilizing β-galactosidase on the modified PSNF surface facilitated formation of stable enzyme binding and exhibited distinguished catalytic performance. Thermal and pH stability were improved significantly while the recyclability was enhanced from four to nine cycles. The evaluation of lactose conversion performance showed an improved GOS yield from 14 to 28% in comparison to free β-galactosidase.

To advance the knowledge of understanding β-galactosidase binding on the PSNF surface, the β-galactosidase/nanofiber nanobiocatalyst structure were comprehensively analyzed. Characterizations on the nanobiocatalyst properties were performed before and after biocatalyst immobilization. The analysis using scanning electron microscope (SEM), fluorescence microscope, Fourier transform infrared spectroscopy (FTIR), and Raman spectroscopy demonstrated successful biocatalyst attachment, homogenous distributions and no conformation changes. The effectiveness factor for lactose conversion into galacto-oligosaccharides (GOS) in a disc-stacked column reactor indicated distinguished biocatalyst performance in comparison to the free counterpart.

Finally, a scalable recirculating spiral reactor was designed in-house and operated for a continuous GOS production using the nanofibers-β-galactosidase nanobiocatalyst. The PSNF-β-galactosidase performed better in GOS production yield by exceeding the free counterpart about 1.5 to 3.7-fold. The variable parameters of the bioreactor system such as reaction time, feed flow rate and initial substrate concentration were found to have a profound effect in optimizing GOS synthesis. The best GOS production yield was determined at 159 g/l with 86% lactose conversion under the optimal operating conditions of 24 h reaction time, 15 ml/min flow rate and 400 g/l initial lactose concentration.

Overall, nanoparticles- and nanofibers-immobilized β-galactosidase nanobiocatalysts were successfully developed and assessed for conversion of lactose into GOS in this study. The nanobiocatalyst assembly demonstrated remarkable selectivity towards transgalactosylation to produce GOS from lactose.Comparing with free enzyme, the immobilized β-galactosidase significantly enhanced enzymatic activities, leading to

excellent bioconversion performance. The distinguished bioengineering perfomance of nanofiber-immobilized β-galactosidase in a scalable recirculating spiral bioreactor indicates their great potential for a large scale and continuous process application. Furthermore, the understanding of the binding mechanism for the enzyme and its nanoscale support surface and the nanobiocatalyst structure can be a key driver for fabricating biocatalyst-nanomaterial hybrids and improving biocatalyst efficiency. In summary, the findings of this study provide new insights into the development of economically and industrially viable nanobiocatalysts for industry-scale bioprocesses.

Table of Contents

List of Tables

List of Figures

CHAPTER 1

Introduction

Chapter 1: Introduction

1.1 Background of Study

Advances in nanotechnology and biotechnology open a new frontier for the development of enzyme-catalyzed bioprocesses which are green and sustainable in comparison with chemical processes. Nevertheless, enzymes constitute the majority of the operational cost in a large scale process and their low stability and reusabilityin a dynamic reactor system impede their industrial applications [1]. Immobilization of the enzymes on nano-structured materials has been recognized as a promising approach to enhance enzyme stability, activity and reusability. The nano-structured materials offer several intrinsic advantages, such as larger surface areas, that allow a higher enzyme loading and reduced mass transfer resistance for substrates [2-3].

Immobilization technology has received a growing interest in the development of biocatalytic techniques as well as enzyme carriers, including natural polymers (*e.g.*cellulose, starch, agarose and chitosan) [4-5], synthetic polymers (*e.g.* ion exchange resin and polyvinyl alcohol) [6-7] or inorganic materials, such as silica [8], zeolite [9] and mesoporous silica [10]. However, enzyme leakage and low stability due to inefficient immobilization protocol remain as the key challenges for industrial applications. The methodologies for recovering biocatalysts have not been well developed. It is, therefore, a focal point to identify enzyme carriers that are technically feasible for the immobilization of enzymes to improve their biocatalytic functions with enhanced stability and recyclability, making the enzyme-catalyzed process economically viable for industrial applications.

Recent development in nanotechnology has provided a wealth of diverse nano-scale carriers that could be applied for enzyme immobilization. A specifically functionalized nanomaterial promises exciting advantages for improving enzyme stability and capability, and biochemical performances. Enzyme immobilization using nano-structure carriers can significantly increase life cycles of the biocatalyst for its reuse, hence reducing the cost of the biocatalytic process. Nanobiocatalyst, an emerging technology that assembles enzyme molecules onto nanomaterial carriers, creates a microenvironment surrounding the enzyme

catalysts that favor desirable chemical kinetics and selectivity for substrates, therefore promoting maximal reaction efficiencies. To date, functional nanomaterials such as nanofibers, nanoparticles, nanotubes, and nanocomposites have been used as enzyme carriers [11-14]. The approaches of immobilization can be accomplished via covalent and non-covalent binding, cross-linking, entrapment or encapsulation [15].

Nevertheless, despite the constant efforts into the development of immobilization techniques and strategies, the employment of the immobilized enzymes in a bioreactor system may lead to a reduction of enzyme activity due to the change of enzyme's unique structures upon immobilization. Enzyme molecules embedded inside enzyme supports that could not directly contact with substrates also promotes ineffective cost management as a result of unreacted biocatalyst occurrence. Hence, the development of novel nanobiocatalysts is a growing biotechnological interest. The integration of enzymes with nanomaterials leads to a hybrid nano-biotechnology assembly that combines the biocatalytic ability of the enzymes with the unique active functions within the nano-structure network. However, how to immobilize multi-enzymes on the functionalized carriers for a continuous process still remains to be a challenge. Furthermore, there is a lack of knowledge for understanding the generic mechanisms and interfacial reactions associated with the nanomaterial-immobilized enzyme system. Such fundamental information is significantly important in the development of the multi-enzyme bioprocess. Till now, there are few studies reporting the influence of local microenvironment of nanobiocatalysts and the structure-function relationship in nanomaterial-immobilized enzyme system. Extensive understanding behind biocatalyst adsorption phenomena on solid surface is also less reported. Moreover, exploring new enzyme nanocarriers, which economically and industrially viable, can be worthy of investigations to nurture the advancements of the nanobiocatalyst-assisted technology and to promote the feasible translation of this bench-scale technology into commercial practices.

The demand of enzymes-catalyzed bioprocesses has been extended to diverse sectors including biocatalysis, pharmaceutical, bioenergy and food industries. Harnessing a green and sustainable waste management in food industry attracts tremendous attention. Cheese whey, the main by-product in casein and cheese manufacturing processes, has been regarded as an organic pollutant in wastewater due to its high organic loading [16]. A cost-effective treatment is therefore highly pursued prior to its safe disposal into eco-system. Through β-galactosidase-catalyzed reaction, bioconversion of lactose-rich wastes into

valuable products endows a promising solution. Lactose can be transgalactosylated into galacto-oligosaccharides (GOS), which offer a range of important health functions in living systems such as prebiotic function and low caloric sugar alternatives [17].

Nanoparticles have strong thermal and mechanical stability. Importantly, nanoparticles offer uniform nanopores and tuneable periodic nanostructures which are beneficial for enhancing mass transfer and molecule diffusion within and enzyme-nanoparticle network [18]. On the other hand, nanofibers offer a high surface-to-volume ratio promoting a high adsorption capacity of enzyme loading. The porosity of nanofibers allows easy penetration of biomoleculesinto all available surfaces. Furthermore, the specific surface characteristics, discrete nanostructures and self-assembling behaviors of nanofibers provide exciting opportunities to develop nanobiocatalysts for bioprocesses using bioreactor systems. Considering these advantages, nanofibers and nanoparticles were therefore chosen as enzyme carriers in this PhD project. The nanomaterials were synthesized and functionalized to facilitate β-galactosidase binding to form nanobiocatalysts assembly. Their adsorption capability, enzymatic stability and functionality in β-galactosidase immobilization for lactose bioconversion to GOS were comprehensively investigated. Other scientific challenges include the understanding of the influence of microenvironment and biocatalyst-nanomaterial interfacial reactions in controlling biocatalyst activities and its bioengineering performance were systematically examined.

1.2 Objectives and Scopes

The aim of this research is to develop a new technology for fabricating nanoparticle-and nonafiber-immobilized β-galactosidase as nanobiocatalysts for lactose bioconversion to galacto-oligosaccharides. Experimental studies have focused on the following research objectives:

- To synthesize and functionalize β-galactosidase nanocarriers from (i) dendrimer-like silica nanoparticles with hierarchical pores and (ii) polystyrene nanofibers.
- To examine the activity, stability and functional ability of immobilized β-galactosidase and the influence on the bioengineering performance in enhancing lactose conversion into galacto-oligosaccharide.

- To advance fundamental knowledge in enzyme adsorption on solid surface and interfacial reactions associated with nanomaterial-immobilized enzyme system.
- To develop and assess a recirculating bioreactor system for high lactose conversion into galacto-oligosaccharide using the nanofibers-based β-galactosidase nanobiocatalyst.

1.3 Thesis Outline

This thesis is written in a publication-based format. Major experimental results are presented in five refereed journal papers (published and to be submitted) which are included in Chapters 3 to 7. The following descriptions provide a short summary of the thesis:

Chapter 1 introduces the project background, and briefly describes current research gaps and the objectives of this study. The outline of the thesis content and the respective motivation of each chapter are also included.

Chapter 2 comprises literature review and studies on the recent development of nanobiocatalyst advancements and applications in bioprocessing engineering. It provides an overview of up-to-date development of novel nanocarriers, and identifies new research and development strategies for fabrication and applications of the nanobiocatalyst in bioprocess, as well as the perspectives and critical challenges associated to the commercialization of this advanced technology. Major part of the literature study has been published in the Journal of Royal Society Interface in 2015. Additional literature studies on understanding protein adsorption phenomena on solid surface and details information about β-galactosidase-catalyzed lactose bioconversion into galacto-oligosaccharides are also elaborated.

Chapter 3 presents the synthesis and performance evaluation of dendrimer-like hierarchical pore silica nanoparticles (HPSNs) as an enzyme carrier. The synthesis, functionalization and characterization of three types of HPSNs are demonstrated and compared. Their performances in term of adsorption yield, recyclability and capability to preserve enzyme activity are evaluated. Finally, their contribution towards enhancing transgalactosylation selectivity to enhance GOS synthesis is studied. This chapter is

presented as a journal paper, which has been published in the Enzyme and Microbial Technology in 2016.

Chapter 4 presents experimental results of (1) the synthesis of polystyrene nanofiber (PSNF), as an enzyme carrier, (2) fabrication of β-galactosidase-PSNF assembly, and (3) assessment of biocatalytic activities of the nanobiocatalytic assembly. The bioengineering performance of β-galactosidase-PSNF in converting lactose into GOS is further investigated by examining the influence of nanoenvironment in enhancing conversion and production yield. This chapter is presented as a journal paper, which has been published in the Journal of Biotechnology in 2016.

Chapter 5 describes the enhancement of enzyme stability and metabolic function of β-galactosidase-PSNF. The importance of surface modification to facilitate β-galactosidase binding is demonstrated. The modified PSNF-Gal is evaluated in term of adsorption capability, enzyme stability at different pH and temperature conditions and recyclability. Their immobilization ability and engineering performance in lactose bioconversion are benchmarked and compared with non-modified PSNF. This chapter is presented as a journal paper, which has been published in the Bioprocess and Biosystem Engineering in 2015.

Chapter 6 demonstrates the understanding of β-galactosidase immobilization on polymer nanofiber surface through integrated characterizations. The effect of chemical modification on PSNF mechanical stability and physiochemical properties is investigated. The biocatalyst attachment, distributions and conformations are examined using advanced analytical devices including SEM, fluorescence microscope, FTIR, and Raman spectroscopy. The effectiveness factor for lactose conversion into galacto-oligosaccharides (GOS) in a disc-stacked column reactor is also demonstrated by comparing to the free counterpart. This chapter is prepared in a publication format to be submitted soon.

Chapter 7 reports the scaling-up of PSNF-Gal in a reactor system. A scalable recirculating spiral reactor is designed and assessed for the GOS production. The kinetic reaction of the immobilized enzyme is compared with free enzyme at similar enzyme concentration. Variable parameters of the biosystem are optimized, including the conversion rate and productivity, effect of flow rate, and effect of substrate concentration. The outcomes from this chapter offer a vital guideline in translation of the bench-scale

nanobiocatalyst technology into industrial application. This chapter is prepared in a publication format to be submitted soon.

Chapter 8 summarizes the key results and findings for this thesis project and the recommendations of future prospective in the development of nanobiocatalysts and their applications for bioengineering industries.

References

1. Illanes, A.; Cauerhff, A.; Wilson, L.; Castro, G. R., Recent trends in biocatalysis engineering. *Bioresource Technology* **2012,***115*, 48-57.
2. Misson, M.; Jin, B.; Chen, B.; Zhang, H., Enhancing enzyme stability and metabolic functional ability of β-galactosidase through functionalized polymer nanofiber immobilization. *Bioprocess and Biosystems Engineering* **2015,***38*, 1915–1923.
3. Ryu, Y. H.; Yeo, K. B.; Ki, M.-R.; Kim, Y. J.; Pack, S. P., Improved stability and reusability of endoglucanase from Clostridium thermocellum by a biosilica-based auto-encapsulation method. *Biochemical Engineering Journal* **2016,***105, Part A*, 144-149.
4. Bryjak, J.; Aniulyte, J.; Liesiene, J., Evaluation of man-tailored cellulose-based carriers in glucoamylase immobilization. *Carbohydrate Research* **2007,***342* (8), 1105-1109.
5. Matto, M.; Husain, Q., Calcium alginate–starch hybrid support for both surface immobilization and entrapment of bitter gourd (Momordica charantia) peroxidase. *Journal of Molecular Catalysis B: Enzymatic* **2009,***57* (1–4), 164-170.
6. Bergamasco, J.; de Araujo, M. V.; de Vasconcellos, A.; Luizon Filho, R. A.; Hatanaka, R. R.; Giotto, M. V.; Aranda, D. A. G.; Nery, J. G., Enzymatic transesterification of soybean oil with ethanol using lipases immobilized on highly crystalline PVA microspheres. *Biomass and Bioenergy* **2013,***59*, 218-233.
7. Guidini, C. Z.; Fischer, J.; Resende, M. M. d.; Cardoso, V. L.; Ribeiro, E. J., B-Galactosidase of Aspergillus oryzae immobilized in an ion exchange resin combining the ionic-binding and crosslinking methods: Kinetics and stability during the hydrolysis of lactose. *Journal of Molecular Catalysis B: Enzymatic* **2011,***71*, 139-145.
8. Kim, H.; Kwon, H.-S.; Ahn, J.; Lee, C.-H.; Ahn, I.-S., Evaluation of a silica-coated magnetic nanoparticle for the immobilization of a His-tagged lipase. *Biocatalysis and Biotransformation* **2009,***27* (4), 246-253.
9. Chang, Y. K.; Chu, L., A simple method for cell disruption by immobilization of lysozyme on the extrudate-shaped NaY zeolite. *Biochemical Engineering Journal* **2007,***35* (1), 37-47.
10. Nabavi Zadeh, P. S.; Mallak, K. A.; Carlsson, N.; Åkerman, B., A fluorescence spectroscopy assay for real-time monitoring of enzyme immobilization into mesoporous silica particles. *Analytical Biochemistry* **2015,***476*, 51-58.
11. Feng, W.; Ji, P., Enzymes immobilized on carbon nanotubes. *Biotechnology Advance* **2011,***29*, 889-895.
12. El-Aassar, M. R., Functionalized electrospun nanofibers from poly (AN-co-MMA) for enzyme immobilization. *Journal of Molecular Catalysis B: Enzymatic* **2013,***85- 86*, 140- 148.

13. Crespilho, F. N.; Iost, R. M.; Travain, S. A.; Oliveira, O. N.; Zucolotto, V., Enzyme immobilization on Ag nanoparticles/polyaniline nanocomposites. *Biosensors and Bioelectronics* **2009,***24* (10), 3073-3077.
14. Cho, E. J.; Jung, S.; Kim, H. J.; Lee, Y. G.; Nam, K. C.; Lee, H. J.; Bae, H. J., Co-immobilization of three cellulases on Au-doped magnetic silica nanoparticles for the degradation of cellulose. *Chemical Communications Cambridge* **2012,***48* (6), 886-8.
15. Misson, M.; Zhang, H.; Jin, B., Nanobiocatalyst advancements and bioprocessing applications. *Journal of Royal Society Interface* **2015,***12* (102), 1-8.
16. Watanabe, T.; Shinozaki, Y.; Suzuki, K.; Koitabashi, M.; Yoshida, S.; Sameshima-Yamashita, Y.; Kuze Kitamoto, H., Production of a biodegradable plastic-degrading enzyme from cheese whey by the phyllosphere yeast Pseudozyma antarctica GB-4(1)W. *Journal of Bioscience and Bioengineering* **2014,***118* (2), 183-187.
17. Osman, A., Chapter 9 - Synthesis of Prebiotic Galacto-Oligosaccharides: Science and Technology. In *Probiotics, Prebiotics, and Synbiotics*, Preedy, R. R. W. R., Ed. Academic Press: **2016**, pp 135-154.
18. Liu, J.; Qiao, S. Z.; Hu, Q. H.; Lu, G. Q., Magnetic nanocomposites with mesoporous structures: Synthesis and applications. *Small* **2011,***7* (4), 425-443.

.

CHAPTER 2

Literature Review

Chapter 2: Nanobiocatalyst Advancements and Bioprocessing Applications

Mailin Misson[1,2], Hu Zhang[1] and Bo Jin[1]

[1]School of Chemical Engineering, The University of Adelaide, Adelaide, South Australia 5000, Australia

[2]Biotechnology Research Institute, Universiti Malaysia Sabah, Jalan UMS, 88400 Kota Kinabalu, Sabah, Malaysia

*Corresponding author:

Email: hu.zhang@adelaide.edu.au

Tel: +61 8 831 33810

Major part published in:

Journal of Royal Society Interface 2015; 12 (102): 1-20

DOI: 10.1098/rsif.2014.0891.

Statement of Authorship

Title of Paper	Nanobiocatalyst Advancements and Bioprocessing Applications
Publication Status	☑ Published ☐ Accepted for Publication ☐ Submitted for Publication ☐ Unpublished and Unsubmitted work written in manuscript style
Publication Details	Mailin Misson, Hu Zhang and Bo Jin Journal of Royal Society Interface 2015; 12 (102): 1-20 DOI: 10.1098/rsif.2014.0891

Principal Author

Name of Principal Author (Candidate)	Mailin Misson		
Contribution to the Paper	Performed literature review, wrote the manuscript.		
Overall percentage (%)	70 %		
Certification:	This paper reports on original research I conducted during the period of my Higher Degree by Research candidature and is not subject to any obligations or contractual agreements with a third party that would constrain its inclusion in this thesis. I am the primary author of this paper.		
Signature		Date	06.02.2016

Co-Author Contributions

By signing the Statement of Authorship, each author certifies that:

i. the candidate's stated contribution to the publication is accurate (as detailed above);

ii. permission is granted for the candidate in include the publication in the thesis; and

iii. the sum of all co-author contributions is equal to 100% less the candidate's stated contribution.

Name of Co-Author	Hu Zhang		
Contribution to the Paper	Supervision of manuscript preparation and evaluation, and acted as corresponding author.		
Signature		Date	18/02/2016

Name of Co-Author	Bo Jin		
Contribution to the Paper	Supervision of manuscript preparation and evaluation		
Signature		Date	19/02/2016

Please cut and paste additional co-author panels here as required.

Abstract

The nanobiocatalyst (NBC) is an emerging innovation that synergistically integrates advanced nanotechnology with biotechnology, and promises exciting advantages for improving enzyme activity, stability, capability, and engineering performances in bioprocessing applications. NBCs are fabricated by immobilizing enzymes with functional nanomaterials as enzyme carriers or containers. In this paper, we review the recent development of novel nanocarriers/nanocontainers with advanced hierarchical porous structures for retaining enzymes, such as nanofibers, mesoporous nanocarriers and nanocages. Strategies for immobilizing enzymes onto nanocarriers made from polymers, silicas, carbons, and metals by physical adsorption, covalent binding, crosslinking or specific ligand spacers are discussed. The resulting NBCs are critically evaluated in terms of their bioprocessing performances. Excellent performances are demonstrated through enhanced NBC catalytic activity and stability due to conformational changes upon immobilization and localised nanoenvironments, and NBC reutilization by assembling magnetic nanoparticles into NBCs to defray high operational cost associated with enzyme production and nanocarrier synthesis. We also highlight several challenges associated with the NBC-driven bioprocess applications, including the maturation of large-scale nanocarrier synthesis, design and development of bioreactors to accommodate NBCs, and long-term operations of NBCs. We suggest these challenges are to be addressed through joint collaboration of chemists, engineers and material scientists. Finally, we have demonstrated great potential of NBCs in manufacturing bioprocesses in the near future through successful laboratory trials of NBCs in carbohydrate hydrolysis, biofuel production and biotransformation.

Keywords: nanobiocatalysts, immobilization, enzyme, nanocarrier, bioprocess

2.1 Introduction

Advances in biotechnology have witnessed a growing interest in the development of green and sustainable bioprocesses using enzymes. The exquisite activity, specificity and selectivity of enzymes have made them as promising biocatalysts for numerous fascinating applications including in biocatalysis biosensor and biomedicine. Biocatalysts promote green processes due to low chemical consumption and no release of toxic by-products. Nevertheless, the major challenges associated with the enzymes-catalyzed bioprocesses are high operational costs due tolow stability and reusabilityof the enzymes when extended to large scale industrial processes. Enzymes immobilization on support materials is rapidly gathering pace in recent years. It has been commonly recognized that such technology is able to shelter and/or stabilize enzymes against chemical and environmental attacks, and importantly the immobilized enzymes could be recovered and reused in a large scale continuous process[1]. The development of immobilization techniques as well as the materials from natural/synthetic polymers or inorganic materialsas enzyme supports has been extensively studied recently, as reported in the review paper by Datta *et al.*[2]. However, employment of the immobilized enzymes in a bioreactor system may lead to a reduction of enzyme activity due to the change of the unique and native structures of enzyme upon immobilization [3], although the enzyme activity and stability can be maintained through optimal immobilization by extensive studies to identify the most suitable immobilization protocols [4]. The methodologies for recovering biocatalysts arealso poorly developed. It is, therefore, a focal point to identify enzyme carriers with biocompatible, robust and separable features.

Recent development in nanotechnology has provided a wealth of diverse nano-scale carriers that could be applied to enzyme immobilization.Immobilization of the enzymes on nanostructured materials has been recognized as a promising approach to enhance enzyme performances. The nanobiocatalyst (NBC) is an emerging innovation that synergistically fuses nanotechnology and biotechnology breakthroughs. The NBC formation encompasses the assembling of enzyme molecules onto nanomaterial carriers to favour desirable chemical kinetics and selectivity for substrates. The functionalized nanocarriers allow assembling enzymes in ordered structures, which act as a nanoscale information storage and processing system. Research has shown that nanostructured materials possess the requirements of the NBCs provide large surface areasthat allow a higher enzyme loading

and reduce mass transfer resistance for substrates [1]. The NBC is a specifically functionalized enzyme-nanocarrier assembly, which promises exciting advantages in improving enzyme stability, capability, and engineering performances, and allowing creation of a microenvironment surrounding the enzyme catalysts for maximal reaction efficiencies. Enzyme immobilization using nanostructured carriers can significantly increase life cycles of the biocatalyst, hence reducing the cost of the biocatalytic process. Betancor and Luckarift [5] described enzyme immobilization onto the nano-scale material as a versatile new technology offers advantages including low cost, rapid immobilization and reaction, similarity of nano size, mild conversion condition, robust activities, mobility, high loading, minimum diffusional limitation, self-assembly and stability. A revolutionary class of biocatalysts can be developed by introducing the unique properties of the nano-scale material such as mobility, confining effects, solution behaviours and interfacial properties into nanobiocatalysts. The preparation, catalytic efficiency and application potential of nanobiocatalysts are significantly different from conventional immobilized enzymes. To date, functional nanomaterials have been used for the development of NBCs such as nanofiber (NF) scaffolds[6], nanotubes (NTs)[7], nanoparticles (NPs)[8], nanocomposites (NCs)[9] and nanosheets (NSs)[10].The increasing interest of NBCs has become a driving force for the fabrication of nanocarriers with unique properties and structures. Advanced nanocarriers such as NFs, nanopores and nanocontainers can significantly enhance the engineering performances of enzymes.

Retaining the enzyme functionality is a major challenge associated with the development of NBCs for bioprocessing applications. Over the past decade, a number of technologies for fabrication of NBC assemblies have been intensively reported. Among the binding mechanisms studied, covalent attachment isexclusively reliable for specific binding sites and circumventing enzyme leaching [11-13]. Meanwhile, in spiteof the simplicity of physical adsorptions, their execution in industrial scale is largely challengeddue to critical enzyme leakage [14-15]. The immobilization strategies are varied depending on the physical and chemical characteristics of both enzymes and nanocarriers, and their interfacial interactions. The NBC assemblyshould also be applicable in the bioprocessing environment without affecting the native enzyme properties. Therefore, NBCs with tremendous biochemical and engineering performance such as enhancedenzyme activity and stability as well as reusability and processabilityare to be pursued.The development of functional nanomaterials as enzyme carriers and supports, and immobilization techniques

have been intensively studied during last two decades, which have been comprehensively reviewed in recent reports[4, 16-19]. However, to our best knowledge, the engineering performances of NBCsand their contributions in the bioprocesses appear to be less reported. Bioprocess operations endow a special niche for the production of valuable and marketable products. With attractive performances in regards to productivity and recyclability, the NBC is a promising candidate for substrate pre-treatment [20], biofuelproduction [21] and biotransformation[22]. An integrated process for industrial bioprocessesusing the NBCs is proposed as sketchedin Figure 2.1, which illustrates the research approach from the synthesis of nanocarriers and enzyme immobilization strategy to execution of a specific function and evaluation of bioprocessing performances of the NBCs.

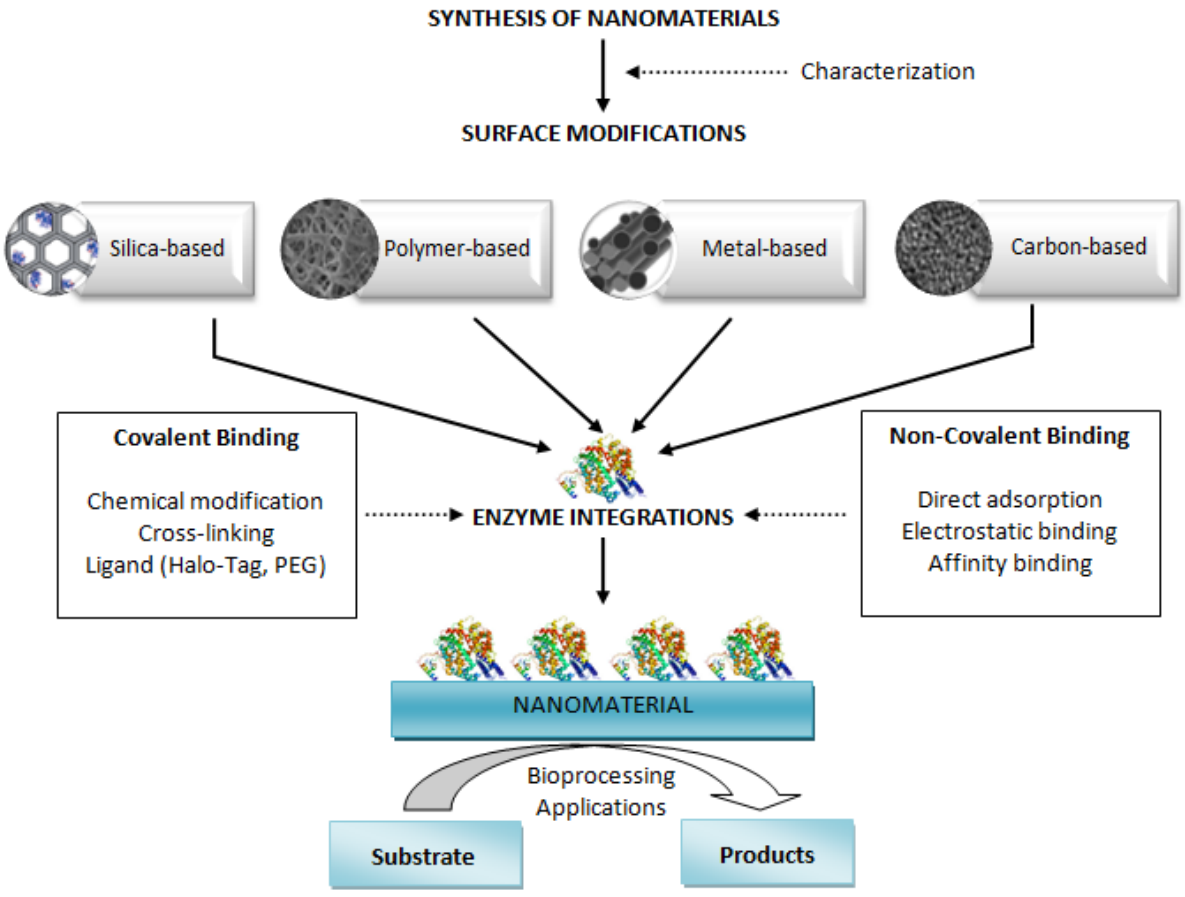

Figure 2.1 Flow diagram demonstrating an integrated process of using advanced nanobiocatalyts for industrial bioprocessing applications.

This article aims to review recent development and applications of the NBCs in industrial bioprocesses. We first discuss the advancements of up-to-date nanocarriers including nanofibers, nanoporous carriers and nanocontainers. We highlight these nanocarrier unique structures and physiochemical properties which are essential for enzyme immobilization. It is also noted that porous microbeads can be classified into these nanocarriers for preparation of biocatalysts since the porous environment is highly compatible with the biological activity of the immobilized biomolecules although the pore size is larger than the mesoporous materials. New strategies for the fabrication and functionalization of NBCs are then addressed for different enzyme nanocarriers and immobilizations. We summarize and evaluate the biocatalytic activities and bioprocessing performance of resulting NBCs. In closing, case studies on NBC bioprocesses for carbohydrate hydrolysis, biofuelproduction and biotransformation are reported.

2.2 Advancements in Nanocarriers for Nanobiocatalysts

NBCs integrate a biological entity for biocatalysis (i.e., enzyme) with a nanomaterialcarrier with unique electronic, optical, magnetic, and external-stimuli responsive properties. There have been many reported technologies for production of specific and processable enzymes, such as recombinant DNA technology to bring the commercial enzyme cost down, directed evolution for pursuing specific traits and widening substrate repertoire, and bioprocessfor making recyclable and durable enzymes for industrial applications. These techniques have been reviewed in detail by Illanes *et al.*[23] and Lopez-Gallego and Schmidt-Dannert [24]. Herewe will focus on the development of nanostructured and nanoporous carriers for the NBC assembly fabrication.

The development of novel nanocarriers with unique functions and characteristics comprises (i) the introduction of functional groups on nanocarriers surface for immobilizing various enzymes or responding to external stimuli, (ii) construction of special structures for increasing the surface area, facilitating substrate diffusion, recycling nanocarriers, or confining enzymes inside nanocages, and (iii) improving processability of nanocarriers such as mechanical and thermal stability.

Hierarchical nanostructures play a significant role in improving the performance of immobilized enzymes in terms of their activity, functionalability and stability. A range of

advanced nanocarriers have been developed and reported in recent studies, including nanoparticle (NP), nanosphere, nanogel, nanocage, nanowire, nanocube, nanorod, nanofiber (NF), nanotube (NT), nanosheet (NS)and nanofilm. Enzyme immobilization onto the NPs has been reviewed by Ansari and Husain [16]. Here,we will only focus on recent research progresses for the development towards applicationof nanofibers, nanoporous carrier, nanocontainers for NBC fabrication.

2.2.1 Nanofibers

Among the nanostructured materials examined for NBC assembly, nanostructured fiber (NF) offers a number of outstanding characteristics, including high enzyme loading and homogenous dispersion in a liquid phase. Furthermore, the high porosity and interconnectivity endow nanostructured fibers with low hindrance for mass transfer. The specific surface characteristics, discrete nanostructures and self-assembling behaviors of NFs provide exciting opportunities to develop NBCs for bioprocesses using bioreactor systems. The integration of enzymes with NFs leads to a hybrid assembly that combines the biocatalytic ability of the enzymes with the unique functions of NFs within the nanostructure network.One-dimensional NFs have been proven as promising nanocarriers in improving biocatalyst performance by considering the factors such as surface area to mass ratio, loading capacity and efficiency, mass transfer resistance, and recyclability. Electrospinning is a commonly used technique to synthesize NFs, due to its simplicity in operation. Fabrication through the electrospinning generates various sizes of fibrous mats, ranging from nanometers to a few micrometre scale[25-27].Except from the single fiber configuration, hybrid structures such as side-by-side, core-shell and hollow NFs can be fabricated from this technique [28]. Side-by-side hybrid fibers (Figure 2.2A) are synthesized by merging two polymer solutionsinto a single jet using a dual-opposite-spinneret electrospinning. Well-aligned and uniform side-by-side fibers may potentially be usedfor carrying two enzymes at the same site.

Feng *et al.*[28] fabricated core-shellNFsby incorporating non-electrospinnable materials into NFs as a core while the shell template was made from electrospinnable polymers. This was achieved by using a facile co-axial electrospinning process, consisting of two syringes for inner (non-electrospinnable) and outer (electrospinnable) solution, respectively.

Removal of the core left the inner part empty so that a hollow structure inside the NFs was generated. These core-shell NFs were applied to a multiple enzyme-catalyzed reaction, involving 3α-hydroxysteroid dehydrogenase, diaphorase and NADH-dehydrogenase. The enzyme mixture solution were fedinto the hollow area while a *N*,*N*-dimethylacetylamide solution of 30 wt% polyurethane sheath was served as a template [29]. This novel polymer NF carrier affords high performance in the multi-enzyme biotransformation. Core shell NF carrier alleviates biomolecules diffusion limitation by controlling the thickness of the sheath and the size of the hollow, which can be tuned by the ratio of inner-outer injection speed during the electrospinning process.

The electrospinning technique can also be useful to fabricate NFs with a hybrid of inorganic/organic material to improve the robustness and mechanical strength of materialsFor example, silica NPs were inserted inside the hollow ultrafine polymer fibers to synthesizea silica-embedded NFcomposite [30-31]. This hybrid nanocomposite can withstand the shear stress during bioprocessing without significant deformation. This feature allows enzyme-loaded NFs to be used in a semi-continuous or continuous bioprocess. Hwang *et al.*[32] reported that uniform quantum-dotsdistribution on polymeric NFsinduced a higher degree of compactness and shape rigidity, resulting in efficient enzyme immobilization.

NFs offer a high surface-to-volume ratio to show a high adsorption capacity of enzyme loading. The porous structures of the NFs allow easy penetration of the moleculesinto all available surfaces. However, the overlapping surfaces of NFs block the enzyme penetration, while some enzyme molecules shielded inside the NFs may not be attacked by the substrate molecules, which reduce enzyme activities. Ros *et al.*[33] reported a chemical modification strategy to increase the surface area of polymer NFs by treating NFs with oxidizing agents such as nitric acid and sulphuric acid.Chemical modification plays an important role in fine-tuning the porous structure of NFs for easy penetration of biomolecules. As the alteration yields an accessible and penetrable surface, enzymes can attach into the inner region of NF carriers. This functional structure also allows optimal substrate diffusion. As a result, the bioconversion of substrates in bioprocessing reactions can be performed effectively without diffusion constraints.

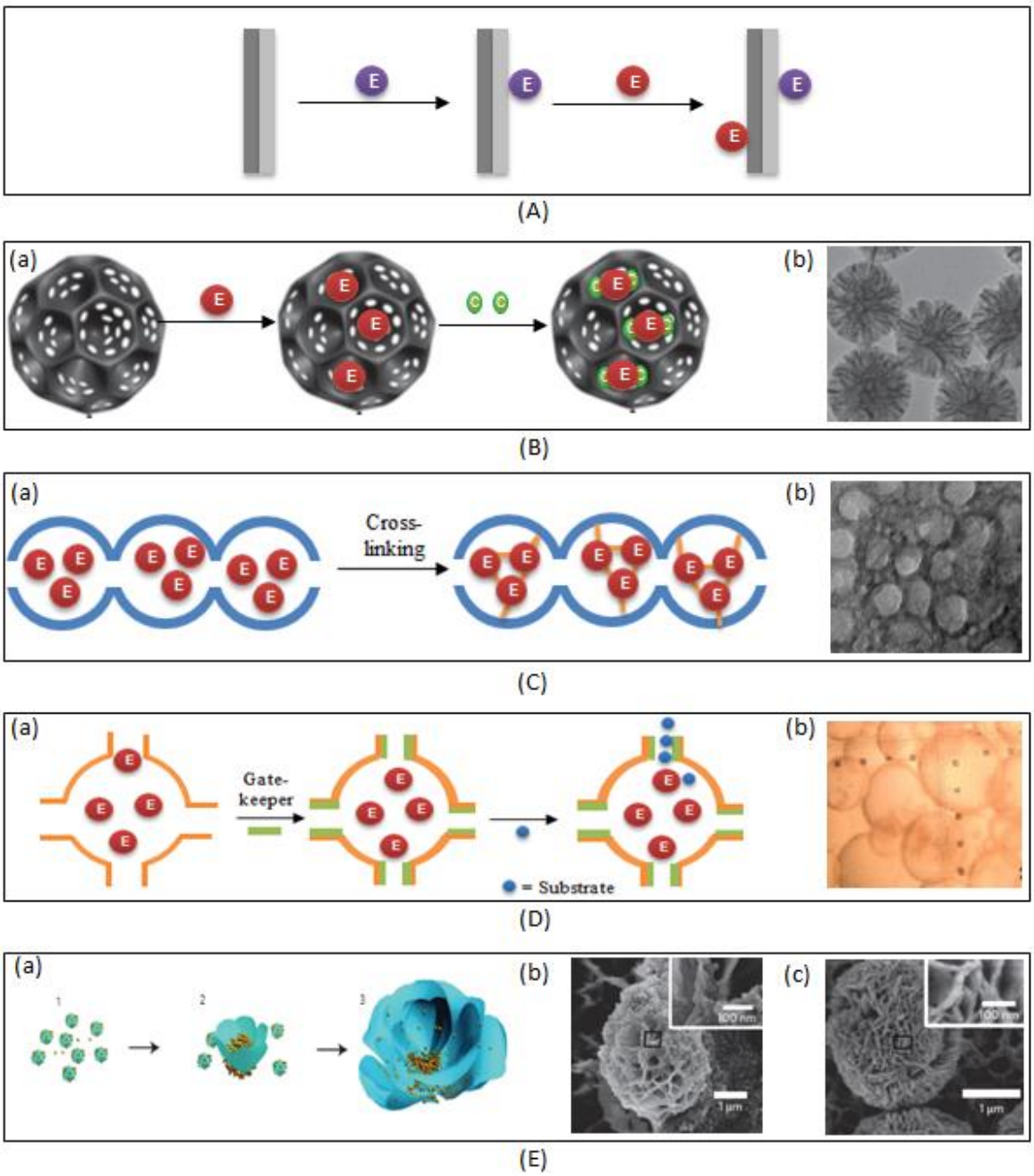

Figure 2.2 Nanocarriers with unique physicochemical properties. (A) Side-by-side hybrid nanofibers promote immobilization of two enzymes to perform simultaneous reactions. (B) Schematic illustration of dendrimer-like nanoporous silica for the co-immobilization of enzyme with co-factors or other biomolecules (a), TEM image of dendrimer-like nanopores silica (b) [34]. (C) Schematic illustration (a) and TEM image [35] (b) of ship-in-a-bottle pore structures to retain and stabilize enzymes inside the nanocages. (D) Schematic illustration (a) and optical micrograph [36] (b) of nanocages with substrate-diffusion gatekeepers to prevent enzyme leaching. (E) Schematic diagram (a) and SEM images of the formation of BSA-incorporated $Cu_3(PO_4)_2.3H_2O$

nanoflowers (spheres in nanoflowers' core as protein molecules) at 12 h (b) and 3 days (c) in enhancing enzyme activity and stability [37].

2.2.2 Nanoporous Carriers

Mesoporous silica and carbon materials are designed with uniform nanopores and tuneable periodic nanostructures, which are promising for controlling release of small and large molecules [38]. The porous structures can offer a high surface area as well as their ability to encapsulate enzymes within the pores to provide a more suitable microenvironment than a planar surface. However, the pore sizes could be vital for enzyme entrapment. In contrast to immobilization protocols, the entrapment does not involve any bond between the enzyme and carrier surface. It has been observed that the enzyme exhibits higher activity and thermal stability when the pore size of the carrier is equivalent to the hydrodynamic size of the enzyme. The enzyme can preserve its native conformation in such a pore size, so that the active sides of the enzyme molecules can facilitate interfacial reactions with substrate molecules. When the pore size of the enzyme carrier is smaller than the enzymes, enzyme molecules are incapable to enter into the pore, resulting in a low enzyme loading. On the other hand, the nanocarriers with pore sizes larger than the enzyme may reduce the enzyme activity, which may be attributed to the enzyme leaching or reduction in the enzyme stability[39-40].

Recently, Du *et al.*[34] developed dendrimer-like silica NPs with hierarchical pores. These silica NPs were synthesized with centre-radial and multiple-scale pores. Large pores were favourable for hosting large biomolecules, while uniform mesopores actedas nanocontainers for encapsulatingsmall molecules. Such unique properties are pertinent across a spectrum of the domains, which are significant in coordinating the diffusion of a range of molecules of different sizes to the interior part of NPs (Figure 2.22B).

The porous structures of the nanocariers can also be beneficial for hybridizing other components to form multiple functional nanocomposites or assemblies. For example, silica mesoporous nanomaterials can be co-synthesized with magnetic NPs to allow the enzyme/nanocarrier complexes to be easily recovered from the aqueous reaction media. Magnetic silica NPs can be synthesized in several ways, including fabricating in a rattle type, and encapsulating magnetic NPs into mesostructured silica nanospheres, aligned

mesoporousshells and pore channels[38].Multifunctional mesoporous silica has been employed in an electrochemical immunosensor [41].

An integrated multifunctional intelligent nanocarrier developed by Motornov *et al.*[42]could be another futuristic biocatalyst supports. The stimuli-responsive nanocarriers are able to be triggered by light[43-44], temperature[45-46], pH[47-48] and ionic strength[49]. Stimuli could be applied either to the material surface or to the biomolecules which encourage or discourage the enzyme-surface interactions. These switchable systems provide unprecedented potential in bioprocess applications[50]. A hybrid of core-shell intelligent particles as an artificial biological cell was developed with an environmental-responsive feature[42]. The core compartments were designed by accommodation offunctional composites composed of polymers, enzymes and NPs, while the shell was responsive to environmental stimuli through opening or closing the selective gates. Special functions were performed by responding to different environmental stimuli. Release of small molecules from the cargo made from enzyme-responsive mesoporous silica was reported in the trials for colon-specific drug delivery [51]. Capped with bridged silsesquioxane as a gatekeeper, the mesoporous MCM-41 were able to open the gate and release entrapped drugs in the presence of a specific enzyme. Rica *et al.*[52] proposed a concept of enzyme-responsive NPs to develop a synergistic biocatalyst-medicine device. They used a cleavableenzyme-linker to modify the polymer-based NPs. The release of the enzymes at the targeted tissue as well as therapeutic biomolecules can be reduced significantly through chemical transformation.This is an exciting futuristic nanoporous complex that can be potentially applied to biocatalysts for bioprocessing applications.

2.2.3 Nanocontainers

Enzymes can be attached to the fiber surface or enclosed inside the pores. However, enzyme leaching can be an issue if only the enzymes are attached by physical adsorption. Enzyme reactivity could be affected due to conformational change or is reduced by exposing to crosslinking reagents. To encapsulate the enzyme molecules inside a nanoscale container is a very promising approach to maintain the enzyme activity, while substrates can be freely diffused into and out of the container.

A nanocontainer with a "ship-in-a-bottle" pore structure was used to prevent the enzyme leaching (Figure 2.2C). The mesoporous silicas had spherical mesocellular cages (around 40 nm) connected by 13 nm-sized mesopores. After the enzyme was adsorbed into the spherical cages with a high degree of enzyme loading, the enzyme was covalently cross-linked by the glutaraldehyde to form enzyme aggregates. These enzyme aggregates had a size range which was less than the cage size (40 nm) but larger than the pore size (13 nm). In this way, the enzyme aggregates were retained inside the nanocages, resulting in a stabilized enzyme activity[35]. The mesoporous silicawasalso modified to show a cage-like porous structureso as to retain enzyme molecules without cross-linking, such as SBA-16 (cubic) and FDU-12(cubic). FDU-12 had isolated cages (about 17nm) which were connected in three dimensions by small pore windows (less than 4nm). Liu *et al.*[36] discovered that when the enzyme molecules were trapped inside the nanocages, the pore entrance was reduced to prevent the possible release of the enzyme molecules, while the pore size was large enough for entry of substrate molecules and exit of products (Figure 2.2D). The nanocages could be formed from biological molecules like DNA, which could assist us in understanding of complicated enzyme reactions inside the biological species and even human bodies. Through DNA self-assembly process, DNA molecules could form various cage structures, including tetrahedra, cubes, octahedra, dodecahedra and icosahedra shapes. Juul *et al.*[53] conducted experiments to control the encapsulation and release of horseradish peroxidase in DNA nanocavity through temperature change. The nanocavity (approximately 10- 12 nm) was covalently closed by 12 double-stranded DNA helices as the edges of the structure. The entrapped enzymes showed catalytic activity inside the DNA cage, and the substrate molecules were able to penetrate the apertures in the DNA lattice into the DNA cages for biocatalytic reactions.

Another exciting enzyme nanocarrier was fabricated as hybrid organic-inorganic nanoflowers, which was an innovative discovery reported in Nature Nanotechnology [37]. They characterized that the resulting microspheres had an average size of less than 2 μm and showed a relatively smooth surface, in which enzymes were mainly located in the core the nanoflower (Figure 2.2E). The crystal structured nanoflowers were used for immobilization of α-lactalbumin, laccase, carbonic anhydrase and lipase. The hybrid nanoflower exhibited enhanced enzymatic activity and stability compared with free enzymes, which may be attributed to the confinement of the enzyme in the core of the

nanoflower. This nanoflower may withstand the harsh environment in the bioprocess operations.

2.3 Strategies for the Development of Nanobiocatalysts

Nanobiocatalysts can be fabricated through the immobilization of enzymes on or encapsulated in a multitude of nanomaterials including polymers, silicas, carbons and metals. Different techniques and methodologies have been explored and developed successfully to retain the enzymes on or in the nanomaterials. These approaches include physical adsorption via electrostatic interactions, hydrophobic interactions, hydrogen bonding or van der Waals forces, covalent binding, cross-linking of enzymes, or physical entrapment or encapsulation. The physical entrapment is mainly determined by the sizes of nanocarrier pores and enzyme molecules, which has been discussed in detail in section 2.3. Other approaches are based on the functional groups on the surfaces of enzymes and nanocarriers employed in the formation of NBCs. The enzyme itself possesses amino (-NH_2), carboxylate (-COOH), thiol (-SH) and hydroxyl (-OH) groups located in lysine, arginine, glutamic and aspartic acid residues [54] which are widely used to interact with functional groups from nanocarriers, while the functional groups on the nanocarriers are introduced via surface modifications. The methodologies for the fabrication of the NBCs can be varied, depending on physical and chemical properties of the nanocarriers and enzymes, as well as applications and processes of the resulting NBCs. These are the focus of this section. A range of nanocarriers and immobilization procedures for fabrication of the NBCs in the bioprocessing applications are tabulated in Table 2.1. The schematic presentations for fabricating NBCs and SEM/TEM images for some of the resulting NBCs are depicted in Figure 2.3 and Figure 2.4, respectively.

2.3.1 Polymer Nanocarriers

Compared to other enzyme nanocarriers, polymer-based materials can be easily produced in large quantities, and importantly the polymer nanocarries can provide a number of reactive groups for fabrication of NBC assemblies with high stability and functional

activities [26, 55-56]. Polymers have been widely used as enzyme supports. However, their huge geometric size is unfavourable due to the diffusion resistance [57]. The molecular structure of conventional polymer materials is uncontrollable, and their physical characteristics such as porosity, pore size or thickness may make the polymer materials unfavourable for enzyme immobilization. Unlike the conventional polymers, nanostructured polymers hold many distinctive properties which benefit the enzyme functionality and stability. The polymer nanocarriers remain the feature of modifiable surfaces of polymers for further biomolecule conjugation. They can be easily fabricated in nanometer-scale, ranging from 30-500 nm with a large surface area [27]. Therefore, they accommodate high enzyme loading and consequently enhance the biological activity [58]. The immobilization of multi-enzymes on polymer nanocarriers builds a molecular bio-network, and thus creates an interfacial microenvironment, which could affect the accessibility of active sites, configuration of enzymes and biochemical mechanisms. Nanogels, NPs, nanocrystals and NFs from polymers have been examined as enzyme hosts in bioprocessing applications [27, 59-60].

Nanogels are cross-linked nano-porous particles produced from hydrophilic polymers. Encapsulation of enzymes inside the nanogels is the most commonly used technique [59]. However, the substrate molecules may experience mass transfer resistance through the nanogel to reach the enzyme molecules. This issue can be overcome by implementing porous structures of the nanogels [61]. Covalent immobilization can be achieved via formation of a covalent linkage between the functional groups of nanogels and enzymes (Figure 2.3A). α-chymotrypsin enzyme was immobilized on mesoporous magnetic nanogels through photochemical *in-situ* polymerization [62]. The enzyme was anchored to the carboxyl-containing support by 1-ethyl-3-(3-dimethylaminepropyl) carbodiimide (EDC) activation. Two or more enzymes also have been co-immobilized on the surface of nanogels [63]. One novel approach was to introduce polymer monomers onto the surface on a single enzyme, and then induce *in-situ* polymerization to form a porous polymeric network with a few nanometer thickness [64]. This method can facilitate substrate entry into the nanogel and their interfacial reactions with the enzyme. The nanogel can also provide a shield for the enzyme itself.

Table 2.1 Strategies for producing nanobiocatalysts for a wide range of bioprocesses applications.

Binding Methods	Supports	Enzymes	Applications	Reference
Electrostatic interaction	Carboxyl-functioned magnetic NPs	Glucoamylase	Hydrolysis	[65]
	magnetic NPs-chitosan	β -galactosidase	Galacto-oligosaccharide production	[66]
Physical adsorption	Zinc oxide NPs	β-galactosidase	Lactose hydrolysis	[1]
	Polyacrylonitrile NFs	Lipase	Biodiesel production	[67]
Chemical modification	Silica NPs	Xylitol dehydrogenase	L-Xylulose production	[54]
Amino functionalization	Silica NPs	Horseradish peroxidase	Biosensor and biodetection	[41]
Thiol linkages	Silver NPs	α-amylase	Starch hyrolysis	[68]
Alkyl grafting	Ferric silica NCs	Lipase	Biodiesel production	[9]
Bioaffinity	Concanavalin A - magnetic NPs	β-galactosidase	Biosensor &Biodetection	[69]
Imidoesterification	Polyacrilonitrile NFs	Lipase	Anti-biofilm	[6]
Hydrophobic	Carbon NTs	Lipase	Biodiesel	[70]

interaction			production	
Covalent by glutaraldehyde	Polyaniline – magnetic NPs	β -galactosidase	Galacto-oligosaccharide production	[58]
	Polysiloxane/polyvinyl alcohol - magnetic NPs	β -galactosidase	Lactose hydrolysis	[71]
	Graphite NSs	Glucoamylase	Glucose production	[10]

Polymeric NPs are also attractive due to their simple synthesis, high stability, uniform size distribution, and abundance of functional groups for enzyme immobilization. Covalent binding is often employed for stabilizing enzyme molecules on NPs. Lipase on magnetic Fe_3O_4–chitosan NPs was realized by using coupling agents, namely EDC and N-hydroxysuccinimide (NHS) [72]. Enzyme binding onto cellulose nanocrystals was initiated by attacking the nucleophilic amino groups of the activated matrix. Mahmoud *et al.*[73] presented such a binding technique in employing cyclodextrin glucanotransferase (CGTase) on cellulose nanocrystals. The attacks on the amino groups occurred after matrix pre-functionalization with carboxylic groups while prior to further activation by NHS/EDC. Meanwhile, carbohydrate or poly-ethylene glycol (PEG), generally known as an enzyme-surface connecting agent [3] were introduced to provide additional platforms of hydrogen bonding and enzyme protection [74].

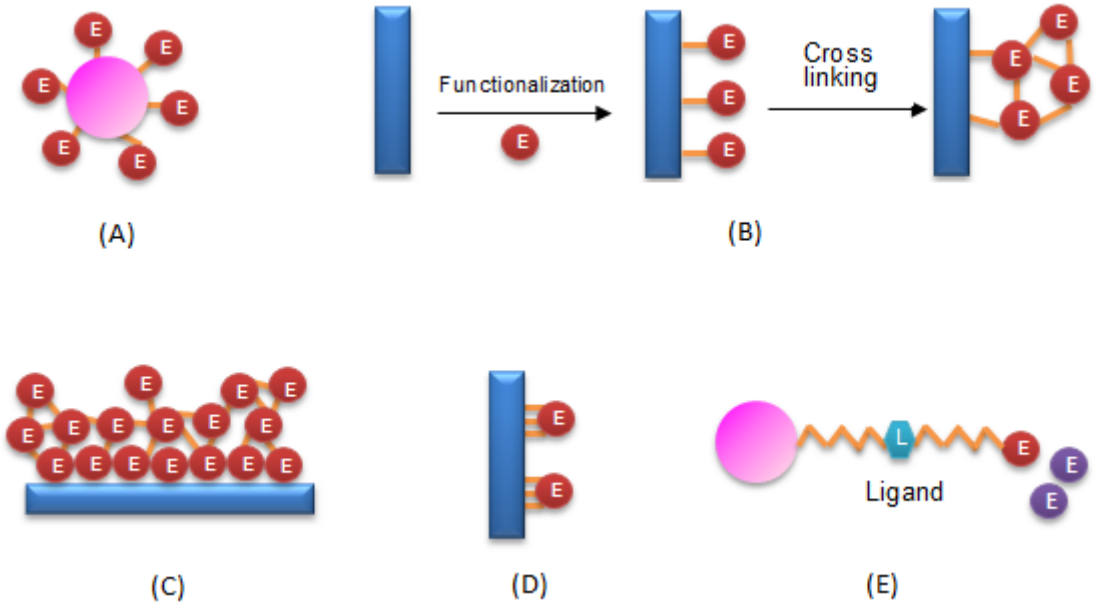

Figure 2.3 Strategies for immobilizing enzyme onto nanocarriers. (A) Covalent linkages between functional groups of nanocarriers and enzymes. (B) Polymeric network using cross-linker agents such as glutaraldehyde and epichlorohydrin. (C) Crosslinking enzyme aggregate coating. (D) Multiple point covalent bonding via short spacer arms on nanocarriers. (e) Spacer molecules such as ligand to promote specific enzyme binding.

Nanofibrous hosts have received increasing attention because of their unique interconnectivity, permeability and separability [75]. Physical adsorption is the most commonly used method for enzyme immobilization onto the NFs. However, the enzyme leaching can be a severe issue for bioprocessing applications. As an alternative, successful immobilization is often employed through covalent binding as confirmed by SEM images (Figure 2.4A) [76]. The hydrophobic surfaces of the polymer NFs can be modified to increase the biocompatibility. For nitrile-rich polymer nanocarriers such as polyacrilonitrile (PAN), enzyme binding onto them is normally activated through imidoesterification between imidoesters of the NFs and amino groups of enzymes [6]. However, their covalent conjugation was inefficient since less than 30% of the initial activity was retained after 10 repeated cycles. Li *et al.*[77] upgraded this technique by using an epichlorohydrin coupling agent when they conjugated catalase onto PANnanofibrous. A rapid enzyme immobilization was achieved using this crosslinking procedure (Figure 2.3B). Experimental data revealed that the amount of attached catalase remained stable after 3 h

reaction, indicating an equilibrium state was reached. However, a drastic activity reduction was simultaneously observed, which was believed due to the detrimental impacts of the epichlorohydrin. Therefore, more effective and non-toxic crosslinking agents are pursued for enzyme immobilization onto PAN NFs.

Co-synthesizing with functionalized polymers is a recently developed strategy to create nanocarrier reactive sites. Co-polymer NFs have been prepared from maleic anhydride and styreme as a new aptasensor platform [55]. The abundance of maleic anhydride promoted high loading of aptamers to ensure sufficient capacity to capture enzymes. For example, Stoilova *et al.*[78] employed this technique for acetylcholinesterase binding. They initially optimized the weight ratio between two polymers to obtain considerable amount of reactive anhydride moieties. The reactive groups potentially formed a facile binding with other functional molecules for specific reactions. The reaction with polyethers, for instance, can form flexible spacers that allow efficient enzyme mobility and reduce steric interference. Consequently, the resultant favourable environment enhanced the storage and thermal stability of the native enzyme.

A combination of enzyme aggregate coating and covalent enzyme attachment has been explored for fabricating enzyme-polymer NF assembles. A thin layer of enzyme molecules were covalently linked to the surface of polymer NFs. When more enzyme molecules were added, they were cross-linked to the first layer of molecules, leading to a crosslinked enzyme aggregate coating (Figure 2.3C) [79]. Enzyme molecules can also be encapsulated inside the polymer NFs by co-electrospinning enzyme in solution with a water-soluble polymer. Consequently, successful enzyme immobilization is achieved by crosslinking the polymer. Alternatively the NBCs can be formed by the coaxial electrospinning with aqueous one or multi enzymes in the core and a water-insoluble polymer in the shell [80].

2.3.2 Silica Nanocarriers

Enzymes can be physically adsorbed onto the mesoporous silica NPs (MSNs) (Figure 2.4B), mainly through hydrophobic/hydrophilic and electrostatic interactions. By tuning the surface properties including the pore geometry, surface charge density, and functional groups, mesoporous silicates have been used to adsorb a variety of enzymes [34, 81-82]. We

have listed several examples of crosslinking enzymes inside the pore and physical encapsulation or entrapment inside a nanocontainer made from silica-based nanocarriers in previous sections 2.2 and 2.3.

Covalent attachment is realized by using crosslinking agents such as glutaraldehyde and carbodiimide derivatives. Zhang *et al.*[54] studied the functionalization of silica NPs by introducing aldehyde, cyanogen, epoxy or carbodiimide groups. The $–NH_2$ and –COOH groups in lysine residues of enzyme are reacted with aldehyde- and epoxy-activated silica nanoparticles. Multiple covalent attachments (Figure 2.3D) are formed in the reactions using these functional groups. Such modifications were applied for immobilization of *Rhizobium etli* CFN42 xylitol dehydrogenase to synthesize various rare sugars. Rekuc *et al.*[83] experimentally revealed that laccase immobilization was also enhanced by readily available functional groups such as $–NH_2$, -OH and oxirane rings from the MSN support.

Using the covalent binding technique, the enzyme is anchored to the surface through any one or more reactive sites. The enzyme displays high efficiency in biocatalysis on some active sites, while the enzyme activity on other sites could be lost. Targeted immobilization has been investigated through specific and focused binding (Figure 2.3E). For example, affinity binding encourages specific molecule bioconjugation onto silica-based supports. It has been implemented on ferric silica NPs by grafting long alkyl groups for lipase binding [9]. The affinity binding resulted in an excellent lipase binding efficiency up to 97%, leading to enhanced stability without major loss of transesterification activity. Besides affinity grafting, metal introduced onto the MSN surfaces can specifically bind to a histidine tag on the enzyme. Cu^{2+} was employed to attach laccase onto mesoporous silica [15]. Consequently, the affinity binding showed a higher adsorption capacity (98.1 mg/g particles) and activity recovery (92.5%) than physical adsorption procedure. Cu- and Ni-modified silicas were also used to specifically bind His-tagged lipase [84-85] and protease inhibitor [86].

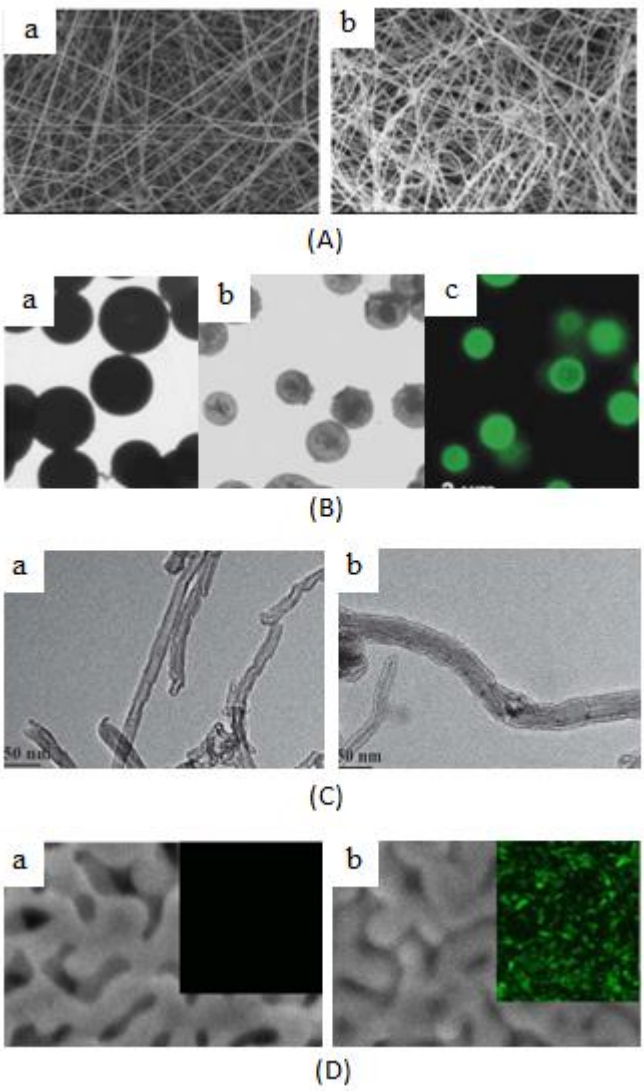

Figure 2.4(A) SEM images of polyacrylonitrile nanofibrous membrane (PNM) (a) and lipase-immobilized PNM (b) [76]. (B) TEM images of catalase-loaded mesoporous spheres (a), removed mesoporous sphere template (b) and CLSM images of microcapsules loaded with FITC-labelled catalase (c) [87]. (C) TEM images of functionalized carbon nanotubes (CNT) (left) and lipase-bound CNT (right) [88]. (D) SEM and fluorescent images of nanoporoous gold composite before (a) and after (b) lipase loading [89].

Another immobilization technique is to form a spacer arm between the enzyme and activated matrix [90]. One approach for spacer arms is carried out through amine activation using glutaraldehyde as a coupling agent. However, although the bridge molecules reduce enzyme leaching, their strong binding may decrease biological activity due to enzyme denaturation.

2.3.3 Carbon Nanocarriers

Carbon-based nanocarriers have been widely employed for enzyme immobilization owing to their inertness, biocompatibility and thermal stability [91-92]. Among them, carbon NTs (CNTs), nanodiamond and graphene derivatives appeared to be the most attractive nanocarriers for producing the NBC assembly. A variety of covalent binding and physical adsorption methods have been studied onto pristine or functional CNTs. CNTs possess a hydrophobic nature which is essential for driving enzyme binding. Enzyme deposition onto single walled CNT can be achieved via simple physical-adsorption without chemical modifications through sequential steps [14]. Using an ionic adsorption technique, α-amylase and urease immobilized onto two-layer alumina silicate halloysite NTs have shown promising stability and reusability [93]. The different charges between NT surface and enzymes enhanced the binding. Both enzymes retained more than 55% of their initial activity after 7 cycles of separation and reaction, as well as preserved more than 90% of its activity after 15- day storage. This simple physical adsorption can also be applied to un-modified multi walled CNTs surfaces, such as lipase adsorption. Prlainovic *et al.*[70] found that the duration for complete enzyme adsorption depended on the medium ionic strength. Based on their observation, the ionic strength enhanced hydrophobic interactions which led to successful enzyme immobilization. In addition, lipase itself contains approximately 28-33% of hydrophobic amino acids, and thus promotes the enzyme to be in open-lid position [94], which can be a driving force for initiating the adsorption process.

Covalent binding has been reported for modified CNT carriers via inducing the reaction of free amine groups on the surface of a protein with carboxylic acid groups on CNTs, confirmed by TEM images in Figure 2.4C. The carboxylic acid groups were introduced by oxidation of CNTs and activation using carbodiimide [95-96]. Lipase [97-98], organophosphorous hydrolase [99-100] and other enzymes have been successfully immobilized onto CNTs. Alternatively, enzyme molecules are covalently attached to linking molecules on the CNT surface via hydrophobic or π-π interactions. Linking molecules can provide specific sites for CNTs to immobilize enzymes, exemplified by 1-pyrenenbutanoic acid succinimidyl ester for horseradish peroxidise [101], a poly(ethylene glycol) based spacer for perhydrolase S54V [102] and Na,Na-bis(carboxymethyl)-l-lysine for His-tagged NADH oxidase [103].

Other carbon-based nanomaterials show similar chemical and physical properties of CNTs and, therefore, similar methods can be used for immobilizing enzymes onto these materials. For example, trypsin was covalently immobilized onto detonated nanodiamonds (3-10 nm) [104], and non-covalent bonds were formed between co-enzyme of glucose oxidase and glucoamylase and chemical reduced graphene oxide nanocarriers [105].

2.3.4 Metal-Based Nanoparticles or Composites

Metal-based nanomaterials have been widely used for fabricating NBCs. Among them, magnetic NPs are one exceptional example due to their high recyclability for biocatalysts. Functional groups, such as amino, carboxylate, thiolate or phosphate, are introduced onto the metal NP surfaces to create strong interfacial reactions with enzyme molecules, and consequently to enhance the enzyme immobilization. Excellent enzyme immobilization on nanoporous gold biocomposite (Figure 2.4D) had resulted in an increase in both biocatalytic performance and enzyme stability [89]. Carbodiimide linkage, for instance, was applied to activate magnetic NPs for cholesterol oxidase immobilization [106] and to modify gold NPs for glucose oxidase immobilizers [107-108]. Multi-functional groups allow enzyme and cofactors, or multienzymes to bind onto one single metal NP, facilitating multi-reaction in a one-pot medium [109]. This catalyst mixture circumvents the laborious and multi-stage operations by shortening long reaction pathways. Amine and carboxylic acid were grafted on multifunctional Fe_3O_4 NPs using robust silane linkages [110]. Mediator thionine, enzyme horseradish peroxidase and secondary anti-human IgG antibody were loaded concurrently onto the modified Fe_3O_4 NPs to produce a highly sensitive label for diagnosing pancreatic cancers.

A thin layer of polymers can be coated onto the surface of metal NPs, on which functional groups are then interacted with enzyme molecules to achieve stable immobilization. Chitosan, PEG, polyvinyl alcohol, and polyethyleneimine (PEI) have been explored for the coating purpose [111-112]. Targeted immobilization onto metal NPs can be achieved through affinity interactions, such as antibody-antigen, and streptavidin-biotin. Biotin groups are first introduced into metal NPs, and then streptavidin is bound to biotin-coated NPs and acts as a spacer arm for the conjugation of biotinylated enzymes. Here are a few excellent examples for immobilization of catalase on activated Au NPs [113] and

glucose oxidase (GOx) on apoferritin NPs [114]. Affinity peptides are often used for modification of the metal NPs as well. The gold binding peptide was the first example of engineered inorganic-binding peptides. Multiple repeats of the peptide were used for directing enzyme self-immobilization on the gold surface [115]. Ligand as a bridging unit in protein bioconjugation can also be modified to promote multifunctional features. Susumu *et al.*[116] modified ligand molecules with dihydrolipoic acid and PEG terminal ends, promoting a simultaneous coupling of biomolecules and dyes to quantum dots. Metal NPs can also be incorporated into CNTs, mesoporous silicas, and polymer nanogels or NFs to synthesize nanocomposites. Fabrication strategies for enzyme immobilization methods onto these nanocomposites are similar to those described above.

There are no universal strategies for constructing NBCs in different processes. The characteristics and relative benefits of the different categories of NBCs are summarizes in Table 2.2. Selection of a specific immobilization strategy depends on many factors, including enzyme molecular structure, application process, and nanocarrier and surface functional groups. However, any strategy should aim at maintaining or improving enzyme functional properties (activity, stability, selectivity and specificity) and being applicable for the NBCs in a bioprocessing environment.

2.4 Engineering Performance of Nanobiocatalysts

Exploitation of NBC technologies are still in the infant stage in bioprocessing industry. Process-related traits of the NBCs are not fully understood. The success of NBC technology in the large-scale manufacturing process relies on four key features: (1) specific activity under the process conditions; (2) stability of the NBCs when exposing to pH / temperature variations, organic solvent interface, high shear stress and other harsh environments; (3) reusability of biocatalysts; and (4) high throughput for large-scale processes. It is economically and technically crucial that the NBCs are able either to maintain stable activities in a long term in a continuous process, or to be recycled for re-use in a batch operation process for many runs in which the NBCs are separated from the reaction media after the reaction is completed. For a continuous operation, stability of the enzyme activity as well as reduction of the enzyme leakage are the main targets for

immobilization, while for batch operations, recyclability and constant enzyme activity of NBCs are the key challenges.

2.4.1 Enzyme Activity and Stability

It is believed that immobilization onto solid supports could reduce the enzyme activity, such as bovine serum albumin[91], penicillin acylase [117] and β-galactosidase [66]. This belief may not be true when enzymes are immobilized onto the nanocarriers. There are many studies on the enhancement of enzyme activity after the enzyme is bioconjugated with nanocarriers. The mechanisms of the enhancement of the enzyme activities through the nanocarrier immobilization have been discussed in detail in a recent review paper [118]. The comparison of the kinetic parameters between free and immobilized enzyme, as well as the key contributions for the performance improvement is summarized in Table 2.3. It is generally accepted that the enhancement of enzyme activity and stability may be due to enzyme conformation change. Immobilization of enzymes onto nanocarriers results in stabilization of active conformation, which promotes the interfacial reactions between the substrate and enzyme reactive sites (Figure 2.5A), while the soluble enzyme in the solution has a freedom in conformation change.

Table 2.2 Characteristics of different types of nanomaterials.

	Polymer Nanocarriers	Silica Nanocarriers	Carbon Nanocarriers	Metal-based Nanoparticles or Composites
Source	Natural and synthetic polymers	Silica	Carbon nanotubes, diamond, graphene	Magnesium, quantum dots, gold, and metal oxides
Configuration	Nanofibers, Nanogels, nanoparticles, nanocontainers	Nanoparticles, mesoporous structures, nanocontainers	Single-wall Nanotube,multi-wall natube, nanofilm	Nanoparticles
Contributor of nanocarriers for nanobiocatalysts	Functional groups available from polymers	Highly porous structures, Introducing external functional groups	Hydrophobic surfaces, introducing external functional groups	Functional group or thin layers of polymers onto metal surfaces Covalent binding
Nanobiocatalyst fabrication	Covalent binding; entrapment, cross-linking	Physical adsorption, entrapment, crosslinking, spacer-arm	Physical adsorption, covalent binding	Covalent binding
Recycle	Attached to macroporous structures or magnetic particles	Attached to magnetic particles	Attached to magnetic particles or separated by density differences	Magnetic or centrifugal separation
Mechanical strength	Weak	Strong	Strong	Strong

Multiple point covalent bonding via short spacer arms on nanocarriers may be a powerful strategy to improve the enzyme activity [9, 66], while physical adsorption of lipase onto nanocarriers via hydrophobic interactions significantly increases the enzyme activity because the open form (active in catalysis) is stabilized when the large hydrophobic groups are exposed to hydrophobic surfaces of nanocarriers as evidenced by Palomo *et al.*[119] and Chen *et al.*[120]. Conformation change may also be induced via some molecules presented in the surfaces of nanocarriers. α-Amylase underwent a conformation change by binding to Ca^{2+} inside $CaHPO_4$ nanocarriers, resulting in a large fraction of enzymes in their allosterically activated form and enhanced enzyme activities [121].

The increased and prolonged enzyme activity can be ascribed to the enhanced stability of nanocarrier-enzyme complexes as well. Enzymes may become denatured due to interactions with hydrophobic interfaces. The enzymes may also become deactivated due to formation of aggregates in the isoelectric point, at high temperature, or in the presence of salts or solvents. Changes in the enzyme structure tend to decrease the enzyme activity. Through immobilization onto nanocarriers, enzymes are shielded from denaturing microenvironments [122], resulting in a higher enzyme activity than the free enzyme. For example, the curvature of CNTs reduced the detrimental interactions between enzyme molecules due to the longer distance between molecules, thereby leading to higher enzyme stability on single-walled CNTs in comparison to flat graphite [123]. Covalent binding mediated by carbodiimide formed a stable bond between amino groups of enzyme and carboxyl groups of functionalized supports [124]. Consequently, it reduced the mobility of protein structure. The rigid structure of the NBCs could promote the enzyme stability to withstand relatively harsh system and operation conditions comparing to free enzymes. Stabilization of β-galactosidase through multipoint covalent attachments was obtained on magnetic Fe_3O_4-chitosan NPs [66]. Jordan *et al.*[125]has revealed a thermal improvement by stabilizing the weak ionic forces and hydrogen bonds through NP activation using a carbodiimide crosslinker. A remarkable stability of cellulases was observed at a broader range of temperatures with an optimum enzymatic activity at 50^{o}C. Trypsin-coated NFs showed a super capability to maintain the enzyme activity after the NBC assembly was repeatedly used for one year and to exhibit great resistance to proteolysis, paving the way for industrial applications [126].

Localized nanoenvironment is an important approach to the improvement of enzyme activity. The nanoenvironment surrounding enzyme molecules may prevent enzyme

deactivation. For example, a hydrophilic environment may reduce the concentration of hydrophobic organic solvents or some gases near to the enzyme to prevent loss of enzyme activity, while a hydrophobic environment may tremendously reduce the detrimental effect of very hydrophilic deactivating molecules, like hydrogen peroxide [127]. The nanoenvironment may provide a localised optimal reaction conditions for the immobilized enzyme, such as pH, ionic strength, and temperature. The presence of peptides on Au NPs helped construct a local pH of 7.7 in comparison to bulk solution of 7.0, thus lipase reaction rates were 3-180 times higher than controls [128]. Gold and silver NPs acted as a conduction centre to facilitate transfer of electrons. Immobilization of redox enzymes onto colloidal gold or silver NPs may help the protein to make possible conducting channels between the prosthetic groups and the gold/silver surface [129]. The nanoenvironment may also facilitate substrate molecules entry into reactive sites of enzymes through a favourable partition or molecular gatekeepers. Cationic substrates were favoured over anionic substrates when Au NPs were coated with anion peptides for α-chymotrypsin [130].

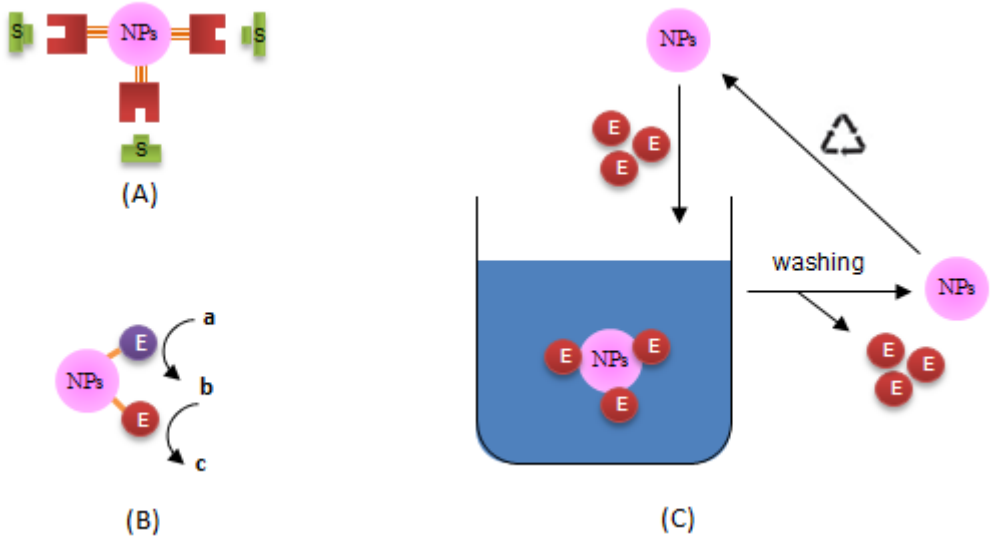

Figure 2.5 Engineering performance of nanobiocatalysts in bioprocess applications. (A) Enhancing enzyme activity by stabilizing the enzyme reactive sites towards the substrate. (B) Accelerating biocatalysis through cascade reactions of the co-immobilized enzymes in one-pot medium. (C) Recycling the nanocarriers after the enzyme activity decays.

Multisubunit and coenzyme immobilized on the same nanocarriers may also contribute to the enhanced enzyme activity. The activity and specificity of multimeric enzymes depend on the architectural structure of subunits. Immobilization of subunits on the same nanosupports can prevent subunit dissociation. In a cascade reaction, two enzymes immobilized in a short distance can accelerate the biocatalysis reactions since the diffusion paths of intermediates are reduced (Figure 2.5B). Glucose oxidease-horseradish peroxidase immobilization onto magnetic NPs was used to demonstrate the concept [131].

Nanocarriers may also restore the enzyme activity of a functionally impaired enzyme. An isolated extracellular pectate lyase had a very low native state activity, but the activity was regained by immobilization of the enzyme onto hydroxyapatite NPs. The activity increased 27.7 fold with a 51 fold increase in half-life at a temperature of 90°C as compared to untreated one [132].

2.4.2 Reusability of Nanobiocatalysts

Feasible reutilization of the biocatalyst is an extremely important requirement in translating NBCs into commercialization. Recovery of NBCs can be a significant issue and downstream processing for their recuperation after the reaction is very complex. Microcarriers or microbeads, however, can be easily separated from reaction medium due to the density difference. Integration of nanostructure with micro- or macro- structures can facilitate the separation of nanobiocatalysts. Nanostructured microparticles can offer the nanoenvironment for enzymatic catalysis and reusability for easy separation. Integration of magnetic technology with the enzyme immobilization on the nanocarriers can enhance recoverability and reusability of the NBCs [133]. NBCs can be separated from the reaction media by simply turning on the magnetic field and attracting magnetic nanocarriers onto magnetic sources. However, some NBCs may be carried away by the reaction media due to weak magnetic forces

.

Table 2.3 Engineering performances of nanobiocatalysts.

Nanocarriers	Enzyme	Binding strategy	Kinetic parameters of NBCs	Kinetic parameter of free enzyme	Contribution for improvement	Reference
Au NPs	Glucose oxidase	Carbodiimide	K_m = 3.74 mM V_{max} = 1.42 μM/min/mg	K_m = 5.85 mM V_{max} = 0.25 μM/min/mg	Conformation change	[108]
Magnetic NPs	Cholesterol oxidase	Carbodiimide	K_m = 0.45 mM V_{max} = 1.64 μM/min/mg	K_m = 2.08 mM V_{max} = 0.67 μM/min/mg	Conformation change	[106]
Ferric silica nano-composites	Lipase	Hydrophobic interaction	K_m = 3.65 mM V_{max} = 131.4 U/mg	K_m = 0.09 mM V_{max} = 133.3 U/mg	Multipoint binding	[9]
Au NPs	Dehydrogenase (MDH) or Citrate synthase (CS)	Physical adsorption	K_m (MDH) = 0.05 mM K_m (CS) = 6 μM V_{max} (MDH) = 5.3 U/mg V_{max} (CS) = 2.7 U/mg	K_m (MDH) = 0.02 mM K_m (CS) = 18 μM V_{max} (MDH) = 8.1 U/mg V_{max} (CS) = 73.6 U/mg	Cascade reaction	[134]

Gold NPs	Lipase	Electrostatic interaction	K_m = 9.10 µM V_{max} = 1.99 µM/sec	K_m = 23.91 µM V_{max} = 1.97 µM/sec	Nanoenvironment (presence of salt)	[135]
nickel-impregnated silica NPs	Diastase	Physical adsorption	K_m = 8,414 mM V_{max} = 4.92µM/min/mg	K_m = 10,176mM V_{max} = 2.71µM/min/mg	Affinity to substrate	[136]
$CaHPO_4$ nano-crystals	α-amylase	Allosteric modulation	K_m> 0. mM	K_m = 0.028-0.073 mM	Conformation change	[121]

Ngo *et al.*[137] further improved this technique through controlling the size of magnetic silica NPs. The particles were dissociated for enzyme loading and reaction, while those particles were re-clustered for easy magnetic separation. This magnetic technique can also be applied to polymer-based nanocarriers. Excellent magnetic response was obtained by coating the magnetic particles with polyaniline [58].

Reutilization is not only applied to nanocarrier-enzyme conjugates, but also to the nanocarriers. Many research findings are focused the reuse potential of immobilized enzyme. However, most of the supports are discarded after enzyme inactivation. Nanocarrier recyclability can lead to a significant reduction of the bioprocessing cost. The synthesis of Au-doped magnetic silica NPs for enzyme immobilization demonstrated nanocarrier recyclability [138]. Cysteine-tagged cellulase, endo-glucanase, exo-glucanase, and β-glucosidase were co-immobilized on the Au NP surface and easily removed by water rinsing as the enzyme activities were decayed (Figure 2.5C). The NPs could be recycled and reused over four times, signifying their robustness against harsh surroundings. Although recycling biocatalysts and nanocarriers through magnetic NPs discussed above can reduce the operation cost, the technique is still in the trial and challenges remain for industrial scale operations. Meanwhile, microcarriers are easy to be separated through sedimentation or centrifugation due to high density. Nevertheless, in contrast to nanocarriers, surface modification such as fine pore adjustment remains as the key challenge in microcarriers.

2.4.3 Processability of Nanobiocatalysts

Although an NBC can achieve a much higher enzyme loading capacity, enzyme activity and stability, as well as mass transfer efficiency, processability of NBCs is limited by the availability of the materials for enzyme carriers and costs for manufacturing nanocarriers. Most of nanocarriers as enzyme immobilizers reported in the literature were produced in the laboratory trials in small quantities. Further studies on economic analysis of overall costs of NBCs for a large-scale production process are needed. Among all nanocarriers discussed above, polymer-based NFs have the tremendous potential for scaling up and meeting the requirement for industrial applications in terms of throughput, reproducibility, and functionality [139]. Another approach to reduce the enzyme purification-associated cost

is to combine the immobilization and purification at the same step. Functional groups of nanocarriers allow selectively binding to target enzymes for immobilization and removing impurities [21]. A high transesterification activity was obtained through simultaneous enzyme purification and immobilization. The NPs were first coated with PEI since PEI was rich in amino groups, which led to a greater binding selectivity and 2-fold purification of the enzyme. As a consequence to the purification, this technique tremendously increased the initial activity to be about 110 times than the unpurified free enzyme.

Weak mechanical strength of nanocarrier-enzyme bioconjugates is another significant issue which limits NBC technologies for wide industrial bioprocesses. A suitable material with strong mechanical strength is needed to support nanocarriers when the bioconjugates are located inside a reactor. Cellulose acetate-based NFs are robust materials with a comparatively high modulus and tensile strength, which are able to bear harsh environments such as agitation and shear force [140]. A protein digestion column has been developed for trypsin-nanoporous silica but trials have not been successful due to a short lifetime of the column [141]. Operation at a low hydrodynamic shear is preferable, for example, using packed bed reactor or monolith column [142]. Four packed-bed reactors have been developed to accommodate bioconjugates in biodiesel production, which provided a longer residence time to enhance the bioconversion rate [143].

Aggregation or clustering of nanocarriers in reaction medium can potentially reduce the surface area of the nanocarriers, leading to low enzyme loading and mass transfer efficiency. It can be a technical challenge to homogeneously distribute enzyme on the nanocarriers during the enzyme immobilization process. Shear may be inserted in the system to prevent aggregation, but this may also damage the fragile structure of enzyme-nanocarrier bioconjugates. For example, poly(styrene-co-maleic anhydride) NFs are hydrophobic and thus, are unlikely to be dispersed in aqueous solution. Nair *et al.*[144]reported a immobilization procedure to use ethanol solution to wash the NFs before immobilizing enzymes. After the enzyme loading, the enzyme-NF complexes were well dispersed in the solution and a continuous flow biocatalysis reactor can be further constructed.

2.5 Applications of Nanobiocatalysts in Bioprocess

Immobilized enzymes have been used for large scale industrial processes, such as glucose isomerase for production of fructose corn syrup (10^7 tonsper annum), lipase for transesterification of food oils (10^5 tons per annum), and penicillin G acylase for antibiotic modification (10^4 tons per annum) [145]. However, the reported studies on the development and application of nanocarrier-based NBCs for bioprocesses are still carried out in the laboratory scale bioreactor or biodevice system. A successful case using NBCs in industrial bioprocesses has not been found in the literature so far. Here, we report the areas which have benefited from these advances, signifying the prospect of designing and operating NBC-based systems in an industrial bioprocess.

2.5.1 Carbohydrate Hydrolysis

Cellulose, starch, empty fruit bunch and microalgae are the commonly used and abundant carbohydrates, which can be potentially hydrolysable substrates for production of valuable chemicals and marketable products. Hydrolysis of these carbohydrates into lower sugars is an essential step. Conventional hydrolysis can be conducted by physical, chemical and/or physio-chemical processes using strong acids or bases under a high temperature and/or a high pressure. Enzymatic hydrolysis has been recognized as an ideal alternative to alter the structure of lignocellulosic, cellulosic and starch materials. Cellulase mixture, which is composed of endoglucanases, cellobiohydrolyases and β-glucosidase, has been explored to breakdown lignocellulosics [125, 138]. Nanocarriers allow simultaneous multiple enzyme co-immobilizations and enhance enzyme stability and activity.

Physical adsorption of cellulase onto superparamagnetic NPs generated a binding efficiency of nearly 100%, and the adsorption capacity reached about 31 mg/g support [146]. Immobilization on the magnetic nanobeads has led to great pH tolerability of cellulase particularly in an alkaline condition, as well as great stability for a long-term storage. Nevertheless, the immobilized enzyme showed a lower biological activity than free enzyme at all tested operating temperatures. Verma *et al.*[147] attached β-glucosidase onto magnetic NPs via glutaraldehyde activation, yielding an immobilization efficiency of about 93%. The cellobiose hydrolysis was significantly increased at 70 ^{o}C in comparison to the

free enzyme. Immobilization of the cellulase mixture onto Au-doped magnetic silica NPs was trialled for the degradation of cellulose [138]. The binding of Au NPs on the surface of functionalized silica NPs created attachment sites for cysteine-tagged enzymes. Although the optimal pH curves were quite similar between the immobilized enzyme and free counterpart, greater pH stability of the immobilized enzyme was demonstrated. The most noteworthy observation was the extension of the enzyme lifetime during thermal inactivation measured at 80^{o}C from 24 h to 36 h (Figure 2.6A). The immobilized enzyme demonstrated enhanced stability and reusability up to seven cycles.

Starch hydrolysis is performed by two enzymes at different operating conditions. Initially, α-amylase hydrolyses starch via a gelatinization and liquefaction process at 105 ^{o}C [148]. The gelatinized starch is further saccharificated using glucoamylase at a lower temperature (50 – 60 ^{o}C) to form reducing sugars mainly composed of glucose. The conjugates of nanoparticles and α-amylase have been used for fast degradation of starch [149]. The product formation rate was increased 1.5 times and the enzyme activity was found to be about 4.7-folds higher than the free enzyme, respectively. The presence of starch during the AgNPs synthesis process was a probable reason for the fast reaction. The starch initially converted silver nitrate into Ag NPs to embed Ag NPs in the helical core of starch molecules. The enzyme degraded the starch helical structure and immobilized onto Ag NPs while the catalyzing sites were kept open towards free starch molecules, which led to a rapid degradation of 9.9 mg free starch within 5 min. High productivity and fast reaction make this discovery economically viable for large-scale production of reducing sugars. In addition, the resulting thiol linkages were able to prevent the particles from forming aggregation. Amyloglucosidase, another starch-hydrolyzing enzyme, was conjugated onto single-walled CNTs by Goh *et al.*[14]. The production cost was defrayed through recycling magnetic NPs-assisted NBC assembly. This study demonstrated that amyloglucosidase retained 40% of its biomass hydrolysis activity within 10 cycle operations. Significant stability was also observed after at least one month storage at 4 ^{o}C.

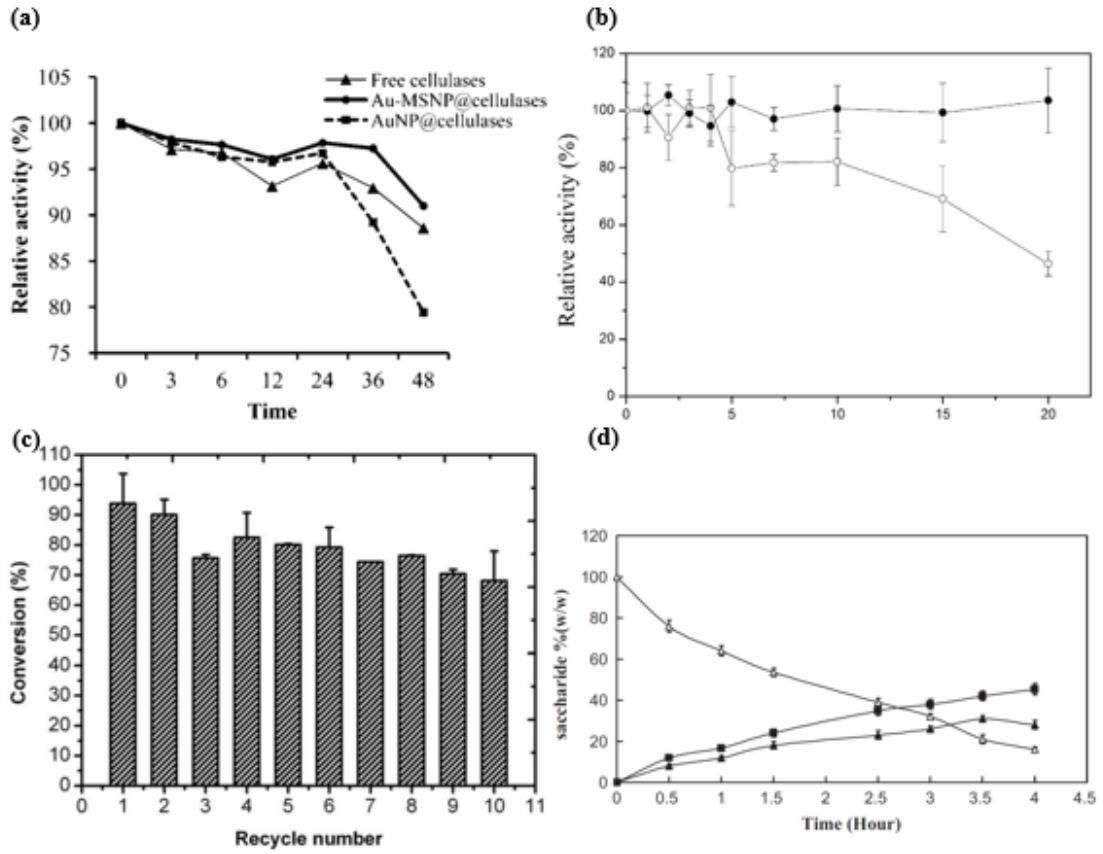

Figure 2.6 Applications of NBCs in Bioprocess. (A) Extension of enzyme activity from 24 h to 36 h by immobilized cellulases on Au-magnetic silica nanoparticles [138]. (B) Storage stability of free lipase (o) and immobilized lipase (●) on polyacrylonitrile nanofibrous membrane [150]. (C) Recyclability of lipase-NPG biocomposite for catalytic conversion of soybean oil to biodiesel [89]. (D) Synthesis of GOS from lactose conversion by β-galactosidase-nanospheres (△lactose, ▲ total galacto-oligosaccharides, ■ monosaccharide) [151].

2.5.2 Biofuel Production

Environmental concerns and fossil fuel shortages have profoundly driven the development of a green and sustainable bioprocessing strategy for biofuel generation through enzymatic technologies. Biofuels derived from bioconversion, such as biodiesel, bioethanol, biohydrogen and biogas, are sustainable and renewable energy sources. Enzymes have been used to replace conventional chemical catalysts. For example, biodiesel production by lipase-based bioprocess is a less energy intensive and more environmentally friendly

technology compared to its production by conventional alkaline catalyzed processes. Another attractive example is the use of enzymes for the hydrolysis of cellulose to produce fermentable sugars for bioethanol production. Nanocarriers have been explored to immobilize enzymes for enhancing their activity and stability.

Biodiesel is normally synthesized in the presence of organic solvents at a high operating temperature. Nanocarriers have been demonstrated to form chemical and thermal-tolerance nanobiocatalysts with a high enzyme loading and enhanced catalytic activity. Core-shell ferric silica nanocomposites (NCs) have been fabricated as a host for *Burkhoderia sp* lipase [9]. Alkyl groups were grafted onto the NCs to create an affinity linker. Binding efficiency was determined to be nearly 100%, demonstrating the affinity can successfully facilitate the binding of lipase. The transesterification activity of biodiesel production was sustained up to 10 cycles. The activity enhancement was also demonstrated by confining *Pseudomonas cepacia* lipase onto polyacrylonitrile (PAN) NFs [67]. Using the physical adsorption method, the enzyme activity was 23-fold higher than that of soluble enzyme. The lipase consistently remained 80% of its initial activity for up to 10 batch reactions. Using the same support, Li *et al.*[150] managed a higher transesterification activity through covalent binding. They initially activated the PAN nitrile groups using amidination reactions prior to reacting with the amino-carrying enzyme. Surprisingly, the immobilized lipase retained almost 100% of the transesterification activity over 10 repeated cycles. Furthermore, the system successfully maintained the same productivity after 20 day storage at 30 ^{o}C, demonstrating that the enzyme stability was significantly improved (Figure 2.6B). To produce a solvent and temperature friendly nanosystem, Wang *et al.*[89] fabricated nanoporous gold (NPG) biocomposites that showed exceptional enzymatic durability against thermal and organic environment. Constructed at a pore size of 35 nm, the enzyme-carried composites allowed encapsulating a large number of biomolecules at various sizes either adsorbing within the pores or on the external surfaces. The NBC-driven system demonstrated a high conversion rate of soybean oil into biodiesel at a longer reaction time for up to 240 h and retained enzymatic activity up to 10 successive batch reactions (Figure 2.6C). The tolerability test over various organic solvents and operating temperatures demonstrated the confined lipase exceeded free enzyme outstandingly. The enzyme was protected inside the small pores of the NPG composites, which provided a sufficient space for substrate molecular mobility as well as retention of enzyme molecules

with less leaching. These remarkable performances in lab-scale pave the way to commercialization of this technology.

β-glucosidase is often used to relieve the product inhibition of cellobiose in the cellulosic ethanol production by converting cellobiose into glucose. The enzyme was coated on NFs to form enzyme aggregates that increased the productivity [152]. The activity of enzyme aggregates was approximately 36-times higher than that of covalent-linked enzymes. The ethanol production from enzyme aggregates was 2.1 times higher. More importantly, after 20 day incubation under a vigorous shaking condition, the activity of enzyme aggregates turned out to increase drastically from 33% to 91%. The tremendous improvement in stabilization may be attributed to the multi-point linkages which may prevent denaturation. Although the development of NBCs is in the infant stage, their contribution in biofuel production has become the major driving force in future research and innovation for bioprocessing engineering.

2.5.3 Biotransformation

Biotransformation through enzymatic reactions has been explored for production of valuable products including drug intermediates and functional food ingredients [22]. β-Galactosidase is generally used to convert lactose-rich dairy wastes into galacto-oligosaccharide (GOS), lactulose and lactosucrose. The bioprocessing performances of the enzymes immobilized onto conventional supports are reported to be less promising. Nanocarriers have been explored for improving the enzyme loading capacity and activity. To improve the GOS production rate, Liu *et al.*[153] used covalent immobilization of the enzyme onto magnetic poly(GMA-EDGMA-HEMA) nanospheres. Epoxy groups on the nanosphere surfaces were reacted with enzyme nucleophilic through a condensation method. A total of 145.6 mg enzyme /g support was successfully adsorbed, indicating a large surface area was available for enzyme attachment. Approximately 2,240 g of GOS per gram adsorbed enzyme were produced. Instead of using the condensation technique, they further grafted polyethyleneimine (PEI) onto the nanospheres as a platform for ionic adsorption [151]. Despite relatively lower enzyme adsorption (86.7 mg/g), the ionic binding however resulted in a higher GOS yield of 4,500 g per gram adsorbed enzyme (Figure 2.6D). The latter retained about 84.6% of its initial activity up to 15 cycles of reactions,

whereas the former only showed 81.5% within 10 operations. In a continuous lactulose synthesis, glutaraldehyde was applied to attach β-galactosidase onto the nanotube microchannel surface [154]. The system successfully mimicked the current industrial practice at a high lactose conversion rate of 78.3%. Moreover, the system constantly maintained the product concentration at about 1.29 g/L for 48 h, operating at a flow rate of 2.5 μL/min. The continuous process is economically viable and very promising for large-scale production of lactulose.

NBCs enable catalytic cascade processes in one site to reduce laborious and multi-step reactions, and promote active reactions in non-aqueous media, mainly in the production of chiral drugs and their precursors. Malate dehydrogenase (MDHase) and/or citrate synthase (CSase) have been co-immobilized onto Au NPs with a diameter of 30 nm for conversion of malate to citrate [134]. The bioconjugates were prepared either by directly adsorbing MDHase followed by CSase, or vice versa, or co-adsorbing two enzymes in the same solution. Higher specific activities and favourable kinetic parameters were obtained by bioconjugating CSase to the NPs before MDHase. In this condition, the individual specific activity for MDHase and CSase were 5.3 U/mg and 2.7 U/mg, while the K_m values were 0.05 mM and 6 μM, respectively. The system promoted efficient sequential reactions by one-step biotransformation, in which the products of MDHase served as substrates for the subsequent CSase reaction. This co-enzyme immobilization leads to a low cost and clean process due to intense reduction on the usage and release of organic solvents.

2.6 Understanding Biocatalyst Adsorption on Nanomaterial

The enzyme immobilization leads to enhancement of enzyme stability and activity beneficial for biocatalytic processes. However, due to sensitivity of protein conformation on solid interface, biocatalysts may encounter structural changes that often facilitate reduction of enzyme activity. Hence, understanding the biocatalyst adsorption phenomena on solid surface is immense research of interest. It can be worthy of investigation to promote widespread applications of enzyme-assisted process.

2.6.1 Factors Affecting Biocatalyst Adsorption

There are many factors controlling biocatalyst adsorption on solid surface including properties of biocatalyst, textural features of surface and influence of external factors [155]. Proteins are complex biopolymers composed of 20 naturally occurring amino acids. The sequence of amino acid in proteins determine their secondary structures such as helixes, β-sheet and turns. β-galactosidase, for instance, consists of four polypeptide chains, each of them is made up of 1023 amino acids within 5 domains [156]. Enzyme itself possesses amino ($-NH_2$), carboxylate (-COOH), thiol (-SH) and hydroxyl (-OH) groups located in lysine, arginine, glutamic and aspartic acid residues which could interact with functional groups from enzyme carriers [54]. Enzyme's domain also has a well-defined hydrophobic core, creating hydrophobic properties to the enzyme that creates a hydrophobic interaction with support surface [157].

The relative size of enzyme and topography of nanomaterials strongly influences the amount of adsorbed enzyme [40]. Enzyme molecules are incapable to enter into the pore of nanoporous when the pore is smaller than the molecular size of enzyme, resulting in a low enzyme loading. In contrast, nanomaterials with pore sizes larger than the enzyme molecular size may reduce the enzyme activity, which may be ascribed to the enzyme leaching or reduction in the enzyme stability [39-40]. Anchoring of biomolecules onto nanoparticles surface may result in a strong binding that may decrease the biological activity of enzyme [90]. The morphology, surface energy, charge and polarity are also among the parameters influencing protein-surface adsorption [155]. It has been reported that proteins adsorb more strongly on non-polar than polar surface, high surface tension than low surface tension, and charged than uncharged substrates [155]. Anand *et al.*[158] demonstrated more rigid adsorbed proteins on non-polar surfaces which were postulated due to destabilization of proteins and conformational reorientations, leading to strong inter protein and protein–surface interactions. Except for glycoporteins that adsorb extensively on hydrophobic planar surfaces as the hydrophobic domains are buried inside a glycans shell [159], most proteins exhibits greater affinity towards hydrophobic than hydrophilic [160].

External parameters such as temperature, pH, ionic strength and buffer composition have a decisive influence on enzyme adsorption behaviour. Koutsoukos *et al.*[161] found an increase protein adsorption at elevated temperature. It can be explained by the entropy gain that become as a major driving force for protein adsorption [162]. The electrostatic state of

proteins is determined by the pH of reaction media. At isoelectric point (pI), the numbers of negative and positive charges of protein are equivalent. Proteins are negatively charged at pH < pI, whereas proteins are positively charged at pH > pI [155]. Their charge could interact with the opposite charge of materials support via electrostatic attractions [163]. The ionic strength, determined by the concentration of dissolved ions, is another parameter that controls protein adsorption. Gessner *et al.*[164] described the increasing surface charge density showed an increase in protein adsorption on polymeric nanoparticles.

2.6.2 Protein Behaviour on Interfaces

The structure of proteins is typically asymmetric and composes of complex molecules of a few nanometers in size. Bovine serume albumin (BSA) is known as a standard protein. Its molecular weight is 79000 while molecular diameter is estimated to be 4.9 nm. Enzyme possesses slightly bigger molecular weight than BSA. The molecular weight of β-galactosidase enzyme, for instance, is 116349 with approximately ca. 7 nm of diameter [165]. The common molecular structures of protein are elliptical, rod-like, or even more sophisticated shapes such as heart-like (BSA), or Y shaped (IgG) [155]. Free protein rotates freely in solution while on a surface the protein will adapt a certain orientation, in which certain part of the protein exposes to the bulk solution while the other part interact with the surface. The active site must be in open-lid position to allow bioreaction with substrates. Rabe *et al.*[155] characterized the structurally-stable protein orientation on surface as 'side-on' or 'end-on' orientation that attached to surface with its long or short axis, respectively.

The orientation changes are highly influenced by the hydrophobicity or hydrophilicity of surface, or the nature of the surface polarity (positively or negatively charged) [155, 166]. As illustrated in Figure 2.7, the possible causes of enzyme conformational changes and inactivation are high charge density (top left) or a hydrophobic surface (top right) [166]. Reduction of unfolding or inactivation of support–enzyme interactions possibly occurs on the enzyme co-immobilized (middle, left) or tethered (middle, right) with hydrophilic polymers. Furthermore, incorrect orientation (below, left) and multilayer formation (below, right) also may result in specific activity reduction.

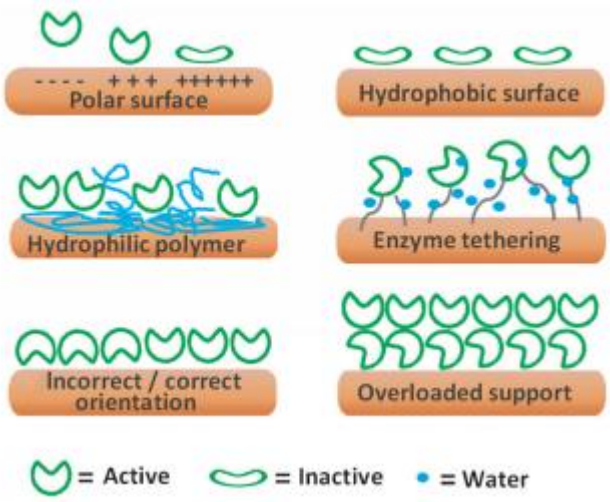

Figure 2.7 Schematic representation of orientation changes of adsorbed enzyme immobilization on different interfaces [166].

It is recognized that the structure of enzyme affects its catalytic efficiency and stability, which influence their potential in biotechnological applications. While enzyme immobilization enables stabilization and continuous operation for significant cost saving, the biocatalyst inevitably undergoes conformational changes upon adsorption to a solid interface. When in contact with surface, the conformation of a protein does not correspond to the free energy minimum of the protein [155]. The surface–protein contact area induces a gain in free energy which causes the protein to maximize their footprint through orientation re-organization, after which conformational changes take place altering protein native structure as have been shown in numerous experimental studies [167-169]. Rabe *et al.*[155] have comprehensively elaborated the factors involved in enzyme conformational changes including the features of enzyme molecule, polar interactions, hydrophobic/hydrophilic interactions, dynamics, material size and topography and enzyme loading. The experimental techniques to elucidate the changes in the secondary structure are elaborated in the section 2.8.3.

2.7 Advanced Characterization of Immobilized Biocatalyst

Integrated analysis studies can be employed to understand the adsorption kinetics of biocatalyst on nanomaterial surface. A number of advanced characterization techniques

are capable of not only providing important information of the surface characteristics of enzyme carriers, but also elucidating enzyme-support interfacial reactions and secondary structures, as reviewed by Bolivar *et al.*[170] who identified the advantages and limitations of each method.

2.7.1 Direct Visualization of Biocatalyst Distribution on Surface

Direct visualization of biocatalyst distribution can be characterized through catalyst imaging using Scanning electron microscope (SEM), Transmission electron microscope (TEM), Raman spectroscopy and Fluorescence microscopy [170]. SEM is able to advance the analysis of bound protein on nanofibers surface. Using SEM technology, Mahmoudifard *et al.*[171] revealed the formation of a homogenous antibodies coating on polyethersolfone electrospun nanofibrous membrane attributed to a hydrophobic interaction. A ruptured coating or biomolecules shrinking into bundles were also demonstrated. SEM micrographs also have been used to indicate the encapsulation of trypsin in electrospun poly (e-caprolactone) nanofibers [172]. Gupta *et al.*[173] postulated the adsorption of lipase in the interfacial region between the polyacrylonitrile nanofibers which confirmed by no change in the surface morphology.

Over the past decades, Fluorescence microscopy has been widely used as a tool in life sciences. Fluorescence microscopy provides an efficient and unique approach to study the fixed and living cells [155, 174]. Selective detection on bound proteins can be achieved by excluding the detection of free proteins that diffuse close to the surface. Fluorescence dyes, such as Fluorescein isothiocyanate [172], amine-reactive fluorescent dyes[175] and fluorescent label Cy5 [176] are useful for protein labelling that emit specific colour under fluorescence microscopy. Fluorescence background is accounted using enzyme-free surface prepared at similar fluorescence condition. An enzyme-loaded surface without fluorescence excitation can be used as negative control. A fluorescence-based strategy has been applied to visualize mechanical forces in structural protein in live cells [177] and for a rapid detection of cellular deoxiribonucleoside triphosphates [178]. Matsuura *et al.*[179] discovered a uniform dispersion of lipase and trypsin co-encapsulated in mesoporous silicas by a combination of differential interference contrast and fluorescence microscopy.

2.7.2 Assessment of Biocatalyst Immobilization

Assessing the location of enzyme upon immobilization is significant to determine whether enzymes are mainly situated inside or adsorbed on the surface of nanocarriers. Thermogravimetric (TGA) is indirect technique that demonstrates the location of enzymes, mainly inside nanoparticle pores by measuring changes in physical and chemical properties such as phase transition, dehydration and decomposition as a function of temperature [180]. Increasing the temperature leads to protein degradation besides evaporating organic materials. The load of enzymes corresponds to the loss of weight after the evaporation process [181].

Ultraviolet-visible (UV) spectroscopy gives information about the modification of adsorption spectra due to protein incorporation such as the content of bound lipase as precipitable protein [182]. The device is suitable for non-opaque carriers. The assessment of protein incorporation also can be carried out using Nitrogen (N_2) absorption [180]. The pore occupation of porous materials is evaluated by measuring N_2 adsorption before and after protein immobilization. In the study by Urabe *et al.*[183], it was observed that the surface area and pore volume available to nitrogen gradually decreased as the haemoglobin concentration increased, indicating an increase in protein loading. Both UV spectroscopy and N_2 absorption techniques, however, face challenges when dealing with a low protein loading.

Fourier transform infrared (FTIR) has been used to detect the formation of interactions between protein and interface. It is a powerful tool to assess the changes in the vibration of silanol groups due to bond formation when they interact with an adsorbing enzyme [180]. For instance, after the immobilization of α-amylase onto functionalized graphene nanosheets, various chemical interactions and bonding were observed [184]. Many prominent peaks were generated including at 1671 cm^{-1} that represents carbonyl amide I bonds whereas bands at 1562 cm^{-1} and 1045 cm^{-1} indicate amide II bonds and C–O–C glycosylated residues, respectively. Verma *et al.*[185] presented new peaks found after incorporation of β-galactosidase onto silicon dioxide nanoparticles. The peak between 3000 and 3500 cm^{-1} was due to vibration modes of O-H and -NH groups. Peaks recorded at 1642 cm^{-1} depict amide II while peaks between 1212 and 1414 cm^{-1} confirmed –CH strecthing, additionally supporting the presence of immobilized β-galactosidase.

2.7.3 Structural Elucidation of Immobilized Biocatalyst

Protein conformational studies are significant in the development of active and stable enzyme in bioreactor system [166]. The structural elucidation of immobilized enzyme can be carried out using Infrared spectroscopy, Circular dichroism (CD) or Raman microscopy. All these techniques provide information about biocatalyst secondary structure and can be applied to diverse types of enzyme carrier [170]. Micro-attenuated total reflection FTIR (micro-ATR FTIR) has been adopted to study the secondary structure of sol-gel immobilized glucose oxidase [186]. Liu *et al.*[187] utilized the combination of sum frequency vibration spectroscopy and attenuated total reflectance FTIR-spectroscopy to characterize the interfacial orientation of immobilized β-galactosidase which was found to exhibit a well-correlation with the tested activity.

Raman spectroscopy is a label-free and non-destructive technique to elucidate protein secondary structure on solid surface [188]. Recent advancement offers the combination of two technologies: i) Raman microscopy, that allows magnification using microscope and thereafter sends the information into spectrometer to analyze signal, ii) Raman spectral imaging or also known as Raman mapping, a method that enables the mapping of spatial resolution of protein molecules and generates chemical images based on sample spectrum. This technique has been employed to analyze the loss of secondary protein structure upon immobilization [189], determine enzyme on solid surface [190] and elucidate enzyme attachment via covalent bond [191]. Confocal Raman microscopy technique has been used to measure conformation and distribution of protein adsorbed in wetted chromatographic particles [189]. Successful binding of tyrosinase on polymeric film of poly(indole-5 carboxylic acid), by chemical coupling to the free carboxylic group of electrochemically formed PIn5COOH, has been proven by in-situ surface enhanced resonance Raman spectra [192]. In other study, three-dimensional Raman spectroscopic imaging of protein crystals deposited on a nanodroplet was demonstrated while two dimensional Raman spectroscopic imaging was used to visualize low concentration region around a growing protein crystal in the nanodroplet [193].

FTIR also can monitor both secondary structure and tertiary fold of immobilized enzyme besides elucidating overall protein conformation and orientation on surface, however, only for non-porous supports [180, 194-195]. Circular dichroism (CD) serves as common alternative or complement of FTIR and Raman spectroscopies. The device is non-

invasive and a convenient applied technique for colloidal particles or transparent material surfaces [180, 196-197], observing the alterations in protein secondary structure occurred due to immobilization protocols [197-199].

In summary, combinations of the characterization approaches and techniques are able to verify the successful incorporation of enzyme and elucidate protein conformational. It might be beneficial to deepen the mechanistic understanding behind protein adsorption and unravel the relationships between enzyme molecule and nanocarrrier. These may facilitate to the development of optimal nanomaterial-immobilized enzyme system which improvises biocatalyst efficiency and stability.

2.8 Nanobiocatalysts for Wastes Conversion into Valuable Products

The demand of enzymes-assisted processes has been extended to diverse sectors including in biocatalysis, pharmaceutical, bioenergy and food industry. One of the applications is to harness a green and sustainable waste management in food industry. One-third of edible foods that are disposed globally as wastes, which have potential as cheap substrates for valuable and marketable products [22]. Around 200 million tons per year of whey are produced worldwidely with an increase rate of about 2 % per year [200]. Whey is a by-product from cheese and casein manufacturing comprises lactose as major constituents (60 - 80 %) [201].Their presence in dairy effluents has been regarded as pollutant due to high organic loading and contributes to eutrophication and toxicity in eco-steams [202]. Hence, a cost-effective treatment has become major concern to the industry. The bioconversion of low-value lactose into value-added products such as galacto-oligosaccharides (GOS) endows a promising solution. GOS is currently being used as a functional ingredient for intestinal regulation and low-caloric sugar alternative to enhance food physicochemical andorganoleptic properties [203-204]. The bioconversion of lactose into GOS is commonly catalysed by β-galactosidase enzyme [205].

2.8.1 Dairy Industry Waste Management

Dairy industry wastes, which are produced with food production like yogurt, cheese, butter, milk and ice cream, are considered as organic pollutant. There is a demand for treatment these wastes due to their high environmental impact. With an index of biodegradability typically in the range 0.4 - 0.8, their wastes are relatively characterized with high biological oxygen demand (BOD) and chemical oxygen demand (COD) in the range of 0.1-100 kgm^{-3} [206]. The presence of milk carbohydrates and proteins such as lactose and casein contributes to organic matter content. Fat and suspended solids are also partially responsible to the contamination levels with values in the range of 0.1-10.6 kgm^{-3}, 0.1-22 kgm^{-3}, respectively. Whey is identified dominating the water stream consists relatively 90 – 95 % of milk volume and containing lactose (60 – 80 %) as major constituents. Worldwidely, more than 10^8 tons of cheese whey is produced annually [207].

High lactose-contained whey has been treated using various techniques, including biological and physicochemical processes, and land application. The approaches of whey management including using various reactor configurations and operating conditions have been extensively studied as reviewed by Prazeres *et al.*[206]. A biological treatment process can be carried out under aerobic or anaerobic conditions. Aerobic process is relatively fast for organic matter degradation at room temperature. However, the variability of effluents properties and extremely high pollution load makes the process inappropriate [206]. Alternatively, anaerobic digestion, conducted at higher temperature (35 ^oC – 37 ^oC) converts the pollutant into beneficial gaseous as alternative energy source. Nevertheless, some proteins are resistant for degradation through these bioprocesses. Thus, there is a need to seek for acclimated or specific microorganisms [208]. The reduction of contaminant load can be accomplished by coagulation-flocculation which is categorized into physicochemical treatment. Protein is precipitated using thermal and isoelectric [209] or coagulant like sodium polyphosphate,sodium hexametaphosphate, iron salts and polyelectrolytes [210-211]. Membrane separation is another physical technique to separate proteins and lactose from cheese whey. It advantageously reduces the wastewater production with possible reuse and clean effluent [212]. Meanwhile, the practice of cheese whey disposal on land generates salts, organic matter and nutrients such as phosphorus, nitrogen, calcium, sodium, potassium, magnesium, chloride, which possess essential properties of fertilizer. However, the resultant soil salinity affects pant growth and fruit

production due to reduce water availability [213]. In addition, the soil structure is destroyed as a consequence of increase conductivity.

2.8.2 Enzymatic Lactose Bioconversion

The recovery of high value-added products from dairy industry wastes provides a green, sustainable and marketable solution. Food wastes are considered as a cheap source of valuable components. Lactose-derived products from β-galactosidase-catalyzed reactions have a large market value and widely used in food and pharmaceutical industries. Products, such as lactulose, lactosucrose and GOS, are known as functional food ingredients with demonstrable health benefits. GOS gains increasing interest as commercial product due to its prebiotic properties and imparting substantial sweet taste to food [71, 214-217]. It stimulates the proliferation of bifidobacteria and lactobacilli in intestine that confers benefits of wellbeing and health [71]. GOS is generally recognised as safe (GRAS) [218] which comply the safety regulation accomplished by the Center for Food Safety and Applied Nutrition's Office of Food Additive Safety [219]. In addition, GOS has low cariogenicity, low caloric values and low sweetness and can be potentially used in range of food products such as fermented milk, breads, jams, confectionery and beverages.

The enzymatic bioconversion of lactose into valuable products has sparked immense biotechnological interest. As an enzyme, β-galactosidase is commonly employed to catalyze bioconversion of lactose into GOS by forming a covalent galactosyl. The reaction occurs through 'shallow' and 'deep' modes of substrate binding [156]. The mechanism of reaction is illustrated in Figure 2.8. β-Galactosidase cleaves lactose molecules forming enzyme-galactosyl complexes before entering either hydrolysis or transgalactosylation pathways. Hydrolysis takes place when water acts a galactosyl acceptor, yielding glucose and galactose as end products, while GOS is generated through nucleophilic-galactosyl reaction in transgalactosylation [220-221]. Sugars that present in the reaction medium can act as the nucleophiles, reacting with enzyme-galactosyl complex, yielding various corresponding products such as GOS, higher GOS, and possibly lactose or isomers. (Figure 2.8a). The reaction conditions generally can be controlled in order to maximize the of GOS production yield. Research has been carried out at elevated temperature, high lactose concentration or lower water activity to favor transgalactosylation [214, 222]. Hydrolysis

dominates at low initial lactose concentration while higher lactose concentrations lead towards transgalatosylation preference. Local nanoenvironment of nanobiocatalysts also has been reported favoring transgalactosylation. The hydrophobicity of enzyme carrier promotes the acceptors such as lactose or smaller units of GOS are preferable at the enzyme catalytic sites [223]. The proposed reaction pathway of lactose bioconversion using the PSNF-Gal due to localized nanoenvironment is presented in Figure 2.8b.

The GOS properties, composition and yield are dependent on the origin of enzymes. The most widely studied are those from *Aspergillus oryzae*[224-225], *Kluyveromyces lactis*[185, 226] and *Bacillus circulans*[220, 227]. β-Galactosidase from *Bacullus circulans* has yielded GOS about 41 % w/w from 400 g/l lactose solution or skim using 1.5 U enzyme [220]. On the other hand, a total of 26 % (w/w) GOS was yielded with 55 % conversion by β-galactosidase from *Aspergillus oryzae* immobilized on magnetic polysiloxane-polyvinyl alcohol [71]. Using similar source of enzyme, Vera *et al.*[228] reported an approximate GOS yield (29 %, w/w) derived from partially dissolved and supersaturated solution lactose. Table 2.4 tabulates the production of GOS which indicates the variability in GOS formation by different source of enzyme and reaction conditions. Bioreactor configuration and operation strategy also affect GOS productivity, yield and purity. Membrane reactor [229], stirred tank reactor [230], packed bed reactor [231], recirculation loop membrane reactor [232] have been assessed for GOS synthesis. The competition of reaction from hydrolysis has become a major challenge in optimization of GOS formation. The generated GOS also can be potentially degraded through reverse chemical reaction. Therefore, a constant study to develop an appropriate system with optimal operating conditions is highly pursued to apply these technologies into large scale operations.

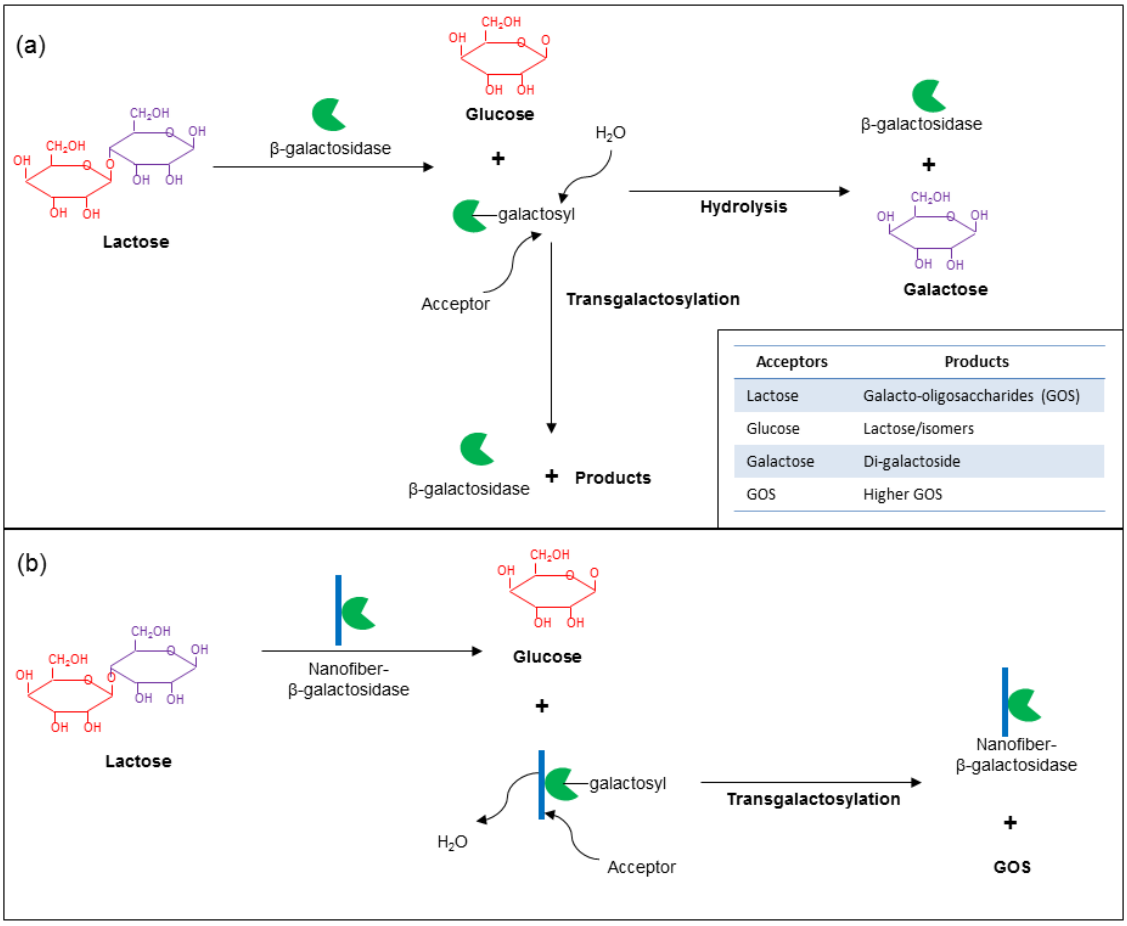

Figure 2.8(a) Thereaction pathway of lactose hydrolysis and transgalactosyslation using free β-galactosidase [233]. (b) Proposed reaction pathway of lactose bioconversion using the PSNF-Gal due to localized nanoenvironment [223].

Table 2.4 Sources of β-galactosidase and reaction conditions for the conversion of lactose into GOS.

Source	Support	Lactose	GOS yield	Conversion	Recyclability	Reference
Aspergillus oryzae	Polysiloxane-polyvinyl alcohol	500 g/l	26 % (w/v)	55 %	10 cycles	[71]
	-	500 g/l	29 % (w/w)	55-60 %	-	[228]
	Cotton cloth	500 g/l	27 (w/v)	50 %	2 weeks (continuous operation)	[218]
	Glyoxyl-agarose	550 g/l	8.5 kg/g enzyme	30 %	10 cycles	[222]
Kluyveromyces lactis	Silicon dioxide nanoparticles	100 g/l	-	100 %	11 cycles	[185]
	Nanosized epoxy	200 g/l	32 % (w/v)	90 %	10 cycles	[153]
	Polymeric Membrane Surfaces	100 mM	13 (w/v)	50 %	5-8 cycles	[234]
			40 (w/v)	10 %		
Bacillus circulans	-	400 g/l	41 (w/v)	50 %	-	[220]

2.9 Conclusion Remarks

Nanobiocatalysts, in which enzymes are incorporated into nano-structured materials, have emerged as a rapidly growing R&D field of nanobiotechnology, which employs and integrates two advanced technologies: nanotechnology and biotechnology. The perspectives of the NBC technology show bright future as well as exciting challenges. These fascinating challenges require joint interdisciplinary collaboration of chemists, engineers, and material scientists. Recent development in nanotechnology has provided a wealth of diverse nano-scale scaffolds that could potentially be applied to the flourishing of NBC-driven industrial bioprocesses. A specifically functionalized nanocarrier-enzyme assembly promises exciting advantages for improving enzyme stability and activity by creating unique nanoenvironments surrounding the enzyme catalysts for maximal reaction efficiencies. Furthermore, enzyme immobilization using nano-structure carriers can significantly increase life cycles of the biocatalyst for its reuse, hence reducing the cost of the biocatalytic process. The integration of enzymes with nanocarriers leads to a hybrid assembly that combines the biocatalytic and specific properties of enzymes with the unique functions within the nanostructure network. However, how to immobilize multi-enzymes on the functionalized nanocarriers to form NBC assembly for a continuous process still remains to be a challenge. Their small size might transform the downstream processing for their recuperation after the reaction is highly complex. Nanostructured microparticles may offer great advantages from both nano and micro worlds for future enzyme carrier trend. Furthermore, there is a lack of fundamental understanding of the generic mechanisms and interfacial reactions associated with the nanomaterial-immobilized enzyme system. Relationships between the enzyme molecules and nanocarrrier properties have not been studied systematically so far. Such fundamental information is significantly important in the development of the multienzyme biocatalytic process. Especially for the cofactor-dependent multireaction systems, how to achieve dynamic interactions among cofactor, enzymes and substrates still awaits in-depth studies from a fundamental point of view. The exploration of multistep enzyme-based bioconversion for large scale operations, particularly involving cofactor-dependent enzymes, presents a profound research interest. It seeks advanced knowledge and innovative technologies for (i) regenerating and reusing the NBCs to minimize the operation costs, (ii) enhancing the stability and performance of

the NBC assembly, and (iii) manipulating multi-enzyme-catalyzed reaction kinetics for maximizing enzyme activity and product yield.

Enzymes in catalyzing a number of bioprocessing domains harness green operations by reducing chemical dependency and releasing non-toxics to the environment. A range of nanocarriers derived from polymers, silica, carbon and metal have been explored to immobilize enzymes or multi-enzymes, making functional and active NBCs. The NBCs demonstrated enhanced enzyme activity and stability, high enzyme loading capacity, and recyclability for bioprocesses. Critical challenges still remain for commercialization. Firstly, cost reduction is the major hurdle for large-scale trials. The major cost is associated with enzyme preparation, immobilization, and nanocarrier synthesis. Recent advances in protein engineering, fermentation and purification technology allow large-scale production of enzymes, while most nanocarriers are still synthesized in the laboratory scale. Secondly, long-term operation of NBCs is required to demonstrate the feasibility in a large-scale operation process. Most NBCs developed in the laboratory trials only demonstrate successfully as a proof-of-concept and very few of them are run up to 10-15 cycles. Stability, activity, leakage and mechanical strength should be evaluated for long-term operation. Thirdly, bioprocess engineers should play a significant role in translating these bench-scale technologies into commercial practices. Most NBCs are developed by material scientists and potential of such NBCs have been raised. However, the realization of the potential relies on bioprocess engineers. Engineering issues should be considered in the early stage of assembling of NBCs. With efforts from material scientists, bioprocessing engineers and biochemists, advanced multifunctional NBCs can be effectively commercialized in a very near future.

References

1. Husain, Q.; Ansari, S. A.; Alam, F.; Azam, A., Immobilization of Aspergillus oryzae beta galactosidase on zinc oxide nanoparticles via simple adsorption mechanism. *International Journal of Biological Macromolecules* **2011,***49* (1), 37-43.
2. Datta, S.; Christena, L. R.; Rajaram, Y. R. S., Enzyme immobilization an overview on techniques and support. *Biotechnology advances* **2012,***3* (1), 1-9.
3. Talbert, J.; Goddard, J., Enzymes on material surfaces. *Colloids and Surfaces. B, Biointerfaces* **2012,***93*, 8-19.

4. Rodrigues, R. C.; Ortiz, C.; Berenguer-Murcia, A.; Torres, R.; Fernandez-Lafuente, R., Modifying enzyme activity and selectivity by immobilization. *Chemical Society Reviews* **2013,***42* (15), 6290-6307.
5. Betancor, L.; Luckarift, H. R., Bioinspired enzyme encapsulation for biocatalysis. *Trends in Biotechnology* **2008,***26* (10), 566-572.
6. Plessis, D. M. d.; Botes, M.; Dicks, L. M. T.; Cloete, T. E., Immobilization of commercial hydrolytic enzymes on poly (acrylonitrile) nanofibers for anti-biofilm activity. *Journal of Chemical Technology & Biotechnology* **2012,***88* (4), 585–593.
7. Wang, L.; Jiang, R., Reversible His-tagged enzyme immobilization on functionalized carbon nanotubes as nanoscale biocatalyst. *Methods in Molecular Biology* **2011,***743*, 95-106.
8. Johnson, P. A.; Park, H. J.; Driscoll, A. J., Enzyme Nanoparticle Fabrication: Magnetic Nanoparticle Synthesis and Enzyme Immobilization. In *Enzyme Stabilization and Immobilization Methods in Molecular Biology*, Minteer, S. D., Ed. Hanna Publisher: **2011**, pp 183-191.
9. Tran, D. T.; Chen, C. L.; Chang, J. S., Immobilization of Burkholderia sp. lipase on a ferric silica nanocomposite for biodiesel production. *Journal of Biotechnology* **2012,***158* (3), 112-9.
10. Ma, Y.-X.; Li, Y.-F.; Zhao, G.-H.; Yang, L.-Q.; Wang, J.-Z.; Shan, X.; Yan, X., Preparation and characterization of graphite nanosheets decorated with Fe3O4 nanoparticles used in the immobilization of glucoamylase. *Carbon* **2012,***50* (8), 2976-2986.
11. Huang, X.; Yu, A.; ZK, X., Covalent immobilization of lipase from Candida rugosa onto poly (acrylonitrile-co-2-hydroxyethyl methacrylate) electrospun fibrous membranes for potential bioreactor application. *Bioresource Technology* **2008,***99*, 5459-5465.
12. Sulek, F.; Drofenik, M.; Habulin, M.; Knez, Z., Surface functionalization of silica-coated magnetic nanoparticles for covalent attachment of cholesterol oxidase. *Journal of Magnetism and Magnetic Materials* **2010,***322* (2), 179-185.
13. Mateo, C.; Palomo, J. M.; Fernandez-Lorente, G.; Guisan, J. M.; Fernandez-Lafuente, R., Improvement of enzyme activity, stability and selectivity via immobilization techniques. *Enzyme and Microbial Technology* **2007,***40* (6), 1451-1463.
14. Goh, W. J.; Makam, V. S.; Hu, J.; Kang, L.; Zheng, M.; Yoong, S. L.; Udalagama, C. N.; Pastorin, G., Iron oxide filled magnetic carbon nanotube-enzyme conjugates for recycling of amyloglucosidase: toward useful applications in biofuel production process. *Langmuir* **2012,***28* (49), 16864-73.
15. Wang, F.; Guo, C.; Yang, L. R.; Liu, C. Z., Magnetic mesoporous silica nanoparticles: fabrication and their laccase immobilization performance. *Bioresource Technology* **2010,***101* (23), 8931-5.
16. Ansari, S. A.; Husain, Q., Potential applications of enzymes immobilized on/in nano materials: A review. *Biotechnology Advances* **2012,***30* (3), 512-523.
17. Cao, M.; Li, Z.; Wang, J.; Ge, W.; Yue, T.; Li, R.; Colvin, V. L.; Yu, W. W., Food related applications of magnetic iron oxide nanoparticles: Enzyme immobilization, protein purification, and food analysis. *Trends in Food Science & Technology* **2012,***27* (1), 47-56.
18. Demarche, P.; Junghanns, C.; Nair, R. R.; Agathos, S. N., Harnessing the power of enzymes for environmental stewardship. *Biotechnology Advances* **2012,***30* (5), 933-53.
19. Verma, M. L.; Barrow, C. J.; Puri, M., Nanobiotechnology as a novel paradigm for enzyme immobilisation and stabilisation with potential applications in biodiesel production. *Applied Microbiology and Biotechnology* **2012,***97*, 23-39.

20. Zieminski, K.; Romanowska, I.; Kowalska, M., Enzymatic pretreatment of lignocellulosic wastes to improve biogas production. *Waste Management* **2012,***32* (6), 1131-7.
21. Solanki, K.; Gupta, M. N., Simultaneous purification and immobilization of Candida rugosa lipase on superparamagnetic Fe3O4 nanoparticles for catalyzing transesterification reactions. *New Journal of Chemistry* **2011,***35* (11), 2551.
22. Galanakis, C. M., Recovery of high added-value components from food wastes: Conventional, emerging technologies and commercialized applications. *Trends in Food Science & Technology* **2012,***26* (2), 68-87.
23. Illanes, A.; Cauerhff, A.; Wilson, L.; Castro, G. R., Recent trends in biocatalysis engineering. *Bioresource Technology* **2012,***115*, 48-57.
24. Lopez-Gallego, F.; Schmidt-Dannert, C., Multi-enzymatic synthesis. *Current Opinion in Chemical Biology* **2010,***14* (2), 174-183.
25. Ignatova, M.; Stoilova, O.; Manolova, N.; Mita, D. G.; Diano, N.; Nicolucci, C.; Rashkov, I., Electrospun microfibrous poly(styrene-alt-maleic anhydride)/ poly(styrene-co-maleic anhydride) mats tailored for enzymatic remediation of waters polluted by endocrine disruptors. *European Polymer Journal* **2009,***45*, 2494–2504.
26. Li, Y.; Quan, J.; White, C. B.; Williams, G. R.; Wu, J.-X.; Zhu, L.-M., Electrospun polyacrylonitrile-glycopolymer nanofibrous membranes for enzyme immobilization. *Journal of Molecular Catalysis B: Enzymatic* **2012,***76*, 15- 22.
27. Park, J.-M.; Kim, M.; Park, H.-S.; Jang, A.; Min, J.; Kim, Y.-H., Immobilization of lysozyme-CLEA onto electrospun chitosan nanofiber for effective antibacterial applications. *International Journal of Biological Macromolecule* **2013,***54*, 37- 43.
28. Feng, C.; Khulbe, K. C.; Matsuura, T.; Tabe, S.; Ismail, A. F., Preparation and characterization of electro-spun nanofiber membranes and their possible applications in water treatment. *Separation and Purification Technology* **2013,***102*, 118-135.
29. Hatzimarinaki, M.; Vamvakaki, V.; Chaniotakis, N., Spectro-electrochemical studies of acetylcholinesterase in carbon nanofiber-bioinspired silica nanocomposites for biosensor development. *Journal of Materials Chemistry* **2009,***19*, 428-433.
30. Kim, J. H.; Kim, J. H.; Choi, E. S.; Yu, H. K.; Kim, J. H.; Wu, Q.; Chun, S. J.; Lee, S. Y.; Lee, S. Y., Colloidal silica nanoparticle-assisted structural control of cellulose nanofiber paper separators for lithium-ion batteries. *Journal of Power Sources* **2013,***242*, 533-540.
31. Yanilmaz, M.; Lu, Y.; Dirican, M.; Fu, K.; Zhang, X., Nanoparticle-on-nanofiber hybrid membrane separators for lithium-ion batteries via combining electrospraying and electrospinning techniques. *Journal of Membrane Science* **2014,***456*, 57-65.
32. Hwang, E. T.; Tatavarty, R.; Lee, H.; Kimb, J.; Gu, M. B., Shape reformable polymeric nanofibers entrapped with QDs as a scaffold for enzyme stabilization. *Journal of Materials Chemistry* **2011,***21*, 5215-5218.
33. Ros, T.; van Dillen, A.; Geus, J.; Koningsberger, D., Surface modification of carbon nanofibers. *Chem. Eur. J* **2002,***8*, 1151-1162.
34. Du, X.; Shi, B.; Liang, J.; Bi, J.; Dai, S.; Qiao, S. Z., Developing functionalized dendrimer-like silica nanoparticles with hierarchical pores as advanced delivery nanocarriers. *Advanced Materials* **2013,***25* (41), 5981–5985.
35. Lee, J.; Kim, J.; Kim, J.; Jia, H.; Kim, M. I.; Kwak, J. H.; Sunmi Jin; Dohnalkova, A.; Park, H. G.; Chang, H. N.; Wang, P.; Grate, J. W.; Hyeon, T., Simple synthesis of hierarchically ordered mesocellular mesoporous silica materials hosting crosslinked enzyme aggregates. *Small* **2005,***1* (7), 744 –753.

36. Liu, J.; Lan, G.; Peng, J.; Li, Y.; Li, C.; Yang, Q., Enzyme confined in silica-based nanocages for biocatalysis in a Pickering emulsion. *Chemical Communications* **2013,***49* (83), 9558.
37. Ge, J.; Lei, J.; Zare, R. N., Protein-inorganic hybrid nanoflowers. *Nature Nanotechnology* **2012,***7* (7), 428-432.
38. Liu, J.; Qiao, S. Z.; Hu, Q. H.; Lu, G. Q., Magnetic nanocomposites with mesoporous structures: Synthesis and applications. *Small* **2011,***7* (4), 425-443.
39. Ikemoto, H.; Chi, Q.; Ulstrup, J., Stability and catalytic kinetics of Horseradish Peroxidase confined in nanoporous SBA-15. *The Journal of Physical Chemistry C* **2010,***114*, 16174–16180.
40. Sang, L. C.; Coppens, M. O., Effects of surface curvature and surface chemistry on the structure and activity of proteins adsorbed in nanopores. *Physical Chemistry Chemical Physics* **2011,***13* (14), 6689.
41. Yang, M.; Li, H.; Javadi, A.; Gong, S., Multifunctional mesoporous silica nanoparticles as labels for the preparation of ultrasensitive electrochemical immunosensors. *Biomaterials* **2010,***31* (12), 3281-3286.
42. Motornov, M.; Roiter, Y.; Tokarev, I.; Minko, S., Stimuli-responsive nanoparticles, nanogels and capsules for integrated multifunctional intelligent systems. *Progress in Polymer Science* **2010,***35*, 174-211.
43. Shi, D.; Matsusaki, M.; Akashi, M., Photo-tunable protein release from biodegradable nanoparticles composed of cinnamic acid derivatives. *Journal of Controlled Release* **2011,***149*, 182-189.
44. Yoon, H. Y.; Koo, H.; Choi, K. Y.; Kwon, I. C.; Choi, K.; Park, J. H.; Kim, K., Photo-crosslinked hyaluronic acid nanoparticles with improved stability for in vivo tumor-targeted drug delivery. *Biomaterials* **2013,***34*, 5273-5280.
45. Wang, A.; Gao, H.; Sun, Y.; Sun, Y.-l.; Yang, Y.-W.; Wu, G.; Wang, Y.; Fan, Y.; Ma, J., Temperature- and pH-responsive nanoparticles of biocompatible polyurethanes for doxorubicin delivery. *International Journal of Pharmaceutics* **2013,***441*, 30-39.
46. Rejinolda, N. S.; Chennazhia, K. P.; Naira, S. V.; Tamurab, H.; Jayakumar, R., Biodegradable and thermo-sensitive chitosan-g-poly(N-vinylcaprolactam) nanoparticles as a 5-fluorouracil carrier. *Carbohydrate Polymers* **2011,***83*, 776-786.
47. Viveka, R.; Babua, V. N.; Thangama, R.; Subramanianc, K. S.; Kannan, S., pH-responsive drug delivery of chitosan nanoparticles as Tamoxifen carriers for effective anti-tumor activity in breast cancer cells. *Colloids and Surfaces B: Biointerfaces* **2013,***111*, 117-123.
48. Hea, Q.; Gao, Y.; Zhang, L.; Zhang, Z.; Gao, F.; Ji, X.; Li, Y.; Shi, J., A pH-responsive mesoporous silica nanoparticles-based multi-drug delivery system for overcoming multi-drug resistance. *Biomaterials* **2011,***32*, 7711-7720.
49. Lorenzo, C. A.; Fernandez, B. B.; Puga, A. M.; Concheiro, A., Crosslinked ionic polysaccharides for stimuli-sensitive drug delivery. *Advanced Drug Delivery Reviews* **2013,***65*, 1148-1171.
50. Colea, M. A.; Voelcker, N. H.; Thissenc, H.; Griesser, H. J., Stimuli-responsive interfaces and systems for the control of protein–surface and cell–surface interactions. *Biomaterials* **2009,***30*, 1827-1850.
51. Li, X.; Tang, T.; Zhou, Y.; Zhang, Y.; Sun, Y., Applicability of enzyme-responsive mesoporous silica supports capped with 2 bridged silsesquioxane for colon-specific drug delivery. *Microporous and Mesoporous Materials* **2013,***184*, 83–89.
52. Rica, R. d. l.; Aili, D.; Stevens, M. M., Enzyme-responsive nanoparticles for drug release and diagnostics. *Advanced Drug Delivery Reviews* **2012,***64*, 967-978.

53. Juul, S.; Iacovelli, F.; Falconi, M.; Kragh, S. L.; Christensen, B.; Frøhlich, R.; Franch, O.; Kristoffersen, E. L.; Stougaard, M.; Leong, K.; Ho, Y.-P.; Sørensen, E. S.; Birkedal, V.; Desideri, A.; Knudsen, B. R., Temperature-Controlled Encapsulation and Release of an Active Enzyme in the Cavity of a Self-Assembled DNA Nanocage. *ACS Nano* **2013,***7* (11), 9724–9734.
54. Zhang, Y. W.; Tiwari, M. K.; Jeya, M.; Lee, J. K., Covalent immobilization of recombinant Rhizobium etli CFN42 xylitol dehydrogenase onto modified silica nanoparticles. *Appl Microbiol Biotechnol* **2011,***90* (2), 499-507.
55. Lee, S. J.; RameshwarTatavarty; Gu, M., Electrospun polystyrene–poly(styrene-co-maleicanhydride) nanofiber as a new aptasensor platform. *Biosensors and Bioelectronics* **2012,***38*, 302-307.
56. Xu, R.; Zhou, Q.; Li, F.; Zhang, B., Laccase immobilization on chitosan/poly(vinyl alcohol) composite nanofibrous membranes for 2,4-dichlorophenol removal. *Chemical Engineering Journal* **2013,***222*, 321-329.
57. Wu, L.; Yuan, X.; Sheng, J., Immobilization of cellulase in nanofibrous PVA membranes by electrospinning. *Journal of Membrane Science* **2005,***250*, 167-173.
58. Neri, D. F. M.; Balcão, V. M.; Dourado, F. O. Q.; Oliveira, J. M. B.; Jr, L. B. C.; Teixeira, J. A., Immobilized B-galactosidase onto magnetic particles coated with polyaniline: Support characterization and galactooligosaccharides production. *Journal of Molecular Catalysis B: Enzymatic* **2011,***70*, 74-80.
59. Lin, M.; Lu, D.; Zhu, J.; Yang, C.; Zhang, Y.; Liu, Z., Magnetic enzyme nanogel (MENG): a universal synthetic route for biocatalysts. *Chemical Communications* **2012,***48* (27), 3315.
60. Lam, E.; Male, K. B.; Chong, J. H.; Leung, A. C.; Luong, J. H., Applications of functionalized and nanoparticle-modified nanocrystalline cellulose. *Trends of Biotechnology* **2012,***30* (5), 283-90.
61. Yan, M.; Ge, J.; Liu, Z.; Ouyang, P., Encapsulation of single enzyme in nanogel withenhanced biocatalytic activity and stability. *Journal of American Chemical Society* **2006,***128*, 11008-11009.
62. Hong, J.; Xu, D.; Gong, P.; Yu, J.; Ma, H.; Yao, S., Covalent-bonded immobilization of enzyme on hydrophilic polymer covering magnetic nanogels. *Microporous and Mesoporous Materials* **2008,***109*, 470-477.
63. Liu, Y.; Du, J.; Yan, M.; Lau, M. Y.; Hu, J.; Han, H.; Yang, O. O.; Liang, S.; Wei, W.; HuiWang; Li, J.; Zhu, X.; Shi, L.; Chen, W.; Ji, C.; Lu, Y., Biomimetic enzyme nanocomplexes and their use as antidotes and preventive measures for alcohol intoxication. *Nanotechnology* **2013,***8*, 187-192.
64. Ge, J.; Yan, M.; Lu, D.; Liu, Z.; Liu, Z., Preparation and characterization of single-enzyme nanogels. *Methods on Molecular Biology* **2011,***743*, 119-130.
65. Guo, C.; Yunhui, M.; Pengfei, S.; Baishan, F., Direct binding glucoamylase onto carboxyl-functioned magnetic nanoparticles. *Biochemical Engineering Journal* **2012,***67*, 120-125.
66. Pan, C.; Hu, B.; Li, W.; Sun, Y.; Ye, H.; Zeng, X., Novel and efficient method for immobilization and stabilization of β-d-galactosidase by covalent attachment onto magnetic Fe3O4–chitosan nanoparticles. *Journal of Molecular Catalysis B: Enzymatic* **2009,***61* (3-4), 208-215.
67. Sakai, S.; Liu, Y.; Yamaguchi, T.; Watanabe, R.; Kawabe, M.; Kawakami, K., Immobilization of Pseudomonas cepacia lipase onto electrospun polyacrylonitrile fibers through physical adsorption and application to transesterification in nonaqueous solvent. *Biotechnol Lett* **2010,***32* (8), 1059-62.

68. Ashly, P. C.; Joseph, M. J.; Mohanan, P. V., Activity of diastase α-amylase immobilized on polyanilines (PANIs). *Food Chemistry* **2011,***127* (4), 1808-1813.
69. Ansari, S. A.; Husain, Q., Lactose hydrolysis from milk/whey in batch and continuous processes by concanavalin A-Celite 545 immobilized Aspergillus oryzae b-galactosidase. *food and bioproducts processing* **2012,***90*, 351-359.
70. Prlainovic, N. Ž.; Bezbradica, D. I.; Knežević-Jugović, Z. D.; Stevanović, S. I.; Avramov Ivić, M. L.; Uskoković, P. S.; Mijin, D. Ž., Adsorption of lipase from Candida rugosa on multi walled carbon nanotubes. *Journal of Industrial and Engineering Chemistry* **2013,***19* (1), 279-285.
71. Neri, D. F. M.; Balcao, V. M.; Costa, R. S.; Rocha, I. C. A. P.; Ferreira, E. M. F. C.; Torres, D. P. M.; Rodrigues, L. R. M.; Jr, L. B. C.; Teixeira, J. A., Galacto-oligosaccharides production during lactose hydrolysis by free Aspergillus oryzae b-galactosidase and immobilized on magnetic polysiloxane-polyvinyl alcohol. *Food Chemistry 128* **2009,***115*, 92-99.
72. Kuo, C.-H.; Liu, Y.-C.; Chang, C.-M. J.; Chen, J.-H.; Chang, C.; Shieh, C.-J., Optimum conditions for lipase immobilization on chitosan-coated Fe3O4 nanoparticles. *Carbohydrate Polymers* **2012,***87*, 2538– 2545.
73. Mahmoud, K. A.; Male, K. B.; Hrapovic, S.; Luong, J. H. T., Cellulose nanocrystal/gold nanoparticle composite as a matrix for enzyme immobilization. *ACS Applied Materials & Interfaces* **2009,***1* (7), 1383-1386.
74. Villalonga, R., Villalonga, M.L., & Gomez, L. , Preparation and functional properties of trypsin modified by carboxymethylcellulose. *Journal of Molecular Catalysis B: Enzymatic* **2000,***10*, 483-490.
75. Wang, Z. G.; Wan, L. S.; Liu, Z. M.; Huang, X. J.; Xu, Z. K., Enzyme immobilization on electrospun polymer nanofibers: An overview. *Journal of Molecular Catalysis B: Enzymatic* **2009,***56* (4), 189-195.
76. Li, S.-F.; Chen, J.-P.; Wu, W.-T., Electrospun polyacrylonitrile nanofibrous membranes for lipase immobilization. *Journal of Molecular Catalysis B: Enzymatic* **2007,***47* (3–4), 117-124.
77. Li, Y.; Quan, J.; Branford-White, C.; Williams, G. R.; Wu, J.-X.; Zhu, L.-M., Electrospun polyacrylonitrile-glycopolymer nanofibrous membranes for enzyme immobilization. *Journal of Molecular Catalysis B: Enzymatic* **2012,***76*, 15-22.
78. Stoilova, O.; Ignatova, M.; Manolova, N.; Godjevargova, T.; Mita, D. G.; Rashkov, I., Functionalized electrospun mats from styrene–maleic anhydride copolymers for immobilization of acetylcholinesterase. *European Polymer Journal* **2010,***46*, 1966-1974.
79. Hong, S.-G.; Kim, H. S.; Kim, J., Highly stabilized lipase in polyaniline nanofibers for surfactant-mediated esterification of ibuprofen. *Langmuir* **2014,***30* (3), 911-915.
80. Ji, X.; Wang, P.; Su, Z.; Ma, G.; Zhang, S., Enabling multi-enzyme biocatalysis using coaxial-electrospun hollow nanofibers: redesign of artificial cells. *Journal of Materials Chemistry B* **2014,***2* (2), 181.
81. Zhang, Y.-W.; Tiwari, M. K.; Jeya, M.; Lee, J.-K., Covalent immobilization of recombinant Rhizobium etli CFN42 xylitol dehydrogenase onto modified silica nanoparticles. *Applied Microbiology and Biotechnology* **2011,***90*, 499-507.
82. Takahashi, H.; Li, B.; Sasaki, T.; Miyazaki, C.; Kajino, T.; Inagaki, S., Catalytic activity in organic solvents and stability of immobilized enzymes depend on the pore size and surface characteristics of mesoporous silica. *Chemistry of Materials* **2000,***12*, 3301-3305.
83. Rekuc, A.; Bryjak, J.; Szymanska, K.; Jarzebski, A. B., Laccase immobilization on mesostructured cellular foams affords preparations with ultra high activity. *Process Biochemistry* **2009,***44*, 191-198.

84. Kim, H.; Kwon, H.-S.; Ahn, J.; Lee, C.-H.; Ahn, I.-S., Evaluation of a silica-coated magnetic nanoparticle for the immobilization of a His-tagged lipase. *Biocatalysis and Biotransformation* **2009,***27* (4), 246–253.
85. Gaffney, D.; Cooney, J.; Magner, E., Modification of mesoporous silicates for immobilization of enzymes. *Topics in Catalysis* **2012,***55* (16-18), 1101-1106.
86. Gaffney, D. A.; O'Neill, S.; O'Loughlin, M. C.; Hanefeld, U.; Cooney, J. C.; Magner, E., Tailored adsorption of His6-tagged protein onto nickel(II)–cyclam grafted mesoporous silica. *Chemical Communications* **2010,***46*, 1124-1126.
87. Yu, A.; Wang, Y.; Barlow, E.; Caruso, F., Mesoporous Silica Particles as Templates for Preparing Enzyme-Loaded Biocompatible Microcapsules. *Advanced Materials* **2005,***17* (14), 1737-1741.
88. Verma, M. L.; Naebe, M.; Barrow, C. J.; Puri, M., Enzyme immobilisation on amino-functionalised multi- walled carbon nanotubes: structural and biocatalytic characterisation. *Plos One* **2013,***8* (9), e73642-e73642.
89. Wang, X.; Liu, X.; Yan, X.; Zhao, P.; Ding, Y.; Xu, P., Enzyme-nanoporous gold biocomposite: Excellent biocatalyst with improved biocatalytic performance and stability. *Plos One* **2011,***6* (9), e24207-e24207.
90. Buthe, A.; Wu, S.; Wang, P., Nanoporous silica glass for the immobilization of interactive enzyme systems. *Methods in Molecular Biology* **2011,***679*, 37-48.
91. Yu, C. H.; Al-Saadi, A.; Shih, S. J.; Qiu, L.; Tam, K. Y.; Tsang, S. C. T., Immobilization of BSA on silica-coated magnetic iron oxide nanoparticle. *The Journal of Physical Chemistry C* **2009,***113*, 537-543.
92. Guo, L.; Zeng, S.; Li, J.; Cui, F.; Cui, X.; Bu, W.; Shi, J., An easy co-casting method to synthesize mesostructured carbon composites with high magnetic separability and acid resistance. *New Journal of Chemistry* **2009,***33* (9), 1926-1931.
93. Zhai, R.; Zhang, B.; Liu, L.; Xie, Y.; Zhang, H.; Liu, J., Immobilization of enzyme biocatalyst on natural halloysite nanotubes. *Catalysis Communications* **2010,***12* (4), 259-263.
94. Foresti, M. L.; Alimenti, G. A.; Ferreira, M. L., Interfacial activation and bioimprinting of Candida rugosa lipase immobilized on polypropylene: effect on the enzymatic activity in solvent-free ethyl oleate synthesis. *Enzyme and Microbial Technology* **2005,***36*, 338-349.
95. Azamian, B. R.; Davis, J. J.; Coleman, K. S.; Bagshaw, C. B.; Green, M. L. H., Bioelectrochemical single-walled carbon nanotubes. *Journal of the American Chemical Society* **2002,***124* (43), 12664-12665.
96. Pedrosa, V. A.; Paliwal, S.; Balasubramanian, S.; Nepal, D.; Davis, V.; Wild, J.; Ramanculov, E.; Simonian, A., Enhanced stability of enzyme organophosphate hydrolase interfaced on the carbon nanotubes. *Colloids and Surfaces B: Biointerfaces* **2010,***77* (1), 69-74.
97. Raghavendra, T.; Basak, A.; Manocha, L. M.; Shah, A. R.; Madamwar, D., Robust nanobioconjugates of Candida antarctica lipase B – Multiwalled carbon nanotubes: Characterization and application for multiple usages in non-aqueous biocatalysis. *Bioresource Technology* **2013,***140*, 103-110.
98. Ji, P.; Tan, H.; Xu, X.; Feng, W., Lipase covalently attached to multiwalled carbon nanotubes as an efficient catalyst in organic solvent. *AIChE Journal* **2010,***56* (11), 3005-3011.
99. Mechrez, G.; Krepker, M. A.; Harel, Y.; Lellouche, J.-P.; Segal, E., Biocatalytic carbon nanotube paper: a 'one-pot' route for fabrication of enzyme-immobilized membranes for organophosphate bioremediation. *Journal of Materials Chemistry B* **2014,***2* (7), 915-922.

100. Zhou, H.; Qu, Y.; Kong, C.; Li, D.; Shen, E.; Ma, Q.; Zhang, X.; Wang, J.; Zhou, J., Catalytic performance and molecular dynamic simulation of immobilized CC bond hydrolase based on carbon nanotube matrix. *Colloids and Surfaces B: Biointerfaces* **2014,***116*, 365-371.
101. Alonso-Lomillo, M. A.; Ruudiger, O.; Maroto-Valiente, A.; Velez, M.; Rodrıguez-Ramos, I.; Munoz, F. J.; Fernandez, V. M.; Lacey, A. L. D., Hydrogenase-coated carbon nanotubes for efficient H2 oxidation. *Nano Letters* **2007,***7* (6), 1603-1608.
102. Dinu, C. Z.; Zhu, G.; Bale, S. S.; Anand, G.; Reeder, P. J.; Sanford, K.; Whited, G.; Kane, R. S.; Dordick, J. S., Enzyme-based nanoscale composites for use as active decontamination surfaces. *Advanced Functional Materials* **2010,***20* (3), 392-398.
103. Wang, L.; Wei, L.; Chen, Y.; Jiang, R., Specific and reversible immobilization of NADH oxidase on functionalized carbon nanotubes. *Journal of Biotechnology* **2010,***150* (1), 57-63.
104. Wei, L.; Zhang, W.; Lu, H.; Yang, P., Immobilization of enzyme on detonation nanodiamond for highly efficient proteolysis. *Talanta* **2010,***80* (3), 1298-1304.
105. Zhao, F.; Li, H.; Jiang, Y.; Wang, X.; Mu, X., Co-immobilization of multi-enzyme on control-reduced graphene oxide by non-covalent bonds: an artificial biocatalytic system for the one-pot production of gluconic acid from starch. *Green Chemistry* **2014,** *16*, 2558-2565
106. Kouassi, G. K.; Irudayaraj, J.; McCarty, G., Examination of Cholesterol oxidase attachment to magnetic nanoparticles. *Journal of Nanobiotechnology* **2005,***3* (1), 1.
107. Li, D.; He, Q.; Cui, Y.; Duan, L.; Li, J., Immobilization of glucose oxidase onto gold nanoparticles with enhanced thermostability. *Biochemical and Biophysical Research Communications* **2007,***355* (2), 488-493.
108. Pandey, P.; Singh, S. P.; Arya, S. K.; Gupta, V.; Datta, M.; Singh, S.; Malhotra, B. D., Application of thiolated gold nanoparticles for the enhancement of glucose oxidase activity. *Langmuir* **2007,***23* (6), 3333-3337.
109. Yiu, H. H. P.; Keane, M. A., Enzyme–magnetic nanoparticle hybrids: new effective catalysts for the production of high value chemicals. *Journal of Chemical Technology & Biotechnology* **2012,***87*, 583-594.
110. Olariu, C. I.; Yiu, H. H. P.; Bouffier, L.; Nedjadi, T.; Eithne Costello; Williams, S. R.; Halloran, C. M.; Rosseinsky, M. J., Multifunctional Fe3O4 nanoparticles for targeted bi-modal imaging of pancreatic cancer. *Journal of Materials Chemistry* **2011,***21*, 12650–12659.
111. Xu, J.; Zeng, F.; Wu, S.; Liu, X.; Hou, C., Gold nanoparticles bound on microgel particles and their application as an enzyme support. *Nanotechnology* **2007,***18*, 265–273.
112. Crespilho, F. N.; Iost, R. M.; Travain, S. A.; Oliveira, O. N.; Zucolotto, V., Enzyme immobilization on Ag nanoparticles/polyaniline nanocomposites. *Biosensors and Bioelectronics* **2009,***24* (10), 3073-3077.
113. Chirra, H. D.; Sexton, T.; Biswal, D.; Hersh, L. B.; Hilt, J. Z., Catalase-coupled gold nanoparticles: Comparison between the carbodiimide and biotin–streptavidin methods. *Acta Biomaterialia* **2011,***7*, 2865–2872.
114. Zhang, Y.; Tang, Z.; Wang, J.; Wu, H.; Lin, C.-T.; Lin, Y., Apoferritin nanoparticle: a novel and biocompatible carrier for enzyme immobilization with enhanced activity and stability. *Journal of Materials Chemistry* **2011,***21*, 17468–17475.
115. Kacar, T.; Zin, M. T.; So, C.; Wilson, B.; Ma, H.; Gul-Karaguler, N.; Jen, A. K.-Y.; Sarikaya, M.; Tamerler, C., Directed self-immobilization of alkaline phosphatase on micro-patterned substrates via genetically fused metal-binding peptide. *Biotechnology and Bioengineering* **2009,***103* (4), 696–705.

116. Susumu, K.; Mei, B. C.; Mattoussi, H., Multifunctional ligands based on dihydrolipoic acid and polyethylene glycol to promote biocompatibility of quantum dots. *Nature Protocol* **2009,***4* (3), 424-436.
117. Chong, A. S. M.; Zhao, X. S., Design of large-pore mesoporous materials for immobilization of penicillin G acylase biocatalyst. *Catalysis Today* **2004,***93-95*, 293–299.
118. Johnson, B. J.; Russ Algar, W.; Malanoski, A. P.; Ancona, M. G.; Medintz, I. L., Understanding enzymatic acceleration at nanoparticle interfaces: Approaches and challenges. *Nano Today* **2014,** (0).
119. Palomo, J. M.; Muñoz, G.; Fernández-Lorente, G.; Mateo, C.; Fernández-Lafuente, R.; Guisán, J. M., Interfacial adsorption of lipases on very hydrophobic support (octadecyl–Sepabeads): immobilization, hyperactivation and stabilization of the open form of lipases. *Journal of Molecular Catalysis B: Enzymatic* **2002,***19-20*, 279-286.
120. Chen, Y. Z.; Yang, C. T.; Ching, C. B.; Xu, R., Immobilization of lipases on hydrophobilized zirconia nanoparticles: Highly enantioselective and reusable biocatalysts. *Langmuir* **2008,***24*, 8877-8884.
121. Wang, L. B.; Wang, Y. C.; He, R.; Zhuang, A.; Wang, X.; Zeng, J.; Hou, J. G., A new nanobiocatalytic system based on allosteric effect with dramatically enhanced enzymatic performance. *Journal of American Chemical Society* **2013,***135* (4), 1272-1275.
122. Xue, R.; Woodley, J. M., Process technology for multi-enzymatic reaction systems. *Bioresource Technology* **2012,***115*, 183-195.
123. Asuri, P.; Karajanagi, S. S.; Yang, H.; Yim, T.-J.; Kane, R. S.; Dordick, J. S., Increasing protein stability through control of the nanoscale environment. *Langmuir* **2006,***22*, 5833-5836.
124. Puri, M.; Barrow, C. J.; Verma, M. L., Enzyme immobilization on nanomaterials for biofuel production. *Trends in Biotechnology* **2013**, *31*(4):215-216.
125. Jordan, J.; Kumar, C. S. S. R.; Theegala, C., Preparation and characterization of cellulase-bound magnetite nanoparticles. *Journal of Molecular Catalysis B: Enzymatic* **2011,***68* (2), 139-146.
126. Kim, J.; Kim, B. C.; Lopez Ferrer, D.; Petritis, K.; Smith, R. D., Nanobiocatalysis for protein digestion in proteomic analysis. *Proteomics* **2010,***10* (4), 687-699.
127. Fernandez-Lafuente, R., Stabilization of multimeric enzymes: Strategies to prevent subunit dissociation. *Enzyme and Microbial Technology* **2009,***45*, 405-418.
128. Zaramella, D.; Scrimin, P.; Prins, L. J., Self-assembly of a catalytic multivalent peptide−nanoparticle complex. *American Chemical Society* **2012,***134*, 8396−8399.
129. Robenek, H., Colloidal gold: Principles, methods, and applications. In *Scanning*, Hayat, M. A., Ed. Wiley Periodicals, Inc: **1990**, pp 244-244.
130. You, C.-C.; Agasti, S. S.; Mrinmoy De, M. J. K.; Rotello, V. M., Modulation of the catalytic behavior of r-Chymotrypsin at monolayer-protected nanoparticle surfaces. *Journal of American Chemical Society* **2006,***128*, 14612-14618.
131. Garcia, J.; Zhang, Y.; Taylor, H.; Cespedes, O.; Webb, M. E.; Zhou, D., Multilayer enzyme-coupled magnetic nanoparticles as efficient, reusable biocatalysts and biosensors. *Nanoscale* **2011,***3* (9), 3721.
132. Dutta, N.; Mukhopadhyay, A.; Dasgupta, A. K.; Chakrabarti, K., Nanotechnology enabled enhancement of enzyme activity and thermostability: Study on impaired pectate lyase from attenuated macrophomina phaseolina in presence of hydroxyapatite nanoparticle. *PLOS ONE* **2013,***8* (5), e63567-e63567.
133. Fuertes, A.; Tartaj, P., Monodisperse carbon-polymer mesoporous spheres with magnetic functionality and adjustable pore-size distribution. *Small* **2007,***3* (275-279).

134. Keighron, J. D.; Keating, C. D., Enzyme:nanoparticle bioconjugates with two sequential enzymes: Stoichiometry and activity of malate dehydrogenase and citrate synthase on Au nanoparticles. *Langmuir* **2010,***26* (24), 18992-19000.
135. Wu, C.-S.; Wu, C.-T.; Yang, Y.-S.; Ko, F.-H., An enzymatic kinetics investigation into the significantly enhanced activity of functionalized gold nanoparticles. *Chemical Communications* **2008,** (42), 5327-5329.
136. Prakasham, R.; Devi, G. S.; Rao, C.; Sivakumar, V. S. S.; Sathish, T.; Sarma, P. N., Nickel-impregnated silica nanoparticle synthesis and their evaluation for biocatalyst immobilization. *Applied Biochemistry and Biotechnology* **2010,***160* (7), 1888-1895.
137. Ngo, T. P. N.; Zhang, W.; Wang, W.; Li, Z., Reversible clustering of magnetic nanobiocatalysts for high-performance biocatalysis and easy catalyst recycling. *Chemical Communications* **2012,***48* (38), 4585.
138. Cho, E. J.; Jung, S.; Kim, H. J.; Lee, Y. G.; Nam, K. C.; Lee, H. J.; Bae, H. J., Co-immobilization of three cellulases on Au-doped magnetic silica nanoparticles for the degradation of cellulose. *Chemical Communications Cambridge* **2012,***48* (6), 886-8.
139. Persano, L.; Camposeo, A.; Tekmen, C.; Pisignano, D., Industrial upscaling of electrospinning and applications of polymer nanofibers: A review. *Macromolecular Materials and Engineering* **2013,***298* (5), 504-520.
140. Konwarh, R.; Karak, N.; Misra, M., Electrospun cellulose acetate nanofibers: The present status and gamut of biotechnological applications. *Biotechnology Advances* **2013,***31*, 421-437.
141. Kim, J.; Grate, J. W.; Wang, P., Nanobiocatalysis and its potential applications. *Trends in Biotechnology* **2008,***26* (11), 639-646.
142. Joo, H.; Lee, J. H., Polyaniline nanofiber coated monolith reactor for enzymatic bioconversion. *Journal of Molecular Catalysis B: Enzymatic* **2010,***67*, 179-183.
143. Wang, X.; Liu, X.; Zhao, C.; Ding, Y.; Xu, P., Biodiesel production in packed-bed reactors using lipase-nanoparticle biocomposite. *Bioresource Technology* **2011,***102* (10), 6352-5.
144. Nair, S.; Kim, J.; Crawford, B.; Kim, S. H., Improving biocatalytic activity of enzyme-loaded nanofibers by dispersing entangled nanofiber structure. *Biomacromolecules* **2007,***8*, 1266-1270.
145. DiCosimo, R.; McAuliffe, J.; Poulose, A. J.; Bohlmann, G., Industrial use of immobilized enzymes. *Chemcial Society Review* **2013,***42* (15), 6437.
146. Khoshnevisan, K.; Bordbar, A. K.; Zare, D.; Davoodi, D.; Noruzi, M.; Barkhi, M.; Tabatabaei, M., Immobilization of cellulase enzyme on superparamagnetic nanoparticles and determination of its activity and stability. *Chemical Engineering Journal* **2011,***171* (2), 669-673.
147. Verma, M. L.; Chaudhary, R.; Tsuzuki, T.; Barrow, C. J.; Puri, M., Immobilization of beta-glucosidase on a magnetic nanoparticle improves thermostability: application in cellobiose hydrolysis. *Bioresource Technology* **2013,***135*, 2-6.
148. Uthumporn, U.; Zaidul, I. S. M.; Karim, A. A., Hydrolysis of granular starch at sub-gelatinization temperature using a mixture of amylolytic enzymes. *Food and Bioproducts Processing* **2010,***88* (1), 47-54.
149. Ernest, V.; Shiny, P. J.; Mukherjee, A.; Chandrasekaran, N., Silver nanoparticles: a potential nanocatalyst for the rapid degradation of starch hydrolysis by alpha-amylase. *Carbohydrate Research* **2012,***352*, 60-4.
150. Li, S.-F.; Fan, Y.-H.; Hu, J.-F.; Huang, Y.-S.; Wu, W.-T., Immobilization of Pseudomonas cepacia lipase onto the electrospun PAN nanofibrous membranes for transesterification reaction. *Journal of Molecular Catalysis B: Enzymatic* **2011,***73* (1-4), 98-103.

151. Liu, J.-F.; Liu, H.; Tan, B.; Chen, Y.-H.; Yang, R.-J., Reversible immobilization of K. fragilis β-galactosidase onto magnetic polyethylenimine-grafted nanospheres for synthesis of galacto-oligosaccharide. *Journal of Molecular Catalysis B: Enzymatic* **2012,***82*, 64-70.
152. Lee, S. M.; Jin, L. H.; Kim, J. H.; Han, S. O.; Na, H. B.; Hyeon, T.; Koo, Y. M.; Kim, J.; Lee, J. H., Beta-glucosidase coating on polymer nanofibers for improved cellulosic ethanol production. *Bioprocess and Biosystems Engineering* **2010,***33* (1), 141-7.
153. Liu, H.; Liu, J.; Tan, B.; Zhou, F.; Qin, Y.; Yang, R., Covalent immobilization of Kluyveromyces fragilis beta-galactosidase on magnetic nanosized epoxy support for synthesis of galacto-oligosaccharide. *Bioprocess and Biosystems Engineering* **2012,***35* (8), 1287-95.
154. Song, Y. S.; Shin, H. Y.; Lee, J. Y.; Park, C.; Kim, S. W., b-Galactosidase-immobilised microreactor fabricated using a novel technique for enzyme immobilization and its application for continuous synthesis of lactulose. *Food Chemistry* **2012,***133* (3), 611-617.
155. Rabe, M.; Verdes, D.; Seeger, S., Understanding protein adsorption phenomena at solid surfaces. *Advances in Colloid and Interface Science* **2011,***162* (1–2), 87-106.
156. Matthews, B. W., The structure of E. coli β-galactosidase. *C. R. Biologies* **2005,** *328* 549–556.
157. Juers, D. H.; Jacobson, R. H.; Wigley, D.; Zhang, X. J.; Huber, R. E.; Tronrud, D. E.; Matthews, B. W., High resolution refinement of beta-galactosidase in a new crystal form reveals multiple metal-binding sites and provides a structural basis for alpha-complementation. *Protein Science : A Publication of the Protein Society* **2000,***9* (9), 1685-1699.
158. Anand, G.; Sharma, S.; Dutta, A. K.; Kumar, S. K.; Belfort, G., Conformational Transitions of Adsorbed Proteins on Surfaces of Varying Polarity. *Langmuir* **2010,***26* (13), 10803-10811.
159. McColl, J.; Yakubov, G. E.; Ramsden, J. J., Complex Desorption of Mucin from Silica. *Langmuir* **2007,***23* (13), 7096-7100.
160. Andrade, J. D.; Hlady, V., Protein adsorption and materials biocompatibility: A tutorial review and suggested hypotheses. In *Biopolymers/Non-Exclusion HPLC*, Springer Berlin Heidelberg: **1986**; Chapter 1, pp 1-63.
161. Koutsoukos, P. G.; Norde, W.; Lyklema, J., Protein adsorption on hematite (α-Fe2O3) surfaces. *Journal of Colloid And Interface Science* **1983,***95* (2), 385-397.
162. Norde, W., Driving Forces For Protein Adsorption At Solid Surfaces *Macromol. Symp.* **1996,***103* (5-18).
163. Bahrami, A.; Hejazi, P., Electrostatic immobilization of pectinase on negatively charged AOT-Fe3O4 nanoparticles. *Journal of Molecular Catalysis B: Enzymatic* **2013,***93*, 1-7.
164. Gessner, A.; Lieske, A.; Paulke, B. R.; Müller, R. H., Influence of surface charge density on protein adsorption on polymeric nanoparticles: analysis by two-dimensional electrophoresis. *European Journal of Pharmaceutics and Biopharmaceutics* **2002,***54* (2), 165-170.
165. Misson, M.; Du, X.; Jin, B.; Zhang, H., Dendrimer-like nanoparticles based β-galactosidase assembly for enhancing its selectivity toward transgalactosylation. *Enzyme and Microbial Technology* **2016,***84*, 68-77.
166. Secundo, F., Conformational changes of enzymes upon immobilisation. *Chemical Society Reviews* **2013,***42* (15), 6250-6261.
167. Sethuraman, A.; Belfort, G., Protein Structural Perturbation and Aggregation on Homogeneous Surfaces. *Biophysical Journal* **2005,***88* (2), 1322-1333.

168. Santore, M. M.; Wertz, C. F., Protein Spreading Kinetics at Liquid−Solid Interfaces via an Adsorption Probe Method†. *Langmuir* **2005,***21* (22), 10172-10178.
169. Giacomelli, C. E.; Norde, W., The Adsorption–Desorption Cycle. Reversibility of the BSA–Silica System. *Journal of Colloid and Interface Science* **2001,***233* (2), 234-240.
170. Bolivar, J. M.; Eisl, I.; Nidetzky, B., Advanced characterization of immobilized enzymes as heterogeneous biocatalysts. *Catalysis Today* **2016,***259, Part 1*, 66-80.
171. Mahmoudifard, M.; Soudi, S.; Soleimani, M.; Hosseinzadeh, S.; Esmaeili, E.; Vossoughi, M., Efficient protein immobilization on polyethersolfone electrospun nanofibrous membrane via covalent binding for biosensing applications. *Materials Science and Engineering: C* **2016,***58*, 586-594.
172. Pinto, S. C.; Rodrigues, A. R.; Saraiva, J. A.; Lopes-da-Silva, J. A., Catalytic activity of trypsin entrapped in electrospun poly(ϵ-caprolactone) nanofibers. *Enzyme and Microbial Technology* **2015,***79–80*, 8-18.
173. Gupta, A.; Dhakate, S. R.; Pahwa, M.; Sinha, S.; Chand, S.; Mathur, R. B., Geranyl acetate synthesis catalyzed by Thermomyces lanuginosus lipase immobilized on electrospun polyacrylonitrile nanofiber membrane. *Process Biochemistry* **2013,***48* (1), 124-132.
174. Ishikawa-Ankerhold, H. C.; Ankerhold, R.; Drummen, G. P. C., Advanced Fluorescence Microscopy Techniques—FRAP, FLIP, FLAP, FRET and FLIM. *Molecules* **2012,***17* (4), 4047-4132.
175. Itoh, T.; Ishii, R.; Matsuura, S.-i.; Hamakawa, S.; Hanaoka, T.; Tsunoda, T.; Mizuguchi, J.; Mizukami, F., Catalase encapsulated in mesoporous silica and its performance. *Biochemical Engineering Journal* **2009,***44* (2–3), 167-173.
176. Suh, C. W.; Kim, M. Y.; Choo, J. B.; Kim, J. K.; Kim, H. K.; Lee, E. K., Analysis of protein adsorption characteristics to nano-pore silica particles by using confocal laser scanning microscopy. *Journal of Biotechnology* **2004,***112* (3), 267-277.
177. Guo, J.; Sachs, F.; Meng, F., Fluorescence-Based Force/Tension Sensors: A Novel Tool to Visualize Mechanical Forces in Structural Proteins in Live Cells. *Antioxidants & Redox Signaling* **2013,***20* (6), 986-999.
178. Wilson, P. M.; LaBonte, M. J.; Russell, J.; Louie, S.; Ghobrial, A. A.; Ladner, R. D., A novel fluorescence-based assay for the rapid detection and quantification of cellular deoxyribonucleoside triphosphates. *Nucleic Acids Research* **2011,***39* (17), e112.
179. Matsuura, S.-i.; Ishii, R.; Itoh, T.; Hanaoka, T.; Hamakawa, S.; Tsunoda, T.; Mizukami, F., Direct visualization of hetero-enzyme co-encapsulated in mesoporous silicas. *Microporous and Mesoporous Materials* **2010,***127* (1–2), 61-66.
180. Carlsson, N.; Gustafsson, H.; Thörn, C.; Olsson, L.; Holmberg, K.; Åkerman, B., Enzymes immobilized in mesoporous silica: A physical–chemical perspective. *Advances in Colloid and Interface Science* **2014,***205*, 339-360.
181. Moelans, D.; Cool, P.; Baeyens, J.; Vansant, E. F., Using mesoporous silica materials to immobilise biocatalysis-enzymes. *Catalysis Communications* **2005,***6* (4), 307-311.
182. Collins, S. E.; Lassalle, V.; Ferreira, M. L., FTIR-ATR characterization of free Rhizomucor meihei lipase (RML), Lipozyme RM IM and chitosan-immobilized RML. *Journal of Molecular Catalysis B: Enzymatic* **2011,***72* (3–4), 220-228.
183. Urabe, Y.; Shiomi, T.; Itoh, T.; Kawai, A.; Tsunoda, T.; Mizukami, F.; Sakaguchi, K., Encapsulation of Hemoglobin in Mesoporous Silica (FSM)—Enhanced Thermal Stability and Resistance to Denaturants. *ChemBioChem* **2007,***8* (6), 668-674.
184. Singh, K.; Srivastava, G.; Talat, M.; Srivastava, O. N.; Kayastha, A. M., α-Amylase immobilization onto functionalized graphene nanosheets as scaffolds: Its

characterization, kinetics and potential applications in starch based industries. *Biochemistry and Biophysics Reports* **2015,***3*, 18-25.
185. Verma, M. L.; Barrow, C. J.; Kennedy, J. F.; Puri, M., Immobilization of beta-d-galactosidase from Kluyveromyces lactis on functionalized silicon dioxide nanoparticles: characterization and lactose hydrolysis. *International journal of biological macromolecules* **2012,***50* (2), 432-7.
186. Delfino, I.; Portaccio, M.; Ventura, B. D.; Mita, D. G.; Lepore, M., Enzyme distribution and secondary structure of sol–gel immobilized glucose oxidase by micro-attenuated total reflection FT-IR spectroscopy. *Materials Science and Engineering: C* **2013,***33* (1), 304-310.
187. Liu, Y.; Ogorzalek, T. L.; Yang, P.; Schroeder, M. M.; Marsh, E. N. G.; Chen, Z., Molecular Orientation of Enzymes Attached to Surfaces through Defined Chemical Linkages at the Solid–Liquid Interface. *Journal of the American Chemical Society* **2013,***135* (34), 12660-12669.
188. Bolivar, J. M.; Eisl, I.; Nidetzk, B., Advanced characterization of immobilized enzymes as heterogeneous biocatalysts. *Catalysis Today* **2015,***259*, 66–80.
189. Xiao, Y.; Stone, T.; Bell, D.; Gillespie, C.; Portoles, M., Confocal Raman Microscopy of Protein Adsorbed in Chromatographic Particles. *Analytical Chemistry* **2012,***84*, 7367-7373.
190. Xiao, Y.; Stone, T.; Moya, W.; Killian, P.; Herget, T., Confocal Raman Characterization of Different Protein Desorption Behaviors from Chromatographic Particles. *Analytical Chemistry* **2014,***86* (2), 1007-1015.
191. Mazur, M.; Krysiński, P.; Michota-Kamińska, A.; Bukowska, J.; Rogalski, J.; Blanchard, G. J., Immobilization of laccase on gold, silver and indium tin oxide by zirconium-phosphonate-carboxylate (ZPC) coordination chemistry. *Bioelectrochemistry* **2007,***71* (1), 15-22.
192. Biegunski, A. T.; Michota, A.; Bukowska, J.; Jackowska, K., Immobilization of tyrosinase on poly(indole-5-carboxylic acid) evidenced by electrochemical and spectroscopic methods. *Bioelectrochemistry* **2006,***69* (1), 41-48.
193. Nitahara, S.; Maeki, M.; Yamaguchi, H.; Yamashita, K.; Miyazaki, M.; Maeda, H., Three-dimensional Raman spectroscopic imaging of protein crystals deposited on a nanodroplet. *The Analyst* **2012,***137* (24), 5730-5735.
194. Shen, L.; Ulrich, N. W.; Mello, C. M.; Chen, Z., Determination of conformation and orientation of immobilized peptides and proteins at buried interfaces. *Chemical Physics Letters* **2015,***619*, 247-255.
195. Schartner, J.; Gavriljuk, K.; Nabers, A.; Weide, P.; Muhler, M.; Gerwert, K.; Kötting, C., Immobilization of Proteins in their Physiological Active State at Functionalized Thiol Monolayers on ATR-Germanium Crystals. *ChemBioChem* **2014,***15* (17), 2529-2534.
196. Kao, K.-C.; Lin, T.-S.; Mou, C.-Y., Enhanced Activity and Stability of Lysozyme by Immobilization in the Matching Nanochannels of Mesoporous Silica Nanoparticles. *The Journal of Physical Chemistry C* **2014,***118* (13), 6734-6743.
197. Ganesan, A.; Moore, B. D.; Kelly, S. M.; Price, N. C.; Rolinski, O. J.; Birch, D. J. S.; Dunkin, I. R.; Halling, P. J., Optical Spectroscopic Methods for Probing the Conformational Stability of Immobilised Enzymes. *ChemPhysChem* **2009,***10* (9-10), 1492-1499.
198. Verma, M. L.; Naebe, M.; Barrow, C. J.; Puri, M., Enzyme Immobilisation on Amino-Functionalised Multi-Walled Carbon Nanotubes: Structural and Biocatalytic Characterisation. *PLoS ONE* **2013,***8* (9), e73642.

199. Petkova, G. A.; Záruba, K.; Král, V., Synthesis of silica particles and their application as supports for alcohol dehydrogenases and cofactor immobilizations: Conformational changes that lead to switch in enzyme stereoselectivity. *Biochimica et Biophysica Acta (BBA) - Proteins and Proteomics* **2012,***1824* (6), 792-801.
200. Illanes, A., Whey upgrading by enzyme biocatalysis. *Electronic Journal of Biotechnology*. **2011,** *14*(6), 1-28.
201. Das, B.; Sarkar, S.; Sarkar, A.; Bhattacharjee, S.; Bhattacharjee, C., Recovery of whey proteins and lactose from dairy waste: A step towards green waste management. *Process Safety and Environmental Protection* **2015**. In Press, corrected proof. doi:10.1016/j.psep.2015.05.006.
202. Watanabe, T.; Shinozaki, Y.; Suzuki, K.; Koitabashi, M.; Yoshida, S.; Sameshima-Yamashita, Y.; Kuze Kitamoto, H., Production of a biodegradable plastic-degrading enzyme from cheese whey by the phyllosphere yeast Pseudozyma antarctica GB-4(1)W. *Journal of Bioscience and Bioengineering* **2014,***118* (2), 183-187.
203. Gosling, A.; Stevens, G. W.; Barber, A. R.; Kentish, S. E.; Gras, S. L., Recent advances refining galactooligosaccharide production from lactose. *Food Chemistry 121* **2010,***121*, 307-318.
204. Ganzle, M. G., Enzymatic synthesis of galacto-oligosaccharides and other lactose derivatives (hetero-oligosaccharides) from lactose. *International Dairy Journal 22 (2012)* **2012,***22*, 116-122.
205. Warmerdam, A.; Zisopoulos, F. K.; Boom, R. M.; Janssen, A. E. M., Kinetic characterization of galacto-oligosaccharide (GOS) synthesis by three commercially important β-galactosidases. *Biotechnology Progress* **2014,***30* (1), 38-47.
206. Prazeres, A. R.; Carvalho, F.; Rivas, J., Cheese whey management: a review. *Journal of Environmental Management* **2012,***110*, 48-68.
207. Grba, S.; Stehlik-Tomas, V.; Stanzer, D.; Vahčić, N.; Škrlin, A., Selection of yeast strain Kluyveromyces marxianus for alcohol and biomass production on whey. *Chemical and Biochemical Engineering Quarterly* **2002,***16* (1), 13-16.
208. Pavlostathis, S. G., Giraldo-Gomez, E., Kinetics of anaerobic treatment. *Water Sci. Technol.* **1991,***24* (8), 35-59.
209. Mišún, D.; Čurda, L.; Jelen, P., Batch and continuous hydrolysis of ovine whey proteins. *Small Ruminant Research* **2008,***79* (1), 51-56.
210. Shi, L.; Zhao, Y.; Zhang, X.; Su, H.; Tan, T., Antibacterial and anti-mildew behavior of chitosan/nano-TiO2 composite emulsion. *Korean J. Chem. Eng.* **2008,***25* (6), 1434-1438.
211. Su, H.; Wang, Z.; Tan, T., Preparation of a surface molecular-imprinted adsorbent for Ni2+ based on Penicillium chrysogenum. *Journal of Chemical Technology & Biotechnology* **2005,***80* (4), 439-444.
212. Minhalma, M.; Magueijo, V.; Queiroz, D. P.; de Pinho, M. N., Optimization of "Serpa" cheese whey nanofiltration for effluent minimization and by-products recovery. *Journal of Environmental Management* **2007,***82* (2), 200-206.
213. Dragone, G.; Mussatto, S. I.; Oliveira, J. M.; Teixeira, J. A., Characterisation of volatile compounds in an alcoholic beverage produced by whey fermentation. *Food Chemistry* **2009,***112* (4), 929-935.
214. Gaur, R.; Pant, H.; Jain, R.; Khare, S. K., Galacto-oligosaccharide synthesis by immobilized Aspergillus oryzae b-galactosidase. *Food Chemistry* **2006,***97*, 426-430.
215. Lu, L.; Xu, S.; Zhao, R.; Zhang, D.; Li, Z.; Li, Y.; Xiao, M., Synthesis of galactooligosaccharides by CBD fusion beta-galactosidase immobilized on cellulose. *Bioresource Technology* **2012,***116*, 327-33.

216. Neri, D. F. M.; Balcao, V. M.; Cardoso, S. M.; Silva, A. M. S.; Domingues, M. d. R. M.; Torres, D. P. M.; Rodrigues, L. R. M.; Jr., L. B. C.; Teixeira, J. A. C., Characterization of galactooligosaccharides produced by b-galactosidase immobilized onto magnetized Dacron. *International Dairy Journal* **2011,***21*, 172-178.
217. Palai, T.; Mitra, S.; Bhattacharya, P. K., Kinetics and design relation for enzymatic conversion of lactose into galacto-oligosaccharides using commercial grade beta-galactosidase. *Journal of Boscience and Bioengineering* **2012,***114* (4), 418-23.
218. Albayrak, N.; Yang, S. T., Production of galacto-oligosaccharides from lactose by aspergillus oryzae B-galactosidase Immobilized on on cotton cloth. *Biotechnology and Bioengineering* **2002,***77* (1), 8-19.
219. Mattia, A.; Merker, R., Regulation of Probiotic Substances as Ingredients in Foods: Premarket Approval or "Generally Recognized as Safe" Notification. *CID* **2008,***46* (2), S115-S118.
220. Rodriguez-Colinas, B.; Poveda, A.; Jimenez-Barbero, J.; Ballesteros, A. O.; Plou, F. J., Galacto-oligosaccharide Synthesis from Lactose Solution or Skim Milk Using the β-Galactosidase from Bacillus circulans. *Journal of Agricultural and Food Chemistry* **2012,***60* (25), 6391-6398.
221. Jovanovic-Malinovska, R.; Fernandes, P.; Winkelhausen, E.; Fonseca, L., Galacto-oligosaccharides Synthesis from Lactose and Whey by beta-Galactosidase Immobilized in PVA. *Applied Biochemistry and Biotechnology* **2012,***168* (5), 1197-211.
222. Huerta, L. M.; Vera, C.; Guerrero, C.; Wilson, L.; Illanes, A., Synthesis of galacto-oligosaccharides at very high lactose concentrations with immobilized -galactosidases from Aspergillus oryzae. *Process Biochem* **2011,***46*, 245-252.
223. Misson, M.; Dai, S.; Jin, B.; Chen, B. H.; Zhang, H., Manipulation of nanofiber-based β-galactosidase nanoenvironment for enhancement of galacto-oligosaccharide production. *Journal of Biotechnology* **2016,***222*, 56-64.
224. Guidini, C. Z.; Fischer, J.; Resende, M. M. d.; Cardoso, V. L.; Ribeiro, E. J., B-Galactosidase of Aspergillus oryzae immobilized in an ion exchange resin combining the ionic-binding and crosslinking methods: Kinetics and stability during the hydrolysis of lactose. *Journal of Molecular Catalysis B: Enzymatic* **2011,***71*, 139-145.
225. Gurdas, S.; Gulec, H. A.; Mutlu, M. M., Immobilization of Aspergillus oryzae β-Galactosidase onto Duolite A568 Resin via Simple Adsorption Mechanism. *Food Bioprocess Technol* **2012,***5*, 904-911.
226. Rodriguez-Colinas, B.; Abreu, M. A. d.; Fernandez-Arrojo, L.; Beer, R. d.; Poveda, A.; Jimenez-Barberos, J.; Haltrich, D.; Olmo, X. A. O. B.; Fernandez-Lobato, M.; Plou, F. J., Production of Galacto-oligosaccharides by the β-Galactosidase from Kluyveromyces lactis: Comparative Analysis of Permeabilized Cells versus Soluble Enzyme. *J. Agric. Food Chem.* **2011,***59*, 10477-10484.
227. Gosling, A.; Alftrén, J.; Stevens, G. W.; Barber, A. R.; Kentish, S. E.; Gras, S. L., Facile Pretreatment of Bacillus circulans β-Galactosidase Increases the Yield of Galactosyl Oligosaccharides in Milk and Lactose Reaction Systems. *Journal of Agricultural and Food Chemistry* **2009,***57* (24), 11570-11574.
228. Vera, C.; Guerrero, C.; Conejeros, R.; Illanes, A., Synthesis of galacto-oligosaccharides by beta-galactosidase from Aspergillus oryzae using partially dissolved and supersaturated solution of lactose. *Enzyme and Microbial Technology* **2012,***50* (3), 188-94.
229. Nath, A.; Bhattacharjee, C.; Chowdhury, R., Synthesis and separation of galacto-oligosaccharides using membrane bioreactor. *Desalination* **2013,***316*, 31-41.
230. Benjamins, E.; Boxem, L.; KleinJan-Noeverman, J.; Broekhuis, T. A., Assessment of repetitive batch-wise synthesis of galacto-oligosaccharides from lactose slurry using

immobilised β-galactosidase from Bacillus circulans. *International Dairy Journal* **2014,***38* (2), 160-168.
231. Sen, P.; Nath, A.; Bhattacharjee, C.; Chowdhury, R.; Bhattacharya, P., Process engineering studies of free and micro-encapsulated β-galactosidase in batch and packed bed bioreactors for production of galactooligosaccharides. *Biochemical Engineering Journal* **2014,***90*, 59-72.
232. Palai, T.; Singh, A. K.; Bhattacharya, P. K., Enzyme, β-galactosidase immobilized on membrane surface for galacto-oligosaccharides formation from lactose: Kinetic study with feed flow under recirculation loop. *Biochemical Engineering Journal* **2014,***88*, 68-76.
233. Shen, Q.; Yang, R.; Hua, X.; Ye, F.; Wang, H.; Zhao, W.; Wang, K., Enzymatic synthesis and identification of oligosaccharides obtained by transgalactosylation of lactose in the presence of fructose using beta-galactosidase from Kluyveromyces lactis. *Food Chemistry* **2012,***135* (3), 1547-54.
234. Gulec, H. A., ImmobılıZatıon of -galactosidase from Kluyveromyces Lactis onto polymeric membrane surfaces: Effect of surface characteristics. *Colloids and Surfaces B: Biointerfaces*. **2013,***104*, 83-90.

CHAPTER 3

Dendrimer-Like Nanoparticles Based β-Galactosidase Assembly for Enhancing Its Selectivity towards Transgalactosylation

Chapter 3: Dendrimer-Like Nanoparticles Based β-Galactosidase Assembly for Enhancing Its Selectivity towards Transgalactosylation

Mailin Misson[1,2], Xin Du[3], Bo Jin[1], Hu Zhang[1*]

[1]School of Chemical Engineering, The University of Adelaide, Adelaide, SA 5000, Australia

[2]Biotechnology Research Institute, Universiti Malaysia Sabah, Jalan UMS, 88400, Kota Kinabalu, Sabah, Malaysia

[3]Research Center for Bioengineering and Sensing Technology, University of Science & Technology Beijing, Beijing 100083, P. R. China

*Corresponding author:

Email: hu.zhang@adelaide.edu.au

Tel: +61 8 831 33810

Published in:

Enzyme and Microbial Technology 2016; 84:68-77

DOI:10.1016/j.enzmictec.2015.12.008

Statement of Authorship

Title of Paper	Dendrimer-like Nanoparticles Based β-galactosidase Assembly for Enhancing Its Selectivity towards Transgalactosylation
Publication Status	☑ Published ☐ Accepted for Publication ☐ Submitted for Publication ☐ Unpublished and Unsubmitted work written in manuscript style
Publication Details	Mailin Misson, Xin Du, Bo Jin, Hu Zhang Enzyme and Microbial Technology 2016;84: 68-77 DOI:10.1016/j.enzmictec.2015.12.008

Principal Author

Name of Principal Author (Candidate)	Mailin Misson		
Contribution to the Paper	Designed and performed experiments, interpreted data and wrote the manuscript.		
Overall percentage (%)	70 %		
Certification:	This paper reports on original research I conducted during the period of my Higher Degree by Research candidature and is not subject to any obligations or contractual agreements with a third party that would constrain its inclusion in this thesis. I am the primary author of this paper.		
Signature		Date	06.02.2016

Co-Author Contributions

By signing the Statement of Authorship, each author certifies that:

i. the candidate's stated contribution to the publication is accurate (as detailed above);

ii. permission is granted for the candidate in include the publication in the thesis; and

iii. the sum of all co-author contributions is equal to 100% less the candidate's stated contribution.

Name of Co-Author	Xin Du		
Contribution to the Paper	Performed some experiments and manuscript evaluation.		
Signature		Date	06.02.2016

Name of Co-Author	Bo Jin		
Contribution to the Paper	Supervised development of work and manuscript evaluation.		
Signature		Date	19/02/2016

Name of Co-Author	Hu Zhang		
Contribution to the Paper	Supervised development of work, data interpretation, manuscript evaluation and acted as corresponding author.		
Signature		Date	18/02/2016

Please cut and paste additional co-author panels here as required

Abstract

Functional nanomaterials have been pursued to assemble nanobiocatalysts since they can provide unique hierarchical nanostructures and localized nanoenvironments for enhancing enzyme specificity, stability and selectivity. Functionalized dendrimer-like hierarchically porous silica nanoparticles (HPSNs) was fabricated for assembling β-galactosidase nanobiocatalysts for bioconversion of lactose to galacto-oligosaccharides (GOS). The nanocarrier was functionalized with amino (NH_2) and carboxyl (COOH) groups to facilitate enzyme binding, benchmarking with non-functionalized HPSNs. Successful conjugation of the functional groups was confirmed by FTIR, TGA and zeta potential analysis. HPSNs-NH_2 showed 1.8-fold and 1.1-fold higher β-galactosidase adsorption than HPSNs-COOH and HPSNs carriers, respectively, with the highest enzyme adsorption capacity of 328 mg/g nanocarrier at an initial enzyme concentration of 8 mg/ml. The HPSNs-NH_2 and β-galactosidase assembly (HPSNs-NH_2-Gal) demonstrated to maintain the highest activity at all tested enzyme concentrations and exhibited activity up to 10 continuous cycles. Importantly, HPSNs-NH_2-Galwas simply recycled through centrifugation, overcoming the challenging problems of separating the nanocarrier from the reaction medium. HPSNs-NH_2-Gal had distinguished catalytic reaction profiles by favoring transgalactosylation, enhancing GOS production of up to 122 g/l in comparison with 56 g/l by free β-galactosidase. Furthermore, it generated up to 46 g/l GOS at a lower initial lactose concentration while the free counterpart had negligible GOS production as hydrolysis was overwhelmingly dominant in the reaction system. Our research findings show the amino-functionalized HPSNs can selectively promote the enzyme activity of β-galactosidase for transgalactosylation, which is beneficial for GOS production.

Keywords: nanobiocatalysis, β-galactosidase, dendrimer-like hierarchical pores silica nanoparticles, galacto-oligosaccharides

3.1 Introduction

The specificity and selectivity of enzyme open a new door for development of green and sustainable enzyme-catalyzed bioprocesses. Enzymatic reactions are environmentally friendly due to low chemical consumption without release of toxic by-products. Nevertheless, the biocatalysts constitute the majority of the operational cost when they are applied in large scale processes, and their low stability and reusabilityin reactor conditions impede their industrial applications [1]. The immobilization of enzyme on support materials is of immense scientific interest. Such technology is able to shelter and/or stabilize enzymes when they are exposed to chemical and environmental harsh conditions. The immobilization also allows the recovery and reuse of these biocatalysts, hence reducing the cost of the biocatalytic process [2-3]. Enzymes have been immobilized onto natural/synthetic polymers or inorganic materials [4]. Despite the fact that optimal immobilization protocols have been extensively studied, retaining the enzyme activity upon immobilization entails persistent investigation. Enzyme activity reduction on support materials remains a significant challenge due to the conformation change upon immobilization [5]. Hence, the development of appropriate enzyme carriers, which can preserve or enhance the enzyme catalytic function, presents a profound research interest.

Nanobiocatalysis, an emerging technology that assembles enzyme molecules onto nanomaterial carriers, synergistically integrates advanced nanotechnology with biotechnology [6]. The technology can increase the enzyme stability and enhance enzyme activity. To date, the enzyme has been immobilized on diverse support materials such as nanofibres [7], nanotubes [8], nanocomposites [9], nanogel [10] and nanoparticles [11]. Silica nanoparticles offer uniform nanopores and tuneable periodic nanostructures which harmonise the diffusion of guest biomolecules with different sizes [12]. It has been recognized that the pore size is vital for enzyme immobilization. Enzyme molecules are incapable to enter into the pore of nanoparticles when the pore is smaller than the molecular size of the enzyme, resulting in a low enzyme loading. In contrast, nanoparticles with pore sizes larger than the enzyme molecular size may reduce the enzyme activity, which may be ascribed to the enzyme leaching or reduction in the enzyme stability[13-14]. Anchoring of biomolecules onto the nanoparticles surface may result in a strong binding that may decrease the biological activity of the enzyme [15]. In addition, chemical reagents in the immobilization protocol such as crosslinking agents (i.e. glutaraldehyde and

epichlorohydrin) lead to a certain level of enzyme activity reduction [16]. Furthermore, enzyme molecules embedded inside the traditional enzyme supports could not directly contact substrates, thus the enzyme supports are unable to maximize the usage of the enzyme, and therefore some of the expensive enzyme is wasted. It is, therefore, constant efforts are being made into exploring robust and functional enzyme carriers.

Dendrimer-like silica nanoparticles with hierarchical pores (HPSNs) were recently developed with unique properties [17]. The carriers have been demonstrated as advanced delivery nanocarriers for siRNA and DNA molecules. The materials were constructed with specific pore structures to increase the surface area for a high loading of biological molecules. Each cavity in the nanostructure can act as a nanobioreactor for enzymatic reaction after the cavity is immobilized with the enzyme. Importantly, the nanocarrier possesses centre-radial open pores that are vital in coordinating diffusion of molecules with different sizes such as substrates and products, and as a result, it enhances the biomolecule interactions as well as reduces the associated mass transfer limitation. Another major issue associated with nanobiocatalysis is to recover nanobiocatalysts from the aqueous solution and reuse them due to their nano-meter size. Magnetic nanoparticles are often employed to realize the recovery by placing them in a magnetic field [18]. For instance, the immobilization of lipase was realized on magnetic chitosan microspheres [19] and Fe_3O_4/poly (styrene-methacrylic acid) magnetic microsphere [20] for enzymatic production of biodiesel from soybean oil. Such an operation poses a significant challenge for scaling up. HPSNs, however, offer easy separation and recovery through sedimentation or centrifugation, which can simplify the recycle process for HPSNs-based nanobiocatalysts.

In the present work, HPSNs were synthesized as nanocarriers to host β-galactosidase. The nanocarriers were functionalized with amino (NH_2) and carboxyl group (COOH) to promote covalent binding with the enzyme. Non-specific binding of the enzyme is expected to occur on the surface of non-functionalized HPSNs. The schematic representation of HPSNs functionalization and enzyme binding is illustrated in Scheme 3.1. The adsorption performance of three types of HPSNs was evaluated through bovine serum albumin (BSA) and β-galactosidase at different protein concentrations. The β-galactosidase activity was compared for the three HPSNs. HPSNs-NH_2 was then chosen to immobilize β-galactosidase for assessing its recyclability up to 10 continuous runs and its performance in converting lactose into galacto-oligosaccharides (GOS).

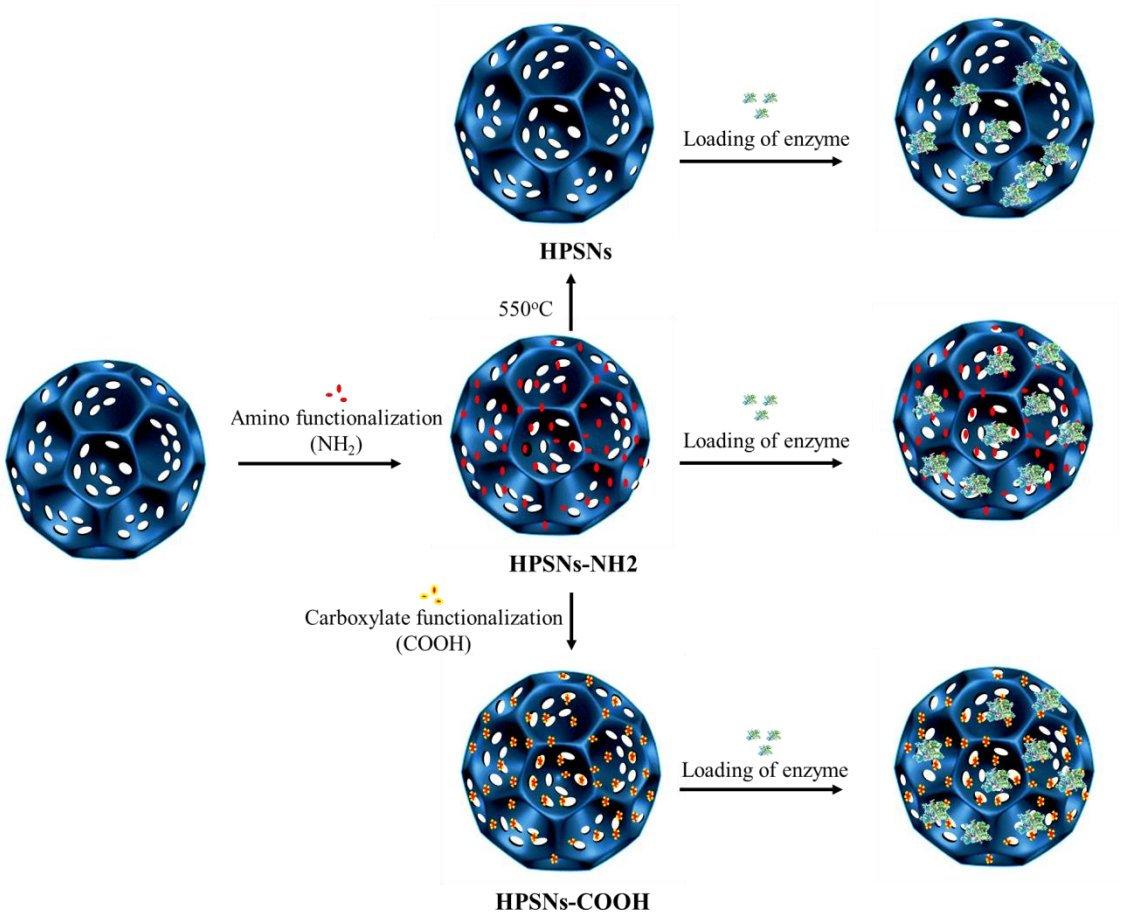

Scheme 3.1 Schematic description on the functionalization of dendrimer-like HPSNs for the loading of β-galactosidase.

3.2 Materials and Methods

3.2.1 Chemicals

Cetyl trimethylammonium bromide (CTAB), ammonia, ethyl ether, ethanol, tetraethoxysilane (TEOS), 3-aminopropyltriethoxysilane (APES), hydrochloric acid (HCl), *N*,*N*-dimethylformamide (DMF), succinic anhydride, triethylamine (TEA), ammonium hydroxide, sodium carbonate and phosphoric acid were of analytical grade without further purification. Bovine serum albumin (BSA), *Kluyveromyces lactis* β-galactosidase, o-nitrophenyl-β-D-glactopyranoside (ONPG) and coomassie brilliant blue G-250 were obtained from Sigma-Aldrich. Potassium phosphate buffer (PBS) (pH 7.2) was procured from Gibson.

3.2.2 Preparation and Functionalization of Nanoparticles

The preparation and functionalization of HPSNs-NH_2 were conducted using the methods developed by Du *et al.*[17]. A total of 0.5 g of CTAB was dissolved in an emulsion system composed of 70 ml of H_2O, 0.8 ml of aqueous ammonia, 15 ml of ethyl ether and 5 ml of ethanol. The mixture was vigorously stirred at 1000 rpm for 0.5 h at room temperature. The stirring was continued for 4 h after addition of a mixture of TEOS (2.5 ml) and APES (0.1 ml). After 4 h, 1 ml of HCl (37 %) was added in order to stop the base-catalyzed reaction. A white precipitate of amino-functionalized silica nanoparticles (HPSNs-NH_2) was obtained from 12 min centrifugation at 4200 rpm. The precipitate was washed with ethanol and water. Treatment with ethanoic HCl (15 ml of concentrated HCl in 120 ml ethanol) was conducted under stirring at 70 ^oC for 24 h to extract CTAB template. The extracted particles, obtained from centrifugation at 4200 rpm for 12 min, were washed with water for three times. HPSNs with the carboxyl group (HPSNs-COOH) was synthesized by reacting HPSNs-NH_2 (50 mg in 20 ml DMF) with succinic anhydride (0.45 g in 5 ml DMF) in the presence of TEA (0.45 ml) for 5 h. Non-functionalized HPSNs was obtained by calcining HPSNs-NH_2 at 550 ^oC for 4 h.

3.2.3 Characterization of Nanoparticles

The characterization of HPSNs-NH_2 and HPSNs-COOH using scanning electron microscopy (SEM) was performed under a Philips XL30 field emission scanning electron microscope operated at 10 kV. Fourier transform infrared (FTIR) spectra of samples were recorded on a Thermo Scientific NICOLET 6700 FTIR spectrometer at room temperature. TriStar II surface area and porosity analyzer from Micromeritics at -196 ˚C was used for nitrogen adsorption-desorption measurements using the volumetric method.Brunauer-Emmett-Teller (BET) specific surface areas were calculated by using adsorption data at a relative pressure range of P/P_0 range of 0.05-0.25. The Barrett, Joyner, and Halenda (BJH) method was used to estimate pore size distributions from adsorption branch of isotherm. The amounts of N_2 adsorbed at the single point of P/P_0=0.99 was used to determine pore volumes. The particle sizes and zeta-potentials dispersed in PBS (pH = 7.5) were measured using a Malvern Zetasizer Nano ZS (Malvern Inst. Ltd., U.K.) equipped with four-side

clear cuvettes or the ZET 5104 cell at room temperature. S60/51920 TGA/DSC (thermogravimetric/differential scanning calorimeter) analyzer from Setaram Instrumentation was used for thermogravimetric analysis (TGA) of samples using an oxidant atmosphere (air, 30 ml/min) (heating ramp of 10 ^{o}C/min from room temperature to 800 ^{o}C).

3.2.4 Enzyme Immobilization on Nanoparticles

Silica nanoparticles (10 mg) were dispersed in 1 ml PBS buffer (pH 7.2) and sonicated for 30 min. The mixtures were mixed into BSA (0-10 mg/ml) or β-galactosidase (0-9 mg/ml) and gently stirred overnight at 4 ^{o}C [21]. The particles were recovered through centrifugation at 4200 rpm for 10 min and washed with water to remove free BSA or enzyme on the surface of nanoparticles. The supernatant and washing solution were collected to measure the concentration of non-adsorbed protein.

3.2.5 Production of Galacto-Oligosaccharides

Lactose (50 to 400 g/l) was prepared by dissolving into PBS (pH 7.2) at 60 ^{o}C. After the solution temperature cooled down to room temperature, free or immobilized enzyme were added and incubated at 37 ^{o}C in an orbital shaker at 200 rpm. Samples were drawn at pre-set intervals for analysis (1-5 h) and immediately heated in boiling water for 5 min to deactivate the enzyme activity [22]. The mixture was centrifuged to separate the supernatant and nanoparticles. The resultant supernatant was filtered using 0.45 μm nylon filters, diluted 40 times and analysed by high performance liquid chromatography (HPLC).

3.2.6 Chemical Analysis

The enzyme concentration was assayed using the method described by Bradford [23]. A total of 100 mg Coomassie brilliant blue G-250 were dissolved in 50 ml of 95% ethanol, 100 ml of 85% phosphoric acid and diluted with water to a final volume of 1 l with gentle mixing.

A total of 100 µl samples was added into 5 ml of the Bradford solution, mixed homogenously, and allowed to react for 5 min and measured at a 595 nm spectrophotometer. Protein concentration was determined based on the calibration curve using BSA as a protein standard. The adsorption yield and adsorption capacity of the immobilized enzyme were calculated using Eqs. (1) and (2), respectively, where P_i is the initial concentration of protein that is subjected for immobilization, P_w and P_s is the amount of protein in washing solution and supernatant, respectively [24].

$$\text{Adsorption yield (\%)} = \frac{[P_i - (P_w + P_s)]}{P_i} \times 100 \quad (1)$$

$$\text{Adsorption capacity (mg/g)} = \frac{[P_i - (P_w + P_s)]}{mass\ of\ nanoparticles} \quad (2)$$

The enzyme activity was measured by mixing 100 samples with 1.7 ml of PBS buffer (pH 7.2) and 0.2 ml of 20 mM ONPG prior to continuous agitation at 37 ^{o}C for 10 min. A total of 2 ml of 1M sodium carbonate was added immediately to stop the reaction before measuring the liberated product spectrophotometrically at 405 nm [25]. The enzyme activity was determined from the plotted o-nitrophenol standard curve. One unit (1 U) of β-galactosidase is defined as the amount of enzyme liberates 1 µmole of o-nitrophenol per min under standard assay conditions. The activity retention of immobilized enzyme was determined using the Eq (3), where α_i is the activity of immobilized enzyme activity, while α_f is the activity of free enzyme at the same concentration [26].

$$\text{Activity retention (\%)} = \frac{a_i}{a_f} \times 100 \quad (3)$$

Saccharides (lactose, glucose, galactose, GOS) were determined using high performance liquid chromatography (HPLC) (Agilent) equipped with an aminex HPX-87H column (300 x 7.8 mm) maintained at 60 ^{o}C and a refractive index detector. H_2SO_4 (8 mmol/l) was used as a mobile phase at a flow rate of 0.5 ml min^{-1}. An approximately 5 µl samples were injected for saccharides analysis [27]. [2727][27][27][27][27][27](Zheng et al., 2006)(Zheng et al., 2006)(Zheng et al., 2006)(Zheng et al., 2006)The lactose conversion

was calculated using Eq (4). The yield (Y) of saccharides (glucose, galactose and GOS) was determined using Eqs (5-7).

$$\text{Conversion (\%)} = \frac{[initial\ lactose]-[final\ lactose]}{[initial\ lactose]} \times 100 \quad (4)$$

$$Y_{glucose}\ (\%) = \frac{[glucose]}{[initial\ lactose]} \times 100 \quad (5)$$

$$Y_{galactose}\ (\%) = \frac{[galactose]}{[initial\ lactose]} \times 100 \quad (6)$$

$$Y_{gos}\ (\%) = \%\ Conversion - \%\ Y_{glucose} - \%\ Y_{galactose} \quad (7)$$

3.2.7 Recyclability

The activity of the immobilized enzyme on HPSNs-NH_2 was continuously monitored for 10 cycles. The enzyme activity was determined using the procedure described in section 2.6. After each assay, the nanoparticle-carrying enzyme was separated from the reaction medium through centrifugation at 4200 rpm for 10 min, and then washed with PBS solution (pH 7.2), dewatered before supplementing with fresh substrate to initiate a new cycle of reaction. The enzyme activity at the first run was considered as control (100%) for the calculation of remaining activity after repeated uses [28].

3.2.8 Statistical Analysis

Experimental studies were carried out in triplicate. The data were analysed using the statistical tool in MS Excel 2010 and presented as a mean value with an average standard deviation of < 5%.

3.3 Results and Discussion

3.3.1 Preparation and Characterization of HPSNs

Three types of dendrimer-like nanoparticles: HPSNs-NH_2, HPSNs-COOH and HPSNs were prepared according to the Scheme 3.1. The surface of HPSNs was functionalized with amino (NH_2) and carboxyl (COOH) groups to facilitate β-galactosidase binding. The enzyme, which possesses amino (-NH_2), carboxyl (-COOH), thiol (-SH) and hydroxyl (-OH) groups located in lysine, arginine, glutamic and aspartic acid residues, could interact with the functional groups on the HPSNs surface [6]. Meanwhile, for HPSNs without functional group, enzyme might perform non-specific binding and randomly attach on the material surface.

Successful conjugation of amino and carboxyl functional groups on the surface of HPSNs is confirmed from the Fourier transforms infrared (FTIR) spectra of HPSNs-NH_2 and HPSNs-COOH (Figure 3.1). The presence of the amino groups is evidenced by weak peaks at 1463 and 1520 cm^{-1} due to N–H bending. Grafting of the carboxylic acid groups is signified by three peaks at 1415, 1554 and 1710 cm^{-1} for carbonyl stretching. Other characterization experiments have also been conducted to demonstrate different groups on the surface of HPSNs. The zeta potentials change from +4.5 (HPSNs-NH_2) to −6.7 (HPSNs-COOH) in PBS solution (Table 3.1). The amount of functional groups attached on HPSNs surface was evaluated through thermogravimetric analysis (TGA) analysis. The surface functional group coverage of the NH_2 group (0.79 mmol NH_2 groups /g product) is found to be greater than the COOH group (0.57 mmol COOH groups /g product). Similar discrepancy for the two functional groups on the HPSN surface is also confirmed by nitrogen sorption, with 0.70 and 0.27 groups/nm^2 based on the specific surface areas for NH_2 and COOH group, respectively. The Brunauer–Emmett–Teller (BET) surface area of HPSNs-NH_2 (747 m^2 g^{-1}) is also higher than HPSNs-COOH (585 m^2 g^{-1}).

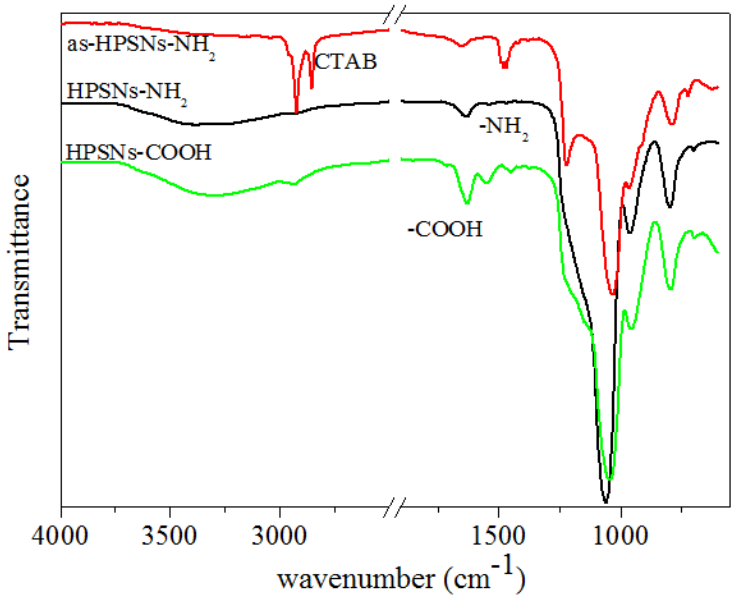

Figure 3.1 FTIR spectra of HPSNs-NH_2 with CTAB template, HPSNs-NH_2 andHPSNs-COOH.

The morphology and pore size of the nanoparticles were also characterized through SEM. Since three types of nanoparticles share very similar images, and only HPSNs-NH_2 are presented in Figure 3.2. It can be seen from Figure 3.2 that uniform sized nanoparticles are prepared with a particle size of 160-250 nm. The nanoparticles have hierachical pores and the center-radial pores were determined to be in the range of 9-117 nm. The average size of uniform mesopores confirmed by the TEM image was ca. 4.5 nm. HPSNs-NH_2 have been demonstrated to be a promising nanocarrier for loading and delivery of therapeutic macromolecules, such as short-interference RNA or plasmid DNA [17]. We will explore the unique structure of this nanocarrier for enzyme immobilization. This multiple-pore structure favors a high enzyme loading and harmonizes diffusion of substrates towards the enzyme on the pore surface, which can promote the interfacial reactions between the substrate and the enzyme.

Table 3.1 Physicochemical properties of HPSNs-NH_2 andHPSNs-COOH.

Properties	HPSNs-NH_2	HPSNs-COOH
pH	7.59	7.54
Particle size (nm)	756	460
Zeta potential (mV)	+4.5	-6.7
BET surface area (m^2 g^{-1})	747	585
Pore size (nm)	4.5	4.3
Total pore volume (cm^3 g^{-1})	1.26	1.19
TGA analysis (mmol groups/g product)	0.79	0.57
N_2 sorption (groups/nm^2)	0.70	0.65

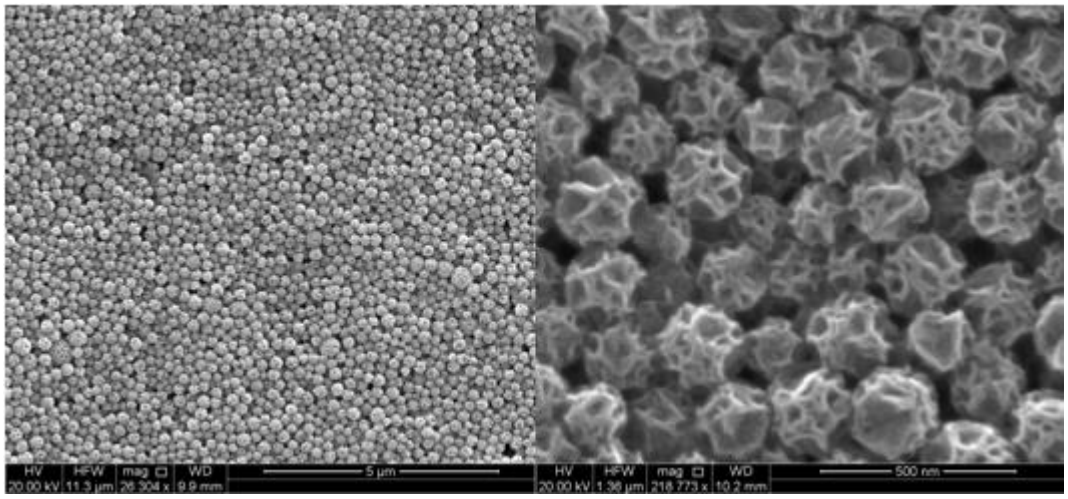

Figure 3.2 SEM images of HPSNs-NH_2 at 5 µm on the left side and 500 nm at the right side.

3.3.2 Immobilization of BSA and β-Galactosidase

High adsorption capacity is one of the major criteria in selecting enzyme carriers. Two parameters have often been used to describe the adsorption performance: adsorption capacity and adsorption yield. The adsorption yield is defined as the percentage of enzymes in the bulk solution transferred to the solid surface. We have used two different proteins to examine the adsorption of the nanocarriers. BSA that often used for evaluation of adsorption was employed for benchmarking the nanocarriers. Comparing with BSA, another enzyme, β-galactosidase, is much larger in size and less negative in zeta potential (Table 3.2). As Figure 3.3(a-b) indicates, HPSNs-NH_2 demonstrates the highest adsorption yield for both BSA (90 %) and β-galactosidase (82 %) at 1 mg/ml concentration. As the enzyme concentration increases, HPSNs-NH_2 are able to retain almost all BSA molecules inside the nanoparticle pores, while nearly 40 % of β-galactosidase molecules are adsorbed at a protein concentration above 4 mg /ml. Meanwhile, the highest yield for HPSNs-COOH is observed below 80 % for both biomolecules at all tested concentrations. When the BSA concentration increases, the adsorption yield starts to slightly reduce. Besides, the adsorption yield also decreases as the enzyme concentration increases, a similar profile as HPSNs-NH_2. The least amount of the bound protein is observed on the non-functionalized HPSNs. Nevertheless, the absorption yield for the enzyme nearly doubles in comparison with BSA. Interestingly, the absorption yield for β-galactosidase on three types of nanocarriers shares a similar trend as the concentration increases.

Table 3.2 Characteristics of β-galactosidase and bovine serum albumin (BSA).

	β-galactosidase	BSA
Molecular weight	116,349	69,000
Isoelectric point	4.6 - 5.1	4.7 - 4.9
Zeta potential (mV)	-2.3	-8.53
Diameter (nm)	7	4.9

Protein adsorption onto the nanocarriers depends on two factors: the available surface for protein molecules and the interaction force between the protein molecules and the functional groups on the nanocarrier surface. The internal surface in the mesopores may be available if the molecular size is smaller than or equivalent to the mesopore size. β-Galactosidase has a high molecule weight of 116349, and the molecular diameter is estimated to be ca. 7 nm, while BSA has a molecular diameter of 4.9 nm (Table 3.2). The mesoporous size is averaged to be around 4.5 nm, which allows BSA molecules to occupy the pore surface, but may block β-galactosidase molecules into the mesopores. There are three possible interaction forces governing protein adsorption on the nanoparticle surface: covalent bonds, electrostatic interactions and non-specific weak binding. BSA and β-galactosidase are able to attach on the HPSNs surface by forming covalent linkages between the grafted NH_2 and COOH groups on the HPSN surface and the COOH and NH_2 group of the protein molecules. Such functional groups on the enzyme have been reported to interact with aldehyde, cyanogen, epoxy and carbodiimide-activated nanoparticles to facilitate xylitol dehydrogenase binding [29].

For the same biomolecules, HPSNs-NH_2 seem to perform better adsoprtion than HPSNs-COOH, which could be explained by a higher BET surface area and a greater functional group coverage of HPSNs-NH_2 than HPSNs-COOH thus provide more active sites for biomolecules binding.In addition, an electrostatic force may also promote protein binding. The negative charge of BSA and β-galactosidase (Table 3.2) could interact with the opposite charge of amino-functionalized HPSNs (Table 3.1). This force could be used to explain the difference between the adsorption of BSA and β-galactosidase onto HPSNs-NH_2. The electrostatic interaction force of HPSNs-NH_2-BSA is higher than that HPSNs-NH_2-β-galactosidase. The reason is probably due to a stronger negative charge of BSA than β-galactosidase, which can facilitate the BSA adsorption onto the mesopores. Protein molecules could also be adsorbed onto the HPSNs surface without any functional groups through non-specific weak binding such as hydrophobic interactions or van der Waals forces [30]. This force becomes more dominant for β-galactosidase as the enzyme concentration increases above 4 mg/ml. Covalent force and electrostatic interactions play a major role at the low enzyme concentration as the functional groups on the nanoparticles are not consumed by the enzyme molecules. As the enzyme concentration increases, extra enzyme molecules are attached to the non-functionalized surface due to the non-specific

binding, and this may also explain why the adsorption yield is similar for three types of nanoparticles at a high enzyme concentration.

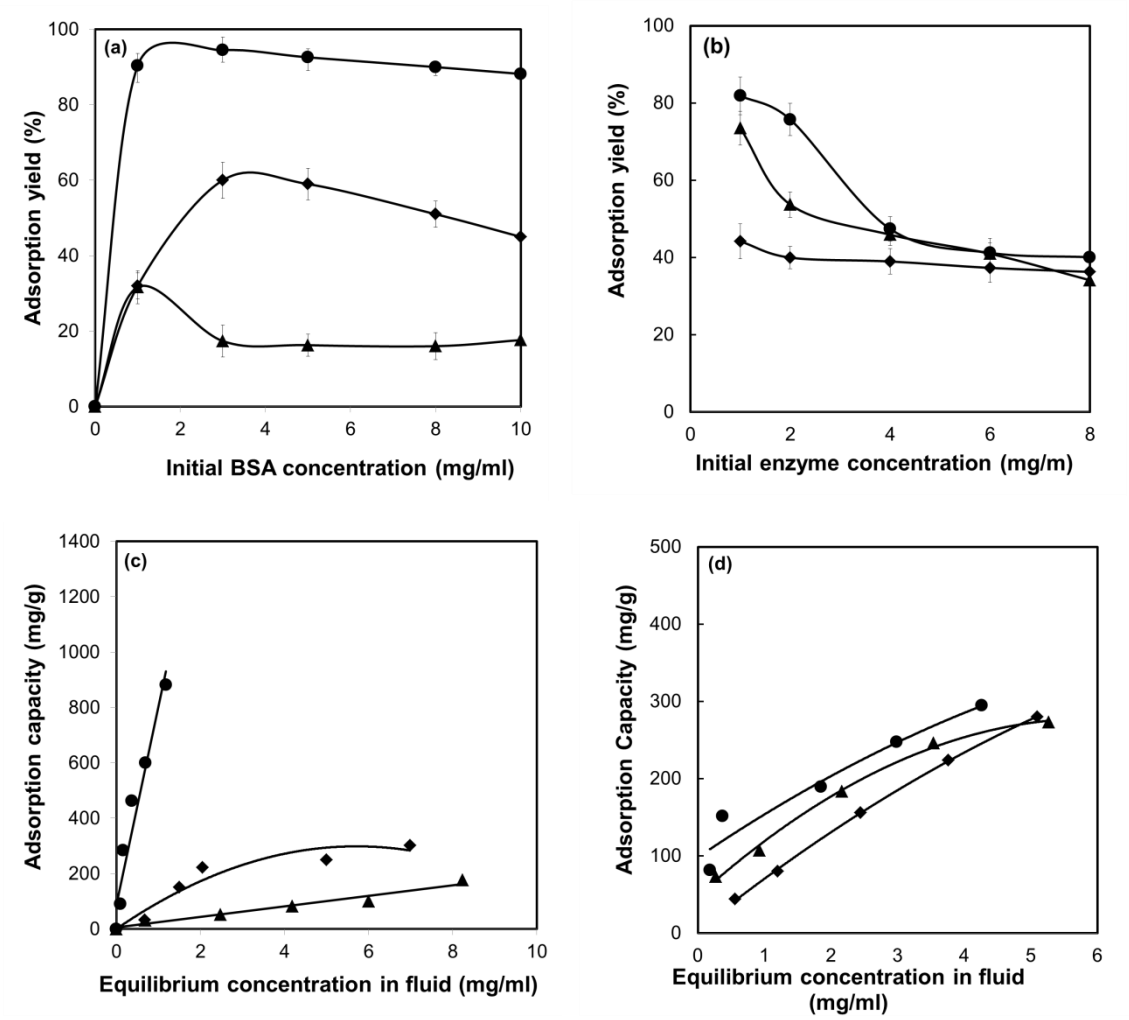

Figure 3.3 Adsorption yield and adsorption capacity of BSA (a, c) and β-galactosidase (b, d) on HPSNs, HPSNs-NH_2 and HPSNs-COOH. (BSA/enzyme concentration: 2-10 mg/ml, incubated at 37 ^oC in pH 7 phosphate buffer solution for overnight at 4 ^oC). ● HPSNs-NH_2,♦ HPSNs-COOH, ▲ HPSNs

In a reactor system, enzyme immobilized through weak binding may easily leak into the reaction medium due to mechanical stress derived from agitation or liquid flow[31-32]. Therefore, the functional groups on the HPSN surface can create specific and strong covalent binding for biomolecules. However, more importantly, the functional groups must

be able to preserve the enzyme catalytic activity through maintaining the enzyme conformation structure.

Another parameter, adsorption capacity defined as the amount of adsorbed enzyme (mg) per gram of enzyme supports, is depicted in Figure 3.3(c-d). The binding capacity is often plotted against the equilibrium enzyme concentration in the liquid solution to determine the adsorption equilibrium relationship. In the case of BSA, HPSNs-NH_2 and HPSNs show a linear relationship between the adsorption capacity and the equilibrium enzyme concentration in the solution at the tested enzyme concentration (0-10 mg/ml). HPSNs-NH_2 have a more sharp slope in the isothermal adsorption profile, which means that HSPNs-NH_2 are able to accommodate a much higher amount of BSA than HPSNs. HPSNs-COOH exhibit a Langmuir isothermal adsorption profile and the maximum adsorption capacity is estimated to be 300 mg BSA/g nanocarrier.

Meanwhile, for β-galactosidase, the Freundlich isotherm ($C_{AS}^{*}=KC_{A}^{*n}$) is the best to correlate the experimental data for three HPSNs. The power indices, n, are 0.3694, 0.8363 and 0.4625 for HPSNs-NH2, HPSNs-COOH and HPSNs, respectively. Since they are below 1.0, the three types of nanoparticles are favorable for enzyme adsorption. At an initial enzyme concentration of 8 mg/ml, all HPSNs carriers exhibit a comparable adsorption yield of 295-328 mg/g, which exceeds other reported carriers summarized in Table 3.3. Cellulase on magnetic chitosan nanoparticles carrier was found to have a lower adsorption capacity (112.3 mg/g) [33]. Laccase loading on metal-mediated mesoporous silica and mesoporous carbon was 98.1 mg/ g [34] particle and 233.3 mg/g [35], respectively. Our enzyme adsorption finding is also in agreement with the previous report [17] in which HPSNs nanocarriers demonstrated to have a high gene loading capacity and high transfection efficiency in the gene delivery application.

3.3.3 Operational Stability of Nanobiocatalysts

The major challenge in the development of the nanobiocatalyst technology is to retain the catalytic activity of the enzyme upon immobilization onto nanocarriers. The enzyme activity was measured using ONPG as the substrate for the enzymes on three carriers, benchmarking with the free enzyme. The initial enzyme concentration was referred to one used for immobilization on three nanocarriers and the formed nanocarrier/enzyme

assemblies were centrifuged and resuspended for enzyme activity measurement. The activity retention was determined by dividing the activity of the immobilized β-galactosidase to the activity of free β-galactosidase. As shown in Figure 3.4, HPSNs-NH_2-Gal exhibits distinguished enzyme stability with 100% activity retention at all tested concentrations, indicating the enzyme catalytic activity was unaffected by the immobilization process. Both HPSNs-COOH and HPSNs provide a lower activity retention at a low enzyme concentration (0.5 mg/ml), approximately 80 % and 60 %, respectively. This low activity retention may be due to a low adsorption yield (Figure 3.3b), which results in less enzyme molecules to react with ONPG. However, as the initial enzyme concentration increases, three nanocarriers have full activity retention. It has been reported that enzyme conformational change upon immobilization reduces the enzyme reactivity [36]. From Figure 3.4, we can conclude that there is no enzyme conformation change when immobilized on three nanocarriers.

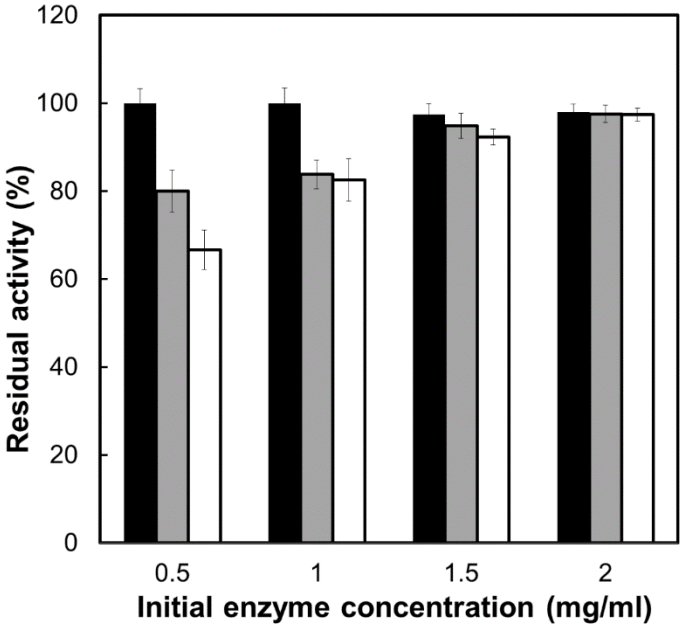

Figure 3.4 Activity retention profiles of free β-galactosidase and immobilized β-galactosidase on HPSNs-NH_2, HPSNs-COOH and HPSNs at various enzyme concentration (0.5-2 mg/ml). The activity of free enzyme at similar concentration at 37 ^oC was selected as a control (100%). ■ HPSNs-NH_2, ▒ HPSNs-COOH and □ HPSNs.

Table 3.3 Adsorption capacity and activity recovery of enzymes on various supports.

Support	Enzyme	Adsorption capacity (mg/g)	Activity retention (%)	Reference
HPSNs-NH_2	β-galactosidase	320	100	This work
		100	100	
HPSNs-COOH	β-galactosidase	280	100	
		74	90	
HPSNs	β-galactosidase	280	100	
		44	70	
Polydopamine-coated iron oxide nanoparticles	Formate dehydrogenase	-	90	[37]
Chitosan	Glucose oxidase	-	77.9	[38]
PGMA-b-PDMAEMA-grafted magnetic nanoparticles	Lipase	500	43.1	[39]

Magnetic mesoporous silica nanoparticles	Laccase	72.6	81.5	[34]
Cu^{2+}-chelated- magnetic mesoporous silica nanoparticles	Laccase	98.1	92.5	[34]
Chitosan	Laccase	20	52	[40]
Magnetic polymer microspheres	Laccase	94.1	65	[41]

Because of its high adsorption yield and activity retention, HPSNs-NH_2 was chosen for further study. Recyclability is a great advantage for immobilized enzyme over free enzyme. Simple recovery of immobilized enzyme and retention of enzyme activity for many runs allow the enzyme to be used in large-scale process, defraying the operation cost. The HPSNs carriers were separated from reaction medium by centrifugation at a mild operation condition (4200 rpm in the lab centrifuge, corresponding to 2397 g), which is applicable in large operation. Separations of nanobiocatalysts are quite challenging, and often magnetic nanoparticle-based nanobiocatalysts are prepared to facilitate separation in a magnetic field. However this operation requires a long separation time and a strong magnetic field, and it also leads to nanobiocatalyst loss after each run [42].

Figure 3.5 presents retention of the β-galactosidase activity on HPSNs-NH_2 after ten cycles. It can be seen that HPSNs-NH_2-Gal can be recycled up to ten times with 20% of its initial activity remaining. It is noted that after five cycles, HPSNs-NH_2-Gal is able to retain 80 % of its initial activity. The decrease of activity is consistent with literature reports. It was reported that the reusability was up to seven cycles [43] or six cycles[44] with the remaining activity was 20% and 35%, respectively.

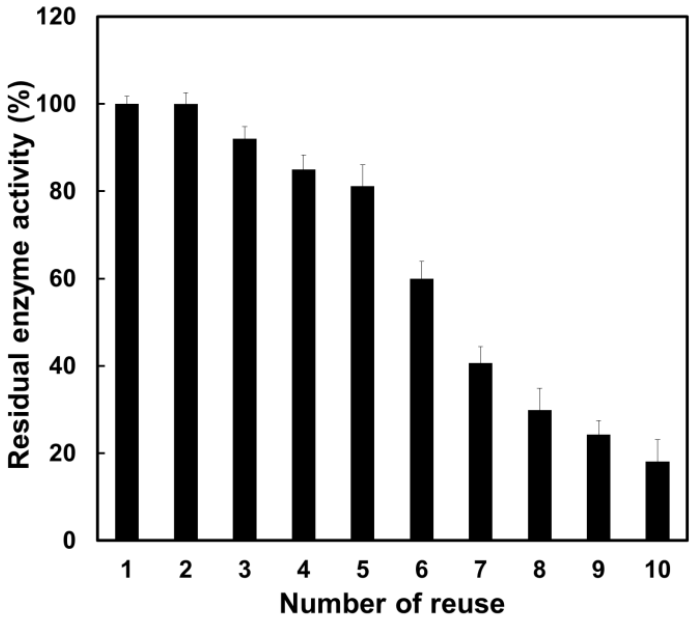

Figure 3.5 Recyclability of immobilized β-galactosidase on HPSNs-NH_2 after 10 repeated cycles. The activity determined at the first cycle (0.45 U/mg) was considered as a control (100%). (Operation conditions: at 37 ^oC with 2 mg/ml enzyme concentration in pH 7).

3.3.4 Production of Galacto-Oligosaccharides

After evaluating the biocatalytic stability, the engineering performance of HPSNs-NH_2-Gal was evaluated for galacto-oligosaccharide (GOS) synthesis, a commercially important functional food. Figure 3.6a-b illustrates the reaction products of lactose bioconversion by free β-galactosidase and HPSNs-NH_2-Gal. The reaction mixtures comprised of glucose, galactose, GOS and remaining lactose. In β-galactosidase-catalyzed reaction, lactose is bioconverted through competitive reactions between hydrolysis and transgalactosylation. Initially, the lactose glycosidic linkages are attacked to form enzyme-galactosyl complexes [45]. Hydrolysis takes place when water acts a galactosyl acceptor, yielding glucose and galactose as end products, while GOS is generated through nucleophilic-galactosyl reaction in transgalactosylation [46-47].

It can be seen in both free and immobilized enzyme that two reactions apparently occur during the first hour reaction time. The remaining lactose is approximately 100 g/l for free β-galactosidase, lower than the unconverted lactose found in HPSNs-NH_2-Gal (160 g/l), indicating the free enzyme demonstrates to have faster lactose reduction. The conversion rate is determined to be 300 g/l/h for the free enzyme and 240 g/l/h for the immobilized enzyme. Despite to that fact, it is found that the free β-galactosidase generates a higher glucose yield which becomes the major product (average 185 g/l). It implies the preferance of the free enzyme towards the hydrolysis reaction. In contrast, the HPSNs-NH_2-Gal yields glucose about 1.7-times lower than the free counterpart, signifying transgalactosylation dominates the lactose bioconversion. Consequently, the GOS yield by HPSNs-NH_2-Gal is 2.6-times higher than the free enzyme.

By extending the reaction time to 5 h, lactose concentration in the free enzyme reaction system experiences a steady and slow decrease. Glucose maintains at the same level as the first hour. A slight increase in GOS and galactose concentration can be found in Figure 3.6a. In the HPSNs-NH_2-Gal catalysed system, lactose concentration has the similar decrease trend as the free enzyme after one hour. However, a steady increase of glucose and galactose concentration can be seen from Figure 3.6b. GOS concentration keeps at between 100 and 122 g/l. In comparison to reported previous studies, the GOS formation by HPSNs-NH_2-Gal is observed to have comparable or even better performance. Employement of β-galactosidase on alginate was described to generate GOS about 87 g/l

[27], 40 g/l by membrane-bound β-galactosidase [48] and 104 g/l on magnetic polysiloxane-polyvinyl alcohol [49].

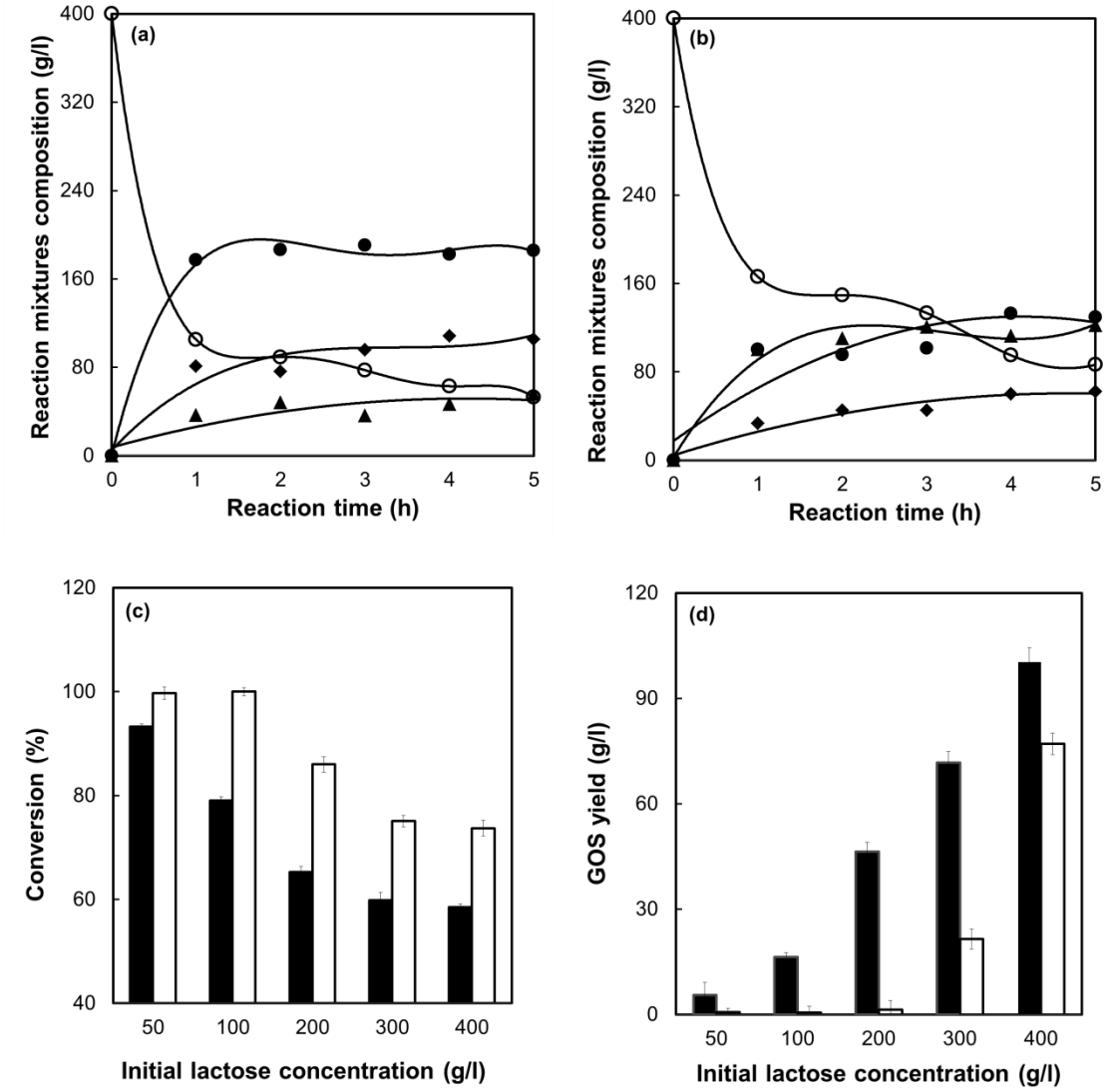

Figure 3.6 The composition of reaction mixture (remaining lactose, glucose, galactose, GOS) by (a) free β-galactosidase and (b) HPSNs-NH2-Gal and (c) the effect of initial lactose concentrations on lactose conversion and (d) GOS yield. (Operation conditions: 2 mg/ml enzyme concentration in pH 7 incubated at 37 oC for 1 h reaction time using 400 g/l lactose for (a-b) and 50-400 g/l for (c-d)).○ Remaining glucose, ▲ GOS, ● glucose, ♦ galactose, ■ HPSNs-NH2-Gal and □ free β-galactosidase.

Figure 3.6c-d presents comparison of the effect of the initial lactose concentration on GOS formation by free β-galactosidase and HPSNs-NH_2-Gal. The conversion trends for

both enzymes decrease with the increasing lactose concentration. Free enzyme is found superior in lactose conversion, up to 100 % below the initial lactose concentration of 100 g/l. Lactose conversion by the free enzyme consistently exceeds HPSNs-NH_2-Gal at all tested concentrations (Figure 3.6c). In contrast, HPSNs-NH_2-Gal performs much better in GOS synthesis than the free counterpart. Figure 3.6d indicates that the free enzyme is unfavourable for GOS formation particularly at a lower lactose concentration. In a diluted solution, water molecules surround the free enzyme reaction sites, therefore, hydrolysis becomes the preferential reaction. When the initial lactose concentration is above 300 g/l, more sugar molecules compete with water molecules and transgalactosylation starts to play a role, which can be seen that GOS production increases sharply. It can be seen that HPSNs-NH_2-Gal shows preference towards transgalactosylation regardless of the initial lactose concentration. While free enzyme does not generate any GOS at a lower lactose concentration up to 200 g/l, HPSNs-NH_2-Gal produces GOS up to 50 g/l. Although GOS yield from HPSNs-NH_2-Gal is still better than that from the free enzyme, the gap is significantly reduced at the initial lactose concentration of 400 g/l. HPSNs microenvironment might have beneficially reduced the diffusion path between the biomolecules and creating a local nanoenvironment with a higher sugar concentration around the enzymatic catalytic sites, promoting more galactosyl-nucleophilic reactions than galactosyl-water activities, therefore, yielding higher GOS than glucose and galactose. This nanoenvironment seems very pronounced at a lower lactose concentrations. As the intital lactose concentration increases, more sugar molecules surrounding the enzymes supress the water activities, and the HPSNs-NH_2-Gal nanobiocatalyst assembly starts to behave like the free enzyme. The nanoenvironment has also been reported to provide a localised optimal reaction condition for immobilized enzyme, such as pH, ionic strength, and temperature [6]. It is evidenced by the increased reaction rates of nanoparticles-bound lipase from 3 to 180 times higher than controls because of a local pH of 7.7 in the nanobiocatalyst assembly [50].

3.4 Conclusion

Functionalized dendrimer-like silica nanoparticles with hierarchical pores were employed as enzyme nanocarriers to form an enzyme-nanocarrier assembly. The functionalization with amino group favoured enzyme binding than carboxylate functional group. The

nanoparticles functionalized with NH_2 group have performed better in adsorption of BSA than COOH group or non-functionalized nanoparticles, and this is also applied to the β-galactosidase adsorption at low enzyme concentration. However, they all had a very similar adsorption yield at higher initial enzyme concentration. The Freundlich isothermal adsorption was found to best fit the experimental data of enzyme adsorption for all three types of nanoparticles. The nanoparticles were found favorable for the enzyme adsorption. The enzyme activity was fully preserved upon immobilization onto three types of nanoparticles. The enzyme assembly with HPSNs-NH_2 was further demonstrated to run up to 10 cycles with 20% of the enzyme activity remaining. Importantly, we have found that the enzyme assembly was able to generate GOS at a much higher yield than free counterpart when the initial lactose concentration is lower than 400 g/l, which means that the enzyme assembly had a preference towards transgalactosylation, while hydrolysis was dominate in the free enzyme solution. At a high initial lactose concentration, the enzyme assembly and free enzyme shared a comparable GOS yield. Our research findings demonstrated the HPSNs can be used to form enzyme-nanocarrier assemblies which have enhanced selectivity towards the required reaction pathways. The findings of the nanocarrier structure-function relationship in enzyme immobilization in this study will provide a useful insight for future development of the hybrid nanobiocatalyst assembly, by correlating and integrating the unique functions of nanocarriers and enzymes. To translate the bench-scale technology into commercial practices, the development of advanced nanoparticle-based enzyme carriers is a critical challenge. Cost reduction as the major hurdle for large-scale trials, long-term stability of the biocatalyst-nanocarrier assembly and operations in a large scale reactor will be addressed in future research.

Acknowledgement

MM gratefully acknowledges the financial support from the Universiti Malaysia Sabah and Malaysian Government. HZ thanks for the 111 Project (B12034). HPLC facility support from Paul Grbin's research group and sugar analysis assistance by Nick Van Holst are highly appreciated. MM also appreciates the technical supports by Jason Peak, Jeffrey Hiorns and Michael Jung from workshop department at School of Chemical Engineering.

References

1. Illanes, A.; Cauerhff, A.; Wilson, L.; Castro, G. R., Recent trends in biocatalysis engineering. *Bioresource Technology* **2012,***115*, 48-57.
2. Cipolatti, E. P.; Silva, M. J. A.; Klein, M.; Feddern, V.; Feltes, M. M. C.; Oliveira, J. V.; Ninow, J. L.; de Oliveira, D., Current status and trends in enzymatic nanoimmobilization. *Journal of Molecular Catalysis B: Enzymatic* **2014,***99*, 56-67.
3. Misson, M.; Jin, B.; Chen, B.; Zhang, H., Enhancing enzyme stability and metabolic functional ability of β-galactosidase through functionalized polymer nanofiber immobilization. *Bioprocess and Biosystems Engineering* **2015,***38*, 1915–1923.
4. Datta, S.; Christena, L. R.; Rajaram, Y. R. S., Enzyme immobilization an overview on techniques and support. *Biotechnology Advances* **2012,***3* (1), 1-9.
5. Zhu, Y.-T.; Ren, X.-Y.; Liu, Y.-M.; Wei, Y.; Qing, L.-S.; Liao, X., Covalent immobilization of porcine pancreatic lipase on carboxyl-activated magnetic nanoparticles: Characterization and application for enzymatic inhibition assays. *Materials Science and Engineering: C* **2014,***38*, 278-285.
6. Misson, M.; Zhang, H.; Jin, B., Nanobiocatalyst advancements and bioprocessing applications. *Journal of Royal Society Interface* **2015,***12* (102), 1-8.
7. Pinto, S. C.; Rodrigues, A. R.; Saraiva, J. A.; Lopes-da-Silva, J. A., Catalytic activity of trypsin entrapped in electrospun poly(ϵ-caprolactone) nanofibers. *Enzyme and Microbial Technology* **2015,***79–80*, 8-18.
8. Wang, L.; Jiang, R., Reversible His-tagged enzyme immobilization on functionalized carbon nanotubes as nanoscale biocatalyst. *Methods in Molecular Biology* **2011,***743*, 95-106.
9. Hong, J.; Yang, W.-Y.; Zhao, Y.-X.; Xiao, B.-L.; Gao, Y.-F.; Yang, T.; Ghourchian, H.; Moosavi-Movahedi, Z.; Sheibani, N.; Li, J.-G.; Moosavi-Movahedi, A. A., Catalase immobilized on a functionalized multi-walled carbon nanotubes–gold nanocomposite as a highly sensitive bio-sensing system for detection of hydrogen peroxide. *Electrochimica Acta* **2013,***89*, 317-325.
10. Zhu, K.; Ye, T.; Liu, J.; Peng, Z.; Xu, S.; Lei, J.; Deng, H.; Li, B., Nanogels fabricated by lysozyme and sodium carboxymethyl cellulose for 5-fluorouracil controlled release. *International Journal of Pharmaceutics* **2013,***441* (1–2), 721-727.
11. Hou, J.; Dong, G.; Ye, Y.; Chen, V., Laccase immobilization on titania nanoparticles and titania-functionalized membranes. *Journal of Membrane Science* **2014,***452*, 229-240.
12. Liu, J.; Qiao, S. Z.; Hu, Q. H.; Lu, G. Q., Magnetic nanocomposites with mesoporous structures: Synthesis and applications. *Small* **2011,***7* (4), 425-443.
13. Ikemoto, H.; Chi, Q.; Ulstrup, J., Stability and catalytic kinetics of Horseradish Peroxidase confined in nanoporous SBA-15. *The Journal of Physical Chemistry C* **2010,***114*, 16174–16180.
14. Sang, L. C.; Coppens, M. O., Effects of surface curvature and surface chemistry on the structure and activity of proteins adsorbed in nanopores. *Physical Chemistry Chemical Physics* **2011,***13* (14), 6689.
15. Buthe, A.; Wu, S.; Wang, P., Nanoporous silica glass for the immobilization of interactive enzyme systems. *Methods in Molecular Biology* **2011,***679*, 37-48.
16. Li, Y.; Quan, J.; Branford-White, C.; Williams, G. R.; Wu, J.-X.; Zhu, L.-M., Electrospun polyacrylonitrile-glycopolymer nanofibrous membranes for enzyme immobilization. *Journal of Molecular Catalysis B: Enzymatic* **2012,***76*, 15-22.

17. Du, X.; Shi, B.; Liang, J.; Bi, J.; Dai, S.; Qiao, S. Z., Developing functionalized dendrimer-like silica nanoparticles with hierarchical pores as advanced delivery nanocarriers. *Advanced Materials* **2013,***25* (41), 5981–5985.
18. Xie, W.; Zang, X., Immobilized lipase on core–shell structured Fe3O4–MCM-41 nanocomposites as a magnetically recyclable biocatalyst for interesterification of soybean oil and lard. *Food Chemistry* **2016,***194*, 1283-1292.
19. Xie, W.; Wang, J., Immobilized lipase on magnetic chitosan microspheres for transesterification of soybean oil. *Biomass and Bioenergy* **2012,***36*, 373-380.
20. Xie, W.; Wang, J., Enzymatic Production of Biodiesel from Soybean Oil by Using Immobilized Lipase on Fe3O4/Poly(styrene-methacrylic acid) Magnetic Microsphere as a Biocatalyst. *Energy & Fuels* **2014,***28* (4), 2624-2631.
21. Yasuda, M.; Nikaido, H.; Glomm, W. R.; Ogino, H.; Ishimi, K.; Ishikawa, H., Enzyme immobilization on amphiphilic polymer particles having grafted polyionic polymer chains. *Biochemical Engineering Journal* **2009,***48* (1), 6-12.
22. Rodriguez-Colinas, B.; Fernandez-Arrojo, L.; Ballesteros, A. O.; Plou, F. J., Galactooligosaccharides formation during enzymatic hydrolysis of lactose: Towards a prebiotic-enriched milk. *Food Chemistry* **2014,***145*, 388-394.
23. Bradford, M. M., A rapid and sensitive method for the quantification of microgram quantities of protein utilizing the principle of protein-dye binding. *Anal Biochem* **1976,***72*, 248-254.
24. Verma, M. L.; Barrow, C. J.; Kennedy, J. F.; Puri, M., Immobilization of beta-d-galactosidase from Kluyveromyces lactis on functionalized silicon dioxide nanoparticles: characterization and lactose hydrolysis. *International Journal of Biological Macromolecules* **2012,***50* (2), 432-7.
25. Ansari, S. A.; Husain, Q., Lactose hydrolysis from milk/whey in batch and continuous processes by concanavalin A-Celite 545 immobilized Aspergillus oryzae b-galactosidase. *Food and Bioproducts Processing* **2012,***90*, 351-359.
26. Zhu, J.; Sun, G., Lipase immobilization on glutaraldehyde-activated nanofibrous membranes for improved enzyme stabilities and activities. *Reactive and Functional Polymers* **2012,***72* (11), 839-845.
27. Zheng, P.; Yu, H.; Professor, Z. S.; Ni1, Y.; Zhang, W.; Fan, Y.; Xu, Y., Production of galacto-oligosaccharides by immobilized recombinant β-galactosidase from Aspergillus candidus. *Biotechnology Journal* **2006,***1* (2), 1464–1470.
28. Husain, Q.; Ansari, S. A.; Alam, F.; Azam, A., Immobilization of Aspergillus oryzae beta galactosidase on zinc oxide nanoparticles via simple adsorption mechanism. *International journal of biological macromolecules* **2011,***49* (1), 37-43.
29. Zhang, Y.-W.; Tiwari, M. K.; Jeya, M.; Lee, J.-K., Covalent immobilization of recombinant Rhizobium etli CFN42 xylitol dehydrogenase onto modified silica nanoparticles. *Applied Microbiology and Biotechnology* **2011,***90*, 499-507.
30. Fernandez, M. F.; Sanroman, M. A.; Moldes, D., Recent developments and applications of immobilized laccase. *Biotechnology Advance* **2013,***31* (8), 1808–1825.
31. Goh, W. J.; Makam, V. S.; Hu, J.; Kang, L.; Zheng, M.; Yoong, S. L.; Udalagama, C. N.; Pastorin, G., Iron oxide filled magnetic carbon nanotube-enzyme conjugates for recycling of amyloglucosidase: toward useful applications in biofuel production process. *Langmuir* **2012,***28* (49), 16864-73.
32. Rahim, S. N. A.; Sulaiman, A.; Hamid, K. H. K.; Edama, N. A.; Baharuddin, A. S., Effect of Agitation Speed for Enzymatic Hydrolysis of Tapioca Slurry Using Encapsulated Enzymes in an Enzyme Bioreactor. *International Journal of Chemical Engineering and Applications* **2015,***6* (1), 38-41.

33. Zang, L.; Qiu, J.; Wu, X.; Zhang, W.; Sakai, E.; Wei, Y., Preparation of Magnetic Chitosan Nanoparticles As Support for Cellulase Immobilization. *Industrial & Engineering Chemistry Research* **2014,***53* (9), 3448-3454.
34. Wang, F.; Guo, C.; Yang, L. R.; Liu, C. Z., Magnetic mesoporous silica nanoparticles: fabrication and their laccase immobilization performance. *Bioresource Technology* **2010,***101* (23), 8931-5.
35. Liu, Y.; Zeng, Z.; Zeng, G.; Tang, L.; Pang, Y.; Li, Z.; Liu, C.; Lei, X.; Wu, M.; Ren, P.; Liu, Z.; Chen, M.; Xie, G., Immobilization of laccase on magnetic bimodal mesoporous carbon and the application in the removal of phenolic compounds. *Bioresource Technology* **2012,***115*, 21-26.
36. Talbert, J.; Goddard, J., Enzymes on material surfaces. *Colloids and Surfaces. B, Biointerfaces* **2012,***93*, 8-19.
37. Gao, X.; Ni, K.; Zhao, C.; Ren, Y.; Wei, D., Enhancement of the activity of enzyme immobilized on polydopamine-coated iron oxide nanoparticles by rational orientation of formate dehydrogenase. *Journal of Biotechnology* **2014,***188*, 36-41.
38. Tang, L.; Yang, R.; Hua, X.; Yu, C.; Zhang, W.; Zhao, W., Preparation of immobilized glucose oxidase and its application in improving breadmaking quality of commercial wheat flour. *Food Chemistry* **2014,***161*, 1-7.
39. Wang, J.; Ji, F.; Xing, J.; Cui, S.; Bao, Y.; Hao, W., Lipase Immobilization onto the Surface of PGMA-b-PDMAEMA-grafted Magnetic Nanoparticles Prepared via Atom Transfer Radical Polymerization. *Chinese Journal of Chemical Engineering* **2014,***2* (11-12), 1333–1339.
40. Zhang, J.; Xu, Z.; Chen, H.; Zong, Y., Removal of 2,4-dichlorophenol by chitosan-immobilized laccase from Coriolus versicolor. *Biochemical Engineering Journal* **2009,***45* (1), 54-59.
41. Wang, F.; Guo, C.; Liu, H.-Z.; Liu, C.-Z., Immobilization of Pycnoporus sanguineus laccase by metal affinity adsorption on magnetic chelator particles. *Journal of Chemical Technology & Biotechnology* **2008,***83* (1), 97-104.
42. Ngo, T. P. N.; Zhang, W.; Wang, W.; Li, Z., Reversible clustering of magnetic nanobiocatalysts for high-performance biocatalysis and easy catalyst recycling. *Chemical Communications* **2012,***48* (38), 4585-4587.
43. Xu, R.; Zhou, Q.; Li, F.; Zhang, B., Laccase immobilization on chitosan/poly(vinyl alcohol) composite nanofibrous membranes for 2,4-dichlorophenol removal. *Chemical Engineering Journal* **2013,***222*, 321-329.
44. Wu, L.; Yuan, X.; Sheng, J., Immobilization of cellulase in nanofibrous PVA membranes by electrospinning. *Journal of Membrane Science* **2005,***250* (1–2), 167-173.
45. Shen, Q.; Yang, R.; Hua, X.; Ye, F.; Wang, H.; Zhao, W.; Wang, K., Enzymatic synthesis and identification of oligosaccharides obtained by transgalactosylation of lactose in the presence of fructose using beta-galactosidase from Kluyveromyces lactis. *Food Chemistry* **2012,***135* (3), 1547-54.
46. Rodriguez-Colinas, B.; Poveda, A.; Jimenez-Barbero, J.; Ballesteros, A. O.; Plou, F. J., Galacto-oligosaccharide Synthesis from Lactose Solution or Skim Milk Using the β-Galactosidase from Bacillus circulans. *Journal of Agricultural and Food Chemistry* **2012,***60* (25), 6391-6398.
47. Jovanovic-Malinovska, R.; Fernandes, P.; Winkelhausen, E.; Fonseca, L., Galacto-oligosaccharides Synthesis from Lactose and Whey by beta-Galactosidase Immobilized in PVA. *Applied Biochemistry and Biotechnology* **2012,***168* (5), 1197-211.
48. Palai, T.; Bhattacharya, P. K., Kinetics of lactose conversion to galacto-oligosaccharides by β-galactosidase immobilized on PVDF membrane. *Journal of Bioscience and Bioengineering* **2013,***115* (6), 668-673.

49. Neri, D. F. M.; Balcao, V. M.; Costa, R. S.; Rocha, I. C. A. P.; Ferreira, E. M. F. C.; Torres, D. P. M.; Rodrigues, L. R. M.; Jr, L. B. C.; Teixeira, J. A., Galacto-oligosaccharides production during lactose hydrolysis by free Aspergillus oryzae b-galactosidase and immobilized on magnetic polysiloxane-polyvinyl alcohol. *Food Chemistry 128* **2009,***115*, 92-99.
50. Zaramella, D.; Scrimin, P.; Prins, L. J., Self-assembly of a catalytic multivalent peptide−nanoparticle complex. *American Chemical Society* **2012,***134*, 8396−8399.

CHAPTER 4

Manipulation of Nanofiber-Based β-Galactosidase Nanoenvironment for Enhancement of Galacto-Oligosaccharide Production

---

Chapter 4: Manipulation of Nanofiber-Based β-Galactosidase Nanoenvironment for Enhancement of Galacto-Oligosaccharide Production

Mailin Misson[1,2], Sheng Dai[1], Bo Jin[1], Bing H Chen[3], Hu Zhang[1*]

[1]School of Chemical Engineering, University of Adelaide, Adelaide, SA 5000, Australia

[2]Biotechnology Research Institute, Universiti Malaysia Sabah, Jalan UMS, 88400, Kota Kinabalu, Sabah, Malaysia

[3]Department of Chemical and Biochemical Engineering, College of Chemistry and Chemical Engineering, Xiamen University, Xiamen, 361005, China

*Corresponding author:

Email: hu.zhang@adelaide.edu.au

Tel: +61 8 831 33810

Published in:

Journal of Biotechnology 2016; 222: 56-64

10.1016/j.jbiotec.2016.02.014

Statement of Authorship

Title of Paper	Manipulation of nanofiber-based β-galactosidase nanoenvironment for enhancement of galacto-oligosaccharide production
Publication Status	☑ Published ☐ Accepted for Publication ☐ Submitted for Publication ☐ Unpublished and Unsubmitted work written in manuscript style
Publication Details	Mailin Misson, Sheng Dai, Bo Jin, Bing H Chen, Hu Zhang Journal of Biotechnology 2016; 222: 56-64 10.1016/j.jbiotec.2016.02.014

Principal Author

Name of Principal Author (Candidate)	Mailin Misson		
Contribution to the Paper	Designed and performed experiments, interpreted data and wrote the manuscript.		
Overall percentage (%)	70 %		
Certification:	This paper reports on original research I conducted during the period of my Higher Degree by Research candidature and is not subject to any obligations or contractual agreements with a third party that would constrain its inclusion in this thesis. I am the primary author of this paper.		
Signature		Date	19.02.2016

Co-Author Contributions

By signing the Statement of Authorship, each author certifies that:

i. the candidate's stated contribution to the publication is accurate (as detailed above);

ii. permission is granted for the candidate in include the publication in the thesis; and

iii. the sum of all co-author contributions is equal to 100% less the candidate's stated contribution.

Name of Co-Author	Sheng Dai		
1. Contribution to the Paper	Supervised development of work and manuscript evaluation.		
Signature		Date	19,02,2016

Name of Co-Author	Bo Jin		
Contribution to the Paper	Supervised development of work and manuscript evaluation.		
Signature		Date	19/02/2016

Name of Co-Author	Bing H Chen		
Contribution to the Paper	Manuscript evaluation		
Signature		Date	2016-02-09

Name of Co-Author	Hu Zhang		
Contribution to the Paper	Supervised development of work, data interpretation, manuscript evaluation and acted as corresponding author.		
Signature		Date	18/02/2016

Please cut and paste additional co-author panels here as required.

Abstract

The nanoenvironment of nanobiocatalysts, such as local hydrophobicity, pH and charge density, plays a significant role in optimizing the enzymatic selectivity and specificity. In this study, *Kluyveromyces lactis* β-galactosidase (Gal) was assembled onto polystyrene nanofibers (PSNFs) to form PSNF-Gal nanobiocatalysts. We proposed that local hydrophobicity on the nanofiber surface could expel water molecules so that the transgalactosylation would be preferable over hydrolysis during the bioconversion of lactose, thus improve the galacto-oligosaccharides (GOS) yield. PSNFs were fabricated by electro-spinning and the operational parameters were optimized to obtain the nanofibers with uniform size and ordered alignment. The resulting nanofibers were functionalized for enzyme immobilization through a chemical oxidation method. The functionalized PSNF improved the enzyme adsorption capacity up to 3100 mg/g nanofiber as well as enhanced the enzyme stability with 80 % of its original activity. Importantly, the functionalized PSNF-Gal significantly improved the GOS yield and the production rate was up to 110 g/l/h in comparison with 37 g/l/h by free β-galactosidase. Our research findings demonstrate that the localized nanoenvironment of the PSNF-Gal nanobiocatalysts favour transgalactosylation over hydrolysis in lactose bioconversion.

Keywords: nanobiocatalyst, galacto-oligosaccharide, β-galactosidase, polymer nanofibers, bioconversion

4.1 Introduction

Advances in biotechnology have led to rapid development of enzyme-catalyzed bioprocesses which are green and sustainable in comparison with chemical processes. Enzymes, a type of biocatalysts able to provide specific and selective activity, have been found in broad applications including biocatalysis, biosensors and medicines. Nevertheless, biocatalysts are no longer economically viable when they are used in large scale processes due to their low stability and reusabilityunder reactor conditions [1]. Therefore, enzyme immobilization on support materials is gaining immense interest from both industry and academia. The immobilization facilitates recovery and recyclability of biocatalysts that enables a cost-effective operation process [2]. A further benefit of immobilization is to enhance enzymatic stability, under either storage or operational conditions, by sheltering and/or stabilizing enzymes against harsh chemical and environmental conditions including extreme pH and temperature [3-4].

Various support materials have been employed for enzyme immobilization including natural polymers *e.g.*cellulose, starch, agarose and chitosan [5-6], synthetic polymers *e.g.* ion exchange resin and polyvinyl alcohol [7-8], or inorganic materials *e.g.* silica [9], zeolite [10] and mesoporous silica [11]. In recent years, assembly of enzymes on nanostructured materials to form nanobiocatalysts has been recognized as a promising approach to enhance enzyme performance. To date, functional nanomaterials such as nanofibers, nanoparticles, nanotubes, and nanocomposites [12-15] have been used as enzyme carriers. The approaches of immobilization can be accomplished via covalent and non-covalent binding, cross-linking, entrapment or encapsulation [16]. Despite constant efforts into optimizing immobilization strategies, reduction of the enzyme activity upon immobilization remains one of key challenges. The activity reduction may be associated with alteration of the unique and native structures of the enzyme [17]. As a consequence, it may significantly affect the performance of the immobilized enzymes in a reactor system. The methodologies for recovering nanobiocatalysts arealso poorly developed. It is, therefore, a focal point to explore recyclable enzyme nanocarriers that can preserve or enhance the enzyme catalytic function, and are suitable for industrial processes.

Cheese whey is a main by-product in casein and cheese manufacturing processes. It has been regarded as organic pollutants in wastewater due to its high organic loading,

which has contributed to significant eutrophication and toxicity in eco-steams [18]. Worldwide, more than 10^8 tons of cheese whey are produced annually, thus a cost-effective treatment technology prior to safe disposal into the environment is highly pursued [19]. Lactose is the major content (60-80 %) of dairy effluents. Bioconversion of the lactose-rich wastes into valuable products endows a promising solution. Lactose can be transgalactosylated into galacto-oligosaccharides (GOS), which offer a range of important health functions in living systems such as prebiotics, low caloric sugar alternatives, and low cariogenicity [20].

β-Galactosidase is the catalyst for bioconversion of lactose into GOS [21]. The enzyme cleaves the lactose molecules forming enzyme-galactosyl complexes before entering either hydrolysis or transgalactosylation pathways. The hydrolysis reaction takes place when water acts a galactosyl acceptor yielding glucose and galactose, while GOS is generated in the transgalactosylation reaction when acceptor molecules, which derived from sugar molecules in reaction medium, surpress the water activity [22]. To enhance GOS production, a localized nanoenvironment can be optimized to promote the transgalactosylation. Meanwhile, due to high cost of β-galactosidase, development of technologies for immobilizing β-galactosidase and enhancing its enzymatic activity and stability has gained momentum in research and development for industrial GOS production.

In this work, we propose to manipulate the local nanoenvironment of β-galactosidase by increasing the local hydrophobicity to reduce the water activity around the enzyme catalytic sites, thus transgalactosylation becomes more preferable than hydrolysis, which leads to a high GOS yield. Polystyrene nanofibers (PSNF) were selected as enzyme nanocarriers because the nanostructured fibers offer intrinsic advantages including high surface area for enzyme loading, and high porosity and interconnectivity to promote low hindrance for mass transfer [16]. The nanofiber surface presents a hydrophobic surface and the solid nanofiber-based nanobiocatalysts can also be recycled. The nanofibers were synthesized using an electrospinning device, and the fabrication process was optimized to generate uniform sized fibers. The PSNF surface was then functionalized through the surface oxidation method to facilitate β-galactosidase binding. The immobilization efficiency was assessed using bovine serum albumin (BSA) and β-galactosidase. Finally, the bioengineering performance of the PSNF-Gal was evaluated in bioconversion of lactose into GOS by benchmarking with the free enzyme.

4.2 Materials and Methods

4.2.1 Chemicals

Polystyrene (molecular weight: 350,000), *N*,*N*-dimethylformamide (DMF) and nitric acid (HNO_3) were of analytical grade without further purification. Bovine serum albumin (BSA), *Kluyveromyces lactis* β-galactosidase, O-nitrophenyl-β-d-glactopyranoside (ONPG), Coomassie Brilliant Blue G-250 and calcium carbonate ($CaCO_3$) were obtained from Sigma-Aldrich. Phosphate buffer saline (PBS), pH 7.2 (10x) were procured from Life Technologies.

4.2.2 Synthesis of Nanofibrous Polystyrene by Electrospinning

The precursor for electrospinning was prepared by dissolving polystyrene (10-30 %, w/v) in DMF with gentle stirring for overnight to form a homogenous solution. The resulting solution was placed inside a 5 ml syringe bearing a needle tip with 1 mm inner diameter, which was connected to a high voltage power supply. The electrospun nanofibers were cast onto a metal-surface collector with a distance of about 10-25 cm from the needle tip. The flow rate was fixed at 2.5 ml/h while the electrospinning was performed within a voltage range of 20-30 kV. The fibers were detached from the collector surface and stored at room temperature for further use.

4.2.3 Enzyme Immobilization on Nanofibers

The surface of polystyrene nanofibers (PS) was modified through surface oxidation to introduce oxygen-containing reactive groups of carboxyl (COOH) and hydroxyl (OH) for enzyme binding [23]. An approximately 1 cm x 2.5 cm piece of nanofibers was immersed in HNO_3 (69 %) for 2 h at room temperature [24]. The acid-modified support was rinsed with water and PBS (pH 7.2) three times to remove excess acid. BSA and β-

galactosidaseimmobilization were carried out by submerging the nanofibers into BSA (0-10 mg/ml) or β-galactosidase (0-9 mg/ml) PBS solution and gently mixed overnight at 4 ^{o}C. Finally, the nanofibers were rinsed thoroughly with water to remove free BSA and β-galactosidase. The supernatant and washing solution were collected to measure the concentration of non-adsorbed proteins.

4.2.4 Enzymatic Activity Assays

The activity assays of free and PSNF- β-galactosidase (PSNF-Gal) were measured according to the procedure described by Ansari and Husain [25]. The reaction mixture containing 0.1 ml of enzyme solution, 1.7 ml of PBS buffer (pH 7.2) and 0.2 ml of 20 mM ONPG were incubated with continuous agitation at 37 ^{o}C for 10 min. The reaction was stopped by adding 2 ml of 1 M sodium carbonate before measuring the liberated product spectrophotometrically at 405 nm. The concentration of product was calculated from the O-nitrophenol standard curve. One unit (1 U) of β-galactosidase is defined as the amount of enzyme which liberates 1 μmole of O-nitrophenol per min under the standard assay condition.

4.2.5 Production of Galacto-Oligosaccharides

Lactose (400 g/l) solution was prepared by dissolving lactose into PBS (pH 7.2) at 60 ^{o}C. Free or immobilized enzymes were added after the solution cooled down to 37 ^{o}C. The mixtures were incubated at 37 ^{o}C in an orbital shaker at 200 rpm. Samples were drawn at designed intervals for analysis during the 5 h reaction period and then immediately heated in boiling water for 5 min to deactivate the enzyme before analysis [26-27]. Samples were filtered using 0.45 μm nylon filters and diluted 40 times prior to high performance liquid chromatography (HPLC) analysis.

4.2.6 Chemical Analysis

The enzyme concentration was analysed using the Bradford method [28]. A total of 100 µl samples were added into 5 ml of the Bradford reagent, mixed homogenously and allowed to react for 5 min. The sample was then measured using a UV spectrophotometer (Shimadzu, Japan) at 595 nm. Protein concentration was determined from a calibration curve using BSA as a standard. The adsorption yield (%) and adsorption capacity (mg/g) of the immobilized enzyme were calculated using Eqs. (1) and (2), where P_i is the initial protein content of the enzyme solution before immobilization, P_w and P_s are the amount of protein in washed solution and supernatant, respectively [29].

$$\text{Adsorption yield (\%)} = \frac{[P_i - (P_w + P_s)]}{P_i} \times 100 \quad (1)$$

$$\text{Adsorption capacity (mg/g)} = \frac{[P_i - (P_w + P_s)]}{nanofiber\ mass} \quad (2)$$

The saccharides (lactose, glucose, galactose, GOS) were determined by HPLC (Agilent, Germany) using an Aminex HPX-87H column (300 x 7.8 mm). The flow rate of a pre-degassed 8 mmol/L-H_2SO_4 mobile phase was set at 0.5 ml min^{-1}. A total of 5 µl samples were injected and the saccharides were detected with a refractive index detector. The column and the detector cell were maintained at 60 ^oC and 40 ^oC, respectively [21]. The conversion (%) was calculated using Eq. (3).

$$\text{Conversion (\%)} = \frac{[initial\ lactose] - [final\ lactose]}{[initial\ lactose]} \times 100 \quad (3)$$

Yield (Y) of glucose, galactose and GOS which represents the fraction with respect to total concentration of initial lactose, was calculated using Eqs. (4-6).

$$Y_{glucose}\ (\%) = \frac{[glucose]}{[Initial\ Lactose]}\ X\ 100\ \% \quad (4)$$

$$Y_{galactose}\ (\%) = \frac{[galactose]}{[Initial\ Lactose]}\ X\ 100\ \% \quad (5)$$

$$Y_{gos}\ (\%) = \%\ Conversion - \%\ Y_{glucose} - \%\ Y_{galactose} \quad (6)$$

4.2.7 Statistical Analysis

Sample collection and analysis were conducted in triplicates. Results were analysed using the statistical tool in MS Excel 2010. Each value corresponds to the mean of independent experiments.

4.3 Results and Discussion

4.3.1 Fabrication and Functionalization of Polystyrene Nanofibers

Structures and the local nanoenvironment of nanocarriers can significantly influence enzyme activity and stability upon immobilization and its bioconversion performance in industrial applications. Large surface areas and minimal defects are two essential criteria for the nanofibers used for β-galactosidase immobilization. Nanofibers with a large surface area are vital to host a high load of enzymes. The presence of defects on the nanomaterial surface could possibly reduce its adsorption capacity. High quality nanofibers are required to be fabricated from an electrospinning process. During the electrospinning process, an electric field charges the polymer solution to create a repulsive force which overcomes the surface tension and leads to a polymer jet eruption from the spinneret tip, thus fiber mats are produced at the collector [30]. A range of operating variables, which could affect the quality and localized physiochemical properties of PS nanofiber, was optimized to obtain high quality nanofibers. The variables comprise of polymer concentration (10-30%, w/v), electric voltage (20-30 kV) and the distance between needle tips and collector (10-25 cm).

A total of 36 trials were carried out based on different combinations of the synthesis conditions as summarized in Table S4.1. The electrospun homogeneity, fiber alignment

and lack of macroscopic defects are normally employed to describe the quality of final products. Good quality nanofibers were obtained from the trials using 20 % (w/v) polymer concentration, basing on homogeneous and droplet-free fiber mats spread on the collector surface by visual inspection. The uniform size and ordered alignment of fibrous mats are further confirmed from microscopic images (Figure 4.1a). It was found that polymer concentration strongly influenced the nanofiber quality. Desirable PSNFs can be obtained using 20% (w/v) PS regardless of the applied voltage or distance. These findings were in agreement with the data reported by An *et al.*[24]. At the lowest polymer concentration (10%, w/v), liquid droplets were produced instead of fibers, probably due to a high surface tension which is associated with a low viscosity of the liquid [31]. In this case, the process is called electrospraying which is used in many industries to obtain aerosols with narrow distributions. In contrast, condensed fibers with major defects were produced using the PS solution at a high concentration (30%, w/v). The defect formation is due to a high viscosity of the PS solution. The resultant PS fibers fused together into a network rather than individual fibers and generated rough and thick mats. This fiber morphology at a high polymer concentration was also demonstrated by Deitzel *et al.*[31] due to its low surface tension. It showed formation of beads on their surface which was observed as black dots under microscopic image (Figure 4.1b), heterogeneous fibers diameters (Figure 4.1c) and disordered alignments (Figure 4.1d), and all these represent a certain level of defects.

The fabricated electrospun mats with high quality were then modified by soaking in HNO_3 solution. Oxidation using HNO_3 has shown a favourable surface modification for protein adsorption [32]. In a previous study, different ratios of HNO_3/H_2SO_4 for modifying polystyrene nanofiber surface were reported [24] and an acid mixing ratio of 4:1 (HNO_3/H_2SO_4) was found to significantly improve the enzyme loading. However, the acidic solution containing sulphuric acid resulted in fibre aggregation. Therefore, surface modification with HNO_3 solution was selected for nanofiber surface treatment. Figure 4.1e and 4.1f show the SEM images of unmodified and HNO_3-treated nanofibers. The acidic oxidation of the fiber surface changes the morphology of the PS fibers. The electrsopun mats becomes shorter fibers as a consequence of the HNO_3 treatment. Such modifications have been proven to create oxygen-containing reactive groups, such as carboxyl (COOH) and hydroxyl (OH), which are able to establish stable binding with biomolecules [23]. As demonstrated by An *et al.*[24], the presence of COOH group on the PS nanofibers facilitated to assemble dehydrogenase on the nanofiber surface as a functional biocatalyst. The

wettability and hydrophobicity have been improved for the modified nanofibers in comparison to the as-spun fibers. Our previous results [24] show that the as-spun fibers are hydrophobic and they float on the water surface. After acidic treatment, the nanofibers are well-dispersed in water.

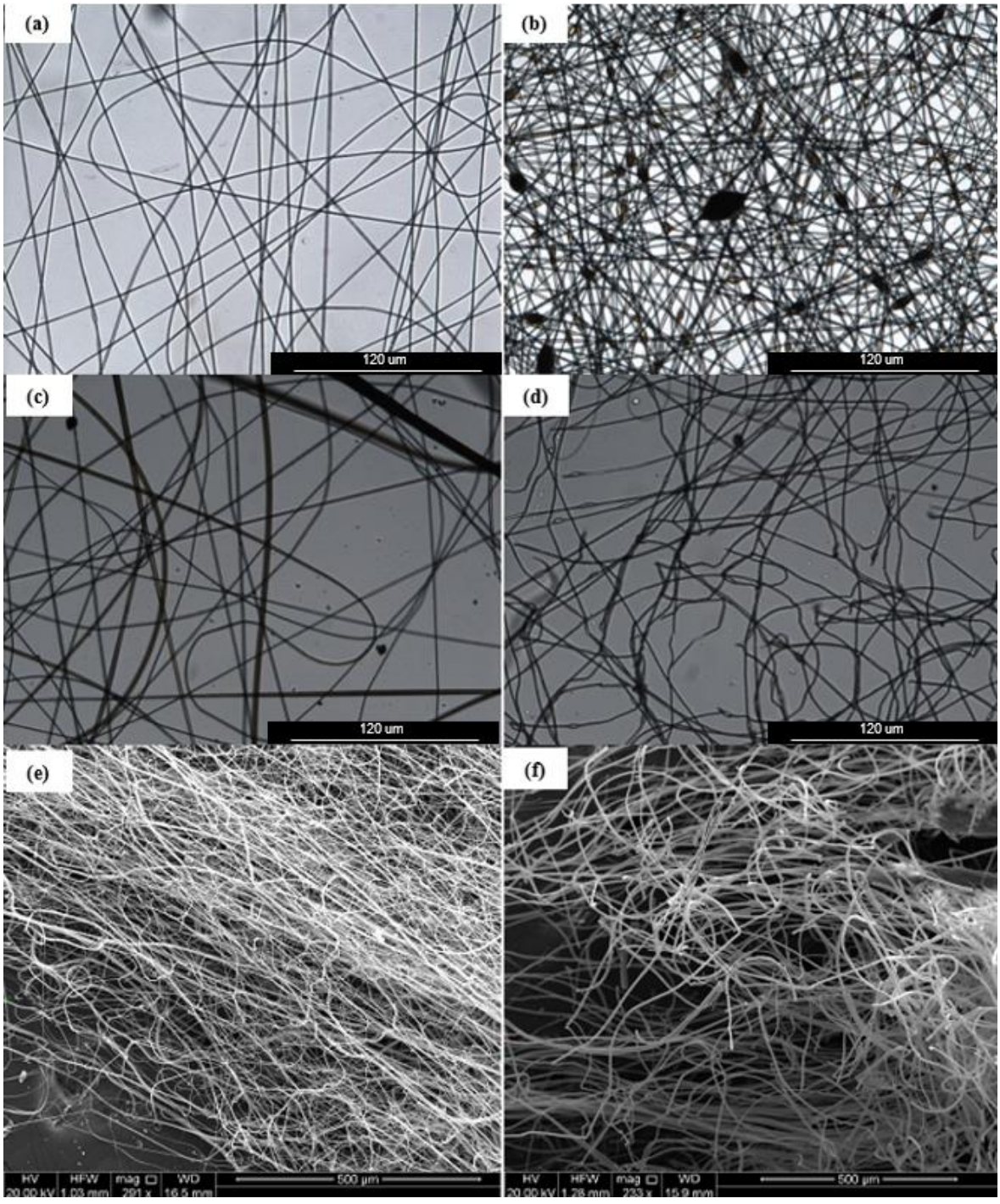

Figure 4.1(a-d) Microscopic images at 40x objective magnification of polystyrene nanofibers (PSNF): (a) nanofibers with uniform diameters (fabrication conditions: 20

% w/v polymer concentration, 25 kV electric voltage, 15 cm distance), (b) nanofibers with beads (black dots) (fabrication conditions: 30 % w/v polymer concentration, 25 kV electric voltage, 10 cm distance), (c) nanofibers with heterogeneous diameter (fabrication conditions: 30 %, w/v polymer concentration, 25 kV electric voltage, 20 cm distance), and (d) nanofibers with coil-like geometry (fabrication conditions: 30 % w/v polymer concentration, 30 kV electric voltage, 25 cm distance). (e-f) SEM images of PSNF: (e) unmodified nanofibers and (f) HNO_3-modified nanofibers.

4.3.2 Immobilization of BSA and β-Galactosidase

Two proteins, BSA and β-galactosidaseat a concentration range of 0 to 10 mg/ml, were used in order to evaluate the protein immobilization performance on the nanofibers before and after HNO_3 treatment (Figure 4.2). BSA and β-galactosidase generally exhibited similar adsorption performance on the nanofibers at all tested concentrations. The maximum adsorption was achieved at protein concentrations around 2 mg/ml and 4 mg/ml for the enzyme and BSA, respectively. Figure 4.2a and 4.2b show that a smaller amount of the bound protein was observed in the case of using unmodified nanofibers. For the PS fibers without surface modification, the proteins may adsorb onto the fibre surface through weak binding such as hydrophobic interactions or van der Waals forces [33]. Thus the hydrophobic nature of the nanofibers drives enzyme deposition. In addition, the enzyme itself contains approximately 28-33% of hydrophobic amino acids which are favourable for hydrophobic binding [34]. Such protein adsorption through hydrophobic interactions has been reported for lipases by Palomo *et al.*[35] and Chen *et al.*[36].

It is notable that the surface modification leads to a substantial increase in the adsorption yield. Approximately 80% of BSA and β-galactosidase were adsorbed on the modified carrier, which was approximately four times that of the unmodified counterpart (20%). It has been recognized that surface oxidation of carbon nanofibers can create more active sites with a large number of carboxylic acid groups, epoxy and hydroxyl groups, which act as anchoring sites for binding protein molecules [37]. A redox enzyme has been successfully employed on electrospun nonwoven poly(acrylonitrile-co-acrylic acid) nanofiber meshes, carrying carboxylic functional groups [38]. In the present work, the binding forces for interfacial reactions might come from hydrogen bonding, electrostatic

force and some hydrophobic interactions [39]. As such, functional groups introduced through the HNO_3 treatment favour and stabilize enzyme adsorption [37].

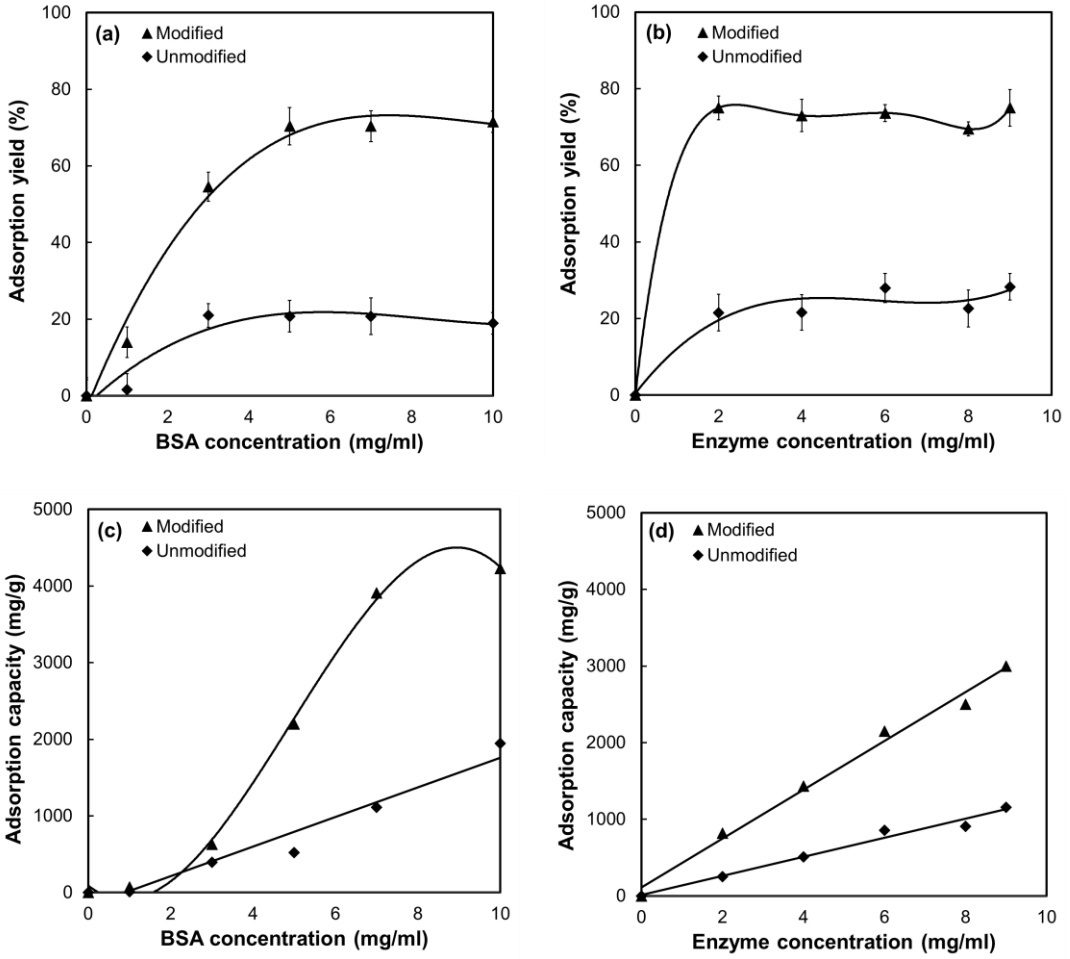

Figure 4.2Adsorption yield and adsorption capacity for (a,c) BSA and (b,d) PSNF-Gal on acid-modified and unmodified nanofiber surface.

High adsorption capacity is one of important criteria for enzyme nanocarriers. Adsorption capacity is defined as the amount of adsorbed enzyme (mg) per gram of enzyme support. The experimental data presented in Figure 4.2c and 4.2d show the effect of acidic treatment of the PS nanofiber surface on the adsorption capacity of BSA and β-galactosidase. It is noted that the nanofibers after treatment by HNO_3have the similar adsorption capacity for both BSA and β-galactosidase. The maximum adsorption capacity was found to be around 4000 mg/g and 3100 mg/g for BSA and β-galactosidase, respectively. The protein adsorption capacity on the treated surface is about 2-fold for BSA

and 3-fold for β-galactosidase in comparison with the untreated surface. The enhancement of adsorption could be ascribed to the protein binding through hydrogen bonding and electrostatic force.

The success in the development of the nanobiocatalysts towards bioprocess applications relies on their excellent performance, especially on enhancing or preserving their catalytic activity and stability upon immobilization. Figure 4.3 presents the specific enzymatic activity of free and immobilized β-galactosidase at different concentrations. The activity of the enzyme immobilized on the nanofiber surface after acidic treatment was found to be comparable with the original activity of the free enzyme. Meanwhile, the decrease in enzyme activity for the unmodified carrier might be associated with the less availability of enzyme as evidenced by a lower adsorption yield as illustrated in Figure 4.2b. In our previous study (Misson et al., 2015a), the PSNF-Gal has shown a promising recyclability. The nanobiocatalyst was demonstrated to retain 30 % of its initial activity after nine operation cycles.

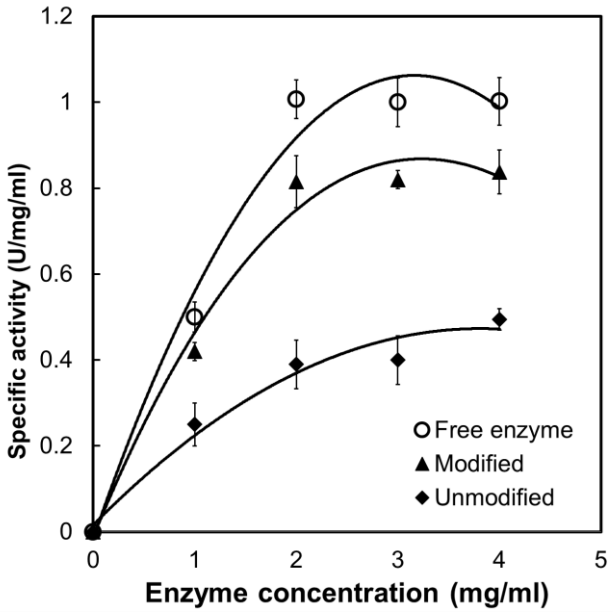

Figure 4.3 Specific enzymatic activity for free β-galactosidase and PSNF-Gal on acid-modified and unmodified nanofiber surface.

4.3.3 Production of Galacto-Oligosaccharides

The performance of PSNF-Gal was further evaluated for bioconversion of lactose into GOS. The reaction product stream from biocatalysis by PSNF-Gal includes glucose, galactose, GOS and the remaining lactose. The saccharides were analysed using HPLC with an Aminex HPX-87H column. GOS are eluted first in the chromatogram, followed by lactose, glucose and galactose [21]. Lactose, glucose and galactose are quantified using chemical standards. The amount of GOS is calculated based on the mass difference between the initial mass of lactose prior to the reaction and summation of the mass of glucose, galactose, and lactose after the reaction.

Figure 4.4a and 4b show the production profiles of lactose bioconversion using free β-galactosidase and PSNF-Gal. Free enzyme demonstrated a rapid lactose conversion during the first hour reaction (Figure 4.4a). The major product was glucose (177 g/l), followed by galactose (80 g/l) and GOS at around 37 g/l. After extending the reaction time from 1 to 5 h, glucose leveled off while lactose decreased at a relatively small order. It is interesting to note that biocoversion using PSNF-Gal has a different reaction profile (Figure 4.4b). The concentrations of glucose and galactose are remarkably lower than those produced by the free β-galactosidase. There is a sharp reduction in lactose concentration and a rapid increase in GOS production during the first hour, resulting in the highest conversion rate of 165 g/l/h, and the production rate of 110 g/l/h, respectively. GOS concentration reduces slightly beyond 2 h, while lactose concentation gradually increases. Lactose and isomers can be possibly re-synthesized through revesible reaction between the galactosyl-enzyme complex and the glucose molecules [40]. Interestingly, the GOS concentration is much higher than that of glucose or galactose using PSNF-Gal up to a reaction time of 5 h. The amount of GOS produced was about 3-fold and 8-fold higher than glucose and galactose, respectively. The PSNF-Gal has the highest GOS production rate of 110 g/l/h in contrast with 37 g/l/h for the free counterpart.

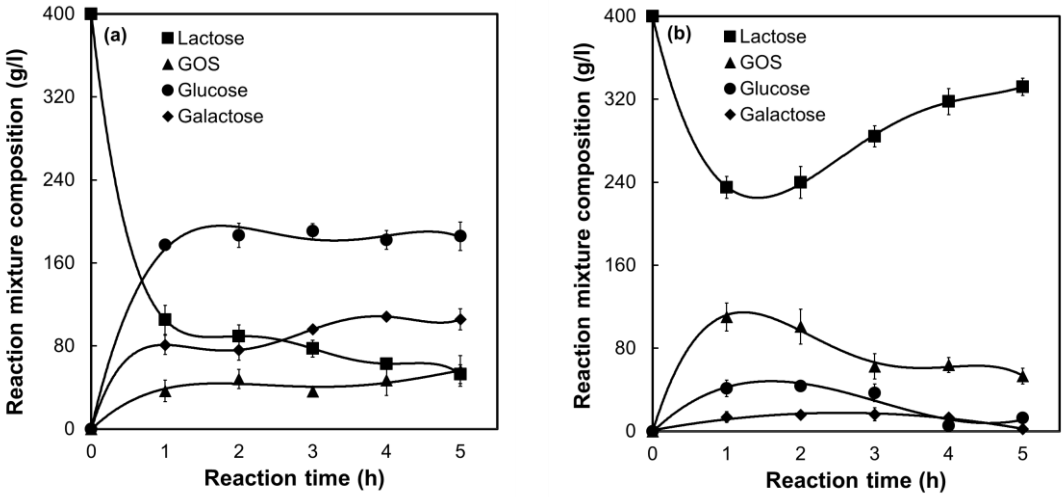

Figure 4.4 Component concentration changes in the product stream at different reaction time for (a) free β-galactosidase and (b) PSNF-Gal. (Operation conditions: incubated at 37 ^{o}C using 400 g/l of initial lactose concentration).

The lactose conversion and the GOS yield are presented in Figure 4.5 for both free β-galactosidase and the PSNF-Gal. Free β-galactosidase offers the advantage for lactose conversion (Figure 4.5a). The amount of converted lactose by free β-galactosidase (86%) is higher than that by PSNF-Gal (41%). The PSNF-Gal, however, appears to have better catalytic capability for synthesizing GOS (Figure 4.5b). A GOS yield of 28% is obtained in the first hour for the PNSF-Gal preparationin comparison with less than 9% for the free enzyme at the same reaction time. The GOS yield can also be calculated based on the consumed lactose, and this yield is estimated to be 67 %. The difference in the GOS yield between the immobilized enzyme and its free counterpart is distinctive, increasing from 12 % to 67 %.The functionalized polystyrene nanofibers-based β-galactosidase has shown comparable bioconversion performance to some of reported immobilized enzyme on various supports for GOS production (Table 4.1) [21-22, 41-44]. This present study used a similar source of enzyme (*Kluyveromyces lactis*) as employed by Klein *et al.*[43] but a different type of enzyme immobilization matrix was selected: polystyrene nanofibers in this work while chitosan macroparticles in Klein *et al.*[43]. The matrix difference can be ascribed to morphology, size, functional groups on the matrix, hydrophobicity, surface charge and others. The local hydrophilic nanoenvironment of chitosan macroparticles could be the key factor for the low GOS yield as water molecules are preferable in the enzyme's active sites. In addition, a packed bed reactor was used by Klein et al. and a low yield of GOS from a continuous operation can be expected.Lactose conversion catalyzed

by β-galactosidase has two different reaction pathways: hydrolysis to glucose and galactose and transgalactosylation to GOS [45-46], which are sketched in Figure 4.6a. According to the proposed pathways, enzyme-galactose complex is formed before entering either hydrolysis or transgalactosylation. Hydrolysis takes place when water acts a galactosyl acceptor, while transgalactosylation occurs when saccharides molecules succeed competing with the water activity [22, 44]. In the free enzyme reaction system, both water and nucleophilic molecules have the equivalent opportunity to enter the enzyme's active site and react with the galactosyl-enzyme complex. Therefore, in the first hour, concentrations for both products from hydrolysis and transgalactosylation increase. After the first hour, the product glucose concentration keeps a constant value, while GOS fluctuates because GOS may be synthesized or hydrolyzed in the system. The increase or decrease of the GOS concentration depends on which reaction becomes preferable in the system.

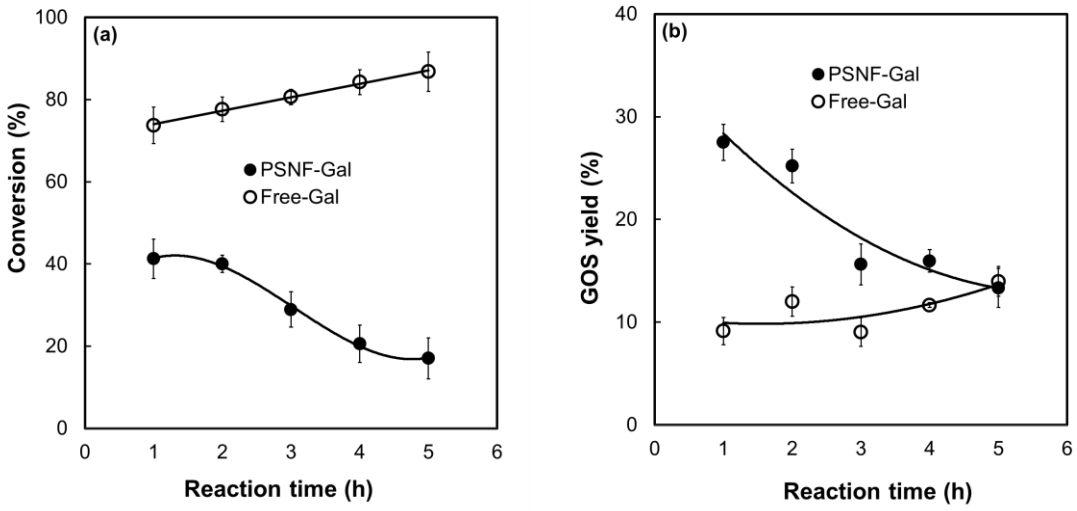

Figure 4.5(a) Lactose conversion and (b) GOS yield using free β-galactosidase (free-Gal) and PSNF-Gal. (Operation conditions: incubated at 37 ^{o}C within 5 h reaction time using 400 g/l of initial lactose concentration).

Table 4.1 Comparison of various types of immobilized β-galactosidases for lactose conversion and GOS production yield.

Enzyme Source	Support material	Initial Lactose (g/L)	Conversion (%)	GOS (g/L)	Reference
Kluyveromyces lactis	Polystyrene nanofibers	400	41	110	This work
Bacillus circulans	Magnetic polysiloxane-polyvinyl alcohol	400	73	198	[44]
Aspergillus oryzae	polyvinyl alcohol	400	75	120	[22]
Aspergillus oryzae	Magnetic polysiloxane-polyvinyl alcohol	400	50	104	[41]
Aspergillus candidus	Alginate	400	-	87	[21]
Bacilus circulans	Membrane surface	200	-	40	[42]
Kluyveromyces lactis	Chitosan macroparticles	400	58	26	[43]

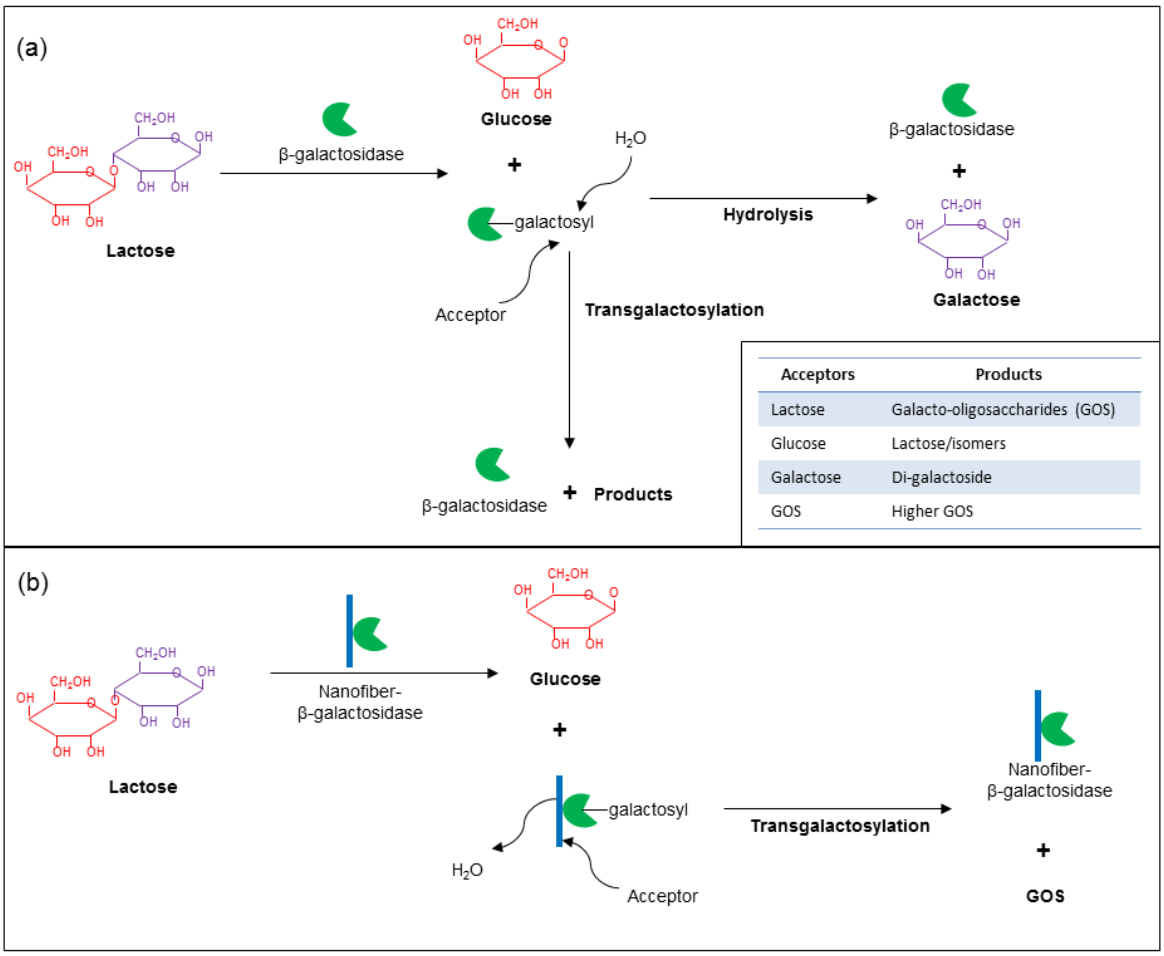

Figure 4.6(a) Thereaction pathway of lactose hydrolysis and transgalactosyslation using free β-galactosidase [45]. (b) Proposed reaction pathway of lactose bioconversion using the PSNF-Gal due to localized nanoenvironment.

In order to promote transgalactosylation catalyzed by β-galactosidase, the local nanoenvironment of the nanofibers is tuned with the hydrophobicity so that acceptors such as lactose or smaller units of GOS are preferable at the enzyme catalytic sites. This hydrophobic property of the nanofiber surface also reduces the water-driven hydrolysis activity. Therefore, the hydrophobic nature of PS nanofibers could be a key factor for GOS formation as presented in Figs. 4 and 5, particularly during the first hour of reaction. Another contributing factor in GOS synthesis may be associated with the reduced diffusion path for biomolecules. Galactose forms a galactosyl –enzyme complex at the enzyme's active sites, and this complex reacts with the acceptors which are produced from the enzymatic reactions and do not immediately diffuse out of the nanofiber surfaces, leading to a preference towards transgalatcosylation reaction. This factor could be used to explain

the reduced gap in GOS formation between PSNF-Gal and its free counterpart after 3-5 h reaction as presented in Figure 4.5. After the nanofibers are exposed to aqueous solution for a few hours, water molecules start to penetrate into the enzymatic catalytic sites as the galactosyl acceptor, and hydrolysis competes with transgalactosylation. When the dynamic balance between both reactions is reached, enzyme on the nanofibers shares the similar performance as free enzyme.

Since PSNF-Gal is able to produce a high GOS yield during the first hour, residence time in the system can be reduced to meet the requiremets of continuous operations in large scale processes. Optimization of the catalytic process in a bioreactor system for continuous operation will be carried out to maximize the GOS yield, which will be expected to be much higher than the initial reported value (110 g/l).

4.4 Conclusion

Polystyrene nanofibers (PSNF) with excellent quality as enzyme carriers were successfully fabricated using electrospinning process. The PSNF surface was modified through chemical oxidation to improve enzyme loading and maintain a high enzyme activity. The lactose conversion by PSNF-Gal catalysis results in a high GOS yield as well as a high production rate. PSNF-Gal may beneficially promote transgalactosylation due to the hydrophobic nature of the polysterene surface. Another contributing factor could be the reduced diffusion path of nuclephilic molecules to facilitate transgalactosylation because these molecules could easily bind to the galactosyl-enzyme complex in such a nanoenvironment. This simple but effective nanobiocatalyst-assisted process may be economically viable for large scale GOS production.

Acknowledgement

MM gratefully acknowledges the financial support from the Universiti Malaysia Sabah and Malaysian Government. HZ thanks for the support from 111 Project (B12034). BHC appreciates the support by the State Key Program of National Natural Science Foundation

of China (No. 21336009). SEM characterization by Masoumeh Zargar, HPLC facility support from Paul Grbin's research group and sugar analysis assistance by Nick Van Holst are highly appreciated.

References

1. Illanes, A.; Cauerhff, A.; Wilson, L.; Castro, G. R., Recent trends in biocatalysis engineering. *Bioresource Technology* **2012,***115*, 48-57.
2. Tran, D. N.; Balkus, K. J., Perspective of recent progress in immobilization of enzymes. *ACS Catalysis* **2011,***1*, 956–968.
3. Sheldon, R. A.; van Pelt, S., Enzyme immobilisation in biocatalysis: why, what and how. *Chemical Society Reviews* **2013,***42* (15), 6223-6235.
4. Misson, M.; Jin, B.; Chen, B.; Zhang, H., Enhancing enzyme stability and metabolic functional ability of β-galactosidase through functionalized polymer nanofiber immobilization. *Bioprocess and Biosystems Engineering* **2015,***38*, 1915–1923.
5. Bryjak, J.; Aniulyte, J.; Liesiene, J., Evaluation of man-tailored cellulose-based carriers in glucoamylase immobilization. *Carbohydrate Research* **2007,***342* (8), 1105-1109.
6. Matto, M.; Husain, Q., Calcium alginate–starch hybrid support for both surface immobilization and entrapment of bitter gourd (Momordica charantia) peroxidase. *Journal of Molecular Catalysis B: Enzymatic* **2009,***57* (1–4), 164-170.
7. Bergamasco, J.; de Araujo, M. V.; de Vasconcellos, A.; Luizon Filho, R. A.; Hatanaka, R. R.; Giotto, M. V.; Aranda, D. A. G.; Nery, J. G., Enzymatic transesterification of soybean oil with ethanol using lipases immobilized on highly crystalline PVA microspheres. *Biomass and Bioenergy* **2013,***59*, 218-233.
8. Guidini, C. Z.; Fischer, J.; Resende, M. M. d.; Cardoso, V. L.; Ribeiro, E. J., B-Galactosidase of Aspergillus oryzae immobilized in an ion exchange resin combining the ionic-binding and crosslinking methods: Kinetics and stability during the hydrolysis of lactose. *Journal of Molecular Catalysis B: Enzymatic* **2011,***71*, 139-145.
9. Kim, H.; Kwon, H.-S.; Ahn, J.; Lee, C.-H.; Ahn, I.-S., Evaluation of a silica-coated magnetic nanoparticle for the immobilization of a His-tagged lipase. *Biocatalysis and Biotransformation* **2009,***27* (4), 246-253.
10. Chang, Y. K.; Chu, L., A simple method for cell disruption by immobilization of lysozyme on the extrudate-shaped NaY zeolite. *Biochemical Engineering Journal* **2007,***35* (1), 37-47.
11. Nabavi Zadeh, P. S.; Mallak, K. A.; Carlsson, N.; Åkerman, B., A fluorescence spectroscopy assay for real-time monitoring of enzyme immobilization into mesoporous silica particles. *Analytical Biochemistry* **2015,***476*, 51-58.
12. Feng, W.; Ji, P., Enzymes immobilized on carbon nanotubes. *Biotechnology Advance* **2011,***29*, 889-895.
13. El-Aassar, M. R., Functionalized electrospun nanofibers from poly (AN-co-MMA) for enzyme immobilization. *Journal of Molecular Catalysis B: Enzymatic* **2013,***85- 86*, 140- 148.

14. Crespilho, F. N.; Iost, R. M.; Travain, S. A.; Oliveira, O. N.; Zucolotto, V., Enzyme immobilization on Ag nanoparticles/polyaniline nanocomposites. *Biosensors and Bioelectronics* **2009,***24* (10), 3073-3077.
15. Cho, E. J.; Jung, S.; Kim, H. J.; Lee, Y. G.; Nam, K. C.; Lee, H. J.; Bae, H. J., Co-immobilization of three cellulases on Au-doped magnetic silica nanoparticles for the degradation of cellulose. *Chemical Communications Cambridge* **2012,***48* (6), 886-8.
16. Misson, M.; Zhang, H.; Jin, B., Nanobiocatalyst advancements and bioprocessing applications. *Journal of Royal Society Interface* **2015,***12* (102), 1-8.
17. Talbert, J.; Goddard, J., Enzymes on material surfaces. *Colloids and surfaces. B, Biointerfaces* **2012,***93*, 8-19.
18. Watanabe, T.; Shinozaki, Y.; Suzuki, K.; Koitabashi, M.; Yoshida, S.; Sameshima-Yamashita, Y.; Kuze Kitamoto, H., Production of a biodegradable plastic-degrading enzyme from cheese whey by the phyllosphere yeast Pseudozyma antarctica GB-4(1)W. *Journal of Bioscience and Bioengineering* **2014,***118* (2), 183-187.
19. Grba, S.; Stehlik-Tomas, V.; Stanzer, D.; Vahčić, N.; Škrlin, A., Selection of yeast strain Kluyveromyces marxianus for alcohol and biomass production on whey. *Chemical and Biochemical Engineering Quarterly* **2002,***16* (1), 13-16.
20. Ganzle, M. G., Enzymatic synthesis of galacto-oligosaccharides and other lactose derivatives (hetero-oligosaccharides) from lactose. *International Dairy Journal 22***2012,***22*, 116-122.
21. Zheng, P.; Yu, H.; Sun, Z.; Ni, Y.; Zhang, W.; Fan, Y.; Xu, Y., Production of galacto-oligosaccharides by immobilized recombinant beta-galactosidase from Aspergillus candidus. *Biotechnology Journal* **2006,***1* (12), 1464-70.
22. Jovanovic-Malinovska, R.; Fernandes, P.; Winkelhausen, E.; Fonseca, L., Galacto-oligosaccharides Synthesis from Lactose and Whey by beta-Galactosidase Immobilized in PVA. *Applied Biochemistry and Biotechnology* **2012,***168* (5), 1197-211.
23. Ros, T. G.; van Dillen, A. J.; Geus, J. W.; Koningsberger, D. C., Surface Oxidation of Carbon Nanofibres. *Chemistry – A European Journal* **2002,***8* (5), 1151-1162.
24. An, H.; Jin, B.; Dai, S., Fabricating polystyrene fiber-dehydrogenase assemble as a functional biocatalyst. *Enzyme and microbial technology* **2015,***68*, 15-22.
25. Ansari, S. A.; Husain, Q., Lactose hydrolysis from milk/whey in batch and continuous processes by concanavalin A-Celite 545 immobilized Aspergillus oryzae b-galactosidase. *Food and Bioproducts Processing* **2012,***90*, 351-359.
26. Rodriguez-Colinas, B.; Fernandez-Arrojo, L.; Ballesteros, A. O.; Plou, F. J., Galactooligosaccharides formation during enzymatic hydrolysis of lactose: Towards a prebiotic-enriched milk. *Food Chemistry* **2014,***145*, 388-394.
27. Lu, L.; Xu, S.; Zhao, R.; Zhang, D.; Li, Z.; Li, Y.; Xiao, M., Synthesis of galactooligosaccharides by CBD fusion beta-galactosidase immobilized on cellulose. *Bioresource technology* **2012,***116*, 327-33.
28. Bradford, M. M., A rapid and sensitive method for the quantification of microgram quantities of protein utilizing the principle of protein-dye binding. *Anal Biochem* **1976,***72*, 248-254.
29. Verma, M. L.; Barrow, C. J.; Kennedy, J. F.; Puri, M., Immobilization of beta-d-galactosidase from Kluyveromyces lactis on functionalized silicon dioxide nanoparticles: characterization and lactose hydrolysis. *International Journal of Biological Macromolecules* **2012,***50* (2), 432-7.
30. Feng, C.; Khulbe, K. C.; Matsuura, T.; Tabe, S.; Ismail, A. F., Preparation and characterization of electro-spun nanofiber membranes and their possible applications in water treatment. *Separation and Purification Technology* **2013,***102*, 118-135.

31. Deitzel, J. M.; Kleinmeyer, J.; Harris, D.; Beck Tan, N. C., The effect of processing variables on the morphology of electrospun nanofibers and textiles. *Polymer* **2001,***42* (1), 261-272.
32. Kaur, J.; Suri, C. R., Direct hapten coated ELISA for immunosensing of low molecular weight analytes. *Protocol Exchange,* **2007**.
33. Fernandez, M. F.; Sanroman, M. A.; Moldes, D., Recent developments and applications of immobilized laccase. *Biotechnology Advance* **2013,***31* (8), 1808–1825.
34. Tudorache, M.; Protesescu, L.; Negoi, A.; Parvulescu, V. I., Recyclable biocatalytic composites of lipase-linked magnetic macro-/nano-particles for glycerol carbonate synthesis. *Applied Catalysis A: General* **2012,***437-438*, 90-95.
35. Palomo, J. M.; Muñoz, G.; Fernández-Lorente, G.; Mateo, C.; Fernández-Lafuente, R.; Guisán, J. M., Interfacial adsorption of lipases on very hydrophobic support (octadecyl–Sepabeads): immobilization, hyperactivation and stabilization of the open form of lipases. *Journal of Molecular Catalysis B: Enzymatic* **2002,***19-20*, 279-286.
36. Chen, H.; Yuan, L.; Song, W.; Wu, Z.; Li, D., Biocompatible polymer materials: Role of protein–surface interactions. *Progress in Polymer Science* **2008,***33* (11), 1059-1087.
37. Stavyiannoudaki, V.; Vamvakaki, V.; Chaniotakis, N., Comparison of protein immobilisation methods onto oxidised and native carbon nanofibres for optimum biosensor development. *Analytical and Bioanalytical Chemistry* **2009,***395* (2), 429-435.
38. Wang, Z. G.; Wan, L. S.; Liu, Z. M.; Huang, X. J.; Xu, Z. K., Enzyme immobilization on electrospun polymer nanofibers: An overview. *Journal of Molecular Catalysis B: Enzymatic* **2009,***56* (4), 189-195.
39. Secundo, F., Conformational changes of enzymes upon immobilisation. *Chemical Society reviews* **2013,***42* (15), 6250-6261.
40. Kim, C.; ES, J.; DK, O., A new kinetic model of recombinant betagalactosidase from Kluyveromyces lactis for both hydrolysis and transgalactosylation reactions. *Biochemical and Biophysical Research Communications* **2004,***316*, 738-743.
41. Neri, D. F. M.; Balcao, V. M.; Costa, R. S.; Rocha, I. C. A. P.; Ferreira, E. M. F. C.; Torres, D. P. M.; Rodrigues, L. R. M.; Jr, L. B. C.; Teixeira, J. A., Galacto-oligosaccharides production during lactose hydrolysis by free Aspergillus oryzae b-galactosidase and immobilized on magnetic polysiloxane-polyvinyl alcohol. *Food Chemistry 128* **2009,***115*, 92-99.
42. Palai, T.; Bhattacharya, P. K., Kinetics of lactose conversion to galacto-oligosaccharides by β-galactosidase immobilized on PVDF membrane. *Journal of bioscience and bioengineering* **2013,***115* (6), 668-673.
43. Klein, M. P.; Fallavena, L. P.; Schöffer, J. d. N.; Ayub, M. A. Z.; Rodrigues, R. C.; Ninow, J. L.; Hertz, P. F., High stability of immobilized β-d-galactosidase for lactose hydrolysis and galactooligosaccharides synthesis. *Carbohydrate Polymers* **2013,***95* (1), 465-470.
44. Rodriguez-Colinas, B.; Poveda, A.; Jimenez-Barbero, J.; Ballesteros, A. O.; Plou, F. J., Galacto-oligosaccharide Synthesis from Lactose Solution or Skim Milk Using the β-Galactosidase from Bacillus circulans. *Journal of Agricultural and Food Chemistry* **2012,***60* (25), 6391-6398.
45. Shen, Q.; Yang, R.; Hua, X.; Ye, F.; Wang, H.; Zhao, W.; Wang, K., Enzymatic synthesis and identification of oligosaccharides obtained by transgalactosylation of lactose in the presence of fructose using beta-galactosidase from Kluyveromyces lactis. *Food Chemistry* **2012,***135* (3), 1547-54.
46. Gaur, R.; Pant, H.; Jain, R.; Khare, S. K., Galacto-oligosaccharide synthesis by immobilized Aspergillus oryzae b-galactosidase. *Food Chemistry* **2006,***97*, 426-430.

Supporting Material

Manipulation of Nanofiber-Based β-Galactosidase Nanoenvironment for Enhancement of Galacto-oligosaccharide Production

Mailin Misson, Sheng Dai, Bo Jin, Bing H Chen, Hu Zhang*

*Corresponding author: Email: hu.zhang@adelaide.edu.au, Tel: +61 88313 3810

Table S4.1

Optimization of operating conditions for polystyrene nanofiber synthesis.

No. of Run	Independent variables			Dependent variables	
	Concentration (w/v %)	Voltage (kV)	Distance (cm)	Fiber Quality	Fiber diameter (μm)
1	30	30	10	Poor	n.a
2	30	30	15	Poor	2.60
3	30	30	20	Poor	2.30
4	30	30	25	Poor	2.41
5	30	25	10	Poor	n.a
6	30	25	15	Poor	2.39
7	30	25	20	Poor	2.43
8	30	25	25	Poor	n.a
9	30	20	10	Poor	n.a
10	30	20	15	Poor	n.a
11	30	20	20	Poor	n.a
12	30	20	25	Poor	n.a
13	20	30	10	Good	1.71
14	20	30	15	Good	1.83
15	20	30	20	Good	1.67

16	20	30	25	Good	1.69
17	20	25	10	Good	1.66
18	20	25	15	Good	1.80
19	20	25	20	Good	1.72
20	20	25	25	Good	1.68
21	20	20	10	Poor	n.a
22	20	20	15	Poor	n.a
23	20	20	20	Poor	n.a
24	20	20	25	Poor	n.a
25	10	30	10	n.a	n.a
26	10	30	15	n.a	n.a
27	10	30	20	n.a	n.a
28	10	30	25	n.a	n.a
29	10	25	10	n.a	n.a
30	10	25	15	n.a	n.a
31	10	25	20	n.a	n.a
32	10	25	25	n.a	n.a
33	10	20	10	n.a	n.a
34	10	20	15	n.a	n.a
35	10	20	20	n.a	n.a
36	10	20	25	n.a	n.a

CHAPTER 5

Enhancing Enzyme Stability and Metabolic Functional Ability of β-Galactosidase through Functionalized Polymer Nanofiber Immobilization

Chapter 5: Enhancing Enzyme Stability and Metabolic Functional Ability of β-Galactosidase through Functionalized Polymer Nanofiber Immobilization

Mailin Misson[1,2], Bo Jin[1], Binghui Chen[3], Hu Zhang[1*]

[1]School of Chemical Engineering, the University of Adelaide, Adelaide, SA 5000, Australia

[2]Biotechnology Research Institute, Universiti Malaysia Sabah, Jalan UMS, 88400, Kota Kinabalu, Sabah, Malaysia

[3]Department of Chemical and Biochemical Engineering, College of Chemistry and Chemical Engineering, Xianmen University, Xiamen, 361005, China

*Corresponding author:

Email: hu.zhang@adelaide.edu.au

Tel: +61 8 831 33810

Published in:

Bioprocess and Biosystems Engineering 2015; 38:1915–1923

DOI 10.1007/s00449-015-1432-5

Statement of Authorship

Title of Paper	Enhancing Enzyme Stability and Metabolic Functional Ability of β-galactosidase through Functionalized Polymer Nanofiber Immobilization
Publication Status	☑ Published ☐ Accepted for Publication ☐ Submitted for Publication ☐ Unpublished and Unsubmitted work written in manuscript style
Publication Details	Mailin Misson, Bo Jin, Binghui Chen, Hu Zhang Bioprocess and Biosystem Engineering 2015; 38:1915–1923 DOI 10.1007/s00449-015-1432-5

Principal Author

Name of Principal Author (Candidate)	Mailin Misson		
Contribution to the Paper	Designed and performed experiments, interpreted data and wrote the manuscript.		
Overall percentage (%)	70 %		
Certification:	This paper reports on original research I conducted during the period of my Higher Degree by Research candidature and is not subject to any obligations or contractual agreements with a third party that would constrain its inclusion in this thesis. I am the primary author of this paper.		
Signature		Date	06.02.2016

Co-Author Contributions

By signing the Statement of Authorship, each author certifies that:

i. the candidate's stated contribution to the publication is accurate (as detailed above);

ii. permission is granted for the candidate in include the publication in the thesis; and

iii. the sum of all co-author contributions is equal to 100% less the candidate's stated contribution.

Name of Co-Author	Bo Jin		
Contribution to the Paper	Supervised development of work and manuscript evaluation.		
Signature		Date	19/02/2016

Name of Co-Author	Bing H Chen		
Contribution to the Paper	Manuscript evaluation		
Signature		Date	2016-02-09

Name of Co-Author	Hu Zhang		
Contribution to the Paper	Supervised development of work, data interpretation, manuscript evaluation and acted as corresponding author.		
Signature		Date	18/02/2016

Please cut and paste additional co-author panels here as required.

Abstract

A functionalized polystyrene nanofiber (PSNF) immobilized β-galactosidase assembly (PSNF-Gal) was synthesised as a nanobiocatalyst aiming to enhance the biocatalyst stability and functional ability. The PSNF fabricated by electrospinning was functionalized through a chemical oxidation method for enzyme binding. The bioengineering performance of the enzyme carriers was further evaluated for bioconversion of lactose to galacto-oligosaccharides (GOS). The modified PSNF-Gal demonstrated distinguished performances to preserve the same activity as the free β-galactosidase at the optimum pH of 7.0, and to enhance the enzyme stability of PSNF-Gal in an alkaline condition up to pH 10. The PSNF assembly demonstrated improved thermal stability from 37 ^{o}C to 60 ^{o}C. The nanobiocatalyst was able to retain 30 % of its initial activity after ninth operation cycles comparing to four cycles with the unmodified counterpart. In contrast with free β-galactosidase, the modified PSNF-Gal enhanced the GOS yield from 14% to 28%. These findings show the chemically modified PSNF-based nanobiocatalyst may be pertinent for various enzyme-catalysed bioprocessing applications.

Keywords: nanobiocatalysts, galacto-oligosaccharides, β-galactosidase, polymer nanofibers, bioconversion

5.1 Introduction

The employment of enzyme on support matrix promises biocatalyst recovery and recyclability. Immobilization allows a continuous operation which is beneficial in reducing the operating cost, making them economically viable for large scale processes. The enzyme immobilization technology has been recognised to shield enzymes against denaturing microenvironments [1]. However, enzymes often encounter activity reduction upon immobilization associated with enzyme conformation changes [2]. There is a great demand to explore new technology for fabricating enzyme carriers. The establishment of the most suitable immobilization protocol is also highly pursued [3].

Nanobiocatalyst, prepared by assembling enzyme on nanomaterial carriers, is an emerging innovation which provides large surface area for high enzyme loading. Their surface is also modifiable to promise advantages in improving enzyme stability, capability, and engineering performances. There have been many reported studies on enhancing enzyme activity and stability associated with nanobiocatalysts. Misson *et al.*[4] described the enzyme enhancement occurs through the stabilization of active conformation that facilitates substrate-enzyme interfacial reactions, while free enzyme has a freedom in the conformation change. It is evidenced by the stabilization of reactive sites of lipase leading to an activity enhancement as reported by Chen *et al.*[5] and Palomo *et al.*[6]. Asuri *et al.*[7] reported that single-walled nanotubes could shelter enzymes and promote higher stability in comparison to flat graphite. The thermal stability of immobilized cellulases on nanoparticles was obtained by stabilizing the binding forces in the presence of the carbodiimide crosslinker [8].

Nanostructured fibers as enzyme immobilizers provide exciting opportunities for the development of enzyme-driven bioreactor systems for bioengineering processes. The nanostructuredfibersare attributed to their specific surface characteristics, discrete nanostructures and self-assembling behaviors [4]. Nanofibers also offer intrinsic advantages including high porosity and interconnectivity which promote low hindrance for mass transfer. The modification of nanofiber surface with strong oxidizing agents is favourable for protein adsorption [9]. The pre-treatment with HNO_3 have been proven to create oxygen-containing reactive groups of carboxyl (COOH) and hydroxyl (OH), which are essential for biomolecule binding [10]. Such modification has successfully assembled dehydrogenase

as a functional biocatalyst [11]. Despite the optimal immobilization has been extensively studied [3], preservation and stabilization of immobilized enzymes in a bioreactor system remains a key challenge. It therefore impedes the translation of these bench-scale technologies into commercial practices.

In this present study, we demonstrated the enhancement of enzyme stability by immobilizing β-galactosidase on acid-modified PSNF. The PSNF was modified through a specially determined chemical oxidation to facilitate enzyme binding. The performance of PSNF-Gal assembly was evaluated in regards to the adsorption capability, enzyme stability and recyclability and benchmarked with the non-modified PSNF. Lastly, their engineering performance was investigated in lactose bioconversion, which abundantly presents in dairy waste industries, into valuable products particularly galacto-oligosaccharides (GOS).

5.2 Materials and Methods

5.2.1 Chemicals

Polystyrene (molecular weight: 350,000), *N*,*N*-dimethylformamide (DMF), nitric acid (HNO_3), and sulphuric acid (H_2SO_4) were analytical grades without further purification. Bovine serum albumin (BSA), *Kluyveromyces lactis* β-galactosidase, O-nitrophenyl-β-d-glactopyranoside (ONPG), Coomassie Brilliant Blue G-250 and calcium carbonate (Ca_2CO_3) were obtained from Sigma-Aldrich. Potassium phosphate buffer (PBS, pH 7.2) were procured from Life Technologies.

5.2.2 Preparation of Nanofibrous Polystyrene by Electrospinning

The precursor for electrospinning was prepared by dissolving polystyrene (20 w/v) in DMF with gentle stirring for overnight to form a homogenous solution. The resultant solution was placed inside a 5-mL syringe bearing a 1-mm inner diameter needle tip which was connected to a high voltage power supply. The electrospun nanofibers were cast onto a metal-surface collector with a distance of about 10 cm from the needle tip. The flow rate was fixed at 2.5 ml/h while the electrospinning was performed at a voltage range of 25 kV.

The polystyrene nanofibers (PSNF) were detached from the collector surface and stored at room temperature for further use.

5.2.3 Enzyme Immobilization on Nanofibers

The surface of PSNF was modified through surface oxidation to introduce functional groups [10]. Approximately 1 cm x 2.5 cm piece of nanofibers sheet were immersed in HNO_3 (69%) for 2 h at room temperature [11]. The modified support was rinsed with water and PBS (pH 7.2) for three times to remove excess acids. β-galactosidase immobilization were carried out by submerging the PSNF into β-galactosidase(2 mg/ml) solution in PBS and gently mixed overnight at 4 ^{o}C by agitation. The enzyme-bound nanofibers were separated from the reaction medium using forceps. Finally, the nanofibers were rinsed thoroughly with water to remove free β-galactosidase. The supernatant and washing solution were collected to measure the concentration of non-adsorbed proteins.

5.2.4 Synthesis of Galacto-Oligosaccharides

Lactose (100- 400 g/l) solution was prepared by dissolving lactose into PBS (pH 7.2) at 60 ^{o}C. Free or immobilized enzymes were added after the solution cooled down to 37 ^{o}C. The mixtures were incubated at 37 ^{o}C in an orbital shaker at 200 rpm. Samples were drawn after 2 h reaction and then immediately heated in boiling water for 5 min to inactivate enzymes [12-13]. Samples were filtered using 0.45 μm nylon filters and diluted 40 times prior to high performance liquid chromatography (HPLC) analysis.

5.2.5 Chemical Analysis

The enzyme concentration was assayed by the Bradford reagent, prepared by mixing 100 mg Coomassie Brilliant Blue G-250 in 50 ml of 95% ethanol, 100 ml of 85% phosphoric acid and diluting the solution with water to a final volume of 1 litre with gentle mixing [14]. A total of 100 μl sample was added into 5 ml of Bradford reagent, mixed homogenously and allowed to react within 2 min - 1 hr. Afterwards, the sample was measured using a UV spectrophotometer (Shimadzu, Japan) at 595 nm. Protein concentration was determined

from a calibration curve using BSA as a standard. The adsorption yield (%) of the immobilized enzyme was calculated using Eqs. (1), where P_i is the initial protein content of enzyme solution before immobilization, P_w and P_s are the amount of protein in washed solution and supernatant [15].

$$\text{Adsorption yield} = \frac{[P_i - (P_w + P_s]}{P_i} x\ 100 \quad (1)$$

Saccharides (lactose, glucose, galactose, GOS) were determined by HPLC (Agilent, Germany) using an Aminex HPX-87H column (300 x 7.8 mm). The flow rate of a pre-degassed 8 mmol/L-H_2SO_4 mobile phase was set at 0.5 ml min^{-1}. A total of 5 µl samples were injected and the saccharides were detected with a refractive index detector. The column and the detector cell were maintained at 60 ^oC and 40 ^oC, respectively [16]. The concentration of total GOS was calculated by the mass balance difference between the initial lactosefeed and the total concentration of remaining lactose, glucose and galactose measured at the end of the reaction [17]. The lactose conversion (%) and GOS yield (%) were calculated using Eq. (2).

$$\text{Lactose conversion } = \frac{[initial\ lactose] - [final\ lactose]}{[initial\ lactose]} \text{ x } 100 \quad (2)$$

5.2.6 Enzymatic Activity Assays

The activity assays of free and immobilized β-galactosidase using 2 mg/ml concentration were measured according to the procedure described by Ansari and Husain [18]. The reaction mixture containing 0.1 ml of enzyme solution, 1.7 ml of phosphate buffer (pH 7.2) and 0.2 ml of 20 mM ONPG were incubated with continuous agitation at 37 ^oC for 10 min. The reaction was stopped by adding 2 ml of 1M sodium carbonate. The liberated product was measured spectrophotometrically at 405 nm and the concentration was calculated from the O-nitrophenol standard curve. One unit (1 U) of β-galactosidase is defined as the amount of enzyme which liberates 1 µmole of O-nitrophenol per min under standard assay condition.

5.2.7 Effect of pH and Temperature of Immobilized Enzyme

The enzyme activity of free and immobilized β-galactosidase on the modified and unmodified PSNF (2 mg/ml) was assayed in PBS buffers at different pHs from 4 to 11. Samples were withdrawn and the residual enzyme activity assay was determined, by defining the activity at pH 7 as a control (100%) for the calculation of other assay conditions. The temperature during agitation was varied from 4 ^{o}C to 70 ^{o}C to study the thermal stability of the enzyme. The activity of enzyme activity incubated at 37 ^{o}C was set as 100% relative activity for each of their respective reactions.

5.2.8 Reusability

Reusability of the immobilized β-galactosidase on modified and unmodified PSNF was assessed in hydrolysing the ONPG substrate using PBS buffer (pH 7) at 37 ^{o}C. After each cycle, immobilized enzyme was separated from supernatant and washed with water for three times. In the next cycle, fresh ONPG was introduced to the immobilized enzyme under same assay conditions. The activity determined at the first cycle was considered as control and attributed to a relative activity of 100% for the determination of remaining activity after repeated uses. Each cycle is defined here as the complete hydrolysis of substrate present in a reaction mixture.

5.2.9 Statistical Analysis

Data was collected in triplicates and analysed using the statistical tool in MS Excel 2010. Each value corresponds to the mean of experimental data with an average standard deviation was <5%.

5.3 Results and Discussion

5.3.1 Immobilization of β-Galactosidase

Nanofibers were fabricated from an electrospinning system which can generate various sized fibrous mats, from nanometers to a few micrometres [19-21]. The synthesis was carried out in the presence of electric field charges to create a repulsive force to the polymer, in which, fibers were generated when the force overcomes the surface tension [22]. Surface modification with strong oxidizing agents was favourable for protein adsorption [9-11]. Figure 5.1 shows the profiles of adsorption capacity of the surface-modified PSNF-Gal. Non-modified PSNF-Gal also was employed under similar operating conditions as a comparative study. It can be seen that the maximum isothermal adsorption was reached within 2 hr immobilization time in both cases. The least adsorption capacity was observed for the case of unmodified PSNF, yielding maximum adsorption merely about 50 mg/g which represents approximately 20 % of adsorption yield.

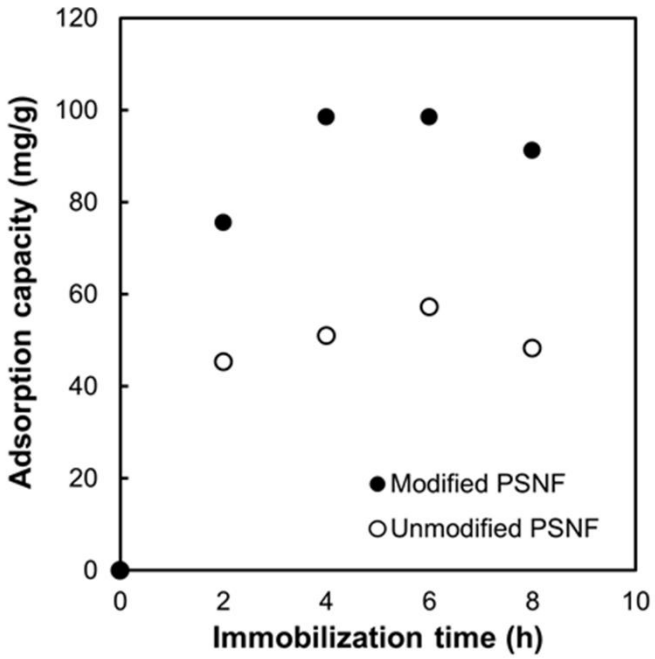

Figure 5.1Adsorption capacity (mg enzyme/ g support material) of the modified PSNF-Gal and unmodified PSNF-Gal. (Enzyme concentration: 2 mg/ml, incubated at 37 ^{o}C in pH 7 phosphate buffer solution).

The characterization of the modified and unmodified PSNF has been carried out in our previous report by scanning electron microscope (SEM) for surface morphology, and the functional groups have been identified using fourier transform infrared spectroscopy

(FTIR) and raman spectroscopy (RS) [11]. The acid-modified nanofibers have been found to contain oxygen-containing reactive groups of carboxyl (COOH) and hydroxyl (OH) for enzyme binding [10]. The enzyme itself possesses amino ($-NH_2$), carboxylate (-COOH), thiol (-SH) and hydroxyl (-OH) groups which can react with the generated functional groups from nanofibers [4]. As a such, the force for binding interaction, as a consequence of the acid modification, could be hydrogen bonding, electrostatic force and some hydrophobic interaction [23]. It is noted that the modified PSNF-Gal exhibited adsorption profiles of nearly 100 mg/g capacity, signifying about 60 % of immobilization yield. The results denote that the surface modification promotes stronger forces of protein binding and leads to a remarkable increase in the adsorption yield. In contrast, the binding of protein on the surface without modification occurs usually through weak binding such as hydrophobic interactions or van der Waals forces [24].

5.3.2 Effect of pH

Figure 5.2 demonstrates the effect of pH on the activity of free β-galactosidase and PSNF-Gal. The maximal enzyme activity was found to be at a neutral pH in all cases study. The origin of enzymes generally influences the optimum pH condition of β-galactosidase. This finding was in agreement with the result reported by Güleç [25] who also used enzyme from *Kluyveromyces lactis*. Ansari *et al.*[26] reported that the highest activity for *Aspergillus oryzae* β-galactosidase occurred at pH 4.5. At a highly acidic (below pH of 5) or basic pH (above pH of 11), β-galactosidase suffered complete loss of enzymatic activity probably due to alteration or distortion of its conformation structure [27]. The unmodified PSNF-Gal demonstrated 50% as its highest activity at the determined optimum condition. It might be associated with the above mentioned lower adsorption yield and weaker enzyme binding. It is interesting to note that the modified PSNF-Gal showed 100 % activity at the similar operating condition. In addition, it exhibited a comparable performance with the soluble enzyme up to a neutral pH (pH 7). Beyond that pH level, the PSNF-Gal had a superior performance by extending the enzyme stability up to pH of 10. The β-galactosidase on the unmodified PSNF also exhibited a noticeable activity enhancement in an alkaline condition comparing with the free counterpart. It signified the enzyme supports have sheltered or stabilized enzyme in the extreme pH environment.

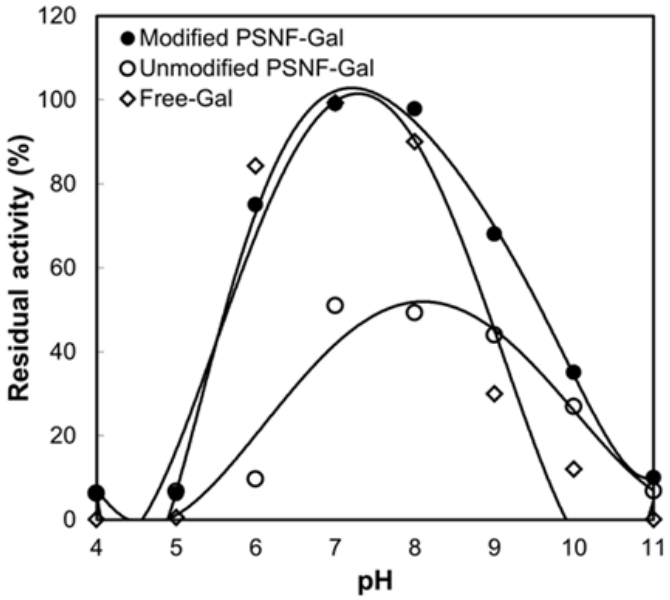

Figure 5.2 Enzyme activity profiles of free-Gal,modified PSNF-Galand unmodified PSNF-Gal at various pH conditions, while keeping at 37 ^{o}C with 2 mg/ml enzyme concentration. The activity of free enzyme (2.08 U/mg) at pH 7 was selected as a control (100%).

5.3.3 Effect of Temperature

Figure 5.3 illustrates the enzyme activity profiles of free and immobilized β-galactosidase at various reaction temperatures. The temperature at 37 ^{o}C was found as the optimal condition in all trials. Interestingly, the modified PSNF-Gal broadened the enzyme stability up to 60 ^{o}C. The modified PSNF-Gal continued to retain about 60 % of its residual activity, while the free β-galactosidase has nearly lost its activity. Meanwhile, the unmodified PSNF exhibited 40 % activity at such a level of heat. At higher temperatures, the enzyme polypeptide chains may rupture, which leads to loss of enzyme activities. The interactions between the polypeptide chains and poymer matrix can maintain the polypeptide chain structure, therefore, the thermal stability is enhanced. Ansari *et al.*[26] found that the ruptures led to enzyme molecules denaturation and consequently loss of its activity. Immobilization of *Aspergillus oryzae* β-galactosidase on zinc oxide nanoparticles also demonstrated the broadening optimal temperatures from 50 ^{o}C to 60 ^{o}C [28].

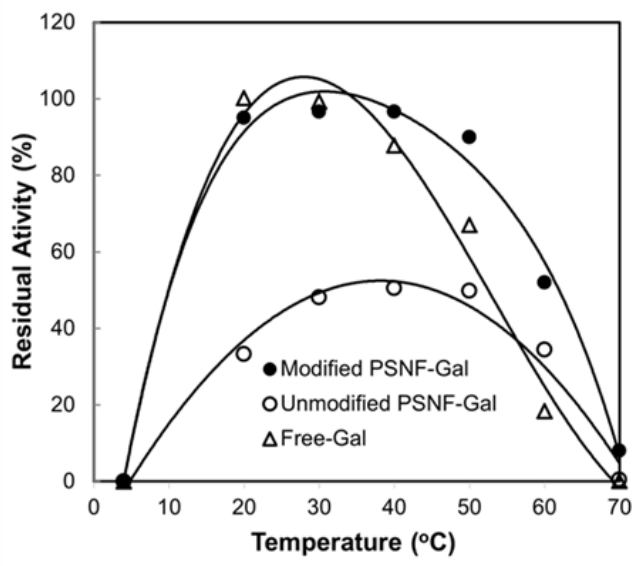

Figure 5.3 Enzyme activity profiles of free-Gal,modified PSNF-Galand unmodified PSNF-Gal at various reaction temperatures, while keeping at 37 ^{o}C with 2 mg/ml enzyme concentration. The activity of free enzyme (2.14 U/mg) at 37 ^{o}C was selected as a control (100%).

5.3.4 Reusability

High cost and instability of enzymes in the reactor are the limitations in translating a lab scale enzyme-catalyzed bioreactor system into a large scale bioprocess. The overall process appears economically viable if the catalytic reaction is in high efficiency and reusability. We conducted a number of bench scale trials to assess the reusability of PSNF-Gal assembly for conversion of lactose to GOS. The reusable potential of the immobilized enzyme provides promising advantages over free enzyme. The recyclability of modified and unmodified PSNF-Gal is shown in Figure 5.4. The first cycle of reaction was considered as a control to measure the remaining activity of enzyme in subsequent cycles. The process of introducing fresh substrate to the immobilized enzyme was repeated until their activity decays. The modified PSNF-Gal retained the remaining 30% of its initial activity after nine cycles comparing with only four cycles when using the non-modified PSNF-Gal. The strong binding of β-galactosidase which is driven by electrostatic and hydrogen bonding might be the probable cause for better recyclability. In general, the enzyme activity of the modified PSNF-Gal was observed to decrease gradually after several repeated uses. Such decreasing pattern of activity was consistent with reported

studies. Previous reports showed nanobiocatalysts recyclability lasted for about seven [29] and six cycles[30] with the remaining activity was 20% and 35%, while employment of enzymes on the Au-doped magnetic silica nanoparticles demonstrated reuse for four times [31]. Hence, these findings in our experiments imply the potential application of the modified PSNF-Gal for continuous operation in a large reactor system.

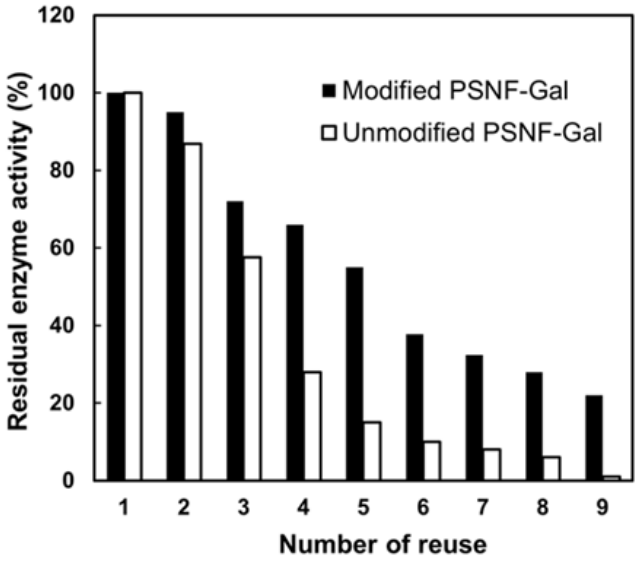

Figure 5.4 Recyclability of the modified PSNF-Gal and unmodified PSNF-Gal. The activity determined at the first cycle (0.24 U/mg and 0.27 U/mg, respectively) was considered as a control (100%). (Operation conditions: at 37 ^{o}C with 2 mg/ml enzyme concentration in pH 7).

5.3.5 Production of Galacto-Oligosaccharides

The performance of the PSNF-Gal in converting lactose into GOS was further investigated. Hydrolysis and transgalactosylation reactions are two catalytic pathways of β-galactosidase in lactose bioconversion. Initially, β-galactosidase-galactose complexes are formed after the biocatalyst attacks lactose molecules before entering hydrolysis or transgalactosylation pathways. Hydrolysis takes place when water acts a galactosyl acceptor, yielding glucose and galactose as products, while galacto-oligosaccharide is formed through transgalactosylation process when nucleophilic molecules succeed in competing the water activity [32-33]. Therefore, the products in the reaction medium of lactose bioconversion possibly contain glucose, galactose, GOS and the remaining lactose.

Figure 5.5 displays the profiles of product distributions in lactose bioconversion by free and immobilized β-galactosidase. Glucose was found to be the major product in free enzyme reaction. The soluble β-galactosidase consistently yielded nearly 50 % of glucose at all tested lactose concentration (Figure 5.5a).The galactose yield however decreased rapidly from 50 % to 10 % when the lactose concentration increased. It was found that both of the immobilized enzymes produced much lower glucose than the free enzyme. In general, the yield of glucose was below 20 % (Figure 5.5b and 5.5c). The GOS yield, on the other hand, increased correspondingly to the lactose concentration in all cases.

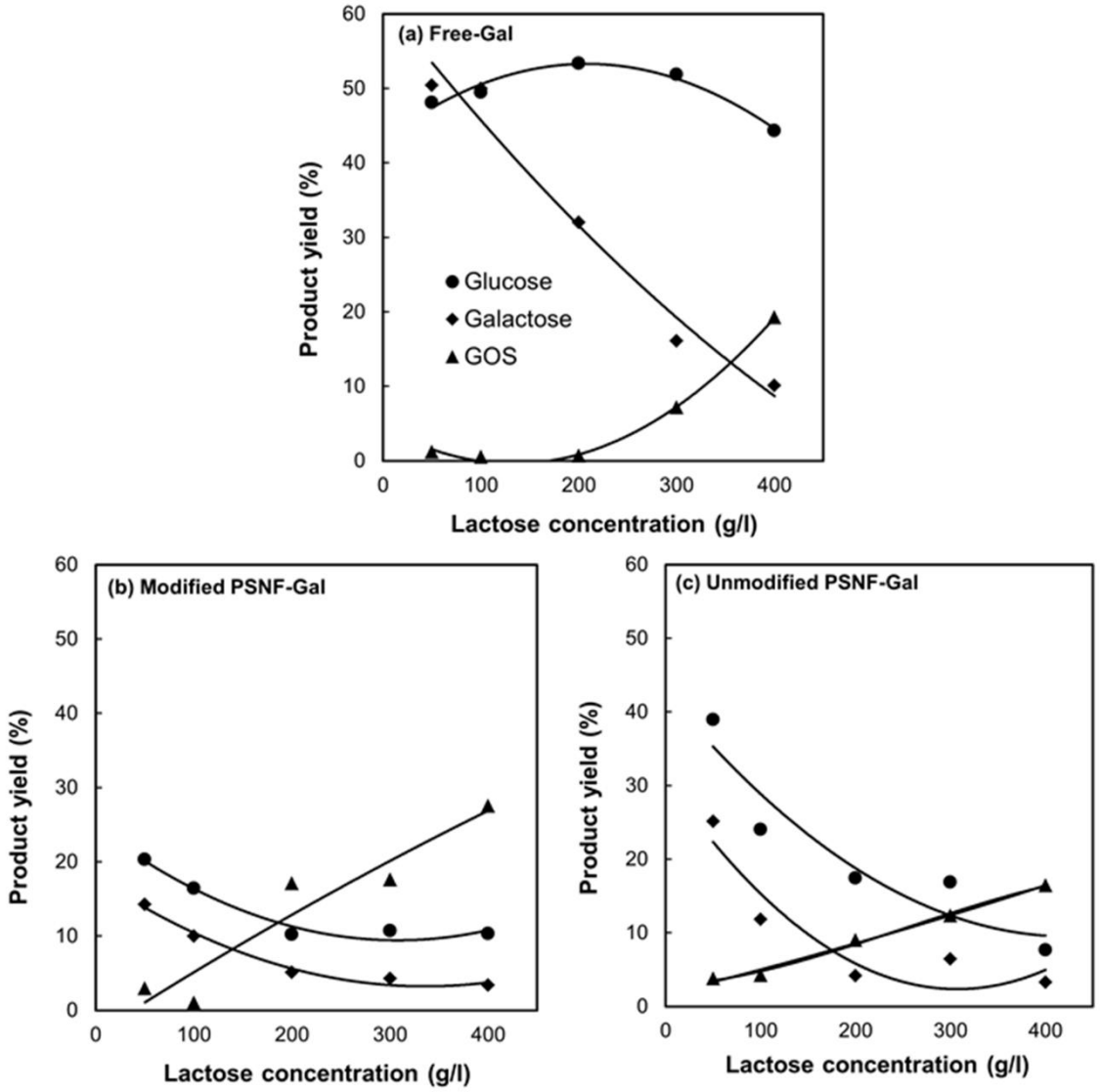

Figure 5.5 Product profiles from lactose bioconversion at different initial lactose concentrations by free-Gal,modified PSNF-Galand unmodified PSNF-Gal. (Operation conditions: at 37 ^{o}C with 2 mg/ml enzyme concentration in pH 7).

Lactose can be converted into glucose and galactose via hydrolysis reaction by the enzyme, while lactose can also react with galactose to form GOS via transgalactosylation using the same enzyme. The immobilized enzyme is more favourable for transgalatosylation than hydrolysis in comparison with free enzyme.This also further explains why the glucose yield by the free enzyme was two times higher than PSNF-Gal in Figure 5.5. Transgalactosylation preferable in PSNF-Gal is also supported by the lower concentration of galactose than glucose.

Figure 5.6 shows the effect of lactose concentration on the conversion and GOS yield by free β-galactosidase and PSNF-Gal. The free β-galactosidase demonstrated complete biconversion at a lower lactose concentration (50 - 100 g/l) while approximately 73 % to 86 % of bioconversion at a higher concentration (200 – 400 g/l) (Figure 5.6a). The bioconversion of the modified and unmodified PSNF-Gal was determined to be roughly 30 % - 40 % at all tested concentrations, about 2-fold lower than the free counterpart. Nevertheless, despite lower bioconversion, the PSNF-Gal assembly exhibited greater GOS synthesis profiles. While there was almost unnoticeable GOS at a lower lactose concentration by the free β-galactosidase, the modified PSNF-Gal demonstrated a total of 16 % GOS and nearly doubled the yield at the highest lactose concentration (28 %) (Figure 5.6b). A gradual increase in GOS production from 4 % to 16 % was also observed by the unmodified PSNF-Gal.

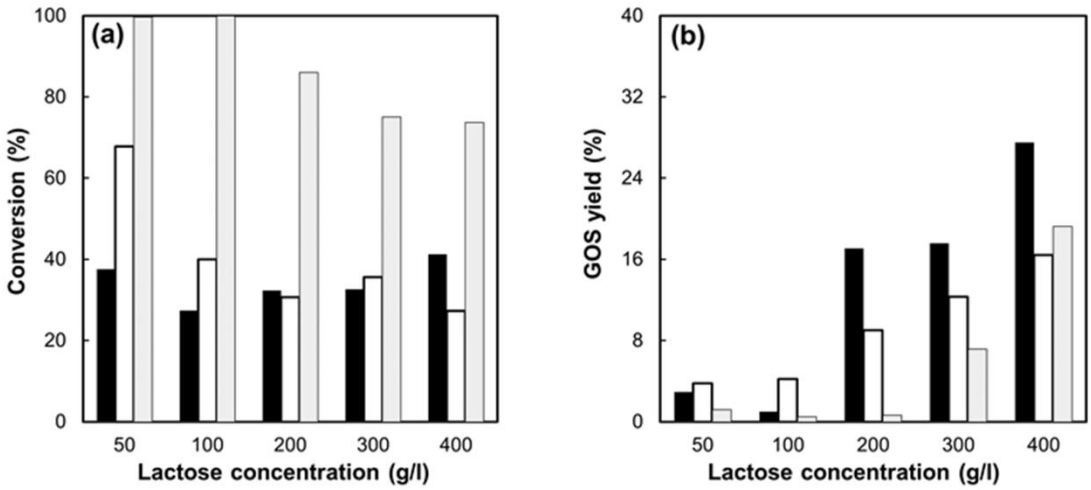

Figure 5.6 Effect of initial lactose concentration on (a) lactose conversion and (b) GOS yield by free-Gal, modified PSNF-Gal and unmodified PSNF-Gal. ■ modified PSNF-Gal,

 unmodified PSNF-Gal, ▒ free-Gal. (Operation conditions: at 37 oC with 2 mg/ml enzyme concentration in pH 7).

For the free enzyme, lactose hydrolysis is the prevailing reaction, especially in the lower concentrations (0~200 g/L), which yields glucose as the major product. It explains a higher conversion rate of lactose but a lower concentration of GOS. At 400 g/L lactose concentration, GOS are produced due to more interactions between galactose and lactose. The transgalactosylation is also supported by the sharp decrease in galactose concentration in Figure 5.5a.At 400 g/L initial lactose concentration, PSNF-Gal has enhanced the GOS yield up to 28% comparing with the highest yield by free β-galactosidase (19 %). The hydrophobic nature of PSNF might potentially repel water from the enzyme active sites, thus reducing the water-driven activity of hydrolysis and ultimately facilitates the reaction to GOS synthesis.

It is also noted that lactose can also be re-produced from glucose and galactose via transgalactosylation in PSNF-Gal and free enzyme. However, lactose from galactose and glucose via transgalactosylation in free enzyme is less than that in immobilized enzyme. Therefore the conversion rate of lactose in free enzyme is around 2 times higher than immobilized enzyme, while the GOS yield in immobilized enzyme is only around 10% higher than that in free enzyme.

In summary, a higher lactose concentration results in a greater yield of GOS. The PSNF-Gal is superior to the free counterpart in the GOS synthesis. The employment of β-galactosidase on modified PSNF was preferable than the unmodified PSNF owing to its greater productivity in addition to its recyclability (Figure 5.4). By benchmarking the findings with previously reported studies as tabulated in Table 5.1, it indicates the modified nanobiocatalyst shows comparable or even greater bioconversion and productivity.

Table 5.1 Comparison on lactose bioconversion, GOS yield, and recyclability of nanobiocatalysts from various types of support materials and sources of enzymes.

Source	Support	Lactose	GOS yield	Conversion	Recyclability	Reference
Aspergillus oryzae	Polysiloxane-polyvinyl alcohol	500 g/l	26% (w/v)	55 %	10 cycles	[34]
	-	500 g/l	29 % (w/w)	55-60 %	-	[35]
	Cotton cloth	500 g/l	27 (w/v)	50 %	2 weeks (continuous operation)	[36]
	Glyoxyl-agarose	550 g/l	8.5kg/g enzyme	30 %	10 cycles	[37]
Kluyveromyces lactis	Nanosized epoxy	200 g/l	32% (w/v)	90 %	10 cycles	[38]
	Polymeric Membrane Surfaces	100 mM	13 (w/v)	50 %	5-8 cycles	[25]
			40 (w/v)	10 %		
	Modified polystyrene nanofibers	400 g/l	28% (w/v)	40%	9 cycles	This study

	Unmodified polystyrene nanofibers	400 g/l	16% (w/v)	27%	4 cycles	This study
Bacillus circulans	-	400 g/l	41 (w/v)	50 %	-	[32]

5.4 Conclusion

A successful immobilization of β-galactosidase on the acid-modified PSNF was demonstrated. The PSNF-Gal nanobiocatalyst assembly exhibited considerable enhancement in enzymatic and metabolic activities at a basic condition and the thermal stability up to 60 ^{o}C, signifying distinguished enzyme stabilizations in the denaturing environments. The surface modification of the nanostructured polymer fibres might have facilitated stable enzyme binding resulted in greater biocatalyst recyclability. Our findings demonstrated the PSNF-Gal doubled the GOS yield comparing using free enzyme, which is of importance for bioengineering process. The highest GOS (28 %) was obtained at 400 g/l lactose. With considerable activity enhancement, recyclability and productivity, the PSNF-Gal was proven as economical and robust biocatalyst for continuous bioprocessing applications.

Acknowledgement

MM gratefully acknowledges the financial support from the Universiti Malaysia Sabah and the Malaysian Government. HZ thanks for the support from 111 Project (B12034). HPLC facility support from Paul Grbin's research group and sugar analysis assistance by Nick Van Holst are highly appreciated. MM also thankful the technical supports by Jason Peak, Jeffrey Hiorns and Michael Jung from workshop department at School of Chemical Engineering.

References

1. Xue, R.; Woodley, J. M., Process technology for multi-enzymatic reaction systems. *Bioresource Technology* **2012,***115*, 183-195.
2. Talbert, J.; Goddard, J., Enzymes on material surfaces. *Colloids and surfaces. B, Biointerfaces* **2012,***93*, 8-19.
3. Rodrigues, R. C.; Ortiz, C.; Berenguer-Murcia, A.; Torres, R.; Fernandez-Lafuente, R., Modifying enzyme activity and selectivity by immobilization. *Chemical Society Reviews* **2013,***42* (15), 6290-6307.
4. Misson, M.; Zhang, H.; Jin, B., Nanobiocatalyst advancements and bioprocessing applications. *Journal of Royal Society Interface* **2015,***12* (102), 1-8.

5. Chen, H.; Yuan, L.; Song, W.; Wu, Z.; Li, D., Biocompatible polymer materials: Role of protein–surface interactions. *Progress in Polymer Science* **2008,***33* (11), 1059-1087.
6. Palomo, J. M.; Muñoz, G.; Fernández-Lorente, G.; Mateo, C.; Fernández-Lafuente, R.; Guisán, J. M., Interfacial adsorption of lipases on very hydrophobic support (octadecyl–Sepabeads): immobilization, hyperactivation and stabilization of the open form of lipases. *Journal of Molecular Catalysis B: Enzymatic* **2002,***19-20*, 279-286.
7. Asuri, P.; Karajanagi, S. S.; Yang, H.; Yim, T.-J.; Kane, R. S.; Dordick, J. S., Increasing protein stability through control of the nanoscale environment. *Langmuir* **2006,***22*, 5833-5836.
8. Jordan, J.; Kumar, C. S. S. R.; Theegala, C., Preparation and characterization of cellulase-bound magnetite nanoparticles. *Journal of Molecular Catalysis B: Enzymatic* **2011,***68* (2), 139-146.
9. Kaur, J.; Suri, C. R., Direct hapten coated ELISA for immunosensing of low molecular weight analytes. *Protocol Exchange* **2007**. doi:10.1038/nprot.2007.508.
10. Ros, T. G.; van Dillen, A. J.; Geus, J. W.; Koningsberger, D. C., Surface oxidation of carbon nanofibres. *Chemistry – A European Journal* **2002,***8* (5), 1151-1162.
11. An, H.; Jin, B.; Dai, S., Fabricating polystyrene fiber-dehydrogenase assemble as a functional biocatalyst. *Enzyme and Microbial Technology* **2015,***68*, 15-22.
12. Rodriguez-Colinas, B.; Fernandez-Arrojo, L.; Ballesteros, A. O.; Plou, F. J., Galactooligosaccharides formation during enzymatic hydrolysis of lactose: Towards a prebiotic-enriched milk. *Food Chemistry* **2014,***145*, 388-394.
13. Lu, L.; Xu, S.; Zhao, R.; Zhang, D.; Li, Z.; Li, Y.; Xiao, M., Synthesis of galactooligosaccharides by CBD fusion beta-galactosidase immobilized on cellulose. *Bioresource Technology* **2012,***116*, 327-33.
14. Bradford, M. M., A rapid and sensitive method for the quantification of microgram quantities of protein utilizing the principle of protein-dye binding. *Analytical Biochemistry* **1976,***72*, 248-254.
15. Verma, M. L.; Barrow, C. J.; Kennedy, J. F.; Puri, M., Immobilization of beta-d-galactosidase from Kluyveromyces lactis on functionalized silicon dioxide nanoparticles: characterization and lactose hydrolysis. *International Journal of Biological Macromolecules* **2012,***50* (2), 432-7.
16. Zheng, P.; Yu, H.; Professor, Z. S.; Ni1, Y.; Zhang, W.; Fan, Y.; Xu, Y., Production of galacto-oligosaccharides by immobilized recombinant β-galactosidase from Aspergillus candidus. *Biotechnology Journal* **2006,***1* (2), 1464–1470.
17. Gosling, A.; Alftrén, J.; Stevens, G. W.; Barber, A. R.; Kentish, S. E.; Gras, S. L., Facile Pretreatment of Bacillus circulans β-Galactosidase Increases the Yield of Galactosyl Oligosaccharides in Milk and Lactose Reaction Systems. *Journal of Agricultural and Food Chemistry* **2009,***57* (24), 11570-11574.
18. Ansari, S. A.; Husain, Q., Lactose hydrolysis from milk/whey in batch and continuous processes by concanavalin A-Celite 545 immobilized Aspergillus oryzae b-galactosidase. *Food and Bioproducts Processing* **2012,***90*, 351-359.
19. Ignatova, M.; Stoilova, O.; Manolova, N.; Mita, D. G.; Diano, N.; Nicolucci, C.; Rashkov, I., Electrospun microfibrous poly(styrene-alt-maleic anhydride)/ poly(styrene-co-maleic anhydride) mats tailored for enzymatic remediation of waters polluted by endocrine disruptors. *European Polymer Journal* **2009,***45*, 2494–2504.
20. Li, Y.; Quan, J.; White, C. B.; Williams, G. R.; Wu, J.-X.; Zhu, L.-M., Electrospun polyacrylonitrile-glycopolymer nanofibrous membranes for enzyme immobilization. *Journal of Molecular Catalysis B: Enzymatic* **2012,***76*, 15- 22.

21. Park, J.-M.; Kim, M.; Park, H.-S.; Jang, A.; Min, J.; Kim, Y.-H., Immobilization of lysozyme-CLEA onto electrospun chitosan nanofiber for effective antibacterial applications. *International Journal of Biological Macromolecule* **2013,***54*, 37- 43.
22. Feng, C.; Khulbe, K. C.; Matsuura, T.; Tabe, S.; Ismail, A. F., Preparation and characterization of electro-spun nanofiber membranes and their possible applications in water treatment. *Separation and Purification Technology* **2013,***102*, 118-135.
23. Stavyiannoudaki, V.; Vamvakaki, V.; Chaniotakis, N., Comparison of protein immobilisation methods onto oxidised and native carbon nanofibres for optimum biosensor development. *Analytical and Bioanalytical Chemistry* **2009,***395* (2), 429-435.
24. Fernandez, M. F.; Sanroman, M. A.; Moldes, D., Recent developments and applications of immobilized laccase. *Biotechnology Advance* **2013,***31* (8), 1808–1825.
25. Güleç, H. A., Immobilization of β-galactosidase from Kluyveromyces lactis onto polymeric membrane surfaces: Effect of surface characteristics. *Colloids and Surfaces B: Biointerfaces* **2013,***104*, 83-90.
26. Ansari, S. A.; Satar, R.; Alam, F.; Alqahtani, M. H.; Chaudhary, A. G.; Naseer, M. I.; Karim, S.; Sheikh, I. A., Cost effective surface functionalization of silver nanoparticles for high yield immobilization of Aspergillus oryzae B-galactosidase and its application in lactose hydrolysis. *Process Biochemistry* **2012,***47*, 2427-2433.
27. Neri, D. F. M.; Balcao, V. M.; Carneiro-da-Cunha, M. G.; Jr., L. B. C.; Teixeir, J. A., Immobilization of b-galactosidase from Kluyveromyces lactis onto a polysiloxane–polyvinyl alcohol magnetic (mPOS–PVA) composite for lactose hydrolysis. *Catalysis Communications* **2008,***9*, 2334–2339.
28. Husain, Q.; Ansari, S. A.; Alam, F.; Azam, A., Immobilization of Aspergillus oryzae beta galactosidase on zinc oxide nanoparticles via simple adsorption mechanism. *International Journal of Biological Macromolecules* **2011,***49* (1), 37-43.
29. Xu, R.; Zhou, Q.; Li, F.; Zhang, B., Laccase immobilization on chitosan/poly(vinyl alcohol) composite nanofibrous membranes for 2,4-dichlorophenol removal. *Chemical Engineering Journal* **2013,***222*, 321-329.
30. Wu, L.; Yuan, X.; Sheng, J., Immobilization of cellulase in nanofibrous PVA membranes by electrospinning. *Journal of Membrane Science* **2005,***250* (1–2), 167-173.
31. Cho, E. J.; Jung, S.; Kim, H. J.; Lee, Y. G.; Nam, K. C.; Lee, H. J.; Bae, H. J., Co-immobilization of three cellulases on Au-doped magnetic silica nanoparticles for the degradation of cellulose. *Chemical Communications Cambridge* **2012,***48* (6), 886-8.
32. Rodriguez-Colinas, B.; Poveda, A.; Jimenez-Barbero, J.; Ballesteros, A. O.; Plou, F. J., Galacto-oligosaccharide synthesis from lactose solution or skim milk using the β-galactosidase from Bacillus circulans. *Journal of Agricultural and Food Chemistry* **2012,***60* (25), 6391-6398.
33. Jovanovic-Malinovska, R.; Fernandes, P.; Winkelhausen, E.; Fonseca, L., Galacto-oligosaccharides Synthesis from Lactose and Whey by beta-galactosidase immobilized in PVA. *Applied Biochemistry and Biotechnology* **2012,***168* (5), 1197-211.
34. Neri, D. F. M.; Balcao, V. M.; Costa, R. S.; Rocha, I. C. A. P.; Ferreira, E. M. F. C.; Torres, D. P. M.; Rodrigues, L. R. M.; Jr, L. B. C.; Teixeira, J. A., Galacto-oligosaccharides production during lactose hydrolysis by free Aspergillus oryzae b-galactosidase and immobilized on magnetic polysiloxane-polyvinyl alcohol. *Food Chemistry 128* **2009,***115*, 92-99.
35. Vera, C.; Guerrero, C.; Conejeros, R.; Illanes, A., Synthesis of galacto-oligosaccharides by beta-galactosidase from Aspergillus oryzae using partially dissolved and supersaturated solution of lactose. *Enzyme and Microbial Technology* **2012,***50* (3), 188-94.

36. Albayrak, N.; Yang, S. T., Production of galacto-oligosaccharides from lactose by aspergillus oryzae B-galactosidase Immobilized on on cotton cloth. *Biotechnology and Bioengineering* **2002,***77* (1), 8-19.
37. Huerta, L. M.; Vera, C.; Guerrero, C.; Wilson, L.; Illanes, A., Synthesis of galacto-oligosaccharides at very high lactose concentrations with immobilized -galactosidases from Aspergillus oryzae. *Process Biochemistry* **2011,***46*, 245-252.
38. Liu, H.; Liu, J.; Tan, B.; Zhou, F.; Qin, Y.; Yang, R., Covalent immobilization of Kluyveromyces fragilis beta-galactosidase on magnetic nanosized epoxy support for synthesis of galacto-oligosaccharide. *Bioprocess and Biosystems Engineering* **2012,***35* (8), 1287-95.

CHAPTER 6

Characterization of β-Galactosidase/Polymer-Nanofibers Nanobiocatalysts and Application for Galacto-Oligosaccharides Production

Chapter 6: Characterization of β-Galactosidase/ Polymer-Nanofibers Nanobiocatalysts and Application for Galacto-Oligosaccharides Production

Mailin Misson[1,2], Bo Jin[1], Hu Zhang[1*]

[1]School of Chemical Engineering, University of Adelaide, Adelaide, SA 5000, Australia

[2]Biotechnology Research Institute, Universiti Malaysia Sabah, Jalan UMS, 88400, Kota Kinabalu, Sabah, Malaysia

*Corresponding author:

Email: hu.zhang@adelaide.edu.au

Tel: +61 8 831 33810

In preparation for submission

2016

Statement of Authorship

Title of Paper	Characterization of β-galactosidase/Polymer-Nanofibers Nanobiocatalysts and Application for Galactoligosaccharides
Publication Status	☐ Published ☐ Accepted for Publication ☐ Submitted for Publication ☑ Unpublished and Unsubmitted work written in manuscript style
Publication Details	Mailin Misson, Bo Jin, Hu Zhang *In preparation for submission.*

Principal Author

Name of Principal Author (Candidate)	Mailin Misson		
Contribution to the Paper	Designed and performed experiments, interpreted data and wrote the manuscript.		
Overall percentage (%)	70 %		
Certification:	This paper reports on original research I conducted during the period of my Higher Degree by Research candidature and is not subject to any obligations or contractual agreements with a third party that would constrain its inclusion in this thesis. I am the primary author of this paper.		
Signature		Date	19.02.2016

Co-Author Contributions

By signing the Statement of Authorship, each author certifies that:

i. the candidate's stated contribution to the publication is accurate (as detailed above);

ii. permission is granted for the candidate in include the publication in the thesis; and

iii. the sum of all co-author contributions is equal to 100% less the candidate's stated contribution.

Name of Co-Author	Bo Jin		
Contribution to the Paper	Supervised development of work and manuscript evaluation.		
Signature		Date	19/02/2016

Name of Co-Author	Hu Zhang		
Contribution to the Paper	Supervised development of work, data interpretation, manuscript evaluation and acted as corresponding author.		
Signature		Date	18/02/2016

Please cut and paste additional co-author panels here as required.

Abstract

Advances in the knowledge of biocatalyst adsorption on an interface can help minimizing enzyme denaturation, which ultimately maintains or improves enzyme functionality. In this study, the nanobiocatalyst prepared by assembling β-galactosidase on chemically modified polystyrene nanofibers (PSNF) was extensively characterized. PSNF were fabricated through electrospinning and modified using a chemical oxidation method to facilitate enzyme binding. Characterizations on the nanobiocatalyst properties were performed before and after biocatalyst immobilization. The findings show surface oxidation has enhanced the nanofiber wettability. A thin layer and homogenous biocatalyst was found to cover the PSNF surface under a scanning electron microscopy (SEM), which was also confirmed from fluorescence images by labelling β-galactosidase with fluorescein isothiocyanat (FITC). Peaks featuring β-galactosidase were identified on the PSNF surface after immobilizing the enzyme based on FTIR spectra, indicating the formation of the nanobiocatalyst due to β-galactosidase adsorption. The biocatalyst distributions and conformations were confirmed from Raman spectral and microscopic analysis. The effectiveness factor for lactose conversion into galacto-oligosaccharides (GOS) in a disc-stacked column reactor demonstrated distinguished biocatalyst performance in comparison to the free counterpart. The characterizations and bioreaction studies indicate successful formation of β-galactosidase-based nanobiocatalyst on the polymer nanofibers while the enzyme conformation structures were retained.

Keywords: β-galactosidase, polymer nanofiber, immobilization, interfacial reaction, conformational change.

6.1 Introduction

Enzyme immobilization onto nanocarriers to form the nanobiocatalyst can enhance enzyme stability and activity, and simplify recycling and downstream processing. However, biocatalysts may encounter structural changes upon immobilization due to protein conformation changes on the interface, which often results in reduction of catalytic activity. Hence, understanding the biocatalyst adsorption phenomena on a solid surface is of a profound research interest. Conformational analysis is a fundamental step to prepare optimal biocatalyst-nanomaterial hybrids and it also provides great insights into improving the biocatalyst efficiency. This analysis can help fabricating biocompatible enzyme carriers, because from an industrial standpoint, specific supports may be requested due to economic processes or easy handling procedures. It has been recognized that investigation of protein adsorption on a solid surface is a fascinating endeavor but a great complexity [1]. In comparison to free enzyme, the presence of enzyme supports or carriers can complicate both experimental data collections and their theoretical interpretations [2].

There are many factors involved in enzyme conformational changes including the features of enzyme molecules and the support material (e.g., size, topography), external factors (e.g., pH and temperature) as well as interaction forces (e.g., polar or hydrophobic/hydrophilic) [2-4]. The sequence of amino acids in proteins determines their secondary structures such as helixes, β-sheet and turns. Alteration of these structures might affect the catalytic reactions due to the change in enzyme orientation and conformational mobility [5]. Exposing hydrophobic amino acids into a hydrophilic environment is also unfavourable to retain the enzyme's native conformation. Small nanopores for bigger biomolecules [6], a high surface charge density [7], and strong biomolecule binding [8] are among the possible causes of enzyme distortion or deactivation. Furthermore, incorrect orientation of enzyme upon binding onto the surface or multilayer formation as a result of high enzyme loading may lead to reduction in the enzyme activity [2].

A number of techniques for advanced characterizations are capable of providing key information of not only the characteristics of enzyme supports, but also of the enzyme distribution on the surface and the interfacial reactions between the enzyme and its support. A review on advanced characterizations of enzymes on immobilized supports has been extensively described by Bolivar *et al.* [9], embracing the immobilization assessment,

catalyst distribution imaging and structural elucidation. The presence of trypsin entrapped in electrospun poly (caprolactone) nanofibers has been demonstrated using SEM, TEM and fluorescence microscopy [10]. In a recent study, micro-attenuated total reflection fourier transform infrared (micro-ATR FTIR) was adopted to study the secondary structure of sol-gel immobilized glucose oxidase [11]. Xiao *et* al. [12] applied a confocal Raman microscopy to measure conformation and distribution of protein adsorbed in wetted chromatographic particles. By combining the frequency vibration spectroscopy and attenuated total reflectance FTIR-spectroscopy, Liu *et al.* [13] found the interfacial orientation of the immobilized β-galactosidase exhibited a well-correlation with the tested activity.

However, unravelling the enzyme behaviour on a confined solid surface still presents a longstanding core challenge. Attempts in understanding enzyme adsorption are restrained by diverse immobilization protocols, which each may require specific approaches to deepen the mechanistic understanding. There are very few studies reporting the fundamental mechanisms and interfacial reactions associated with the nanomaterial-immobilized nanobiocatalyst. The guidelines for selecting appropriate nanocarriers for the immobilized enzyme molecules have yet to be established.

In this work, the assembly of β-galactosidase on a chemically-modified polystyrene nanofiber (PSNF) surface was investigated. Nanofibers have been known as a great enzyme carrier due to its intrinsic advantages including a high surface area for enzyme loading, a high porosity and excellent interconnectivity [14]. β-Galactosidase was chosen to catalyze the bioconversion of lactose in dairy industry wastes into galactooligosaccharides (GOS). GOS is a high value functional food ingredient, offering a range of important health functions in living systems including prebiotic benefits and low caloric sugar alternatives [15]. The PSNF surface was treated with oxidizing agents to create oxygen-containing reactive groups such as carboxyl (COOH) and hydroxyl (OH) to facilitate β-galactosidase binding [16-17]. To maximize the enzyme catalytic activity towards synthesis of GOS, the β-galactosidase/PSNF nanobiocatalyst has been physically and chemically characterized to understand the enzyme/support interactions. The nanobiocatalyst was further evaluated in a column reactor for its performance in synthesizing GOS. The correlation between the enzyme conformation structure and its engineering performance was built, which may provide great insights for fabricating other nanobiocatalysts.

6.2 Materials and Methods

Polystyrene polymer (molecular weight: 350,000), *N*,*N*-dimethylformamide (DMF) and nitric acid (HNO_3) were of analytical grade without further purification. Fluorescein isothiocyanate (FITC), bovine serum albumin (BSA) and *Kluyveromyces lactis* β-galactosidase were purchased from Sigma-Aldrich, lactose monohydrate by Chem Supply and potassium phosphate buffer (PBS, pH 7.2) by Life Technologies.

6.2.1 Synthesis of Polymer Nanofibers

Approximately 10 ml of polystyrene (20 %, w/v) was dissolved in DMF solvent in a flask at 100 rpm for overnight at room temperature. The resultant homogenous solution was placed inside a 5-mL syringe in an electrospinning device. The syringe attached to a 1-mm inner diameter needle tip which was connected to a Glassman high voltage power supply (25 kV). The flow rate of the polymer solution was controlled at 2.5 ml/h by an Adelab Scientific syringe pump. The electrospun polystyrene nanofibers (PSNF) were cast onto a metal-surface collector. The distance between the needle tip and the collector was fixed about 10 cm. The PSNF was detached from the collector surface and stored at room temperature until further use.

6.2.2 β-Galactosidase Immobilization Procedure

The PSNF surface was modified by immersing nanofiber mats (1.5 cm radius), approximately 20-30 mg, into 5 ml HNO_3 (69%) for 2 h at room temperature [17]. The acid-modified support was rinsed with water for three times to remove excess acid and further equilibrated with PBS solution (pH 7.2) overnight prior to enzyme immobilization. β-galactosidase immobilization was carried out by submerging the modified PSNF into β-galactosidasesolution in PBS (2 mg/ml). The mixtures were gently mixed overnight at 4 ^{o}C. The β-galactosidase–loading PSNF were rinsed thoroughly with water to remove unbound enzyme.

6.2.3 Characterization of Polymer Nanofibers

The textural properties of untreated PSNF, treated PSNF, and β-galactosidase-loaded treated PSNF were characterized using scanning electron microscopy (SEM) under a Philips XL30 field emission scanning electron microscope operated at 10 kV. A small piece of each sample was placed on a metal support and coated with a layer of platinum (5 μm) by ion sputtering before SEM analysis.

An Attension Theta Optical Tensiometer was used to measure the contact angle of the treated and untreated PSNFs. A thin layer of the PSNF samplewith a homogenous surface was located on a glass microscope slide before a water droplet was introduced onto the surface. The One Attension software was used to analyse the wettability properties of the samples.

A Zeiss Axio Fluorescence microscope was used to image the presence and distribution of FITC-labelled β-galactosidase on the polymer nanofiber surface. The labelled samples were prepared by mixing a proportion of 100 mg of β-galactosidase with 10 μg of FITC in 1 ml ethanol (70 %) solution with gentle mixing before addition of PSNF. The β-galactosidase-PSNF assembly was allowed to react for 2 h at 4 ^{o}C in a dark condition. A thin layer of the PSNF loading FITC-labelled β-galactosidase was placed onto a glass microscope slide, observed under the fluorescence microscope and analysed using the Zen2 software. A PSNF-Gal without fluorescence excitation was used as a negative control.

Fourier transform infrared (FTIR) spectra of the free β-galactosidase,β-galactosidase-loaded PSNF and β-galactosidase-free PSNF were recorded on a Thermo Scientific NICOLET 6700 FTIR spectrometer at room temperature. Background spectra were first acquired prior to each sample measurement. The analysis was controlled using the OMNIC software.

The Confocal Raman spectroscopy was carried out using a Horriba XploRA™PLUS confocal Raman microscopy equipped with a charge coupled device (CCD) detector. Samples were placed onto a glass microscope slide and focused at a 50x objective-lens magnification. Laser at 532 nm was used to excite the sample. Spectra were collected at

600 gr/mm diffraction grafting with an acquisition time (s) of 0.5 and analyzed using the LabSpec 6 software.

6.2.4 Lactose Bioconversion into Galacto-Oligosaccharides

Lactose conversion was carried out in an in-housecolumn reactor consisting of six holders, each containing a disc-like layer of β-galactosidase-loading PSNF (1.5 cm radius). The holders were stacked on top of each other to form a 12-cm height column with a total working volume of 6 ml. The substrate from a reservoir tank was fed into the column from the top inlet through the Eur-Pharm silicone tubing. A Masterflex 7021-24 (USA) pump was used to control the feed flow rate. The resulting products were collected at the bottom outlet of the column,channelled back into the reservoir tank and recirculated into the reactor system. Lactose in the feed reservoir was prepared by dissolving it into PBS (pH 7.2) at 60 ^{o}C and then cooling down to 37 ^{o}C prior to reactions. Samples were drawn after 24 h for carbohydrate analysis. They are immediately heated in boiling water for 5 min to deactivate enzymes [18-19]. Samples were filtered using 0.45 μm nylon filters and diluted prior to carbohydrate analysis using high performance liquid chromatography (HPLC). The yield of conversion and products were determined using Eq. (1-4) while the effectiveness factor of immobilization was calculated using Eq. (5), where brackets represent the mass concentration.

$$\text{Conversion (\%)} = \frac{[Initial\ lactose]-[Final\ lactose]}{[Initial\ lactose]} \times 100\% \quad (1)$$

$$\text{Glucose (\%)} = \frac{[Glucose]}{[Initial\ Lactose]} \times 100\% \quad (2)$$

$$\text{Galactose (\%)} = \frac{[Galactose]}{[Initial\ Lactose]} \times 100\% \quad (3)$$

$$\text{GOS (\%)} = \%\ conversion - \%\ glucose - \%\ galactose \quad (4)$$

$$\text{Effectiveness factor} = \frac{[GOS]_{immobilized\ enzyme}}{[GOS]_{free\ enzyme}} \quad (5)$$

6.2.5 Chemical Analysis

Remaining substrate and products were analysed in Agilent 1100 Series HPLC using an Aminex HPX-87H column (300 x 7.8 mm) with a refractive index detector, pump and an autosampler. The flow rate of a pre-degassed mobile phase (8mmol/L-H_2SO_4) was set at 0.5 ml min^{-1}. The column and the detector cell were maintained at 60 ^oC and 40 ^oC, respectively [20]. Chromatograms were integrated using the ChemStation software.

6.3 Results and Discussion

6.3.1 Textural Properties of Polymer Nanofibers

The properties of polymer nanofibers play an important role in binding β-galactosidase and enzyme-catalyzed reactions. To modify the surface property for enzyme immobilization and biocatalysis, the surface was chemically modified using a strong oxidizing agent for 2 h, 10 h and 24 h to create oxygen-containing reactive groups such as carboxyl (COOH) and hydroxyl (OH) which may facilitate β-galactosidase binding [17]. The effect of surface modifications on mechanical stability and wettability of the nanofibers was examined. Figure 6.1 indicates that the nanofiber surface pretreatment led to changes in the surface properties. In comparison with the non-modified PSNF that exhibited a smooth surface and a homogenous structure (Figure 6.1a) with a diameter of 1.06 μm for a single nanofiber, surface damages were observed on the pre-treated PSNF witnessing minimal defects at 2-h pretreated PSNF but the dimension was nearly the same as the non-modified PSNF (Figure 6.1b), while longer pretreatment (for 10 h or 24 h) (Figure 6.1c-d) resulted in more destruction, making the surface rougher and more heterogeneous with some observable small pieces ripped off from the original nanofibers, and shrinking the size of the diameter for single nanofibers. The 2-h pretreated PSNF was therefore selected for further characterization and compared with the untreated PSNF.

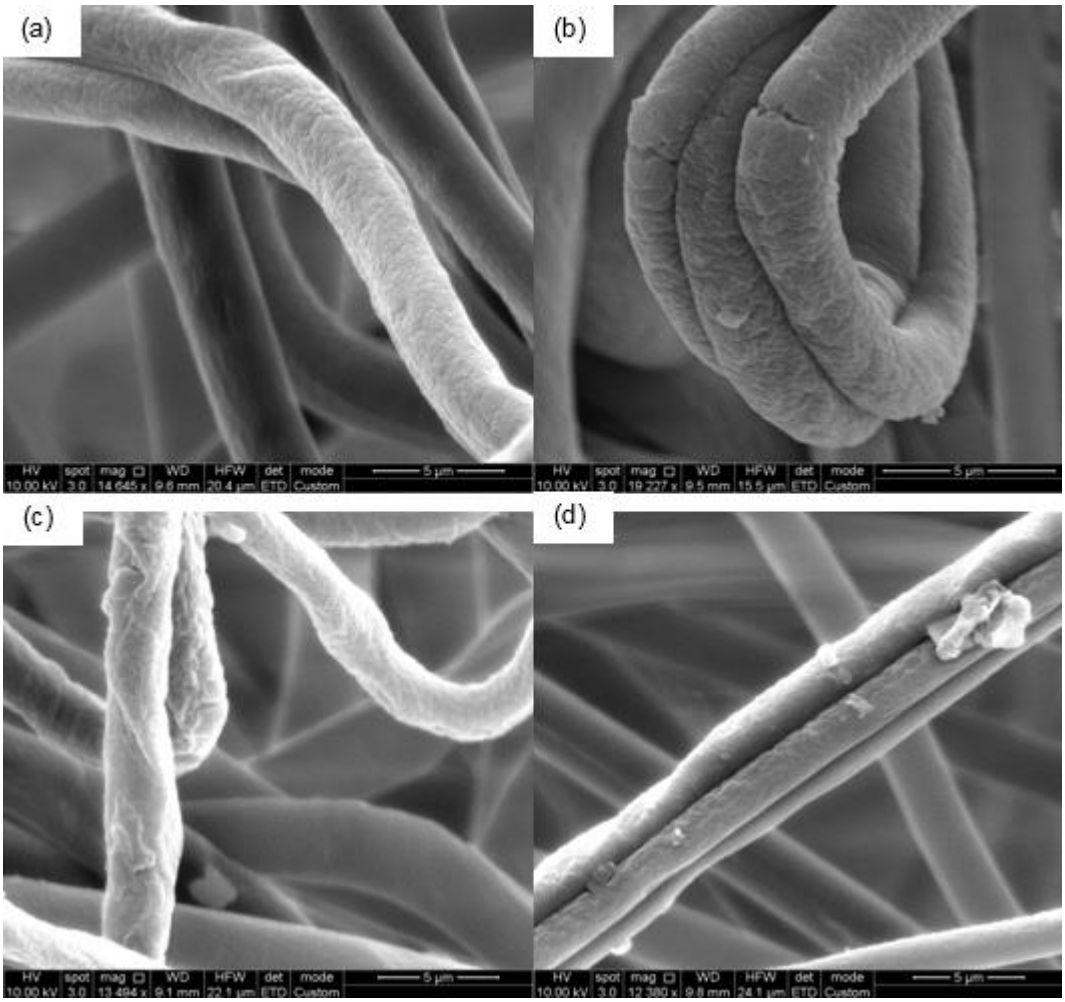

Figure 6.1 SEM images of (a) untreated, (b) 2 h acid treated, (c) 10 h acid-treated, and (d) 24 h acid-treated nanofibers.

Surface treatment not only resulted in morphological changes for the nanofibers, but also the wettability of the surface. Wettability, governed by the chemical composition and the surface geometrical microstructure, has been recognized as one of the most important properties for nanofibrous materials [21]. Poor wettability of polystyrene nanofibers has hampered their applications due to adhesion with other materials and heterogeneous dispersion in an aqueous solution [22]. The wettability of the 2-h treated and untreated PSNF was characterized by contact angles (Table 6.1) and the angle θ is generally known as the wetting angle [23]. A small contact angle represents greater hydrophilicity or wettability. It can be seen that the treated PSNF exhibited a smaller contact angle (84°) than the untreated PSNF (106°). It indicates the surface modification has increased the PSNF wettability. A possible explanation for this might be due to the introduction of OH or COOH groups that have brought a hydrophilic feature on the interface. The presence of these active groups on

the surface-oxidized polymer surface has been confirmed in detailed characterizations reported in previous work [17]. The wettability behaviour was also found correlated with the surface roughness. A higher wettability (θ <90°) occurred on a rougher surface (Figure 6.1b) in comparison with the wettability (θ >90°) of the native PSNF (Figure 6.1a). Therefore, surface modifications by the oxidative method not only have changed the surface morphology of nanofibers but also improved the fiber wettability.

Table 6.1 Contact angle measurement of nanofibers.

Nanofibers	Contact Angle [°]
Untreated PSNF	106
2 h acid-treated PSNF	84

6.3.2 Physical Characterization of Polymer Nanofibers/ β-Galactosidase Nanobiocatalysts

After the nanofibers were treated, they were employed for preparation of nanobiocatalysts. One of the key issues for the nanobiocatalyst is the distribution of bound proteins on the support nanocarriers. The most common method is to visualize the morphological changes of the nanofibers after enzyme immobilization under a SEM, alternatively, the distribution can be analyzed from the fluorescence-assisted images under a fluorescence microscope after the enzyme is tagged with fluorescence molecules [9]. Although minor cracking is noticed on some nanofibers, all enzyme-loading nanofibers have nearly identical thickness, which means that a thin layer and uniform coating of enzyme covers the PSNF surface, which can be observed by comparing the SEM images of β-galactosidase-free PSNF (Figure 6.2a-b) and β-galactosidase-loaded PSNF (Figure 6.2c-d). These findings are consistent with a recent study that presented a homogenous antibody coating on the polyethersolfone electrospun nanofibrous membrane due to hydrophobic interactions [24].

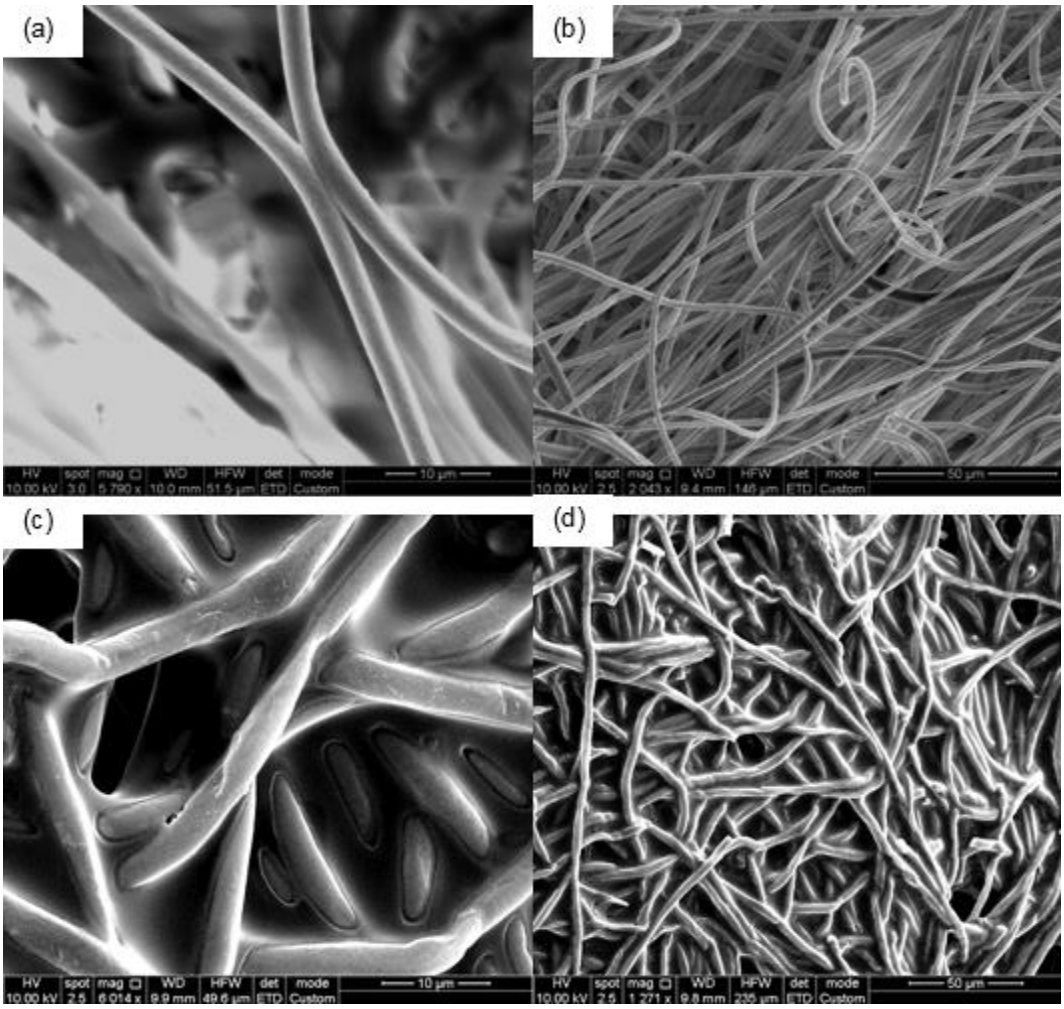

Figure 6.2 SEM images of (a-b) β-galactosidase-free PSNF and (c-d) β-galactosidase-loaded PSNF at 10 µm and 50 µm.

The fluorescence microscope that provides an efficient and unique approach to study fixed and living cells [25] was also used to demonstrate the successful immobilization of β-galactosidase on the nanofiber surface. A fluorescence-based strategy has been applied to visualize structural proteins in live cells [26] and to rapidly detect cellular deoxiribonucleoside triphosphates [27]. In this study, the enzyme was initially labelled with FITC, immobilized onto PSNF surface afterwards and imaged directly by a fluorescence microscope (Figure 6.3). The observation was compared with the negative control of PSNF-β-gal without fluorescence excitation as shown in Figure 6.3c. PSNF without enzyme under the same fluorescence conditions was used to account for the fluorescence background (Figure 6.3a). As Figure 6.3b indicates, the nanobiocatalyst consisting of

electrospun PSNF fibers and FITC-labeled β-galactosidase emitted green fluorescence, indicating the presence of homogenously distributed enzyme on the fiber surface.

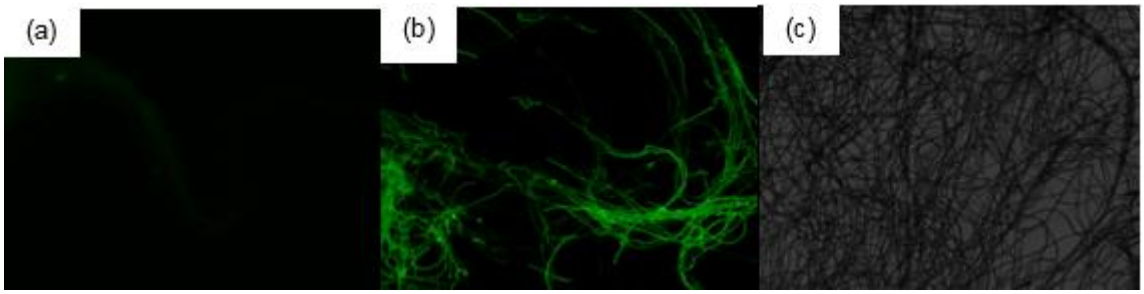

Figure 6.3 Visualization of FITC-tagged enzyme using fluorescene microscope: (a) PSNF fluorescence background, (b) FITC-PSNF-β-Gal fluorescence image excitation (c) negative control PSNF-β-gal without fluorescence excitation.

6.3.3 Chemical Characterization of Polymer Nanofibers/ β-Galactosidase Nanobiocatalysts

The attachment of β-galactosidase on nanofibers surface was further clarified using FTIR analysis. FTIR is a powerful tool to assess the formation of protein-surface interactions by detecting the bond formation generated by the wavelength and intensity of IR radiation [28]. Figure 6.4 shows the FTIR spectra of β-galactosidase-free PSNF, free β-galactosidase and β-galactosidase-loaded PSNF.

The characteristic signals of the β-galactosidase-free PSNF are represented by the peaks at 3100, 1493, 1451, 1150, 905, 754, and 700 cm^{-1} (Figure 6.4a). Meanwhile, the β-galactosidase spectra show the peaks at 3290, 1640, 1405, 1310, 1230, 1100 and 1050 cm^{-1}(Figure 6.4b). After assembling β-galactosidase on PSNF, three new peaks were detected at 3290, 1641 and 1230 cm^{-1} (Figure 6.4c) in comparison with PSNF alone (Figure 6.4a). These characteristic peaks correspond to the spectra generated by β-galactosidase. According to Verma *et al.* [29], the vibrations of O-H and N-H groups of enzyme occur between 3000 and 3500 cm^{-1} while there is no peak at this range for PSNF. Therefore, the peak recorded at 3290 cm^{-1} is due to the presence of the immobilized β-galactosidase. Similarly, the peak at 1641 cm^{-1} corresponds to C=O stretch vibrations of peptide linkages produced by amide I protein [28] whereas the signal at 1230 cm^{-1} ascribes to C-N stretching

and N-H bending. The FTIR analysis indicates successful incorporation of β-galactosidase on the polymer nanofibers.

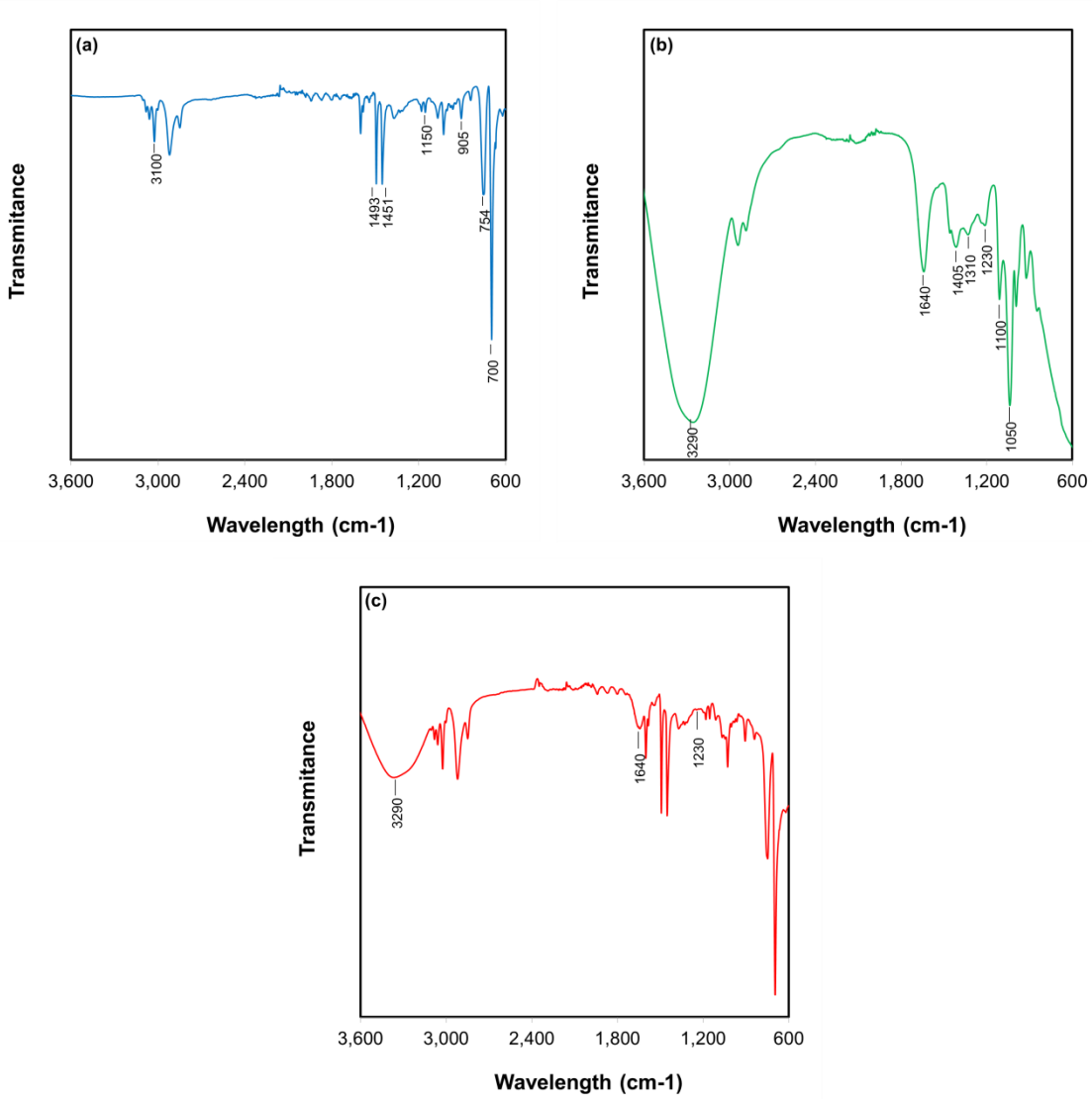

Figure 6.4 FTIR spectra of (a) β-galactosidase-free PSNF, (b) free β-galactosidase and (c) β-galactosidase-loaded PSNF.

Raman spectroscopy is a label-free and non-destructive technique to analyze the protein secondary structure [30]. Recent advancement of this technology offers the combination of (i) Raman microscopy, a method that allows visualization of the localized zone of a sample under a microscope and collection of generated Raman signals for that zone using a spectrometer, and (ii) Raman spectral imaging, also known as Raman

mapping, a method that enables the mapping of the spatial resolution of protein molecules and generates chemical images based on Raman spectrum of sample.

Both techniques were employed in this study as illustrated in Figure 6.5 to analyze the β-galactosidase-free PSNF and the β-galactosidase-loaded PSNF. Similar to the FTIR analysis, the difference of the spectra between the β-galactosidase-free and β-galactosidase-loaded PSNF represents the protein adsorbed on the polymer nanofibers. According to the Raman microscopy analysis (Figure 6.5a-b), new bands were detected at 1096, 1339, 1450, 1536, 1667 cm^{-1} in the β-galactosidase-loaded PSNF. The frequency observed at 1667 cm^{-1} is a characteristic peak for β-sheet conformation produced by amide I due to C=O stretching vibration with minor contributions of C-N stretching and N-H bending [31]. The finding is also in agreement with [12] that reported the detection of the amide I structure to confirm the protein adsorption on chromatographic particles. However, the limitation of this standard optical microscopy is lack of accuracy in localizing biocatalyst on the nanomaterial supports. The microscopic analysis was carried out at a randomly chosen location on the sample surface. It may generate a low intensity/no Raman signal for the protein secondary structure at a location with minimal or no presence of β-galactosidase.

Raman mapping studies, which can generate false colour images based on the material composition and structure, were therefore executed. The generated image describes the distribution of biomolecules on the support surface. As Figure 6.5c depicts, two different images were generated representing the biocatalyst and the support surface. PSNF was denoted by the red spectrum proven by its location beneath the green spectrum of β-galactosidase. The accumulated spectra of the image at a location of x = -5 μm and y = -1 μm show two images are overlapping, indicating binding of the enzyme on the nanofiber surface (Figure 6.5d). For every pixel of the imaging a complete spectrum can be acquired for further analysis. The spectra at the selected location can be identified and translated into Raman signals based on their molecular structures, as illustrated in Figure 6.5e and 6.5f for the red and green spectrum, respectively. Although the Raman microscope and Raman mapping show considerable consistence in identifying and elucidating the conformation structure of a protein, in comparison to Figure 6.5b (Raman spectrum), more new bands (930, 1100, 1245, 1340, 1400, and 1450 cm^{-1}) with a stronger intensity were generated in Figure 6.5f (Raman mapping). The band at 1245 cm^{-1} represents amide III vibrations attributed to the C-N stretching vibrations and N-H bending

with small contributions from C-C and C-O vibrations [32]. Amide III band can be correlated with the amide I due to the complementary protein structure, comprising three assignment categories: i) α-helix ((1270-1300 cm^{-1}), ii) random coil (1243-1253 cm^{-1}) and iii) β-sheet (1229-1235 cm^{-1})[33]. The band at 1245 cm^{-1} is therefore identified to exhibit a random coil assignment. Moreover, a tryptophan amino acid was found at 1340 and 1360 cm^{-1} bands [34], additionally supporting the presence of immobilized β-galactosidase.

The SEM and fluorescence microscopy images altogether with FTIR and Raman analysis manifest the distribution and attachment of β-galactosidase onto the PSNF surface. No apparent band shifting in FTIR analysis for the immobilized β-galactosidase comparing with the free enzyme suggests no changes in the secondary structures of the biocatalysts.

6.3.4 Production of GOS by the Nanobiocatalyst in a Column Reactor

After examining the the nanobiocatalyst structure, the performance of the immobilized β-galactosidase in lactose conversion in a column reactor was evaluated as displayed in Figure 6.6. Lactose conversion is generally performed in two different pathways: (1) hydrolysis when water acts as the galactosyl acceptor, yielding glucose and galactose as the main products, or (2) transgalactosylation when nucleophilic molecules replace water to generate galacto-oligosaccharide (GOS). GOS is highly pursued due to their health functionalities [35-36]. Therefore, the transgalactosylation pathway is prefered in such a reactor. Meanwhile, lactose concentration in the dairy wastes needs to be reduced to minimize the environment impact, therefore, lactose conversion is also considered in the catalytic process.

The conversion improved with an increase in feeding rate, reaching a peak of 83 % at a feeding rate of 150 g/h before displaying a declining profile (Figure 6.6a). The formation of GOS, glucose and galactose at different feed rates shared a similar trend with conversion (Figure 6.6b). The highest yielded GOS was 36 % while glucose and galactose were 32 % and 16 %, respectively. It was observed that up to the optimum condition (150 g/h feeding rate), the GOS formation exceeded the yield of glucose and galactose which implies the transgalactosylation was preferred at a slower supply of lactose into the reactor. An increase in the feed rate resulted in a comparable transgalactosylationand hydrolysis rate, however, further increase in the feed rate led to hydrolysis dominated in the reactor.

At a faster feeding rate, the contact time for the interfacial reaction between lactose nucleophiles and the enzyme-galactosyl complex reduced, and more water molecules constantly penetrated into the enzyme-galactosyl complex site and occupied the site, therefore, water activity is dominant in the catalytic site. Thus, small yield of GOS was found at a higher feed rate.

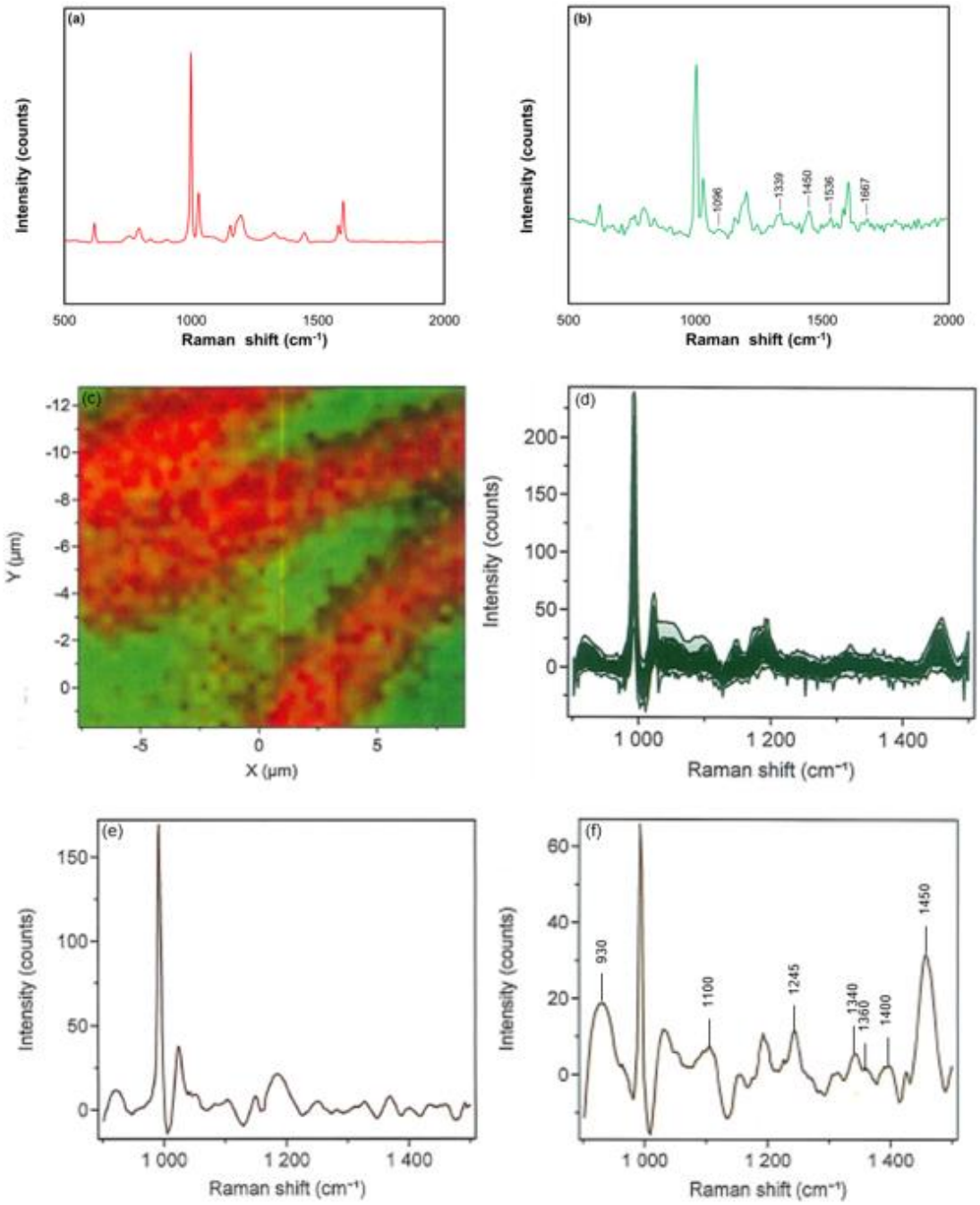

Figure 6.5 Raman spectrum analysis of (a) β-galactosidase-free PSNF and (b) β-galactosidase-loaded PSNF, (c) Raman mapping false colour image of β-galactosidase-loaded PSNF, scale bar 2μm, (c) accumulated signals for the red and

green spectrum, (d) Raman signals for the red spectra, (e) Raman signals for the green spectra.

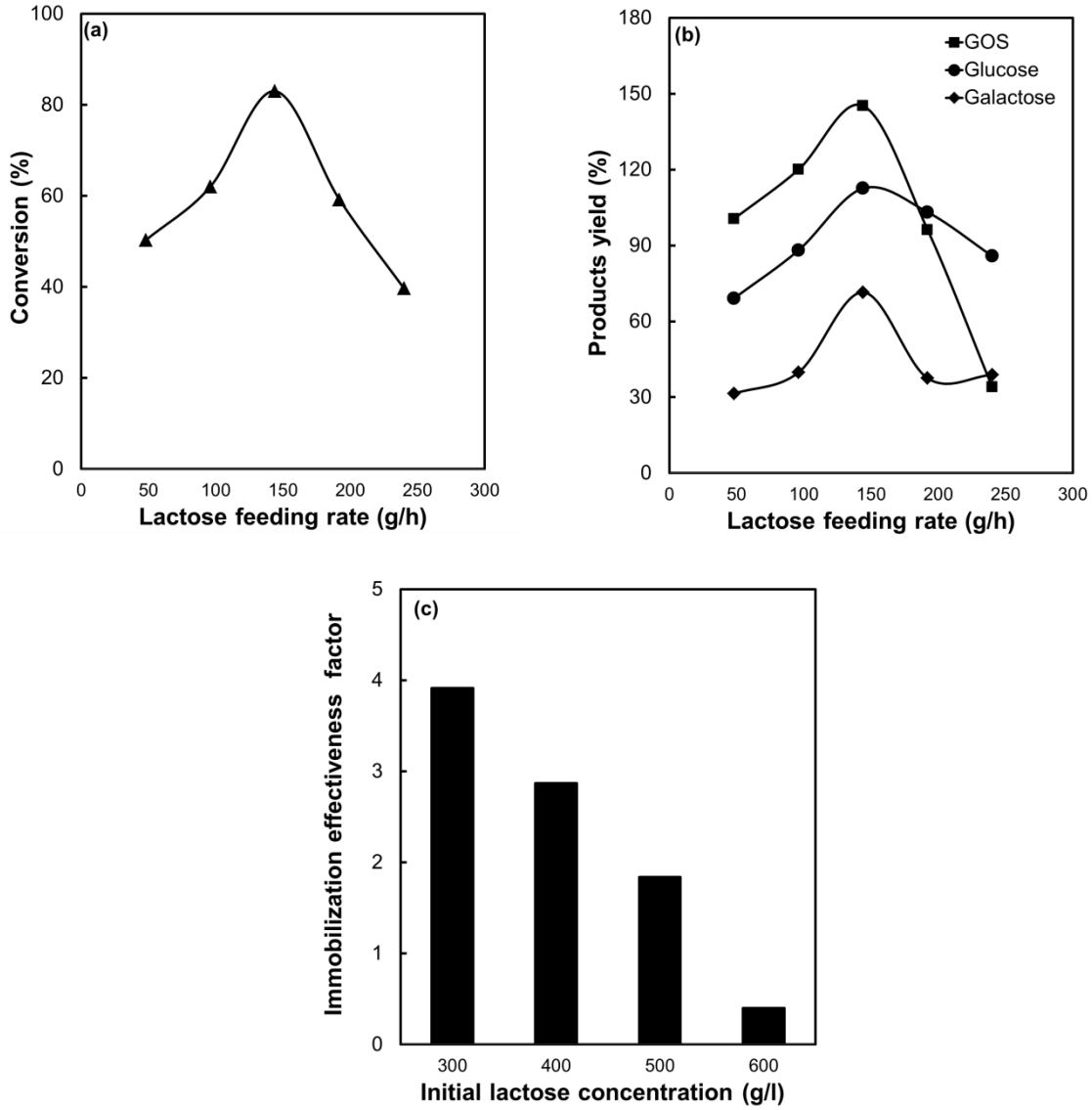

Figure 6.6 The effect of substrate feeding rate on (a) lactose conversion and (b) production yield and (c) the immobilization effectiveness factor at different initial lactose concentration by PSNF-Gal. Reactions were conducted at 37 ^{o}C using 2 mg/ml enzyme concentration in pH 7 for 24 h reaction time in recirculationg stacked column reactor.

The catalytic effectiveness factor is one of the important parameters for evaluating immobilized enzymes in industrial applications [37]. It is determined by dividing the activity of the immobilized enzyme by that of the corresponding free enzyme at the same amount.

The parameter is used to benchmark the activity of the immobilized β-galactosidase as depicted in Figure 6.6c. Apparently, the effectiveness factor is dependent on the substrate concentration. It declined significantly when the lactose concentration increased. The findings are consistent with the report by Liese *et al.* [37] that the substrate concentration influences the effectiveness factor. At a high lactose concentration of 600 g/l, it was observed the activity of the free β-galactosidase exceeded the immobilized enzyme. It has been recognized that lactose has a low solubility and forms a crystal-like substance at a high concentration [38]. Comparing with the immobilized biocatalyst, enzyme in free solution had a greater diffusion rate to facilitate a higher bioconversion of lactose prior to occurrence of crystallization. The effectiveness factor, however, was favourable at a substrate concentration below 600 g/l. At 300 g/l lactose, the effectiveness factor was approximately 8 times higher than that at 600 g/l. It may conclude that the immobilized biocatalyst was superior to the free counterpart at a lower initial lactose concentration in the column reactor. The performance of the immobilized β-galctosidase on the polymer nanofibers was also comparable or greater than that in other reported studies (Table 6.2), indicating remarkable stability and activity of the biocatalyst under the operational conditions.

Table 6.2 Comparison on lactose bioconversion and GOS yield by immobilized enzymes in various types of support materials.

Source of β-galactosidase	Reactor	Support material	Lactose g/l	Conversion %	GOS %	Reference
Kluyveromyces lactis	Batch spiral reactor	Polystyrene nanofibers	400	82	36	This work
Kluyveromyces lactis	Batch process	Modified polystyrene nanofibers	400	40	28	[39]
Kluyveromyces lactis	Continuous ultrafiltration membrane reactor	Membrane	300	76	80	[40]
Bacillus circulans	Repetitive batch-wise	Eupergit C250L	550	-	64	[41]
Bacillus circulans	Repeated batch	Glyoxyl agarose	500	60	39	[42]
Bacillus circulans	Batch process	-	400	50	41	[43]
Aspergillus oryzae	Batch process	Polysiloxane-polyvinyl alcohol	500	55	26	[44]

6.4 Conclusion

A comprehensive analysis study has been carried out to advance the understanding of β-galactosidase/nanofiber nanobiocatalyst structure. The homogenous biocatalyst distribution on the support surface was demonstrated by SEM and fluorescence microscopy images. The FTIR showed a few feature peaks of enzymes on the surface of the enzyme-loaded PSNF, indicate successful biocatalyst attachment on the PSNF surface. In comparison with the free enzyme signals, no shifting of bands was observed, suggesting the native structures of biocatalyst were retained. The biocatalyst amide I and other structures were identified by Raman microscopic examinations. Raman mapping further supports the distribution of β-galactosidase on the PSNF surface. These observations were well correlated with the biocatalyst bio-engineering performance comparing with the free enzyme in a bioreactor, signifying the native conformation of biocatalysts has been well preserved, thus leading to remarkable biocatalyst stability and activity under the operational conditions. The findings of this study provide useful insights into understanding of the structure and interfacial reactions of nanomaterial-enzyme assemblies.

Acknowledgement

MM gratefully acknowledges the financial support from the Universiti Malaysia Sabah and the Malaysian Government. The HPLC facility support from Paul Grbin's research group and sugar analysis assistance by Nick Van Holst, Raman analysis assistance by Umar Azhar, analytical supports by Dr Qiuhong Hu at Analytical Lab School of Chemical Engineering, and the SEM analysis from Adelaide Microscope are highly appreciated.

References

1. Rabe, M.; Verdes, D.; Seeger, S., Understanding protein adsorption phenomena at solid surfaces. *Advances in Colloid and Interface Science* **2011,***162* (1–2), 87-106.
2. Secundo, F., Conformational changes of enzymes upon immobilisation. *Chemical Society Reviews* **2013,***42* (15), 6250-6261.
3. Ba, O. M.; Hindie, M.; Marmey, P.; Gallet, O.; Anselme, K.; Ponche, A.; Duncan, A. C., Protein covalent immobilization via its scarce thiol versus abundant amine groups: Effect on orientation, cell binding domain exposure and conformational lability. *Colloids and Surfaces B: Biointerfaces* **2015,***134*, 73-80.
4. Zhuang, W.; Zhang, Y.; Zhu, J.; An, R.; Li, B.; Mu, L.; Ying, H.; Wu, J.; Zhou, J.; Chen, Y.; Lu, X., Influences of geometrical topography and surface chemistry on the stable immobilization of adenosine deaminase on mesoporous TiO2. *Chemical Engineering Science* **2016,***139*, 142-151.
5. Talbert, J.; Goddard, J., Enzymes on material surfaces. *Colloids and Surfaces. B, Biointerfaces* **2012,***93*, 8-19.
6. Sang, L. C.; Coppens, M. O., Effects of surface curvature and surface chemistry on the structure and activity of proteins adsorbed in nanopores. *Physical Chemistry Chemical Physics* **2011,***13* (14), 6689.
7. Xie, Y.; Zhou, J.; Jiang, S., Parallel tempering monte carlo simulations of lysozyme orientation on charged surfaces. *The Journal of Chemical Physics* **2010,***132* (6), 065101.
8. Koutsopoulos, S.; Patzsch, K.; Bosker, W. T. E.; Norde, W., Adsorption of trypsin on hydrophilic and hydrophobic surfaces. *Langmuir* **2007,***23* (4), 2000-2006.
9. Bolivar, J. M.; Eisl, I.; Nidetzky, B., Advanced characterization of immobilized enzymes as heterogeneous biocatalysts. *Catalysis Today* **2016,***259, Part 1*, 66-80.
10. Pinto, S. C.; Rodrigues, A. R.; Saraiva, J. A.; Lopes-da-Silva, J. A., Catalytic activity of trypsin entrapped in electrospun poly(ϵ-caprolactone) nanofibers. *Enzyme and Microbial Technology* **2015,***79–80*, 8-18.
11. Delfino, I.; Portaccio, M.; Ventura, B. D.; Mita, D. G.; Lepore, M., Enzyme distribution and secondary structure of sol–gel immobilized glucose oxidase by micro-attenuated total reflection FT-IR spectroscopy. *Materials Science and Engineering: C* **2013,***33* (1), 304-310.
12. Xiao, Y.; Stone, T.; Bell, D.; Gillespie, C.; Portoles, M., Confocal Raman Microscopy of Protein Adsorbed in Chromatographic Particles. *Analytical Chemistry* **2012,***84*, 7367-7373.
13. Liu, Y.; Ogorzalek, T. L.; Yang, P.; Schroeder, M. M.; Marsh, E. N. G.; Chen, Z., Molecular Orientation of Enzymes Attached to Surfaces through Defined Chemical Linkages at the Solid–Liquid Interface. *Journal of the American Chemical Society* **2013,***135* (34), 12660-12669.
14. Misson, M.; Zhang, H.; Jin, B., Nanobiocatalyst advancements and bioprocessing applications. *Journal of Royal Society Interface* **2015,***12* (102), 1-8.
15. Ganzle, M. G., Enzymatic synthesis of galacto-oligosaccharides and other lactose derivatives (hetero-oligosaccharides) from lactose. *International Dairy Journal 22 (2012)* **2012,***22*, 116-122.
16. Ros, T. G.; van Dillen, A. J.; Geus, J. W.; Koningsberger, D. C., Surface oxidation of carbon nanofibres. *Chemistry – A European Journal* **2002,***8* (5), 1151-1162.
17. An, H.; Jin, B.; Dai, S., Fabricating polystyrene fiber-dehydrogenase assemble as a functional biocatalyst. *Enzyme and Microbial Technology* **2015,***68*, 15-22.

18. Monteil, C.; Bar, N.; Retoux, R.; Henry, J.; Bernay, B.; Villemin, D., Partially phosphonated polyethylenimine-coated nanoparticles as convenient support for enzyme immobilization in bioprocessing. *Sensors and Actuators B: Chemical* **2014,***192* (0), 269-274.
19. Lu, L.; Xu, S.; Zhao, R.; Zhang, D.; Li, Z.; Li, Y.; Xiao, M., Synthesis of galactooligosaccharides by CBD fusion beta-galactosidase immobilized on cellulose. *Bioresource Technology* **2012,***116*, 327-33.
20. Zheng, P.; Yu, H.; Sun, Z.; Ni, Y.; Zhang, W.; Fan, Y.; Xu, Y., Production of galacto-oligosaccharides by immobilized recombinant beta-galactosidase from Aspergillus candidus. *Biotechnology Journal* **2006,***1* (12), 1464-70.
21. Zhu, Y.; Feng, L.; Xia, F.; Zhai, J.; Wan, M.; Jiang, L., Chemical dual-responsive wettability of superhydrophobic PANI-PAN coaxial nanofibers. *Macromolecular Rapid Communications* **2007,***28* (10), 1135-1141.
22. Huang, F. L.; Wang, Q. Q.; Wei, Q. F.; Gao, W. D.; Shou, H. Y.; Jiang, S. D., Dynamic wettability and contact angles of poly(vinylidene fluoride) nanofiber membranes grafted with acrylic acid. *eXPRESS Polymer Letters* **2010,***4* (9), 551-558.
23. Grodzka, J.; Pomianowski, A., Wettability versus Hydrophilicity. *Physicochemical Problems of Mineral Processing* **2006,***40*, 5-18.
24. Mahmoudifard, M.; Soudi, S.; Soleimani, M.; Hosseinzadeh, S.; Esmaeili, E.; Vossoughi, M., Efficient protein immobilization on polyethersolfone electrospun nanofibrous membrane via covalent binding for biosensing applications. *Materials Science and Engineering: C* **2016,***58*, 586-594.
25. Ishikawa-Ankerhold, H. C.; Ankerhold, R.; Drummen, G. P. C., Advanced Fluorescence Microscopy Techniques—FRAP, FLIP, FLAP, FRET and FLIM. *Molecules* **2012,***17* (4), 4047-4132.
26. Guo, J.; Sachs, F.; Meng, F., Fluorescence-Based Force/Tension Sensors: A Novel Tool to Visualize Mechanical Forces in Structural Proteins in Live Cells. *Antioxidants & Redox Signaling* **2013,***20* (6), 986-999.
27. Wilson, P. M.; LaBonte, M. J.; Russell, J.; Louie, S.; Ghobrial, A. A.; Ladner, R. D., A novel fluorescence-based assay for the rapid detection and quantification of cellular deoxyribonucleoside triphosphates. *Nucleic Acids Research* **2011,***39* (17), e112.
28. Kong, J.; Yu, S., Fourier transform infrared spectroscopic analysis of protein secondary structures. *Acta Biochimica et Biophysica Sinica* **2007,***39* (8), 549-559.
29. Verma, M. L.; Barrow, C. J.; Kennedy, J. F.; Puri, M., Immobilization of beta-d-galactosidase from Kluyveromyces lactis on functionalized silicon dioxide nanoparticles: characterization and lactose hydrolysis. *International Journal of Biological Macromolecules* **2012,***50* (2), 432-7.
30. Bolivar, J. M.; Eisl, I.; Nidetzk, B., Advanced characterization of immobilized enzymes as heterogeneous biocatalysts. *Catalysis Today* **2015,***259*, 66–80.
31. Yang, H.; Yang, S.; Kong, J.; Dong, A.; Yu, S., Obtaining information about protein secondary structures in aqueous solution using Fourier transform IR spectroscopy. *Nat. Protocols* **2015,***10* (3), 382-396.
32. Barth, A.; Zscherp, C., What vibrations tell us about proteins. *Q. Rev. Biophys.* **2002,***35* (4), 369-430.
33. Cai, S.; Singh, B. R., Identification of β-turn and random coil amide III infrared bands for secondary structure estimation of proteins. *Biophysical Chemistry* **1999,***80* (1), 7-20.
34. Takeuchi, H., Raman structural markers of tryptophan and histidine side chains in proteins. *Biopolymers* **2003,***72* (5), 305-317.

35. Yoo, H. S.; Kim, T. G.; Park, T. G., Surface-functionalized electrospun nanofibers for tissue engineering and drug delivery. *Advanced Drug Delivery Reviews* **2009,***61* (12), 1033-1042.
36. Jovanovic-Malinovska, R.; Fernandes, P.; Winkelhausen, E.; Fonseca, L., Galacto-oligosaccharides synthesis from lactose and whey by beta-galactosidase immobilized in PVA. *Applied Bochemistry and Biotechnology* **2012,***168* (5), 1197-211.
37. Liese, A.; Hilterhaus, L., Evaluation of immobilized enzymes for industrial applications. *Chemical Society Reviews* **2013,***42* (15), 6236-6249.
38. Machado, J.; Coutinho, J.; Maceso, E., Solid–liquid equilibrium of a-lactose in ethanol/water. . *Fluid Phase Equilib* **2000,***173*, 121-134.
39. Misson, M.; Jin, B.; Chen, B.; Zhang, H., Enhancing enzyme stability and metabolic functional ability of β-galactosidase through functionalized polymer nanofiber immobilization. *Bioprocess and Biosystems Engineering* **2015,***38*, 1915–1923.
40. Ren, H.; Fei, J.; Shi, X.; Zhao, T.; Cheng, H.; Zhao, N.; Chen, Y.; Ying, H., Continuous ultrafiltration membrane reactor coupled with nanofiltration for the enzymatic synthesis and purification of galactosyl-oligosaccharides. *Separation and Purification Technology* **2015,***144*, 70-79.
41. Benjamins, E.; Boxem, L.; KleinJan-Noeverman, J.; Broekhuis, T. A., Assessment of repetitive batch-wise synthesis of galacto-oligosaccharides from lactose slurry using immobilised β-galactosidase from Bacillus circulans. *International Dairy Journal* **2014,***38* (2), 160-168.
42. Urrutia, P.; Mateo, C.; Guisan, J. M.; Wilson, L.; Illanes, A., Immobilization of Bacillus circulans β-galactosidase and its application in the synthesis of galacto-oligosaccharides under repeated-batch operation. *Biochemical Engineering Journal* **2013,***77*, 41-48.
43. Rodriguez-Colinas, B.; Poveda, A.; Jimenez-Barbero, J.; Ballesteros, A. O.; Plou, F. J., Galacto-oligosaccharide synthesis from lactose solution or skim milk using the β-galactosidase from Bacillus circulans. *Journal of Agricultural and Food Chemistry* **2012,***60* (25), 6391-6398.
44. Neri, D. F. M.; Balcao, V. M.; Costa, R. S.; Rocha, I. C. A. P.; Ferreira, E. M. F. C.; Torres, D. P. M.; Rodrigues, L. R. M.; Jr, L. B. C.; Teixeira, J. A., Galacto-oligosaccharides production during lactose hydrolysis by free Aspergillus oryzae b-galactosidase and immobilized on magnetic polysiloxane-polyvinyl alcohol. *Food Chemistry 128* **2009,***115*, 92-99.

CHAPTER 7

High Galacto-Oligosaccharide Production in Recirculating Spiral Reactor by Polymer Nanofiber Immobilized β-Galactosidase

Chapter 7: High Galacto-Oligosaccharide Production in Recirculating Spiral Reactor by Polymer Nanofiber Immobilized β-Galactosidase

Mailin Misson[1,2], Bo Jin[1], Hu Zhang[1*]

[1]School of Chemical Engineering, The University of Adelaide, Adelaide, SA 5000, Australia

[2]Biotechnology Research Institute, Universiti Malaysia Sabah, Jalan UMS, 88400, Kota Kinabalu, Sabah, Malaysia

*Corresponding author:

Email: hu.zhang@adelaide.edu.au

Tel: +61 8 831 33810

In preparation for submission

2016

Statement of Authorship

Title of Paper	Recirculating Spiral Bioreactor for Galactooligosaccharide Production from Nanofiber-supported Nanobiocatalysts
Publication Status	☐ Published ☐ Accepted for Publication ☐ Submitted for Publication ☑ Unpublished and Unsubmitted work written in manuscript style
Publication Details	Mailin Misson, Bo Jin, Hu Zhang *In preparation for submission.*

Principal Author

Name of Principal Author (Candidate)	Mailin Misson		
Contribution to the Paper	Designed and performed experiments, interpreted data and wrote the manuscript.		
Overall percentage (%)	70 %		
Certification:	This paper reports on original research I conducted during the period of my Higher Degree by Research candidature and is not subject to any obligations or contractual agreements with a third party that would constrain its inclusion in this thesis. I am the primary author of this paper.		
Signature		Date	19.02.2016

Co-Author Contributions

By signing the Statement of Authorship, each author certifies that:

i. the candidate's stated contribution to the publication is accurate (as detailed above);

ii. permission is granted for the candidate in include the publication in the thesis; and

iii. the sum of all co-author contributions is equal to 100% less the candidate's stated contribution.

Name of Co-Author	Bo Jin		
Contribution to the Paper	Supervised development of work and manuscript evaluation.		
Signature		Date	19/02/2016

Name of Co-Author	Hu Zhang		
Contribution to the Paper	Supervised development of work, data interpretation, manuscript evaluation and acted as corresponding author.		
Signature		Date	18/02/2016

Please cut and paste additional co-author panels here as required.

Abstract

Design of an economically and industrially viable reactor system in which functions and bioengineering performance of biocatalysts are greatly enhanced has been pursued. This study presents development of a recirculating spiral reactor for the β-galactosidase/ polymer nanofiber assembly (PSNF-Gal), aiming for continuous galacto-oligosaccharides (GOS) production. The spiral reactor was fabricated in-house and assessed by comparing the conversion of lactose to GOS by the PSNF-Gal with free β-galactosidase.The variable parameters of the system were optimized including reaction time (6-30 h), feed flow rate (2-18 ml/min) and initial substrate concentration (300-700 g/l).It was found that the GOS selectivity of the PSNF-Gal exceeded the free counterpart about 1.5 to 3.7-fold. The maximum conversion rate was 42 g lactose/l/h and the GOS productivity rate was 23 g/l/h observed at 6 h reaction time. An increase in the flow rate resulted in enhanced lactose bioconversion and GOS formation, however, further increase beyond 15 ml/min led to a significant decrease in GOS synthesis and enzyme leaching. Although lactose conversion was decreased about 1.6 times, an increase in the initial lactose concentration from 300 to 700 g/l has enhanced the GOS yield around 1.7 times. The best yield for GOS synthesis was determined to be 159 g/l with 86% lactose conversion at 24 h reaction time, 15 ml/min flow rate and 400 g/l initial lactose concentration. The initial results demonstrate the potential of the recirculating spiral bioreactor for industrial scale production of GOS.

Keywords**:** nanobiocatalyst, galacto-oligosaccharide, β-galactosidase, polymer nanofibers, bioconversion, recirculating spiral bioreactor

7.1 Introduction

The role of enzymes as biocatalysts has driven rapid biotechnology advancements in the area of harnessing green and sustainable processes. The demand of biocatalysts has extended to diverse sectors including in biocatalysis, pharmaceutics, bioenergy and food industries. In recent years, there has been a growing interest to promote an integrated waste management using enzyme-assisted technologies. Enzymes provide specific and selective activity. Hence, promising opportunities arise in generating marketable and valuable products from waste sources. Whey is a by-product from cheese and casein manufacturing in which lactose is the major constituent (60-80% on a dry matter basis) in whey. Dairy effluents have been regarded as pollutants due to a high organic loading that contributes to eutrophication and toxicity in eco-streams [1].Worldwide, more than 10^8 tons of cheese whey are produced annually and the quantities increase corresponding to the growing demand of cheese [2]. Thus, cost-effective treatment of dairy effluents has become a major concern to the dairy industry.

Enzymatic bioconversion of lactose in the dairy effluents into value-added products, such as galacto-oligosaccharides (GOS) by β-galactosidase endows a promising solution. GOS are used as a functional ingredient for intestinal regulation and a low-caloric sugar alternative to enhance food physicochemical and organoleptic properties [3-4]. There are two simultaneous reaction pathways during β-galactosidase biocatalysis of lactose, hydrolysis or transgalactosylation. After cleaving the lactose molecules, β-galactosidase-galactosyl complexes are formed. Glucose and galactose are generated via hydrolysis when water acts a galactosyl acceptor, while transgalactosylation is dominant to produce GOS when nucleophile molecules surpress the water activity [5]. Therefore, bioreactor conditions and the enzyme local nanoenvironment should be controlled to favor the transgalactosylation pathway for GOS production [6].

β-Galactosidase has been immobilized on nanofibers to enhance enzyme recyclability, stability and functionality, and to allow continuous operation [7-8] due to the specific characteristics of nanofibers, such as their high surface area, discrete nanostructures and self-assembling behaviors as well as high porosity and interconnectivity [9]. A number of bioreactor configurations and operation modes have been evaluated for nanostructure-supported nanobiocatalysts, including continuous packed-bed reactors,

recirculated reactors in a batch mode, and membrane reactors in a fed-batch mode [10-11]. However, there are very few reports on bioreactors for nanofiber-based nanobiocatalysts. Such a bioreactor should be able to preserve the immobilized enzyme activity under the bioreactor operational conditions. It has been recognized that maintaining long-term enzyme stability in a bioreactor system remains a key challenge. Hence, it is a focal point of interest to design a reactor system that can provide an optimal macro-environment for facilitating biocatalytic reactions, preserving enzyme functionalities, as well as sheltering enzymes against harsh external environmental conditions, such as mechanical shear stress.

In the present study, a scalable recirculating spiral reactor system was fabricated for the immobilized β-galactosidase polymer nanofiber assembly (PSNF-Gal), aiming for enhancing the GOS production. The PSNF-Gal was spread on the surface of a spiral mesh support to achieve homogenous distribution of biocatalysts inside the reactor, which is beneficial for maximizing the interfacial reaction between substrates and enzyme reactive sites and consequently promoting a high lactose bioconversion into GOS. This approach also allows a simple biocatalyst recovery procedure, and prevents aggregation or clustering behaviours of nanofiber mats in the aqueous solution so that the enzyme carriers are well dispersed to prevent diffusion limitation. The feed was recirculated through the system at a designed flow rate, which determined the number of feed recirculation cycle in the reactor, for a better opportunity of reactant-enzyme activities. The operating conditions were optimized by varying the reaction time, feed flow rate and substrate concentration and benchmarked with free β-galactosidase. This study provides new insights into translation of the bench-scale enzyme-assisted technology to a manufacture scale.

7.2 Materials and Methods

7.2.1 Materials

Polystyrene (molecular weight: 350,000), *N*,*N*-dimethylformamide (DMF), nitric acid (HNO_3), and sulphuric acid (H_2SO_4) were of analytical grade without further purification. Bovine serum albumin (BSA) and *Kluyveromyces lactis* β-galactosidase were supplied by

Sigma-Aldrich, lactose monohydrate by Chem Supply and potassium phosphate buffer (PBS, pH 7.2) by Life Technologies.

7.2.2 Synthesis and Functionalization of Nanofibrous Polystyrene

20 % (w/v) polystyrene were dissolved in 10 ml DMF with gentle stirring for overnight to form a homogenous solution. The resultant solution as the precursor for electrospinning was placed inside a 5-ml syringe bearing a 1-mm inner diameter needle tip which was connected to a 25 kV voltage power supply. The flow rate of the polymer solution was fixed at 2.5 ml/h. The electrospun polystyrene nanofibers (PSNF) were cast onto a metal-surface collector with a distance of about 10 cm from the tip. The PSNF was detached from the collector surface and stored at room temperature for further use.

The surface of PSNF was modified through surface oxidation to introduce functional groups. Approximately 250 mg of PSNF sheet was placed on the surface of 12 x 8 cm polypropylene mesh. The mesh support was rolled to form spiral PSNF mats and immersed in HNO_3 (69%) for 2 h at room temperature [12]. The spiral PSNF was rinsed with water thoroughly for three times to ensure that the surface was entirely acid-free and the PSNF was further equilibrated with PBS solution (pH 7.2) for overnight prior to enzyme immobilization.

7.2.3 Immobilization Procedure

The spiral PSNF was submerged into β-galactosidase solution (2 mg/ml in PBS) (pH 7.2) for overnight at 4 ^{o}C. The spiral PSNF-Gal was then separated from the supernatant using forceps and washed with water for three times to remove unbound proteins. The supernatant and washing solutions were collected to measure the concentration of non-adsorbed proteins.

7.2.4 Experimental Set-up of Recirculating Spiral Reactor for GOS Synthesis

The enzymatic lactose conversion was carried out in a recirculating spiral PSNF-Gal reactor. The reactor system comprises a reservoir tank maintained at 37 ^{o}C, a Masterflex 7021-24 (USA) pump to control the feed flow rate and a 25-ml cylindrical reactor containing enzyme-carrying nanofiber sheets fitted on spiral-formed mesh supports. The schematic diagram of the reactor system is illustrated in Figure 7.1. The reservoir tank and the reactor were connected by Eur-Pharm silicone tubing. Lactose in the feed reservoir was prepared by dissolving lactose into PBS (pH 7.2) at 60 ^{o}C and cooled down into 37 ^{o}C before reaction. A peristaltic pump was used to feed lactose from the bottom inlet of the reactor, passed through the spiral PSNF-Gal, and channeled back into the feed reservoir through the top outlet. Variable parameters including reaction time (6-30 h), flow rate (2-18 ml/min) and substrate concentration (300-700 g/l) were tested to optimize the GOS synthesis. Flow rate, controlled by the pump, determines the total cycle of feed recirculation and retention time inside the reactor, calculated using Eq. 1 and 2, respectively. Enzyme leakage was evaluated by measuring the protein content in the feeding solution. Samples were also drawn at pre-set intervals for carbohydrate analysis and immediately heated in boiling water for 5 min to deactivate enzymes [13-14]. Samples were filtered using 0.45 μm nylon filters and diluted prior to carbohydrate analysis using high performance liquid chromatography (HPLC).

$$\text{Total cycle } (h^{-1}) = \frac{Flow\ rate\ (ml/min)}{Feed\ working\ volume\ (ml)}\ X\ 60 \quad (1)$$

$$\text{Retention time (h)} = \frac{Reactor\ volume\ (ml)}{Flow\ rate\ (ml/min)}\ X\ \frac{1}{60} \quad (2)$$

7.2.5 Analytical Methods

The enzyme leakage in reaction mediumwas measured according to the procedure described by Bradford [15]. Approximately 100 mg Coomassie Brilliant Blue G-250 was mixed with 50 ml of 95% ethanol, 100 ml of 85% phosphoric acid. The solution was

diluted with water to a final volume of 1 litre with gentle mixing. A total of 100 µl sample was added into 5 ml of Bradford reagent, mixed homogenously and allowed to react within 5 min. The sample was measured using a UV spectrophotometer (Shimadzu, Japan) at 595 nm. The concentration was determined from a calibration curve using BSA as a standard.

The remaining substrates and products were analyzed in Agilent 1100 Series HPLC equipment with a refractive index detector, a pump and an autosampler and an Aminex HPX-87H column (300 x 7.8 mm). The flow rate of a pre-degassed 8 mmol/L-H_2SO_4 mobile phase was set at 0.5 ml min^{-1}. The column and the detector cell were maintained at 60 ^oC and 40 ^oC, respectively[16]. Chromatograms were integrated using the ChemStation software.

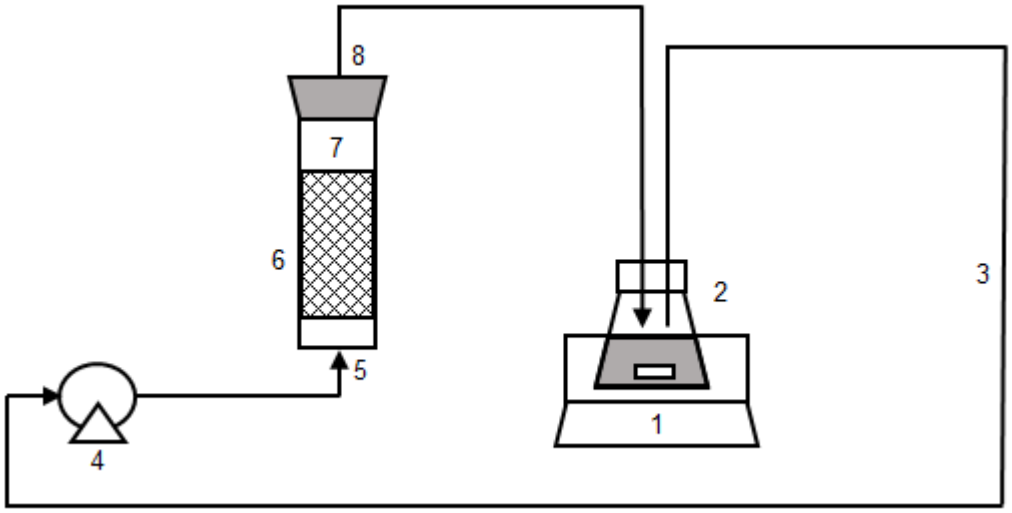

Figure 7.1 Schematic diagram of spiral PSNF-GAL reactor system for lactose bioconversion. (1) Temperature-controlled magnetic stirrer, (2) feeding tank, (3) silicone tubing, (4) peristaltic pump, (5) inlet, (6) spiral PSNF-Gal, (7) reactor, (8) outlet.

7.2.6 Conversion and Productivity

The performance of PSNF-Gal in spiral reactor system was appraised in terms of lactose conversion (X), conversion rate, product yield (Y), volumetric productivity rate (Q_v) and GOS selectivity.

Corresponding yield of substrate conversion (X), which represents the percentage of initial lactose that has reacted during the reaction, was determined using Eq 3.

$$X_{lactose}\ (\%) = \frac{[Initial\ lactose]-[Final\ lactose]}{[Initial\ lactose]} \times 100\ \% \quad (3)$$

Where brackets represent the mass concentration.

Corresponding products yield (Y), which represents the fraction of products (glucose, galactose, GOS) with respect to total concentration of initial lactose, was calculated using Eqs 4-5.

$$Y_{product}\ (\%) = \frac{[Product]}{[Initial\ Lactose]}\ X\ 100\ \% \quad (4)$$

$$Y_{GOS}\ (\%) = 100\ \% - \%\ Y_{lactose} - \%\ Y_{glucose} - \%\ Y_{galactose} \quad (5)$$

GOS selectivity, which is defined as the ratio of the amount of GOS to the amounts of all products formed in reaction medium, was determined using Eq 6.

$$\text{GOS selectivity} = \frac{Y_{GOS}}{Y_{GOS} + Y_{glucose} + Y_{galactose}} \quad (6)$$

the ratio of the amount of GOS to the amounts of all products formed in reaction medium.

Corresponding conversion rate and volumetric productivity rate (Q_v), which represents the average conversion or productivity over the running time of reaction, was determined using Eqs 7-8.

$$\text{Conversion rate} = \frac{[Initial\ lactose]-[Final\ lactose]}{t} \quad (7)$$

$$Q_v = \frac{[Product]}{t} \quad (8)$$

Where t is the running time of reaction and expressed as g product per liter per hour (g/l/h).

7.2.7 Statistical Analysis

Sample collection and analysis were conducted in triplicate. Results were analysed using the statistical tool in MS Excel 2010. Each value corresponds to the mean of independent experiments conducted in triplicates.

7.1 Results and Discussion

7.3.1 Development and Assessment of Recirculating Spiral Reactor

In order to evaluate the bioengineering performance of PSNF-Gal in a scalable reactor for GOS synthesis, a recirculating spiral reactor was designed and fabricated in-house. As the flow rate increases, the total cycle number of recirculation increases while the retention time reduces correspondingly as tabulated in Table 7.1.The results show that the conversion increased with the increasing recirculation cycle. The results are in good agreement with the findings by Kim *et al.*[17] that showed an enhance treatment rate with increased batch cycles.

Table 7.1 The flow rate of lactose feeding with the corresponding total recirculation cycle, residence time and resulting lactose conversion in the spiral PSNF-Gal reactor system.

Flow rate (ml/min)	Total recirculation cycle (h^{-1})	Retention time (h)	Conversion (%)
2	2	12.5	61
5	5	5.0	68
9	9	2.8	72
12	12	2.1	80
15	15	1.7	86
18	18	1.3	88

In β-galactosidase-catalyzed reaction, lactose conversion has two different reaction pathways: (1) hydrolysis to glucose and galactose and (2) transgalactosylation to GOS [18-19].Transgalactosylation occurs when nucleophilic moleculesacts a galactosyl acceptor, while hydrolysis takes place when water acts as the acceptor [5, 20]. Therefore, the products from β-galactosidase-catalysed reaction include glucose, galactose, GOS and the remaining lactose.

The bioconversion and the GOS selectivity of PSNF-Gal were benchmarked with free β-galactosidase as shown in Figure 7.2 (a,b). The GOS selectivity represents the preference of lactose conversion into GOS, which is determined by dividing the amount of GOS products to that of all products in the reaction medium (GOS, glucose and galactose) [21]. The free enzyme was able tocompletely convert lactose at all tested concentrations. In contrast, the PSNF-Gal PSNF-Gal demonstrated a gradual decrease in the conversion (Figure 7.2a). These observations are likely to be correlated to obstacle-free diffusion of substrates into and products out of the enzyme sites, yielding greater conversion than PSNF-Gal. In terms of GOS selectivity, however, the PSNF-Gal was found to be superior to the free counterpart. The selectivity was consistently above 0.4, about 1.5-3.7 times of that of free counterpart. The findings imply the transgalactosylation reaction dominated in the immobilized enzyme while the free counterpart favored hydrolysis reaction.

Initial lactose concentration is one of the important parameters that affect GOS production. As can be seen in Figure 7.2, apparently the conversion and production profiles are largely dependent on the initial lactose concentration. The highest lactose conversion (87 %) by PSNF-Gal was achieved using 300 g/l and 400 g/l initial lactose concentration (Figure 7.2a). The PSNF-Gal experienced about 86 % to 54 % decrease in conversion when the lactose concentration was further increased to 700 g/l. A longer enzymatic reaction time may be required to catalyse the conversion of more lactose molecules at the same reactant volume and reaction time.Furthermore, the reduction of conversion might be related to the low solubility of lactose, which formscrystal-like substances at a high concentration.It has been reported that the solubility of lactose in water is 250 g/l at 40 ^{o}C [22]. Vera *et al.*[23] performed the reactions at an elevated temperature at 55 ^{o}C, yielding about 29 g GOS/100 g lactose. The present work was conducted at a similar initial lactose concentration, and a total of 46 g GOS/100 g lactose was generated (Figure 7.2c).

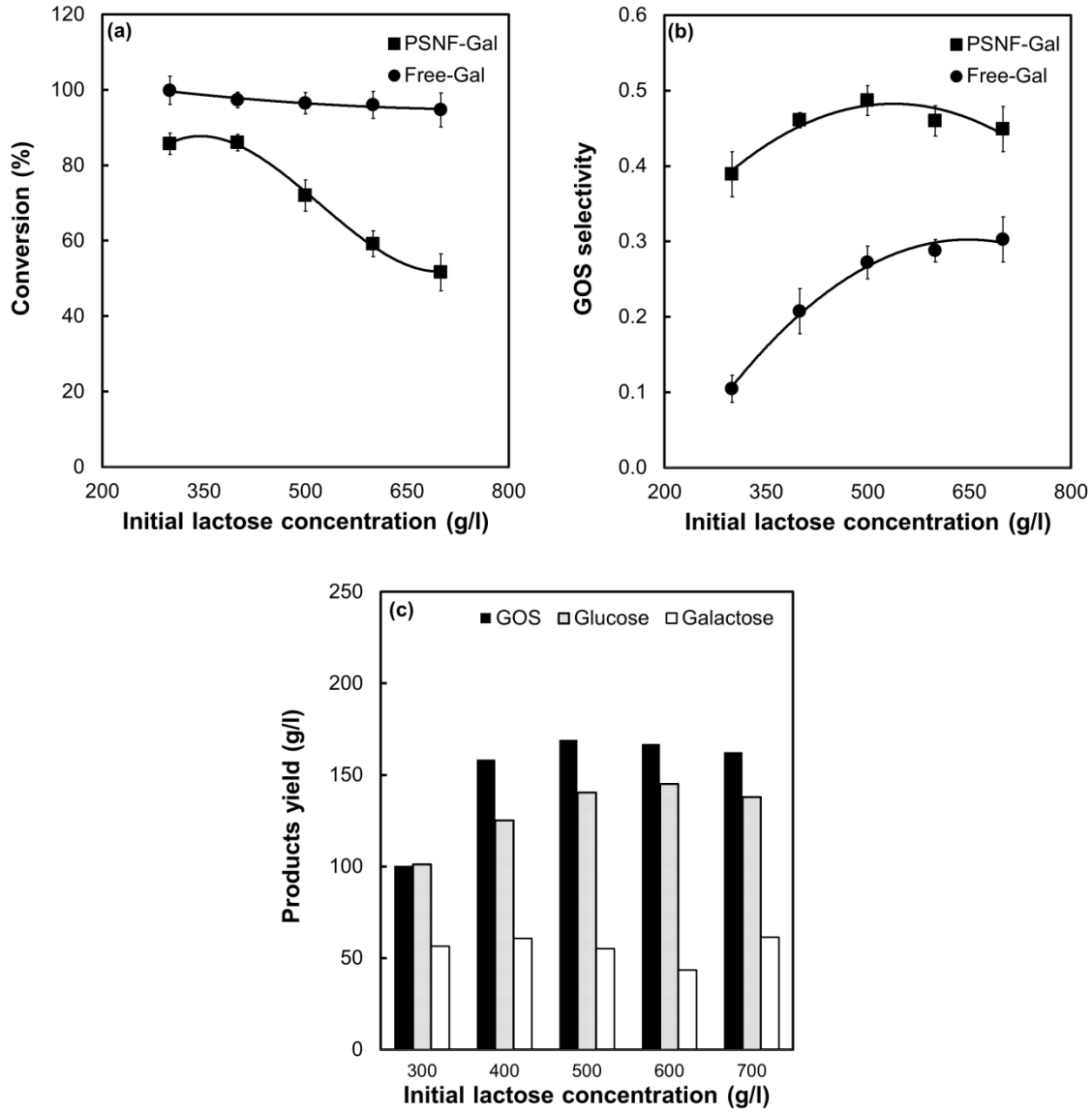

Figure 7.2(a, b) Comparison of free enzyme and immobilized enzyme on lactose conversion and GOS selectivity at various lactose concentrations. (c) The effect of initial lactose concentration on product yield by PSNF-Gal. Reactions were conducted on 300-700 g/l lactose at 15 ml/min feed flow rate, using 2 mg/ enzyme concentration at 37 ^{o}C in pH 7 for 24 h reaction time.

A maximum GOS yield (165 g/l) was obtained at 400 g/l lactose, 1.7 times of that GOS concentration at 300 g/l lactose (Figure 7.2c) (Figure 7.2c). Further increasing the concentration, however, would not result in an improvement of GOS yield. While galactose formation remained constant around 50 g/l, glucose synthesis increased with increasing the initial lactose concentration prior to reaching the plateau around 140 g/l at 500 g/l lactose. It is also noted that GOS and glucose was comparable at the lowest initial

lactose concentration, indicating both hydrolysis and transgalactosylation reaction occurred simultaneously. It has been recognized that lactose hydrolysis is predominant at a lower lactose concentration (below 30%, w/w), therefore a low concentration of GOS would be produced [24]. By increasing the lactose concentration, the GOS yield was higher than glucose approximately 10 to 15%, implying a preference towards transgalactosylation. These findings are in accordance with the recent studies indicating a transgalactosylation preference at high lactose concentrations [21, 24-25]. Since lactose nucleophiles act as acceptorsfor galactosyl-enzyme complex and compete with water to form GOS, lactose concentration has a significant influence on GOS synthesis.

7.3.2 Time-Course of Conversion Rate and Productivity in Recirculating Spiral Reactor

The temporal profiles for lactose bioconversion using PSNF-Gal in the recirculating spiral reactor are presented in Figure 7.3. A rapid reduction in lactose concentration was observed during the first 6 hour reaction, and the lactose concentration was gradually reduced thereafterand reached a steady state after 24 h with the remaining unconverted lactose at 56 g/l. GOS synthesis reached the plateau after 6 h reaction time.While glucose was about 2-fold higher than galactose, both products however demonstrated an increase yield with the increasing reaction time. The findings indicate transgalactosylation was dominated in the reaction during the first 6 hour reaction when lactose was rapidly bio-converted. The results could be attributed to the abundant lactose nucleophiles at the beginning of reaction, which compete with water molecules to react with the galactosyl-enzyme complex. However, as the concentration of lactose reduced when the reaction continued, the yield of hydrolysis products gradually increased until glucose concentration was comparable with GOS at 30 h reaction time. At such condition, both water and nucleophilic molecules might have the equivalent opportunity to enter the enzyme sites and react with galactosyl-enzyme complex.

The conversion rate and productivity rate of PSNF-Gal are presented in Figure 7.3, which are defined as the average conversion or productivity over the running time of reaction.Figure 7.3b shows a steep decrease in the conversion rate from 42 g/l/h to 12 g/l/h when the reaction time was prolonged from 6 h to 30 h.Similarly, the product formation

rates also exhibited a decline trend as illustrated in Figure 7.3c. The productivity rate of GOS and glucose reduced about 81% and 66%, respectively, while galactose showed slight reduction.As a high throughput and productivity are greatly pursuedin bioprocesses, a longer reaction time is less favourable. Our study has shown that a longer reaction time is less economical for GOS production.The maximum GOS yield (139 g/l, Figure 7.3a) could be harvested as early as 6 h, presenting a corresponding conversion and productivity rate of 42 g/l/h and 23 g/l/h.

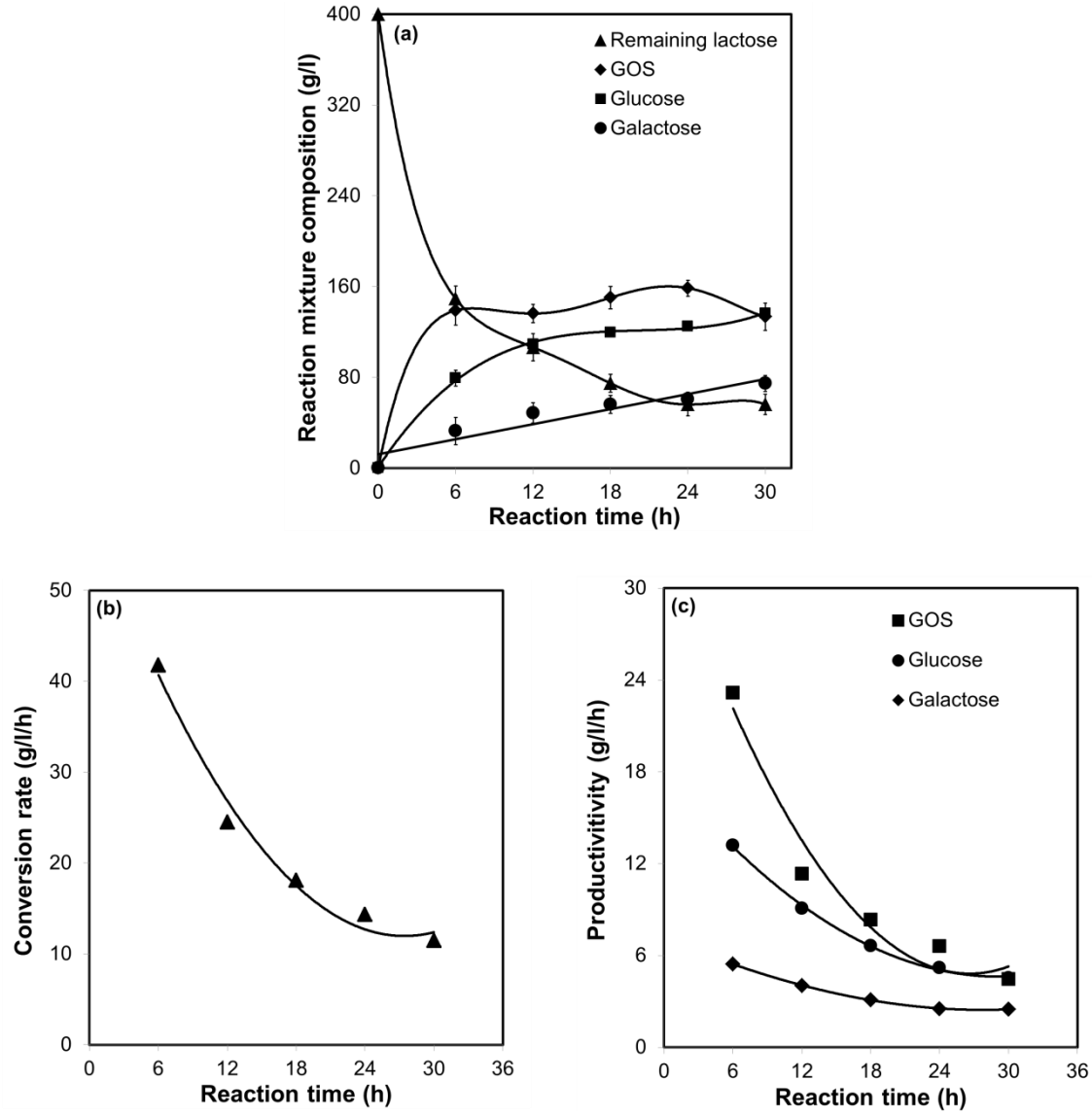

Figure 7.3(a) The composition of reaction mixtures (b) conversion rate and (c) productivity rate of PSNF-Gal in recirculating spiral reactor. Reactions were conducted on 400 g/l initial lactose concentration, feed flow rate at 15 ml/min lactose/h at 37 ^{o}C using 2 mg/ml enzyme concentration in pH 7 for 30 h reaction time.

7.3.3 Effect of Flow Rate on Galacto-Oligosaccharide Synthesis

Feed flow rate may have an impact on the residence time, the enzyme-substrate reaction and the enzyme leakage out of the nanobiocatalyst assembly. The effect of flow rate on lactose reduction, production yield, GOS selectivity and enzyme leakage was presented in Figure 7.4. Feed flow generally creates a convective motion to facilitate mass transfer of reactants towards and products away from PSNF-Gal [21]. As the flow rate increased from 2 to 18 ml/min, the concentration of remaining lactose reduced significantly from 162 g/l into 47 g/l (Figure 7.4a). It corresponds to a greater conversion at a higher flow rate as described in Table 7.1.

As Figure 7.4b indicates, an increase in the flow rate, however, had a less significant effect on glucose and galactose formation. The synthesis for both products nearly remained constant at the flow rate between 0-15 ml/min. The yield of galactose was 60 g/l, approximately half the glucose concentration (120 g/l). At a flow rate below 5 ml/min, the glucose yield was found 1.5 times higher than GOS. On the other hand, at 5 ml/min flow rate, an equivalent amount of glucose and GOS was observed that indicates a comparable activity of water and nucleophilic molecules, that competed each other to act as galactosyl acceptor [5], which yielded a fairly equal reaction between hydrolysis and transgalactosylation. Beyond 5 ml/min flow rate, the GOS yield surpassed glucose remarkably reaching a peak at 15 ml/min flow rate suggesting transgalactosylation may be dominated at a higher flow rate.The trend of findings imply the bioreactor conditions can be controlled to favor transgalactosylation pathway, which is in agreement to our previous study that has demonstrated the local environment of enzyme plays significant roles in GOS production [6].

An increase in the flow rate to 18 ml/min, however, led to a significant GOS decrease from 174 g/l into 145 g/l. By further extending the rate, hydrolysis seems to exceed transgalactosylation as the yield of hydrolysis products increased while GOS synthesis experienced a decline. A possible explanation for this might be due to ashorter contact time between lactose nucleophiles and enzyme-galactosyl complexat a faster feeding rate, which is evident by a low residence time (1.3 h) in Table 7.1. Therefore, it minimized the GOS synthesis and diverted the reaction into the hydrolysis pathway.

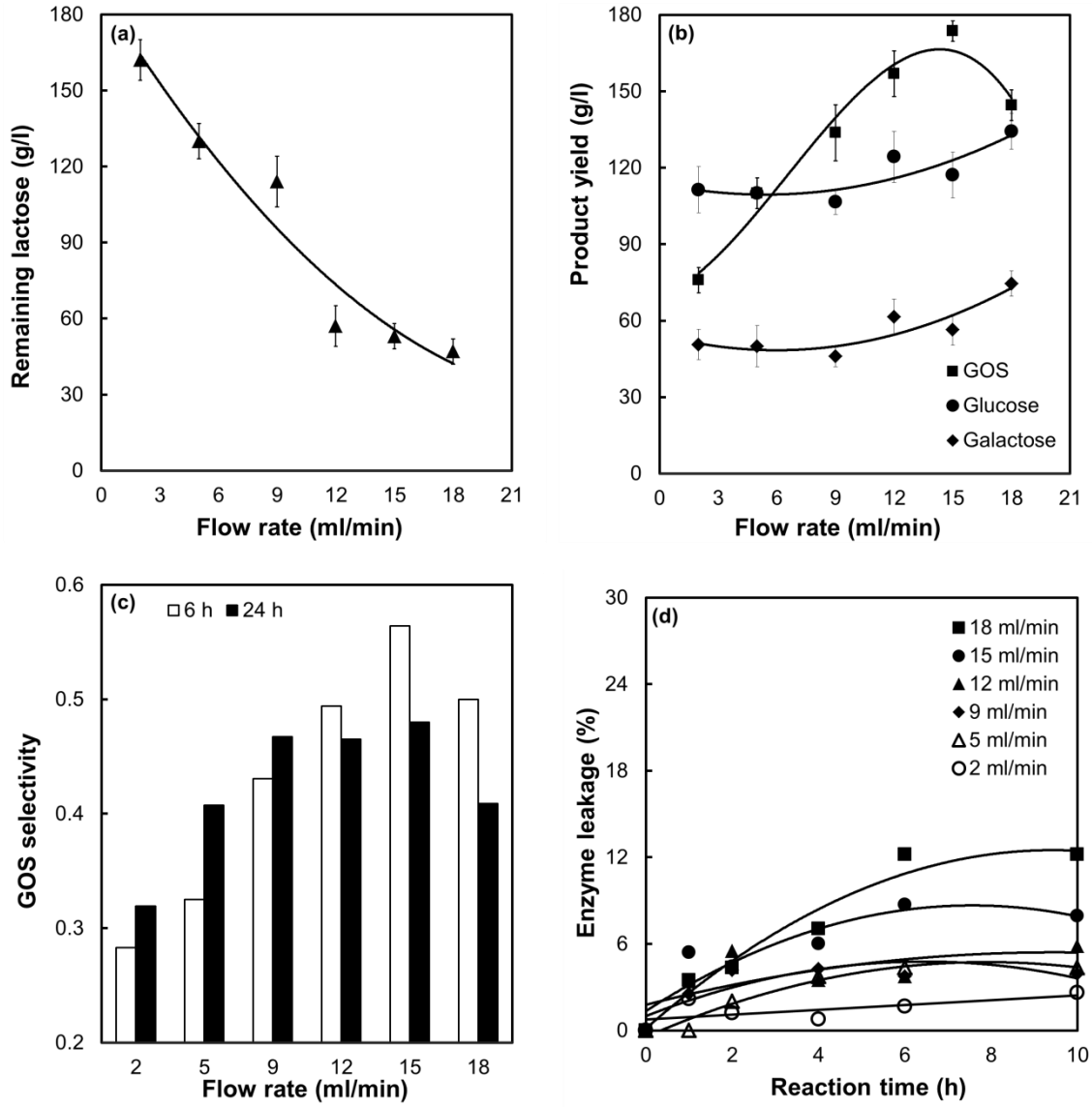

Figure 7.4 The effect of feed flow rate on (a) lactose reduction, (b) product yield, (c) GOS selectivity, and (d) enzyme leakage of immobilized β-galactosidase in recirculating spiral reactor. Reactions were conducted on 400 g/l initial lactose concentration, at 37 ^{o}C using 2 mg/ml enzyme concentration in pH 7 for 24 h reaction time.

The effect of flow rate on GOS selectivity was evaluated at two different reaction times: 6 h and 24 h as shown in Figure 7.4c. Both cases demonstrated an improved GOS selectivity as the flow rate increased. The selectivity, however, dropped at a flow rate beyond 15 ml/min, probably due to preference of hydrolysis inβ-galactosidase-catalyzed lactose conversion at a higher flow rate. Besides, a substantial correlation was also observed between the reaction time and the flow rate towards GOS selectivity.At a flow

rate below 9 ml/min, the GOS selectivity obtained at 24 h was higher than 6 h while a contradictoryfinding was observed at a higher flow rate.The data obtained indicatethat GOS selectivity was favoured at a slower flow rate with a longer reaction time (24 h) or a higher flow rate with a shorter reaction time (6 h).

The main weakness in enzyme-catalyzed processes is leaching of the immobilized enzyme into its reaction medium. Hence, a minimal enzyme leakage is often the biotechnological interest. It technically determines the binding stability of enzyme on support materials against mechanical shear stress in a reactor.Figure 7.4d reveals that there has been an accelerationof enzyme loss with an increase in flow rate. The leaching has surpassed 10 % at the highest flow rate (18 ml/min).The finding is broadly consistent with the results reported by Rahim *et al.*[26]. A minimal enzyme leakage (2.9 %) was observed at the lowest flow rate,which might be due to weak nature of the enzyme binding forces [27]. At 5-15 ml/min, the enzyme leakage was about 7 % indicating lower level of loss in comparison with a recent study that described approximately 40% glucose oxidase was released from a calcium alginate carrier [28]. The evidence from the experimental data suggests that the designed reactor system may possibly prevent biocatalysts loss at a flow rate of 5-15 ml/min.

Overall, the performance of the recirculating spiral PSNF-Gal reactor showed comparable or greater performance in comparison with other reported studies using different reactor configuration systems or operating modes as summarized in Table 7.2 [10, 29-31]. More importantly, comparing to the static feed as reported in our previous study [8], the process in the recirculating spiral reactor enhanced the bioconversion from 40 to 86% and the GOS yield from 110 to 169 g/l. Summing up the experimental results, it can be concluded that the newly developed PSNF-Gal recirculating spiral reactor provides suitable microenvironments that maximize the biocatalytic performance and demonstrates a its potential for large-scale operations.

7.4 Conclusion

A scalable recirculating spiral reactor system for the β-galactosidasepolymer nanofiber assembly (PSNF-Gal) was successfully developed and assessed for galacto-oligosaccharides (GOS) synthesis.PSNF-Gal exceeded free counterpart for the GOS selectivity of regardless of the initial lactose concentration. Prolonged reaction time benefited for a greater bioconversion but became unfavourable for GOS productivity. The maximum GOS yield could be harvested as early as 6 h, yielding a conversion rate and a productivity rate of 42 g/l/h and 23 g/l/h. An increase in flow rate resulted in enhanced bioconversion and GOS formation, as a consequence of higher feed recirculation cycles that promoted greater enzyme-substrate interfacial reaction. A high GOS selectivity was obtained at a slower flow rate with a longer reaction time or a shorter reaction time with a higher flow rate. A low level (7%) of enzyme loss could be achieved when applying a flow rate below 15 ml/min. Transgalactosylation was found to become dominant over hydrolysis at a higher initial lactose concentration. At the optimum operating conditions, the maximum lactose conversion was 86 % with a GOS yield about 159 g/l. By benchmarking with previous reported systems for lactose bioconversion, the developed recirculating spiral reactor shows distinguished bioengineering perfomances which may hold great potential for various large-scale enzyme-assisted bioprocessess.

Table 7.2 Comparison on lactose bioconversion and GOS yield by immobilized enzymes in various types of support materials.

Source of β-galactosidase	Reactor	Support material	Lactose (g/l)	Conversion (%)	GOS (g/l)	Reference
Kluyveromyces lactis	Batch spiral reactor	Polystyrene nanofibers	400	86	159	This work
			500	71	169	
			600	52	172	
Kluyveromyces lactis	Batch process	Modified polystyrene nanofibers	400	40	110	[8]
Talaromyces thermophilus	Batch packed bed	Eupergit C	200	80	80	[29]
	Continuous packed bed	Eupergit C	200	50	50	
Aspergillus oryzae	Batch reactor	-	400	-	115	[10]
	Fed-batch reactor		580	-	218	

Aspergillus oryzae	Batch reactor	-	400	70	100	[31]
Bacillus circulans	Repeated batch	Glyoxyl agarose	500	60		[30]

Acknowledgement

MM gratefully acknowledges the financial support from the Universiti Malaysia Sabah and the Malaysian Government. The HPLC facility support from Paul Grbin's research group and sugar analysis assistance by Nick Van Holst, and technical supports by Jason Peak, Jeffrey Hiorns and Michael Jung from workshop department at School of Chemical Engineering are highly appreciated.

References

1. Watanabe, T.; Shinozaki, Y.; Suzuki, K.; Koitabashi, M.; Yoshida, S.; Sameshima-Yamashita, Y.; Kuze Kitamoto, H., Production of a biodegradable plastic-degrading enzyme from cheese whey by the phyllosphere yeast Pseudozyma antarctica GB-4(1)W. *Journal of Bioscience and Bioengineering* **2014,***118* (2), 183-187.
2. Grba, S.; Stehlik-Tomas, V.; Stanzer, D.; Vahčić, N.; Škrlin, A., Selection of yeast strain Kluyveromyces marxianus for alcohol and biomass production on whey. *Chemical and Biochemical Engineering Quarterly* **2002,***16* (1), 13-16.
3. Gosling, A.; Stevens, G. W.; Barber, A. R.; Kentish, S. E.; Gras, S. L., Recent advances refining galactooligosaccharide production from lactose. *Food Chemistry 121* **2010,***121*, 307-318.
4. Ganzle, M. G., Enzymatic synthesis of galacto-oligosaccharides and other lactose derivatives (hetero-oligosaccharides) from lactose. *International Dairy Journal 22* **2012,***22*, 116-122.
5. Jovanovic-Malinovska, R.; Fernandes, P.; Winkelhausen, E.; Fonseca, L., Galacto-oligosaccharides Synthesis from Lactose and Whey by beta-Galactosidase Immobilized in PVA. *Applied Biochemistry and Biotechnology* **2012,***168* (5), 1197-211.
6. Misson, M.; Dai, S.; Jin, B.; Chen, B. H.; Zhang, H., Manipulation of nanofiber-based β-galactosidase nanoenvironment for enhancement of galacto-oligosaccharide production. *Journal of Biotechnology* **2016,***222*, 56-64.
7. Misson, M.; Du, X.; Jin, B.; Zhang, H., Dendrimer-like nanoparticles based β-galactosidase assembly for enhancing its selectivity toward transgalactosylation. *Enzyme and Microbial Technology* **2016,***84*, 68-77.
8. Misson, M.; Jin, B.; Chen, B.; Zhang, H., Enhancing enzyme stability and metabolic functional ability of β-galactosidase through functionalized polymer nanofiber immobilization. *Bioprocess and Biosystems Engineering* **2015,***38*, 1915–1923.
9. Misson, M.; Zhang, H.; Jin, B., Nanobiocatalyst advancements and bioprocessing applications. *Journal of Royal Society Interface* **2015,***12* (102), 1-8.
10. Vera, C.; Guerrero, C.; Illanes, A.; Conejeros, R., Fed-batch synthesis of galacto-oligosaccharides with Aspergillus oryzae β-galactosidase using optimal control strategy. *Biotechnology Progress* **2014,***30* (1), 59-67.
11. Ren, H.; Fei, J.; Shi, X.; Zhao, T.; Cheng, H.; Zhao, N.; Chen, Y.; Ying, H., Continuous ultrafiltration membrane reactor coupled with nanofiltration for the enzymatic

synthesis and purification of galactosyl-oligosaccharides. *Separation and Purification Technology* **2015,***144*, 70-79.
12. An, H.; Jin, B.; Dai, S., Fabricating polystyrene fiber-dehydrogenase assemble as a functional biocatalyst. *Enzyme and Microbial Technology* **2015,***68*, 15-22.
13. Rodriguez-Colinas, B.; Fernandez-Arrojo, L.; Ballesteros, A. O.; Plou, F. J., Galactooligosaccharides formation during enzymatic hydrolysis of lactose: Towards a prebiotic-enriched milk. *Food Chemistry* **2014,***145*, 388-394.
14. Lu, L.; Xu, S.; Zhao, R.; Zhang, D.; Li, Z.; Li, Y.; Xiao, M., Synthesis of galactooligosaccharides by CBD fusion beta-galactosidase immobilized on cellulose. *Bioresource technology* **2012,***116*, 327-33.
15. Bradford, M. M., A rapid and sensitive method for the quantification of microgram quantities of protein utilizing the principle of protein-dye binding. *Analytical Biochemistr* **1976,***72*, 248-254.
16. Zheng, P.; Yu, H.; Sun, Z.; Ni, Y.; Zhang, W.; Fan, Y.; Xu, Y., Production of galacto-oligosaccharides by immobilized recombinant beta-galactosidase from Aspergillus candidus. *Biotechnology Journal* **2006,***1* (12), 1464-70.
17. Kim, J.; Lee, S.; Lee, C., Comparative study of changes in reaction profile and microbial community structure in two anaerobic repeated-batch reactors started up with different seed sludges. *Bioresource Technology* **2013,***129*, 495-505.
18. Shen, Q.; Yang, R.; Hua, X.; Ye, F.; Wang, H.; Zhao, W.; Wang, K., Enzymatic synthesis and identification of oligosaccharides obtained by transgalactosylation of lactose in the presence of fructose using beta-galactosidase from Kluyveromyces lactis. *Food Chemistry* **2012,***135* (3), 1547-54.
19. Gaur, R.; Pant, H.; Jain, R.; Khare, S. K., Galacto-oligosaccharide synthesis by immobilized Aspergillus oryzae b-galactosidase. *Food Chemistry* **2006,***97*, 426-430.
20. Rodriguez-Colinas, B.; Poveda, A.; Jimenez-Barbero, J.; Ballesteros, A. O.; Plou, F. J., Galacto-oligosaccharide Synthesis from Lactose Solution or Skim Milk Using the β-Galactosidase from Bacillus circulans. *Journal of Agricultural and Food Chemistry* **2012,***60* (25), 6391-6398.
21. Palai, T.; Singh, A. K.; Bhattacharya, P. K., Enzyme, β-galactosidase immobilized on membrane surface for galacto-oligosaccharides formation from lactose: Kinetic study with feed flow under recirculation loop. *Biochemical Engineering Journal* **2014,***88*, 68-76.
22. Machado, J.; Coutinho, J.; Maceso, E., Solid–liquid equilibrium of a-lactose in ethanol/water. . *Fluid Phase Equilib* **2000,***173*, 121-134.
23. Vera, C.; Guerrero, C.; Conejeros, R.; Illanes, A., Synthesis of galacto-oligosaccharides by beta-galactosidase from Aspergillus oryzae using partially dissolved and supersaturated solution of lactose. *Enzyme and Microbial Technology* **2012,***50* (3), 188-94.
24. Torres, D. P. M.; Gonçalves, M. d. P. F.; Teixeira, J. A.; Rodrigues, L. R., Galacto-Oligosaccharides: Production, Properties, Applications, and Significance as Prebiotics. *Comprehensive Reviews in Food Science and Food Safety* **2010,***9* (5), 438-454.
25. Albayrak, N.; Yang, S. T., Production of galacto-oligosaccharides from lactose by aspergillus oryzae B-galactosidase Immobilized on on cotton cloth. *Biotechnology and Bioengineering* **2002,***77* (1), 8-19.
26. Rahim, S. N. A.; Sulaiman, A.; Hamid, K. H. K.; Edama, N. A.; Baharuddin, A. S., Effect of Agitation Speed for Enzymatic Hydrolysis of Tapioca Slurry Using Encapsulated Enzymes in an Enzyme Bioreactor. *International Journal of Chemical Engineering and Applications* **2015,***6* (1), 38-41.

27. Kweon, D.-H.; Kim, S.-G.; Han, N. S.; Lee, J. H.; Chung, K. M.; Seo, J.-H., Immobilization of Bacillus macerans cyclodextrin glycosyltransferase fused with poly-lysine using cation exchanger. *Enzyme and Microbial Technology* **2005,***36* (4), 571-578.
28. Blandino, A.; Macías, M.; Cantero, D., Glucose oxidase release from calcium alginate gel capsules. *Enzyme and Microbial Technology* **2000,***27* (3–5), 319-324.
29. Nakkharat, P.; Haltrich, D., b-Galactosidase from Talaromyces thermophilus immobilized. *World J Microbiol Biotechnol* **2007,***23*, 759-764.
30. Urrutia, P.; Mateo, C.; Guisan, J. M.; Wilson, L.; Illanes, A., Immobilization of Bacillus circulans β-galactosidase and its application in the synthesis of galacto-oligosaccharides under repeated-batch operation. *Biochemical Engineering Journal* **2013,***77*, 41-48.
31. Urrutia, P.; Rodriguez-Colinas, B.; Fernandez-Arrojo, L.; Ballesteros, A. O.; Wilson, L.; Illanes, A.; Plou, F. J., Detailed Analysis of Galactooligosaccharides Synthesis with β-Galactosidase from Aspergillus oryzae. *Journal of Agricultural and Food Chemistry* **2013,***61* (5), 1081-1087.

CHAPTER 8

Conclusions and Future Directions

Chapter 8: Conclusions and Future Directions

8.1 Conclusions

This research study focuses on the fabrication of nanoparticle- and nanofiber-based β-galactosidase nanobiocatalysts for conversion of dairy industry wastes into galacto-oligosaccharide (GOS) through an improved and feasible process with the potential for industrial scale manufacturing. The nanocarriers were synthesized and functionalized to facilitate enzyme binding and their performance in enzyme adsorption capability and stability were extensively evaluated. The structure-function relationship for the nanocarriers, the enzyme-nanocarrier nanoenvironment at the catalytic sites and the nanobiocatalyst structure were studied, aiming to enhance the bioengineering performance of the nanobiocatalysts. The main conclusions derived from the findings presented in Chapters 3 to 7 are summarized below:

In Chapter 3, the fabrication of dendrimer-like silica nanoparticles (HPSNs) with hierarchical pores and functionalization with amino (NH_2) and carboxyl group (COOH) were performed and benchmarked with non-functionalized HPSNs. Experimental results show both bovine serum albumin (BSA) and β-galactosidase exhibit preferential affinity towards the amino-functionalized HPSNs. The enzyme activity was fully preserved upon immobilization onto three types of nanoparticles. The enzyme assembly with HPSNs-NH_2 was further demonstrated to run up to 10 cycles with 20% of the enzyme activity remaining. Importantly, we have found that the enzyme assembly was able to generate GOS at a much higher yield than free counterpart when the initial lactose concentration is lower than 400 g/l, which means that the enzyme assembly had a preference towards transgalactosylation, while hydrolysis was dominant in the free enzyme solution. At a high initial lactose concentration, the enzyme assembly and free enzyme shared a comparable GOS yield. Our research findings demonstrated the HPSNs can be used to form enzyme-nanocarrier assemblies which have enhanced selectivity towards the required reaction pathways. The findings of the nanocarrier structure-function relationship in enzyme immobilization will provide a useful insight for future development of the hybrid

nanobiocatalyst assembly, by correlating and integrating the unique functions of nanocarriers and enzymes.

In Chapter 4, polystyrene nanofibers (PSNFs) with excellent quality were successfully fabricated using an electrospinning device by optimizing the operational parameters including polymer concentration, electric voltage and distance between discharge needle tips and the collector. Under these optimum conditions, uniform size and ordered alignment for fibrous mats can be obtained. Surface modification through chemical oxidation has improved enzyme loading and activity. The lactose conversion by PSNF-Gal catalysis results in a high GOS yield as well as a high production rate. The PSNF-Gal may beneficially promote transgalactosylation due to the hydrophobic nature of the polysterene surface. Another contributing factor could be the reduced diffusion path of the nuclephilic molecules and these molecules could easily bind to the galactosyl-enzyme complex in such a nanoenvironment. This simple but effective nanobiocatalyst-assisted process may be economically viable for large scale GOS production.

In Chapter 5, the stability and catalytic ability of β-galactosidase through functionalized PSNF immobilization have been evaluated. A successful immobilization of β-galactosidase on the acid-modified PSNF was demonstrated. The PSNF-Gal nanobiocatalyst assembly exhibited considerable enhancement in enzymatic and catalytic activities at a basic condition and the thermal stability up to 60 ^{o}C, signifying distinguished enzyme stabilizations in the denaturing environments. The surface modification of the nanostructured polymer fibres might have facilitated stable enzyme binding resulted in greater biocatalyst recyclability. Our findings demonstrated the PSNF-Gal doubled the GOS yield comparing with free enzyme, which is of importance for a bioengineering process. The highest GOS (28 %) was obtained at 400 g/l lactose. With considerable activity enhancement, recyclability and productivity, the PSNF-Gal was proven as economical and robust biocatalyst for continuous bioprocessing applications.

In Chapter 6, a comprehensive analysis study has been carried out to advance the understanding of β-galactosidase/nanofiber nanobiocatalyst structure. The homogenous biocatalyst distribution on the support surface was demonstrated by SEM and fluorescence microscopy images. The FTIR showed a few new peaks on the surface of the enzyme-loaded PSNF, indicating successful biocatalyst attachment on the PSNF surface. In comparison with the free enzyme FTIR signals, no shifting of bands was observed,

suggesting the native structures of the biocatalyst were retained. The biocatalyst amide I and other structures were identified by Raman microscopic examinations. These observations were well correlated with the biocatalyst engineering performance in a column bioreactor, signifying the native conformation of the nanobiocatalyst has been well preserved, thus leading to remarkable biocatalyst stability and activity under the operational conditions. The findings of this study provide useful insights into understanding of the structure and interfacial reactions of nanobiocatalyst assemblies.

In Chapter 7, an in-house recirculating spiral reactor for the PSNF-β-galactosidase assembly has been successfully developed and assessed for galacto-oligosaccharides (GOS) synthesis. The results show the PSNF-β-galactosidase exceeds its free counterpart in the GOS selectivity regardless of the initial lactose concentration. A prolonged reaction time benefits a greater bioconversion but becomesunfavorable for GOS productivity. A high GOS selectivity is obtained at a slower flow rate with a longer reaction time or a shorter reaction time with a higher flow rate. An acceptable level of enzyme loss can be achieved when applying a flow rate below 15 ml/min. Transgalactosylation is found to become dominant over hydrolysis at a higher initial lactose concentration. Under the optimum operating conditions, the maximum lactose conversion is 86 % with a GOS yield about 159 g/l. By benchmarking with previous reported systems for lactose bioconversion, the developed recirculating spiral reactor shows distinguished bioengineering perfomance which may hold great potential for large-scale enzyme-assisted bioprocessess.

As a conclusion, this study has successfully developed nanoparticles and nanofibers-based nanobiocatalysis technology for conversion of lactose-rich dairy industry wastes into GOS. In comparison to the free counterpart, the immobilized β-galactosidase remarkably enhances the enzymatic activities and the nanoenvironment of the nanobiocatalyst favors transgalactosylation over hydrolysis. Moreover, this is one of few studies to understand the enzyme adsorption phenomena on a nano-sized solid surface throughcomprehensive analysis. The nanobiocatalyst in the recirculating reactor demonstrates a promising engineering solution for a continuous and large scale operation for GOS production.

8.2 Future Directions

The incorporation of β-galactosidase onto polymer nanofibers forming nanobiocatalysts integrates the advances in both nanotechnology and biotechnology. The perspectives of the nanobiocatalyst technology show significant potential as well as bright future. Translating this bench-scale technology into commercial practices still remains a critical challenge. Several key issues need to be addressed for future development to promote the feasibility of the nanobiocatalyst into real practices. To realize this laboratory-scale technology into industrial applications, cost reduction as the major hurdle for large-scale trials, long-term stability of the β-galactosidase/nanofiber-nanobiocatalystassembly and operations in a large scale reactor should be taken into consideration.

Reduction in the operation cost that is generally associated with enzyme preparation, immobilization and nanocarrier synthesis should be considered. Large-scale production of β-galactosidase can be made possible through the advances in protein engineering, fermentation and purification technology.

Long-term nanobiocatalyst operation is required to demonstrate its feasibility in a large-scale operation process. At present, the nanobiocatalyst developed in the laboratory trials in this study only demonstrates successfully as a proof-of-concept and it can run up to 9 cycles with 20% of activity remaining. Further research on appropriate strategies to assemble β-galactosidase on the nanocarriers will be required to ensure that the proposed immobilization approaches should be able to hold the enzymes strongly on the nanocarrier surface, but also at the same time to retain their functionality and stability.

Besides, the β-galactosidase/nanofiber-nanobiocatalyst needs also to be tested by treating real dairy wastewater. The process feasibility should be investigated to develop an economically and industrially viable system for generating GOS from the wastewater.

Finally, further study on how to separate and purify the GOS product from the reaction medium is also needed. If these technical issues could be addressed successfully, the β-galactosidase/nanofiber nanobiocatalystwith long-term operation stability will render an economical process for commercialization in a very near future.

.

APPENDIXES

Published Papers

Appendix 1

Nanobiocatalyst Advancements and Bioprocessing Applications

Journal of Royal Society Interface 2015; 12 (102): 1-20
DOI: 10.1098/rsif.2014.0891

Misson, M., Zhang, H. & Jin, B. (2015). Nanobiocatalyst advancements and bioprocessing applications.
Journal of Royal Society Interface, 12(102), 1-20

Appendix 2

Dendrimer-like Nanoparticles Based β-Galactosidase Assembly for Enhancing Its Selectivity towards Transgalactosylation

Enzyme and Microbial Technology 2016; 84: 68-77
DOI:10.1016/j.enzmictec.2015.12.008

Enzyme and Microbial Technology 84 (2016) 68–77

Contents lists available at ScienceDirect

Enzyme and Microbial Technology

journal homepage: www.elsevier.com/locate/emt

Dendrimer-like nanoparticles based β-galactosidase assembly for enhancing its selectivity toward transgalactosylation

Mailin Misson[a,b], Xin Du[c], Bo Jin[a], Hu Zhang[a,*]

[a] School of Chemical Engineering, The University of Adelaide, Adelaide, SA 5000, Australia
[b] Biotechnology Research Institute, Universiti Malaysia Sabah, Jalan UMS, 88400 Kota Kinabalu, Sabah, Malaysia
[c] Research Center for Bioengineering and Sensing Technology, University of Science & Technology Beijing, Beijing100083, PR China

ARTICLE INFO

Article history:
Received 12 November 2015
Received in revised form
16 December 2015
Accepted 17 December 2015
Available online 23 December 2015

Keywords:
Nanobiocatalysis
β-Galactosidase
Dendrimer-like hierarchical pores silica nanoparticles
Galacto-oligosaccharides

ABSTRACT

Functional nanomaterials have been pursued to assemble nanobiocatalysts since they can provide unique hierarchical nanostructures and localized nanoenvironments for enhancing enzyme specificity, stability and selectivity. Functionalized dendrimer-like hierarchically porous silica nanoparticles (HPSNs) was fabricated for assembling β-galactosidase nanobiocatalysts for bioconversion of lactose to galacto-oligosaccharides (GOS). The nanocarrier was functionalized with amino (NH_2) and carboxyl (COOH) groups to facilitate enzyme binding, benchmarking with non-functionalized HPSNs. Successful conjugation of the functional groups was confirmed by FTIR, TGA and zeta potential analysis. HPSNs-NH_2 showed 1.8-fold and 1.1-fold higher β-galactosidase adsorption than HPSNs-COOH and HPSNs carriers, respectively, with the highest enzyme adsorption capacity of 328 mg/g nanocarrier at an initial enzyme concentration of 8 mg/ml. The HPSNs-NH_2 and β-galactosidase assembly (HPSNs-NH_2-Gal) demonstrated to maintain the highest activity at all tested enzyme concentrations and exhibited activity up to 10 continuous cycles. Importantly, HPSNs-NH_2-Gal was simply recycled through centrifugation, overcoming the challenging problems of separating the nanocarrier from the reaction medium. HPSNs-NH_2-Gal had distinguished catalytic reaction profiles by favoring transgalactosylation, enhancing GOS production of up to 122 g/l in comparison with 56 g/l by free β-galactosidase. Furthermore, it generated up to 46 g/l GOS at a lower initial lactose concentration while the free counterpart had negligible GOS production as hydrolysis was overwhelmingly dominant in the reaction system. Our research findings show the amino-functionalized HPSNs can selectively promote the enzyme activity of β-galactosidase for transgalactosylation, which is beneficial for GOS production.

1. Introduction

The specificity and selectivity of enzyme open a new door for development of green and sustainable enzyme-catalyzed bioprocesses. Enzymatic reactions are environmentally friendly due to low chemical consumption without release of toxic by-products. Nevertheless, the biocatalysts constitute the majority of the operational cost when they are applied in large scale processes, and their low stability and reusability in reactor conditions impede their industrial applications [1]. The immobilization of enzyme on support materials is of immense scientific interest. Such technology is able to shelter and/or stabilize enzymes when they are exposed to chemical and environmental harsh conditions. The immobilization also allows the recovery and reuse of these biocatalysts, hence reducing the cost of the biocatalytic process [2,3]. Enzymes have been immobilized onto natural/synthetic polymers or inorganic materials [4]. Despite the fact that optimal immobilization protocols have been extensively studied, retaining the enzyme activity upon immobilization entails persistent investigation. Enzyme activity reduction on support materials remains a significant challenge due to the conformation change upon immobilization [5]. Hence, the development of appropriate enzyme carriers, which can preserve or enhance the enzyme catalytic function, presents a profound research interest.

Nanobiocatalysis, an emerging technology that assembles enzyme molecules onto nanomaterial carriers, synergistically integrates advanced nanotechnology with biotechnology [7]. The technology can increase the enzyme stability and enhance enzyme activity. To date, the enzyme has been immobilized on diverse support materials such as nanofibres [8], nanotubes

* Corresponding author.
E-mail address: hu.zhang@adelaide.edu.au (H. Zhang).

http://dx.doi.org/10.1016/j.enzmictec.2015.12.008
0141-0229/

[9], nanocomposites [10], nanogel [11] and nanoparticles [12]. Silica nanoparticles offer uniform nanopores and tuneable periodic nanostructures which harmonise the diffusion of guest biomolecules with different sizes [13]. It has been recognized that the pore size is vital for enzyme immobilization. Enzyme molecules are incapable to enter into the pore of nanoparticles when the pore is smaller than the molecular size of the enzyme, resulting in a low enzyme loading. In contrast, nanoparticles with pore sizes larger than the enzyme molecular size may reduce the enzyme activity, which may be ascribed to the enzyme leaching or reduction in the enzyme stability [14,15]. Anchoring of biomolecules onto the nanoparticles surface nay result in a strong binding that may decrease the biological activity of the enzyme [16]. In addition, chemical reagents in the immobilization protocol such as crosslinking agents (i.e., glutaraldehyde and epichlorohydrin) lead to a certain level of enzyme activity reduction [6]. Furthermore, enzyme molecules embedded inside the traditional enzyme supports could not directly contact substrates, thus the enzyme supports are unable to maximize the usage of the enzyme, and therefore some of the expensive enzyme is wasted. It is, therefore, constant efforts are being made into exploring robust and functional enzyme carriers.

Dendrimer-like silica nanoparticles with hierarchical pores (HPSNs) were recently developed with unique properties [17]. The carriers have been demonstrated as advanced delivery nanocarriers for siRNA and DNA molecules. The materials were constructed with specific pore structures to increase the surface area for a high loading of biological molecules. Each cavity in the nanostructure can act as a nanobioreactor for enzymatic reaction after the cavity is immobilized with the enzyme. Importantly, the nanocarrier possesses centre-radial open pores that are vital in coordinating diffusion of molecules with different sizes such as substrates and products, and as a result, it enhances the biomolecule interactions as well as reduces the associated mass transfer limitation. Another major issue associated with nanobiocatalysis is to recover nanobiocatalysts from the aqueous solution and reuse them due to their nano-meter size. Magnetic nanoparticles are often employed to realize the recovery by placing them in a magnetic field [18]. For instance, the immobilization of lipase was realized on magnetic chitosan microspheres [19] and Fe_3O_4/poly(styrene-methacrylic acid) magnetic microsphere [20] for enzymatic production of biodiesel from soybean oil. Such an operation poses a significant challenge for scaling up. HPSNs, however, offer easy separation and recovery through sedimentation or centrifugation, which can simplify the recycle process for HPSNs-based nanobiocatalysts.

In the present work, HPSNs were synthesized as nanocarriers to host β-galactosidase. The nanocarriers were functionalized with amino (NH_2) and carboxyl group (COOH) to promote covalent binding with the enzyme. Non-specific binding of the enzyme is expected to occur on the surface of non-functionalized HPSNs. The schematic representation of HPSNs functionalization and enzyme binding is illustrated in Scheme 1. The adsorption performance of three types of HPSNs was evaluated through bovine serum albumin (BSA) and β-galactosidase at different protein concentrations. The β-galactosidase activity was compared for the three HPSNs. HPSNs-NH_2 was then chosen to immobilize β-galactosidase for assessing its recyclability up to 10 continuous runs and its performance in converting lactose into galacto-oligosaccharides (GOS).

2. Materials and methods

2.1. Chemicals

Cetyl trimethylammonium bromide (CTAB), ammonia, ethyl ether, ethanol, tetraethoxysilane (TEOS), 3-aminopropyltriethoxysilane (APES), hydrochloric acid (HCl), *N*,*N*-dimethylformamide (DMF), succinic anhydride, triethylamine (TEA), ammonium hydroxide, sodium carbonate and phosphoric acid were of analytical grade without further purification. Bovine serum albumin (BSA), Kluyveromyces lactis β-galactosidase, *o*-nitrophenyl-β-D-glactopyranoside (ONPG) and coomassie brilliant blue G-250 were obtained from Sigma–Aldrich. Potassium phosphate buffer (PBS) (pH 7.2) was procured from Gibson.

2.2. Preparation and functionalization of nanoparticles

The preparation and functionalization of HPSNs-NH_2 were conducted using the methods developed by Du et al. [17]. A total of 0.5 g of CTAB was dissolved in an emulsion system composed of 70 ml of H_2O, 0.8 ml of aqueous ammonia, 15 ml of ethyl ether and 5 ml of ethanol. The mixture was vigorously stirred at 1000 rpm for 0.5 h at room temperature. The stirring was continued for 4 h after addition of a mixture of TEOS (2.5 ml) and APES (0.1 ml). After 4 h, 1 ml of HCl (37%) was added in order to stop the base-catalyzed reaction. A white precipitate of amino-functionalized silica nanoparticles (HPSNs-NH_2) was obtained from 12 min centrifugation at 4200 rpm. The precipitate was washed with ethanol and water. Treatment with ethanoic HCl (15 ml of concentrated HCl in 120 ml ethanol) was conducted under stirring at 70 °C for 24 h to extract CTAB template. The extracted particles, obtained from centrifugation at 4200 rpm for 12 min, were washed with water for three times. HPSNs with the carboxyl group (HPSNs-COOH) was synthesized by reacting HPSNs-NH_2 (50 mg in 20 ml DMF) with succinic anhydride (0.45 g in 5 ml DMF) in the presence of TEA (0.45 ml) for 5 h. Non-functionalized HPSNs was obtained by calcining HPSNs-NH_2 at 550 °C for 4 h.

2.3. Characterization of nanoparticles

The characterization of HPSNs-NH_2 and HPSNs-COOH using scanning electron microscopy (SEM) was performed under a Philips XL30 field emission scanning electron microscope operated at 10 kV. Fourier transform infrared (FTIR) spectra of samples were recorded on a Thermo Scientific NICOLET 6700 FTIR spectrometer at room temperature. TriStar II surface area and porosity analyzer from Micromeritics at −196 °C was used for nitrogen adsorption–desorption measurements using the volumetric method. Brunauer–Emmett–Teller (BET) specific surface areas were calculated by using adsorption data at a relative pressure range of P/P_0 range of 0.05–0.25. The Barrett, Joyner, and Halenda (BJH) method was used to estimate pore size distributions from adsorption branch of isotherm. The amounts of N_2 adsorbed at the single point of $P/P_0 = 0.99$ was used to determine pore volumes. The particle sizes and zeta-potentials dispersed in PBS (pH 7.5) were measured using a Malvern Zetasizer Nano ZS (Malvern Inst. Ltd., U.K.) equipped with four-side clear cuvettes or the ZET 5104 cell at room temperature. S60/51920 TGA/DSC (thermogravimetric/differential scanning calorimeter) analyzer from Setaram Instrumentation was used for thermogravimetric analysis (TGA) of samples using an oxidant atmosphere (air, 30 ml/min) (heating ramp of 10 °C/min from room temperature to 800 °C).

2.4. Enzyme immobilization on nanoparticles

Silica nanoparticles (10 mg) were dispersed in 1 ml PBS buffer (pH 7.2) and sonicated for 30 min. The mixtures were mixed into BSA (0–10 mg/ml) or β-galactosidase (0–9 mg/ml) and gently stirred overnight at 4 °C [21]. The particles were recovered through centrifugation at 4200 rpm for 10 min and washed with water to remove free BSA or enzyme on the surface of nanoparticles. The supernatant and washing solution were collected to measure the concentration of non-adsorbed protein.

2.5. Production of galacto-oligosaccharides

Lactose (50–400 g/l) was prepared by dissolving into PBS (pH 7.2) at 60 °C. After the solution temperature cooled down to room temperature, free or immobilized enzyme were added and incubated at 37 °C in an orbital shaker at 200 rpm. Samples were drawn at pre-set intervals for analysis (1–5 h) and immediately heated in boiling water for 5 min to deactivate the enzyme activity [22]. The mixture was centrifuged to separate the supernatant and nanoparticles. The resultant supernatant was filtered using 0.45 μm nylon filters, diluted 40 times and analyzed by high performance liquid chromatography (HPLC).

2.6. Chemical analysis

The enzyme concentration was assayed using the method described by Bradford [23]. A total of 100 mg Coomassie brilliant blue G-250 were dissolved in 50 ml of 95% ethanol, 100 ml of 85% phosphoric acid and diluted with water to a final volume of 1 l with gentle mixing. A total of 100 μl sample was added into 5 ml of the Bradford solution, mixed homogenously, and allowed to react for 5 min and measured at a 595 nm spectrophotometer. Protein concentration was determined based on the calibration curve using BSA as a protein standard. The adsorption yield and adsorption capacity of the immobilized enzyme were calculated using Eqs. (1) and (2), respectively, where P_i is the initial concentration of protein that is subjected for immobilization, P_w and P_s are the amount of protein in washing solution and supernatant, respectively [24].

$$\text{Adsorption yield}\,(\%) = \frac{\left[P_i - (P_w + P_s)\right]}{P_i} \times 100 \quad (1)$$

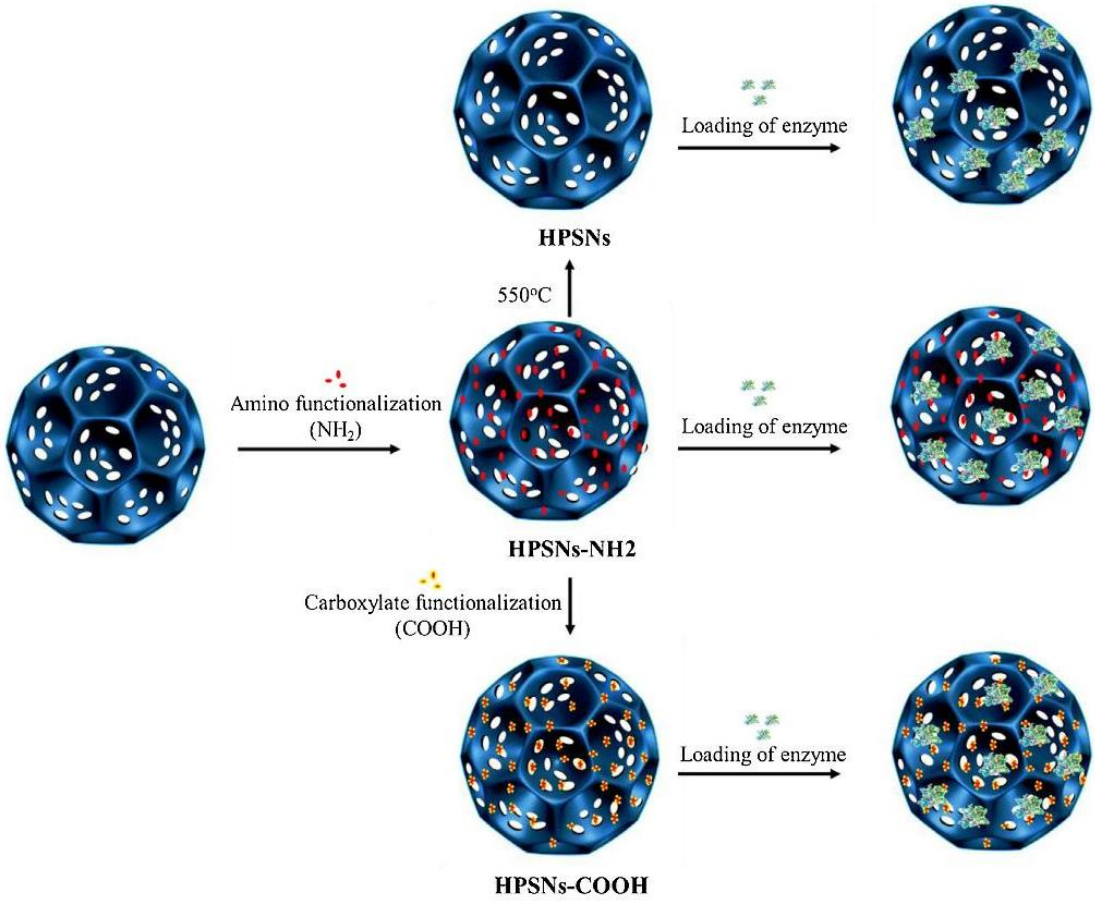

Scheme 1. Schematic description on the functionalization of dendrimer-like HPSNs for the loading of β-galactosidase.

$$\text{Adsorption capacity (mg/g)} = \frac{[P_i - (P_w + P_s)]}{\text{mass of nanoparticles}} \quad (2)$$

The enzyme activity was measured by mixing 100 samples with 1.7 ml of PBS buffer (pH 7.2) and 0.2 ml of 20 mM ONPG prior to continuous agitation at 37 °C for 10 min. A total of 2 ml of 1 M sodium carbonate was added immediately to stop the reaction before measuring the liberated product spectrophotometrically at 405 nm [25]. The enzyme activity was determined from the plotted *o*-nitrophenol standard curve. One unit (1 U) of β-galactosidase is defined as the amount of enzyme liberates 1 μmole of *o*-nitrophenol per minute under standard assay conditions. The activity retention of immobilized enzyme was determined using Eq. (3), where α_i is the activity of immobilized enzyme activity, while α_f is the activity of free enzyme at the same concentration [26].

$$\text{Activity retention}(\%) = \frac{\alpha_i}{\alpha_f} \times 100 \quad (3)$$

Saccharides (lactose, glucose, galactose, GOS) were determined using high performance liquid chromatography (HPLC) (Agilent) equipped with an aminex HPX-87H column (300 × 7.8 mm) maintained at 60 °C and a refractive index detector. H_2SO_4 (8 mmol/l) was used as a mobile phase at a flow rate of 0.5 ml min^{-1}. An approximately 5 μl samples were injected for saccharides analysis [27]. The lactose conversion was calculated using Eq. (4) [27,26,22–24]. The yield (Y) of saccharides (glucose, galactose and GOS) was determined using Eqs. (5)–(7).

$$\text{Conversion}(\%) = \frac{[\text{initial lactose}] - [\text{final lactose}]}{[\text{initial lactose}]} \times 100 \quad (4)$$

$$Y_{\text{glucose}}(\%) = \frac{[\text{glucose}]}{[\text{initial lactose}]} \times 100 \quad (5)$$

$$Y_{\text{galactose}} = (\%) \frac{[\text{galactose}]}{[\text{initial galactose}]} \times 100 \quad (6)$$

$$Y_{\text{gos}}(\%) = \%\text{Conversion} - \%Y_{\text{glucose}} - \%Y_{\text{galactose}} \quad (7)$$

2.7. Recyclability

The activity of the immobilized enzyme on HPSNs-NH_2 was continuously monitored for 10 cycles. The enzyme activity was determined using the procedure described in Section 2.6. After each assay, the nanoparticle-carrying enzyme was separated from the reaction medium through centrifugation at 4200 rpm for 10 min, and then washed with PBS solution (pH 7.2), dewatered before supplementing with fresh substrate to initiate a new cycle of reaction. The enzyme activity at the first run was considered as control (100%) for the calculation of remaining activity after repeated uses [28].

2.8. Statistical analysis

Experimental studies were carried out in triplicate. The data were analyzed using the statistical tool in MS Excel 2010 and presented as a mean value with an average standard deviation of <5%.

3. Results and discussion

3.1. Preparation and characterization of HPSNs

Three types of dendrimer-like nanoparticles: HPSNs-NH_2, HPSNs-COOH and HPSNs were prepared according to Scheme 1. The surface of HPSNs was functionalized with amino (NH_2) and carboxyl (COOH) groups to facilitate β-galactosidase binding. The enzyme, which possesses amino ($-NH_2$), carboxyl ($-$COOH), thiol

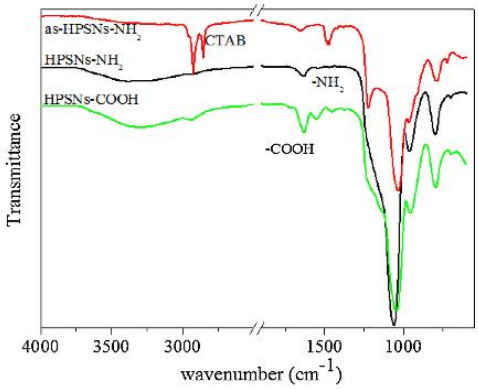

Fig. 1. FTIR spectra of HPSNs-NH_2 with CTAB template, HPSNs-NH_2 and HPSNs-COOH.

Table 1
Physicochemical properties of HPSNs-NH_2 and HPSNs-COOH.

	HPSNs-NH_2	HPSNs-COOH
pH	7.59	7.54
Particle size (nm)	756	460
Zeta potential (mV)	+4.5	−6.7
BET surface area ($m^2\ g^{-1}$)	747	585
Pore size (nm)	4.5	4.3
Total pore volume ($cm^3\ g^{-1}$)	1.26	1.19
TGA analysis (mmol groups/g product)	0.79	0.57
N_2 sorption (groups/nm^2)	0.70	0.65

(−SH) and hydroxyl (−OH) groups located in lysine, arginine, glutamic and aspartic acid residues, could interact with the functional groups on the HPSNs surface [7]. Meanwhile, for HPSNs without functional group, enzyme might perform non-specific binding and randomly attach on the material surface.

Successful conjugation of amino and carboxyl functional groups on the surface of HPSNs is confirmed from the Fourier transforms infrared (FTIR) spectra of HPSNs-NH_2 and HPSNs-COOH (Fig. 1). The presence of the amino groups is evidenced by weak peaks at 1463 and 1520 cm^{-1} due to N—H bending. Grafting of the carboxylic acid groups is signified by three peaks at 1415, 1554 and 1710 cm^{-1} for carbonyl stretching. Other characterization experiments have also been conducted to demonstrate different groups on the surface of HPSNs. The zeta potentials change from +4.5 (HPSNs-NH_2) to −6.7 (HPSNs-COOH) in PBS solution (Table 1). The amount of functional groups attached on HPSNs surface was evaluated through thermogravimetric analysis (TGA) analysis. The surface functional group coverage of the NH_2 group (0.79 mmol NH_2 groups/g product) is found to be greater than the COOH group (0.57 mmol COOH groups/g product). Similar discrepancy for the two functional groups on the HPSN surface is also confirmed by nitrogen sorption, with 0.70 and 0.27 groups/nm^2 based on the specific surface areas for NH_2 and COOH group, respectively. The Brunauer–Emmett–Teller (BET) surface area of HPSNs-NH_2 (747 $m^2\ g^{-1}$) is also higher than HPSNs-COOH (585 $m^2\ g^{-1}$).

The morphology and pore size of the nanoparticles were also characterized through SEM. Since three types of nanoparticles share very similar images, and only HPSNs-NH_2 are presented in Fig. 2. It can be seen from Fig. 2 that uniform sized nanoparticles are prepared with a particle size of 160–250 nm. The nanoparticles have hierachical pores and the center-radial pores were determined to be in the range of 9–117 nm. The average size of uniform mesopores confirmed by the TEM image was ca. 4.5 nm. HPSNs-NH_2 have been demonstrated to be a promising nanocarrier for loading and delivery of therapeutic macromolecules, such as short-interference RNA or plasmid DNA [17]. We will explore the unique structure of this nanocarrier for enzyme immobilization. This multiple-pore structure favors a high enzyme loading and harmonizes diffusion of substrates towards the enzyme on the pore surface, which can promote the interfacial reactions between the substrate and the enzyme.

Table 2
Characteristics of β-galactosidase and bovine serum albumin (BSA).

	β-Galactosidase	BSA
Molecular weight	116,349	69,000
Isoelectric point	4.6–5.1	4.7–4.9
Zeta potential (mV)	−2.3	−8.53
Diameter (nm)	7	4.9

3.2. Immobilization of BSA and β-galactosidase

High adsorption capacity is one of the major criteria in selecting enzyme carriers. Two parameters have often been used to describe the adsorption performance: adsorption capacity and adsorption yield. The adsorption yield is defined as the percentage of enzymes in the bulk solution transferred to the solid surface. We have used two different proteins to examine the adsorption of the nanocarriers. BSA that often used for evaluation of adsorption was employed for benchmarking the nanocarriers. Comparing with BSA, another enzyme, β-galactosidase, is much larger in size and less negative in zeta potential (Table 2). As Fig. 3(a, b) indicates, HPSNs-NH_2 demonstrates the highest adsorption yield for both BSA (90%) and β-galactosidase (82%) at 1 mg/ml concentration. As the enzyme concentration increases, HPSNs-NH_2 are able to retain almost all BSA molecules inside the nanoparticle pores, while nearly 40% of β-galactosidase molecules are adsorbed at a protein concentration above 4 mg/ml. Meanwhile, the highest yield for HPSNs-COOH is observed below 80% for both biomolecules at all tested concentrations. When the BSA concentration increases, the adsorption yield starts to slightly reduce. Besides, the adsorption yield also decreases as the enzyme concentration increases, a similar profile as HPSNs-NH_2. The least amount of the bound protein is observed on the non-functionalized HPSNs. Nevertheless, the absorption yield for the enzyme nearly doubles in comparison with BSA. Interestingly, the absorption yield for β-galactosidase on three types of nanocarriers shares a similar trend as the concentration increases.

Protein adsorption onto the nanocarriers depends on two factors: the available surface for protein molecules and the interaction force between the protein molecules and the functional groups on the nanocarrier surface. The internal surface in the mesopores may be available if the molecular size is smaller than or equivalent to the mesopore size. β-Galactosidase has a high molecule weight of 116,349, and the molecular diameter is estimated to be ca. 7 nm, while BSA has a molecular diameter of 4.9 nm (Table 2). The mesoporous size is averaged to be around 4.5 nm, which allows BSA molecules to occupy the pore surface, but may block β-galactosidase molecules into the mesopores. There are three possible interaction forces governing protein adsorption on the nanoparticle surface: covalent bonds, electrostatic interactions and non-specific weak binding. BSA and β-galactosidase are able to attach on the HPSNs surface by forming covalent linkages between the grafted NH_2 and COOH groups on the HPSN surface and the COOH and NH_2 group of the protein molecules. Such functional groups on the enzyme have been reported to interact with aldehyde, cyanogen, epoxy and carbodiimide-activated nanoparticles to facilitate xylitol dehydrogenase binding [29]. For the same biomolecules, HPSNs-NH_2 seem to perform better adsoprtion than HPSNs-COOH, which could be explained by a higher BET surface

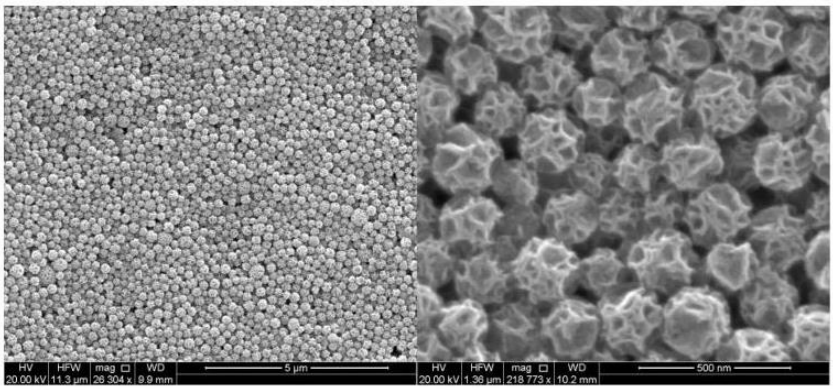

Fig. 2. SEM images of HPSNs-NH_2 at 5 μm on the left side and 500 nm at the right side.

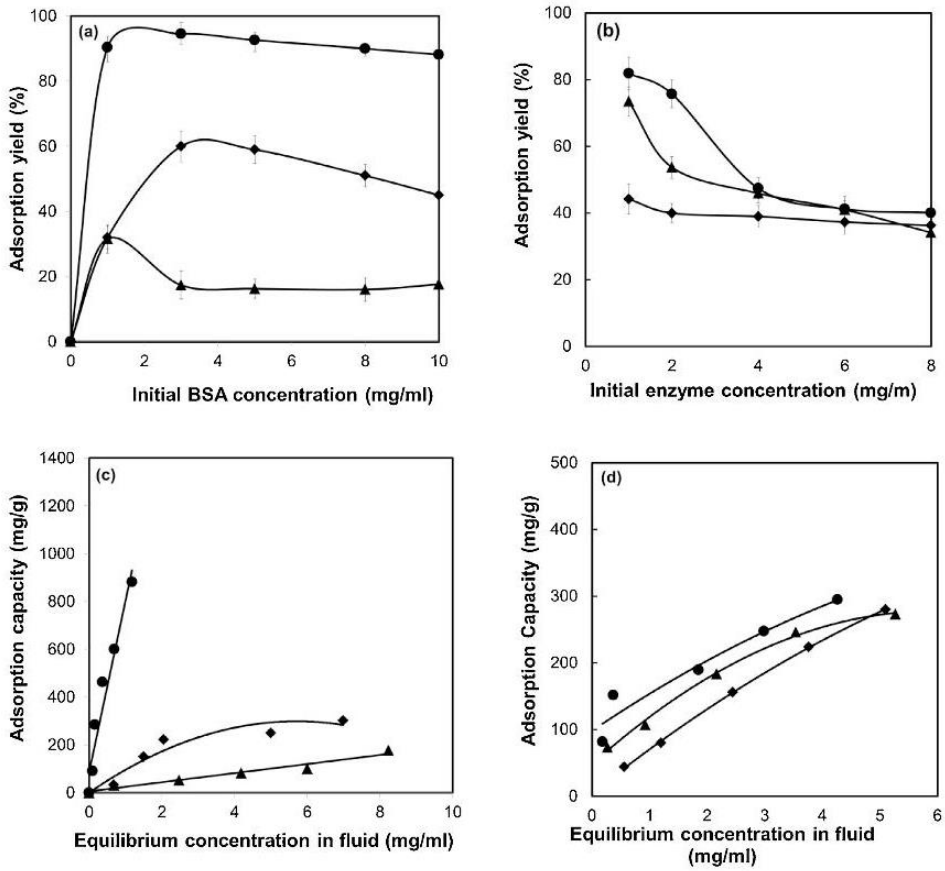

Fig. 3. Adsorption yield and adsorption capacity of BSA (a, c) and β-galactosidase (b, d) on HPSNs, HPSNs-NH_2 and HPSNs-COOH. (BSA/enzyme concentration: 2–10 mg/ml, incubated at 37 °C in pH 7 phosphate buffer solution for overnight at 4 °C). ● HPSNs-NH_2, ♦ HPSNs-COOH, ▲ HPSNs.

area and a greater functional group coverage of HPSNs-NH_2 than HPSNs-COOH thus provide more active sites for biomolecules binding. In addition, an electrostatic force may also promote protein binding. The negative charge of BSA and β-galactosidase (Table 2) could interact with the opposite charge of amino-functionalized HPSNs (Table 1). This force could be used to explain the difference between the adsorption of BSA and β-galactosidase onto HPSNs-NH_2. The electrostatic interaction force of HPSNs-NH_2-BSA is higher than that HPSNs-NH_2-β-galactosidase. The reason is probably due to a stronger negative charge of BSA than β-galactosidase, which can facilitate the BSA adsorption onto the mesopores. Protein molecules could also be adsorbed onto the HPSNs surface

without any functional groups through non-specific weak binding such as hydrophobic interactions or van der Waals forces [30]. This force becomes more dominant for β-galactosidase as the enzyme concentration increases above 4 mg/ml. Covalent force and electrostatic interactions play a major role at the low enzyme concentration as the functional groups on the nanoparticles are not consumed by the enzyme molecules. As the enzyme concentration increases, extra enzyme molecules are attached to the non-functionalized surface due to the non-specific binding, and this may also explain why the adsorption yield is similar for three types of nanoparticles at a high enzyme concentration.

In a reactor system, enzyme immobilized through weak binding may easily leak into the reaction medium due to mechanical stress derived from agitation or liquid flow [31,32]. Therefore, the functional groups on the HPSN surface can create specific and strong covalent binding for biomolecules. However, more importantly, the functional groups must be able to preserve the enzyme catalytic activity through maintaining the enzyme conformation structure.

Another parameter, adsorption capacity defined as the amount of adsorbed enzyme (mg) per gram of enzyme supports, is depicted in Fig. 3(c, d). The binding capacity is often plotted against the equilibrium enzyme concentration in the liquid solution to determine the adsorption equilibrium relationship. In the case of BSA, HPSNs-NH_2 and HPSNs show a linear relationship between the adsorption capacity and the equilibrium enzyme concentration in the solution at the tested enzyme concentration (0–10 mg/ml). HPSNs-NH_2 have a more sharp slope in the isothermal adsorption profile, which means that HSPNs-NH_2 are able to accommodate a much higher amount of BSA than HPSNs. HPSNs-COOH exhibit a Langmuir isothermal adsorption profile and the maximum adsorption capacity is estimated to be 300 mg BSA/g nanocarrier.

Meanwhile, for β-galactosidase, the Freundlich isotherm ($C_{AS}^* = KC_A^{*n}$) is the best to correlate the experimental data for three HPSNs. The power indices, *n*, are 0.3694, 0.8363 and 0.4625 for HPSNs-NH2, HPSNs-COOH and HPSNs, respectively. Since they are below 1.0, the three types of nanoparticles are favorable for enzyme adsorption. At an initial enzyme concentration of 8 mg/ml, all HPSNs carriers exhibit a comparable adsorption yield of 295–328 mg/g, which exceeds other reported carriers summarized in Table 3. Cellulase on magnetic chitosan nanoparticles carrier was found to have a lower adsorption capacity (112.3 mg/g) [33]. Laccase loading on metal-mediated mesoporous silica and mesoporous carbon was 98.1 mg/g [34] particle and 233.3 mg/g [35], respectively. Our enzyme adsorption finding is also in agreement with the previous report [17] in which HPSNs nanocarriers demonstrated to have a high gene loading capacity and high transfection efficiency in the gene delivery application.

3.3. Operational stability of nanobiocatalysts

The major challenge in the development of the nanobiocatalyst technology is to retain the catalytic activity of the enzyme upon immobilization onto nanocarriers. The enzyme activity was measured using ONPG as the substrate for the enzymes on three carriers, benchmarking with the free enzyme. The initial enzyme concentration was referred to one used for immobilization on three nanocarriers and the formed nanocarrier/enzyme assemblies were centrifuged and resuspended for enzyme activity measurement. The activity retention was determined by dividing the activity of the immobilized β-galactosidase to the activity of free β-galactosidase. As shown in Fig. 4, HPSNs-NH_2-Gal exhibits distinguished enzyme stability with 100% activity retention at all tested concentrations, indicating the enzyme catalytic activity was unaffected by the immobilization process. Both HPSNs-COOH and HPSNs provide a lower activity retention at a low enzyme concentration (0.5 mg/ml), approximately 80% and 60%, respectively. This low activity retention may be due to a low adsorption yield (Fig. 3(b)), which results in less enzyme molecules to react with ONPG. However, as the initial enzyme concentration increases, three nanocarriers have full activity retention. It has been reported that enzyme conformational change upon immobilization reduces the enzyme reactivity [36]. From Fig. 4, we can conclude that there is no enzyme conformation change when immobilized on three nanocarriers.

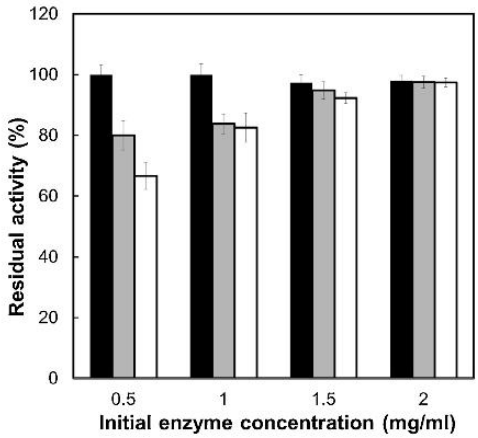

Fig. 4. Activity retention profiles of free β-galactosidase and immobilized β-galactosidase on HPSNs-NH_2, HPSNs-COOH and HPSNs at various enzyme concentration (0.5–2 mg/ml). The activity of free enzyme at similar concentration at 37 °C was selected as a control (100%). ■ HPSNs-NH_2, ▒ HPSNs-COOH and □ HPSNs.

Because of its high adsorption yield and activity retention, HPSNs-NH_2 was chosen for further study. Recyclability is a great advantage for immobilized enzyme over free enzyme. Simple recovery of immobilized enzyme and retention of enzyme activity for many runs allow the enzyme to be used in large-scale process, defraying the operation cost. The HPSNs carriers were separated from reaction medium by centrifugation at a mild operation condition (4200 rpm in the lab centrifuge, corresponding to 2397 g), which is applicable in large operation. Separations of nanobiocatalysts are quite challenging, and often magnetic nanoparticle-based nanobiocatalysts are prepared to facilitate separation in a magnetic field. However this operation requires a long separation time and a strong magnetic field, and it also leads to nanobiocatalyst loss after each run [37].

Fig. 5 presents retention of the β-galactosidase activity on HPSNs-NH_2 after ten cycles. It can be seen that HPSNs-NH_2-Gal can be recycled up to ten times with 20% of its initial activity remaining. It is noted that after five cycles, HPSNs-NH_2-Gal is able to retain 80% of its initial activity. The decrease of activity is consistent with literature reports. It was reported that the reusability was up to seven cycles [38] or six cycles [39] with the remaining activity was 20% and 35%, respectively.

3.4. Production of galacto-oligosaccharides

After evaluating the biocatalytic stability, the engineering performance of HPSNs-NH_2-Gal was evaluated for galacto-oligosaccharide (GOS) synthesis, a commercially important functional food. Fig. 6(a, b) illustrates the reaction products of lactose bioconversion by free β-galactosidase and HPSNs-NH_2-Gal. The reaction mixtures comprised of glucose, galactose, GOS and remaining lactose. In β-galactosidase-catalyzed reaction, lactose is bioconverted through competitive reactions between hydrolysis and transgalactosylation. Initially, the lactose glycosidic linkages

Table 3
Adsorption capacity and activity recovery of enzymes on various supports.

Support	Enzyme	Adsorption capacity (mg/g)	Activity retention (%)	References
HPSNs-NH2	β-Galactosidase	320 100	100 100	This work
HPSNs-COOH	β-Galactosidase	280 74	100 90	
HPSNs	β-Galactosidase	280 44	100 70	
Polydopamine-coated iron oxide nanoparticles	Formate dehydrogenase	–	90	[46]
Chitosan	Glucose oxidase	–	77.9	[47]
PGMA-b-PDMAEMA-grafted magnetic nanoparticles	Lipase	500	43.1	[48]
Magnetic mesoporous silica nanoparticles	Laccase	72.6	81.5	[34]
Cu^{2+}-chelated- magnetic mesoporous silica nanoparticles	Laccase	98.1	92.5	[34]
Chitosan	Laccase	20	52	[49]
Magnetic polymer microspheres	Laccase	94.1	65	[50]

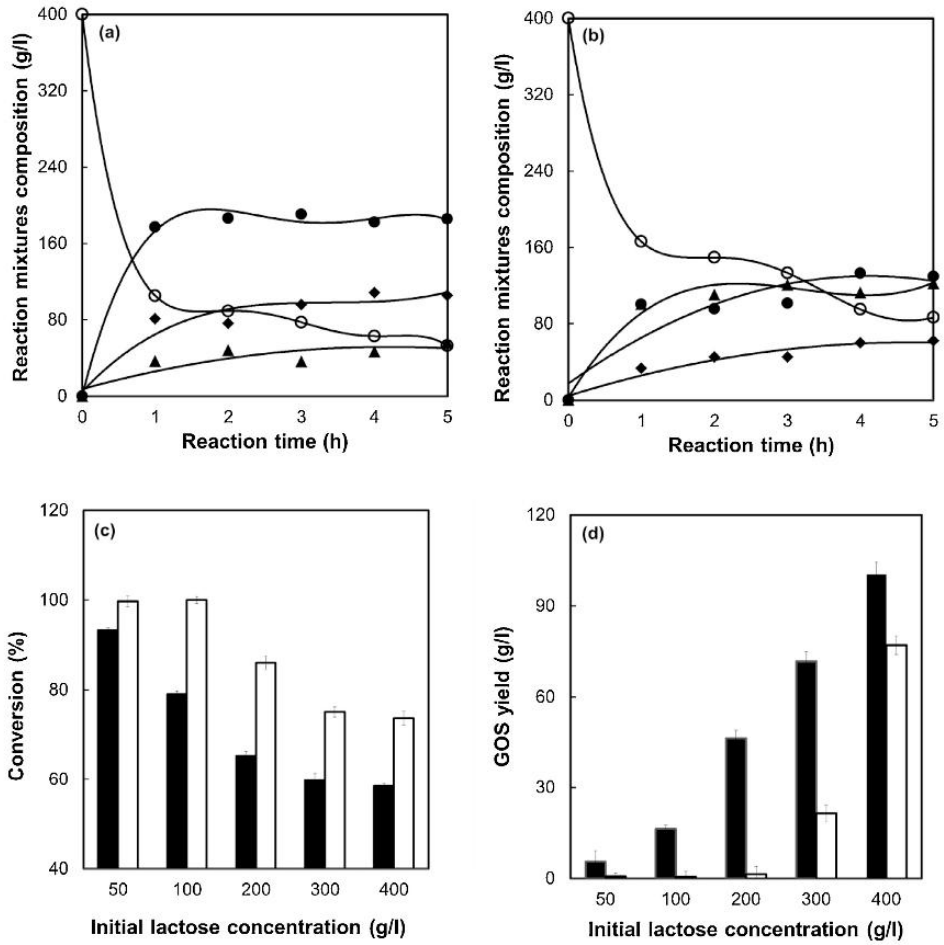

Fig. 6. The composition of reaction mixture (remaining lactose, glucose, galactose, GOS) by (a) free β-galactosidase and (b) HPSNs-NH_2-Gal and (c) the effect of initial lactose concentrations on lactose conversion and (d) GOS yield. (Operation conditions: 2 mg/ml enzyme concentration in pH 7 incubated at 37 °C for 1 h reaction time using 400 g/l lactose for (a, b) and 50–400 g/l for (c, d)).○ Remaining glucose, ▲ GOS, ● glucose, ♦ galactose, ■ HPSNs-NH_2-Gal and □ free β-galactosidase.

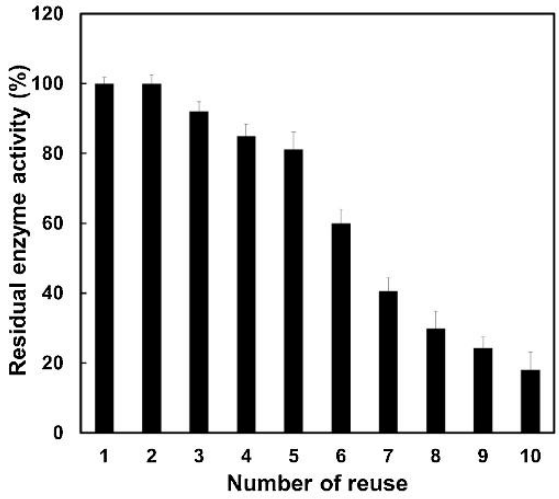

Fig. 5. Recyclability of immobilized β-galactosidase on HPSNs-NH_2 after 10 repeated cycles. The activity determined at the first cycle (0.45 U/mg) was considered as a control (100%). (Operation conditions: at 37 °C with 2 mg/ml enzyme concentration in pH 7).

are attacked to form enzyme–galactosyl complexes [40]. Hydrolysis takes place when water acts a galactosyl acceptor, yielding glucose and galactose as end products, while GOS is generated through nucleophilic–galactosyl reaction in transgalactosylation [41,42].

It can be seen in both free and immobilized enzyme that two reactions apparently occur during the first hour reaction time. The remaining lactose is approximately 100 g/l for free β-galactosidase, lower than the unconverted lactose found in HPSNs-NH_2-Gal (160 g/l), indicating the free enzyme demonstrates to have faster lactose reduction. The conversion rate is determined to be 300 g/l/h for the free enzyme and 240 g/l/h for the immobilized enzyme. Despite to that fact, it is found that the free β-galactosidase generates a higher glucose yield which becomes the major product (average 185 g/l). It implies the preferance of the free enzyme toward the hydrolysis reaction. In contrast, the HPSNs-NH_2-Gal yields glucose about 1.7-times lower than the free counterpart, signifying transgalactosylation dominates the lactose bioconversion. Consequently, the GOS yield by HPSNs-NH_2-Gal is 2.6-times higher than the free enzyme.

By extending the reaction time to 5 h, lactose concentration in the free enzyme reaction system experiences a steady and slow decrease. Glucose maintains at the same level as the first hour. A slight increase in GOS and galactose concentration can be found in Fig. 6(a). In the HPSNs-NH_2-Gal catalyzed system, lactose concentration has the similar decrease trend as the free enzyme after one hour. However, a steady increase of glucose and galactose concentration can be seen from Fig. 6(b). GOS concentration keeps at between 100 and 122 g/l. In comparison to reported previous studies, the GOS formation by HPSNs-NH_2-Gal is observed to have comparable or even better performance. Employement of β-galactosidase on alginate was described to generate GOS about 87 g/l [27], 40 g/l by membrane-bound β-galactosidase [43] and 104 g/l on magnetic polysiloxane–polyvinyl alcohol [44].

Fig. 6(c, d) presents comparison of the effect of the initial lactose concentration on GOS formation by free β-galactosidase and HPSNs-NH_2-Gal. The conversion trends for both enzymes decrease with the increasing lactose concentration. Free enzyme is found superior in lactose conversion, up to 100% below the initial lactose concentration of 100 g/l. Lactose conversion by the free enzyme consistently exceeds HPSNs-NH_2-Gal at all tested concentrations (Fig. 6(c)). In contrast, HPSNs-NH_2-Gal performs much better in GOS synthesis than the free counterpart. Fig. 6(d) indicates that the free enzyme is unfavourable for GOS formation particularly at a lower lactose concentration. In a diluted solution, water molecules surround the free enzyme reaction sites, therefore, hydrolysis becomes the preferential reaction. When the initial lactose concentration is above 300 g/l, more sugar molecules compete with water molecules and transgalactosylation starts to play a role, which can be seen that GOS production increases sharply. It can be seen that HPSNs-NH_2-Gal shows preference toward transgalactosylation regardless of the initial lactose concentration. While free enzyme does not generate any GOS at a lower lactose concentration up to 200 g/l, HPSNs-NH_2-Gal produces GOS up to 50 g/l. Although GOS yield from HPSNs-NH_2-Gal is still better than that from the free enzyme, the gap is significantly reduced at the initial lactose concentration of 400 g/l. HPSNs microenvironment might have beneficially reduced the diffusion path between the biomolecules and creating a local nanoenvironment with a higher sugar concentration around the enzymatic catalytic sites, promoting more galactosyl–nucleophilic reactions than galactosyl–water activities, therefore, yielding higher GOS than glucose and galactose. This nanoenvironment seems very pronounced at a lower lactose concentrations. As the intital lactose concentration increases, more sugar molecules surrounding the enzymes supress the water activities, and the HPSNs-NH_2-Gal nanobiocatalyst assembly starts to behave like the free enzyme. The nanoenvironment has also been reported to provide a localized optimal reaction condition for immobilized enzyme, such as pH, ionic strength, and temperature [7]. It is evidenced by the increased reaction rates of nanoparticles-bound lipase from 3 to 180 times higher than controls because of a local pH of 7.7 in the nanobiocatalyst assembly [45].

4. Conclusion

Functionalized dendrimer-like silica nanoparticles with hierarchical pores were employed as enzyme nanocarriers to form an enzyme-nanocarrier assembly. The functionalization with amino group favored enzyme binding than carboxylate functional group. The nanoparticles functionalized with NH_2 group have performed better in adsorption of BSA than COOH group or non-functionalized nanoparticles, and this is also applied to the β-galactosidase adsorption at low enzyme concentration. However, they all had a very similar adsorption yield at higher initial enzyme concentration. The Freundlich isothermal adsorption was found to best fit the experimental data of enzyme adsorption for all three types of nanoparticles. The nanoparticles were found favorable for the enzyme adsorption. The enzyme activity was fully preserved upon immobilization onto three types of nanoparticles. The enzyme assembly with HPSNs-NH2 was further demonstrated to run up to 10 cycles with 20% of the enzyme activity remaining. Importantly, we have found that the enzyme assembly was able to generate GOS at a much higher yield than free counterpart when the initial lactose concentration is lower than 400 g/l, which means that the enzyme assembly had a preference toward transgalactosylation, while hydrolysis was dominate in the free enzyme solution. At a high initial lactose concentration, the enzyme assembly and free enzyme shared a comparable GOS yield. Our research findings demonstrated the HPSNs can be used to form enzyme-nanocarrier assemblies which have enhanced selectivity toward the required reaction pathways. The findings of the nanocarrier structure-function relationship in enzyme immobilization in this study will provide a useful insight for future development of the hybrid nanobiocatalyst assembly, by correlating and integrating

the unique functions of nanocarriers and enzymes. To translate the bench-scale technology into commercial practices, the development of advanced nanoparticle-based enzyme carriers is a critical challenge. Cost reduction as the major hurdle for large-scale trials, long-term stability of the biocatalyst-nanocarrier assembly and operations in a large scale reactor will be addressed in future research.

Conflict of interests

The authors confirm that there are no known conflicts of interest.

Acknowledgments

MM gratefully acknowledges the financial support from the Universiti Malaysia Sabah and Malaysian Government. HZ thanks for the 111 Project (B12034). HPLC facility support from Paul Grbin's research group and sugar analysis assistance by Nick Van Holst are highly appreciated. MM also appreciates the technical supports by Jason Peak, Jeffrey Hiorns and Michael Jung from workshop department at School of Chemical Engineering.

References

[1] A. Illanes, A. Cauerhff, L. Wilson, G.R. Castro, Recent trends in biocatalysis engineering, Bioresour. Technol. 115 (2012) 48–57.
[2] E.P. Cipolatti, M.J.A. Silva, M. Klein, V. Feddern, M.M.C. Feltes, J.V. Oliveira, et al., Current status and trends in enzymatic nanoimmobilization, J. Mol. Catal. B: Enzym. 99 (2014) 56–67.
[3] M. Misson, B. Jin, B. Chen, H. Zhang, Enhancing enzyme stability and metabolic functional ability of β-galactosidase through functionalized polymer nanofiber immobilization, Bioprocess Biosyst. Eng. 38 (2015) 1915–1923.
[4] S. Datta, L.R. Christena, Y.R.S. Rajaram, Enzyme immobilization an overview on techniques and support, Biotechnol. Adv. 3 (2012) 1–9.
[5] Y.-T. Zhu, X.-Y. Ren, Y.-M. Liu, Y. Wei, L.-S. Qing, X. Liao, Covalent immobilization of porcine pancreatic lipase on carboxyl-activated magnetic nanoparticles: characterization and application for enzymatic inhibition assays, Mater. Sci. Eng.: C 38 (2014) 278–285.
[6] Y. Li, J. Quan, C. Branford-White, G.R. Williams, J.-X. Wu, L.-M. Zhu, Electrospun polyacrylonitrile-glycopolymer nanofibrous membranes for enzyme immobilization, J. Mol. Catal. B: Enzym. 76 (2012) 15–22.
[7] M. Misson, H. Zhang, B. Jin, Nanobiocatalyst advancements and bioprocessing applications, J. R. Soc. Interface 12 (2015) 1–8.
[8] S.C. Pinto, A.R. Rodrigues, J.A. Saraiva, J.A. Lopes-Da-Silva, Catalytic activity of trypsin entrapped in electrospun poly(ϵ-caprolactone) nanofibers, Enzyme Microb. Technol. 79–80 (2015) 8–18.
[9] L. Wang, R. Jiang, Reversible His-tagged enzyme immobilization on functionalized carbon nanotubes as nanoscale biocatalyst, Methods Mol. Biol. 743 (2011) 95–106.
[10] J. Hong, W.-Y. Yang, Y.-X. Zhao, B.-L. Xiao, Y.-F. Gao, T. Yang, et al., Catalase immobilized on a functionalized multi-walled carbon nanotubes—gold nanocomposite as a highly sensitive bio-sensing system for detection of hydrogen peroxide, Electrochim. Acta 89 (2013) 317–325.
[11] K. Zhu, T. Ye, J. Liu, Z. Peng, S. Xu, J. Lei, et al., Nanogels fabricated by lysozyme and sodium carboxymethyl cellulose for 5-fluorouracil controlled release, Int. J. Pharm. 441 (2013) 721–727.
[12] J. Hou, G. Dong, Y. Ye, V. Chen, Laccase immobilization on titania nanoparticles and titania-functionalized membranes, J. Membr. Sci. 452 (2014) 229–240.
[13] J. Liu, S.Z. Qiao, Q.H. Hu, G.Q. Lu, Magnetic nanocomposites with mesoporous structures: synthesis and applications, Small 7 (2011) 425–443.
[14] H. Ikemoto, Q. Chi, J. Ulstrup, Stability and catalytic kinetics of horseradish peroxidase confined in nanoporous SBA-15, J. Phys. Chem. C 114 (2010) 16174–16180.
[15] L.C. Sang, M.O. Coppens, Effects of surface curvature and surface chemistry on the structure and activity of proteins adsorbed in nanopores, Phys. Chem. Chem. Phys. 13 (2011) 6689.
[16] A. Buthe, S. Wu, P. Wang, Nanoporous silica glass for the immobilization of interactive enzyme systems, Methods Mol. Biol. 679 (2011) 37–48.
[17] X. Du, B. Shi, J. Liang, J. Bi, S. Dai, S.Z. Qiao, Developing functionalized dendrimer-like silica nanoparticles with hierarchical pores as advanced delivery nanocarriers, Adv. Mater. 25 (2013) 5981–5985.
[18] W. Xie, X. Zang, Immobilized lipase on core–shell structured Fe_3O_4–MCM-41 nanocomposites as a magnetically recyclable biocatalyst for interesterification of soybean oil and lard, Food Chem. 194 (2016) 1283–1292.
[19] W. Xie, J. Wang, Immobilized lipase on magnetic chitosan microspheres for transesterification of soybean oil, Biomass Bioenergy 36 (2012) 373–380.
[20] W. Xie, J. Wang, Enzymatic production of biodiesel from soybean oil by using immobilized lipase on Fe_3O_4/poly(styrene-methacrylic acid) magnetic microsphere as a biocatalyst, Energy Fuels 28 (2014) 2624–2631.
[21] M. Yasuda, H. Nikaido, W.R. Glomm, H. Ogino, K. Ishimi, H. Ishikawa, Enzyme immobilization on amphiphilic polymer particles having grafted polyionic polymer chains, Biochem. Eng. J. 48 (2009) 6–12.
[22] B. Rodriguez-Colinas, L. Fernandez-Arrojo, A.O. Ballesteros, F.J. Plou, Galactooligosaccharides formation during enzymatic hydrolysis of lactose: towards a prebiotic-enriched milk, Food Chem. 145 (2014) 388–394.
[23] M.M. Bradford, A rapid and sensitive method for the quantification of microgram quantities of protein utilizing the principle of protein-dye binding, Anal. Biochem. 72 (1976) 248–254.
[24] M.L. Verma, C.J. Barrow, J.F. Kennedy, M. Puri, Immobilization of beta-D-galactosidase from Kluyveromyces lactis on functionalized silicon dioxide nanoparticles: characterization and lactose hydrolysis, Int. J. Biol. Macromol. 50 (2012) 432–437.
[25] S.A. Ansari, Q. Husain, Lactose hydrolysis from milk/whey in batch and continuous processes by concanavalin A-celite 545 immobilized *Aspergillus oryzae* b-galactosidase, Food Bioprod. Process. 90 (2012) 351–359.
[26] J. Zhu, G. Sun, Lipase immobilization on glutaraldehyde-activated nanofibrous membranes for improved enzyme stabilities and activities, React. Funct. Polym. 72 (2012) 839–845.
[27] P. Zheng, H. Yu, Z.S. Professor, Y. Ni1, W. Zhang, Y. Fan, et al., Production of galacto-oligosaccharides by immobilized recombinant β-galactosidase from *Aspergillus candidus*, Biotechnol. J. 1 (2006) 1464–1470.
[28] Q. Husain, S.A. Ansari, F. Alam, A. Azam, Immobilization of *Aspergillus oryzae* beta galactosidase on zinc oxide nanoparticles via simple adsorption mechanism, Int. J. Biol. Macromol. 49 (2011) 37–43.
[29] Y.-W. Zhang, M.K. Tiwari, M. Jeya, J.-K. Lee, Covalent immobilization of recombinant *Rhizobium etli* CFN42 xylitol dehydrogenase onto modified silica nanoparticles, Appl. Microbiol. Biotechnol. 90 (2011) 499–507.
[30] M.F. Fernandez, M.A. Sanroman, D. Moldes, Recent developments and applications of immobilized laccase, Biotechnol. Adv. 31 (2013) 1808–1825.
[31] W.J. Goh, V.S. Makam, J. Hu, L. Kang, M. Zheng, S.L. Yoong, et al., Iron oxide filled magnetic carbon nanotube-enzyme conjugates for recycling of amyloglucosidase: toward useful applications in biofuel production process, Langmuir 28 (2012) 16864–16873.
[32] S.N.A. Rahim, A. Sulaiman, K.H.K. Hamid, N.A. Edama, A.S. Baharuddin, Effect of agitation speed for enzymatic hydrolysis of tapioca slurry using encapsulated enzymes in an enzyme bioreactor, Int. J. Chem. Eng. Appl. 6 (2015) 38–41.
[33] L. Zang, J. Qiu, X. Wu, W. Zhang, E. Sakai, Y. Wei, Preparation of magnetic chitosan nanoparticles as support for cellulase immobilization, Ind. Eng. Chem. Res. 53 (2014) 3448–3454.
[34] F. Wang, C. Guo, L.R. Yang, C.Z. Liu, Magnetic mesoporous silica nanoparticles: fabrication and their laccase immobilization performance, Bioresour. Technol. 101 (2010) 8931–8935.
[35] Y. Liu, Z. Zeng, G. Zeng, L. Tang, Y. Pang, Z. Li, et al., Immobilization of laccase on magnetic bimodal mesoporous carbon and the application in the removal of phenolic compounds, Bioresour. Technol. 115 (2012) 21–26.
[36] J. Talbert, J. Goddard, Enzymes on material surfaces, Colloids Surf. B Biointerfaces 93 (2012) 8–19.
[37] T.P.N. Ngo, W. Zhang, W. Wang, Z. Li, Reversible clustering of magnetic nanobiocatalysts for high-performance biocatalysis and easy catalyst recycling, Chem. Commun. 48 (2012) 4585.
[38] R. Xu, Q. Zhou, F. Li, B. Zhang, Laccase immobilization on chitosan/poly(vinyl alcohol) composite nanofibrous membranes for 2,4-dichlorophenol removal, Chem. Eng. J. 222 (2013) 321–329.
[39] L. Wu, X. Yuan, J. Sheng, Immobilization of cellulase in nanofibrous PVA membranes by electrospinning, J. Membr. Sci. 250 (2005) 167–173.
[40] Q. Shen, R. Yang, X. Hua, F. Ye, H. Wang, W. Zhao, et al., Enzymatic synthesis and identification of oligosaccharides obtained by transgalactosylation of lactose in the presence of fructose using beta-galactosidase from *Kluyveromyces lactis*, Food Chem. 135 (2012) 1547–1554.
[41] B. Rodriguez-Colinas, A. Poveda, J. Jimenez-Barbero, A.O. Ballesteros, F.J. Plou, Galacto-oligosaccharide synthesis from lactose solution or skim milk using the β-galactosidase from *Bacillus circulans*, J. Agric. Food Chem. 60 (2012) 6391–6398.
[42] R. Jovanovic-Malinovska, P. Fernandes, E. Winkelhausen, L. Fonseca, Galacto-oligosaccharides Synthesis from lactose and whey by beta-galactosidase immobilized in PVA, Appl. Biochem. Biotechnol. 168 (2012) 1197–1211.
[43] T. Palai, P.K. Bhattacharya, Kinetics of lactose conversion to galacto-oligosaccharides by β-galactosidase immobilized on PVDF membrane, J. Biosci. Bioeng. 115 (2013) 668–673.
[44] D.F.M. Neri, V.M. Balcao, R.S. Costa, I.C.a.P. Rocha, E.M.F.C. Ferreira, D.P.M. Torres, et al., Galacto-oligosaccharides production during lactose hydrolysis by free *Aspergillus oryzae* b-galactosidase and immobilized on magnetic polysiloxane-polyvinyl alcohol, Food Chem. 128 (115) (2009) 92–99.
[45] D. Zaramella, P. Scrimin, L.J. Prins, Self-assembly of a catalytic multivalent peptide–nanoparticle complex, Am. Chem. Soc. 134 (2012) 8369–8396.
[46] X. Gao, K. Ni, C. Zhao, Y. Ren, D. Wei, Enhancement of the activity of enzyme immobilized on polydopamine-coated iron oxide nanoparticles by rational orientation of formate dehydrogenase, J. Biotechnol. 188 (2014) 36–41.

[47] L. Tang, R. Yang, X. Hua, C. Yu, W. Zhang, W. Zhao, Preparation of immobilized glucose oxidase and its application in improving breadmaking quality of commercial wheat flour, Food Chem. 161 (2014) 1–7.
[48] J. Wang, F. Ji, J. Xing, S. Cui, Y. Bao, W. Hao, Lipase immobilization onto the surface of PGMA-b-PDMAEMA-grafted magnetic nanoparticles prepared via atom transfer radical polymerization, Chin. J. Chem. Eng. 2 (2014) 1333–1339.
[49] J. Zhang, Z. Xu, H. Chen, Y. Zong, Removal of 2,4-dichlorophenol by chitosan-immobilized laccase from *Coriolus versicolor*, Biochem. Eng. J. 45 (2009) 54–59.
[50] F. Wang, C. Guo, H.-Z. Liu, C.-Z. Liu, Immobilization of *Pycnoporus sanguineus* laccase by metal affinity adsorption on magnetic chelator particles, J. Chem. Technol. Biotechnol. 83 (2008) 97–104.

Appendix 3

Manipulation of Nanofiber-based β-Galactosidase Nanoenvironment for Enhancement of Galacto-Oligosaccharide Production

Journal of Biotechnology 2016;
10.1016/j.jbiotec.2016.02.014

Journal of Biotechnology 222 (2016) 56–64

Contents lists available at ScienceDirect

Journal of Biotechnology

journal homepage: www.elsevier.com/locate/jbiotec

Manipulation of nanofiber-based β-galactosidase nanoenvironment for enhancement of galacto-oligosaccharide production

Mailin Misson [a,b], Sheng Dai [a], Bo Jin [a], Bing H. Chen [c], Hu Zhang [a,*]

[a] School of Chemical Engineering, University of Adelaide, Adelaide SA 5000, Australia
[b] Biotechnology Research Institute, Universiti Malaysia Sabah, Jalan UMS, 88400 Kota Kinabalu, Sabah, Malaysia
[c] Department of Chemical and Biochemical Engineering, College of Chemistry and Chemical Engineering, Xiamen University, Xiamen 361005, China

ARTICLE INFO

Article history:
Received 1 September 2015
Received in revised form 5 February 2016
Accepted 8 February 2016
Available online 10 February 2016

Keywords:
Nanobiocatalyst
Galacto-oligosaccharide
β-galactosidase
Polymer nanofibers
Bioconversion

ABSTRACT

The nanoenvironment of nanobiocatalysts, such as local hydrophobicity, pH and charge density, plays a significant role in optimizing the enzymatic selectivity and specificity. In this study, *Kluyveromyces lactis* β-galactosidase (Gal) was assembled onto polystyrene nanofibers (PSNFs) to form PSNF-Gal nanobiocatalysts. We proposed that local hydrophobicity on the nanofiber surface could expel water molecules so that the transgalactosylation would be preferable over hydrolysis during the bioconversion of lactose, thus improve the galacto-oligosaccharides (GOS) yield. PSNFs were fabricated by electro-spinning and the operational parameters were optimized to obtain the nanofibers with uniform size and ordered alignment. The resulting nanofibers were functionalized for enzyme immobilization through a chemical oxidation method. The functionalized PSNF improved the enzyme adsorption capacity up to 3100 mg/g nanofiber as well as enhanced the enzyme stability with 80% of its original activity. Importantly, the functionalized PSNF-Gal significantly improved the GOS yield and the production rate was up to 110 g/l/h in comparison with 37 g/l/h by free β-galactosidase. Our research findings demonstrate that the localized nanoenvironment of the PSNF-Gal nanobiocatalysts favour transgalactosylation over hydrolysis in lactose bioconversion.

1. Introduction

Advances in biotechnology have led to rapid development of enzyme-catalyzed bioprocesses which are green and sustainable in comparison with chemical processes. Enzymes, a type of biocatalysts able to provide specific and selective activity, have been found in broad applications including biocatalysis, biosensors and medicines. Nevertheless, biocatalysts are no longer economically viable when they are used in large scale processes due to their low stability and reusability under reactor conditions (Illanes et al., 2012). Therefore, enzyme immobilization on support materials is gaining immense interest from both industry and academia. The immobilization facilitates recovery and recyclability of biocatalysts that enables a cost-effective operation process (Tran and Balkus, 2011). A further benefit of immobilization is to enhance enzymatic stability, under both storage or operational conditions, by sheltering and/or stabilizing enzymes against harsh chemical and environmental conditions including extreme pH and temperature (Misson et al., 2015a; Sheldon and van Pelt, 2013).

Various support materials have been employed for enzyme immobilization including natural polymers e.g. cellulose, starch, agarose and chitosan (Bryjak et al., 2007; Matto and Husain, 2009), synthetic polymers e.g. ion exchange resin and polyvinyl alcohol (Bergamasco et al., 2013; Guidini et al., 2011), or inorganic materials e.g. silica (Kim et al., 2009), zeolite (Chang and Chu, 2007) and mesoporous silica (Nabavi Zadeh et al., 2015). In recent years, assembly of enzymes on nanostructured materials to form nanobiocatalysts has been recognized as a promising approach to enhance enzyme performance. To date, functional nanomaterials such as nanofibers, nanoparticles, nanotubes, and nanocomposites (Cho et al., 2012; Crespilho et al., 2009; El-Aassar, 2013; Feng and Ji, 2011) have been used as enzyme carriers. The approaches of immobilization can be accomplished via covalent and non-covalent binding, cross-linking, entrapment or encapsulation (Misson et al., 2015b). Despite constant efforts into optimizing immobilization strategies, reduction of the enzyme activity upon immobilization remains one of key challenges. The activity reduction may be associated with alteration of the unique and native structures of the enzyme (Talbert and Goddard, 2012). As a consequence, it may significantly affect

* Corresponding author.
E-mail address: hu.zhang@adelaide.edu.au (H. Zhang).

http://dx.doi.org/10.1016/j.jbiotec.2016.02.014
0168-1656/

the performance of the immobilized enzymes in a reactor system. The methodologies for recovering nanobiocatalysts are also poorly developed. It is, therefore, a focal point to explore recyclable enzyme nanocarriers that can preserve or enhance the enzyme catalytic function, and are suitable for industrial processes.

Cheese whey is a main by-product in casein and cheese manufacturing processes. It has been regarded as organic pollutants in wastewater due to its high organic loading, which has contributed to significant eutrophication and toxicity in eco-steams (Watanabe et al., 2014). Worldwide, more than 10^8 tons of cheese whey are produced annually, thus a cost-effective treatment technology prior to safe disposal into the environment is highly pursued (Grba et al., 2002). Lactose is the major content (60–80%) of dairy effluents. Bioconversion of the lactose-rich wastes into valuable products endows a promising solution. Lactose can be transgalactosylated into galacto-oligosaccharides (GOS), which offer a range of important health functions in living systems such as prebiotics, low caloric sugar alternatives, and low cariogenicity (Ganzle, 2012).

β-Galactosidase is the catalyst for bioconversion of lactose into GOS (Zheng et al., 2006). The enzyme cleaves the lactose molecules forming enzyme-galactosyl complexes before entering either hydrolysis or transgalactosylation pathways. The hydrolysis reaction takes place when water acts a galactosyl acceptor yielding glucose and galactose, while GOS is generated in the transgalactosylation reaction when acceptor molecules, which derived from sugar molecules in reaction medium, surpress the water activity (Jovanovic-Malinovska et al., 2012). To enhance GOS production, a localized nanoenvironment can be optimized to promote the transgalactosylation. Meanwhile, due to high cost of β-galactosidase, development of technologies for immobilizing β-galactosidase and enhancing its enzymatic activity and stability has gained momentum in research and development for industrial GOS production.

In this work, we propose to manipulate the local nanoenvironment of β-galactosidase by increasing the local hydrophobicity to reduce the water activity around the enzyme catalytic sites, thus transgalactosylation becomes more preferable than hydrolysis, which leads to a high GOS yield. Polystyrene nanofibers (PSNF) were selected as enzyme nanocarriers because the nanostructured fibers offer intrinsic advantages including high surface area for enzyme loading, and high porosity and interconnectivity to promote low hindrance for mass transfer (Misson et al., 2015b). The nanofiber surface presents a hydrophobic surface and the solid nanofiber-based nanobiocatalysts can also be recycled. The nanofibers were synthesized using an electrospinning device, and the fabrication process was optimized to generate uniform sized fibers. The PSNF surface was then functionalized through the surface oxidation method to facilitate β-galactosidase binding. The immobilization efficiency was assessed using bovine serum albumin (BSA) and β-galactosidase. Finally, the bioengineering performance of the PSNF-Gal was evaluated in bioconversion of lactose into GOS by benchmarking with the free enzyme.

2. Materials and methods

2.1. Chemicals

Polystyrene (molecular weight: 350,000), *N,N*-dimethylformamide (DMF) and nitric acid (HNO_3) were of analytical grade without further purification. Bovine serum albumin (BSA), *Kluyveromyces lactis* β-galactosidase, O-nitrophenyl-β-D-glactopyranoside (ONPG), Coomassie Brilliant Blue G-250 and calcium carbonate ($CaCO_3$) were obtained from Sigma-Aldrich. Phosphate buffer saline (PBS), pH 7.2 (10×) were procured from Life Technologies.

2.2. Synthesis of nanofibrous polystyrene by electrospinning

The precursor for electrospinning was prepared by dissolving polystyrene (10–30%, w/v) in DMF with gentle stirring for overnight to form a homogenous solution. The resulting solution was placed inside a 5 ml syringe bearing a needle tip with 1 mm inner diameter, which was connected to a high voltage power supply. The electrospun nanofibers were cast onto a metal-surface collector with a distance of about 10–25 cm from the needle tip. The flow rate was fixed at 2.5 ml/h while the electrospinning was performed within a voltage range of 20–30 kV. The fibers were detached from the collector surface and stored at room temperature for further use.

2.3. Enzyme immobilization on nanofibers

The surface of polystyrene nanofibers (PS) was modified through surface oxidation to introduce oxygen-containing reactive groups of carboxyl (COOH) and hydroxyl (OH) for enzyme binding (Rus et al., 2002). An approximately 1 cm × 2.5 cm piece of nanofibers was immersed in HNO_3 (69%) for 2 h at room temperature (An et al., 2015). The acid-modified support was rinsed with water and PBS (pH 7.2) three times to remove excess acid. BSA and β-galactosidase immobilization were carried out by submerging the nanofibers into BSA (0–10 mg/ml) or β-galactosidase (0–9 mg/ml) PBS solution and gently mixed overnight at 4 °C. Finally, the nanofibers were rinsed thoroughly with water to remove free BSA and β-galactosidase. The supernatant and washing solution were collected to measure the concentration of non-adsorbed proteins.

2.4. Enzymatic activity assays

The activity assays of free and PSNF- β-galactosidase (PSNF-Gal) were measured according to the procedure described by Ansari and Husain (2012). The reaction mixture containing 0.1 ml of enzyme solution, 1.7 ml of PBS buffer (pH 7.2) and 0.2 ml of 20 mM ONPG were incubated with continuous agitation at 37 °C for 10 min. The reaction was stopped by adding 2 ml of 1 M sodium carbonate before measuring the liberated product spectrophotometrically at 405 nm. The concentration of product was calculated from the O-nitrophenol standard curve. One unit (1 U) of β-galactosidase is defined as the amount of enzyme which liberates 1 μmol of O-nitrophenol per min under the standard assay condition.

2.5. Production of galacto-oligosaccharides

Lactose (400 g/l) solution was prepared by dissolving lactose into PBS (pH 7.2) at 60 °C. Free or immobilized enzymes were added after the solution cooled down to 37 °C. The mixtures were incubated at 37 °C in an orbital shaker at 200 rpm. Samples were drawn at designed intervals for analysis during the 5 h reaction period and then immediately heated in boiling water for 5 min to deactivate the enzyme before analysis (Lu et al., 2012; Rodriguez-Colinas et al., 2014). Samples were filtered using 0.45 μm nylon filters and diluted 40 times prior to high performance liquid chromatography (HPLC) analysis.

2.6. Chemical analysis

The enzyme concentration was analysed using the Bradford method (Bradford, 1976). A total of 100 μl sample was added into 5 ml of the Bradford reagent, mixed homogenously and allowed to react for 5 min. The sample was then measured using a UV spectrophotometer (Shimadzu, Japan) at 595 nm. Protein concentration was determined from a calibration curve using BSA as a standard. The adsorption yield (%) and adsorption capacity (mg/g) of the immobilized enzyme were calculated using Eqs. (1) and (2), where

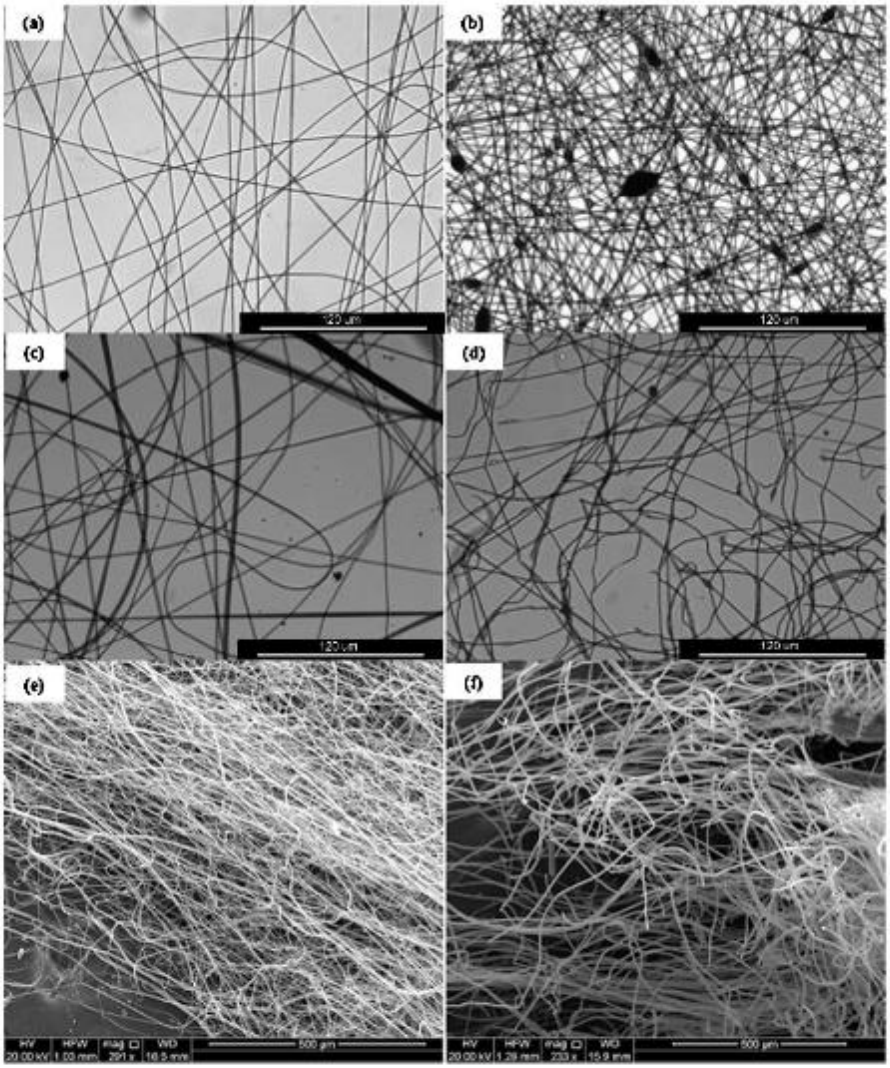

Fig. 1. (a–d) Microscopic images at 40× objective magnification of polystyrene nanofibers (PSNF): (a) nanofibers with uniform diameters (fabrication conditions: 20% w/v polymer concentration, 25 kV electric voltage, 15 cm distance), (b) nanofibers with beads (black dots) (fabrication conditions: 30%, w/v polymer concentration, 25 kV electric voltage, 10 cm distance), (c) nanofibers with heterogeneous diameter (fabrication conditions: 30%, w/v polymer concentration, 25 kV electric voltage, 20 cm distance), and (d) nanofibers with coil-like geometry (fabrication conditions: 30% w/v polymer concentration, 30 kV electric voltage, 25 cm distance). (e, f) SEM images of PSNF: (e) unmodified nanofibers and (f) HNO_3-modified nanofibers.

P_i is the initial protein content of the enzyme solution before immobilization, P_w and P_s are the amount of protein in washed solution and supernatant, respectively (Verma et al., 2012).

$$\text{Adsorption yield}(\%) = \frac{[P_i - (P_w + P_s)]}{P_i} \times 100 \quad (1)$$

$$\text{Adsorption capacity}(\text{mg/g}) = \frac{[P_i - (P_w + P_s)]}{\text{nano fiber mass}} \quad (2)$$

The saccharides (lactose, glucose, galactose, GOS) were determined by HPLC (Agilent, Germany) using an Aminex HPX-87H column (300 × 7.8 mm). The flow rate of a pre-degassed 8 mmol/L-H_2SO_4 mobile phase was set at 0.5 ml min^{-1}. A total of 5 µl samples was injected and the saccharides were detected with a refractive index detector. The column and the detector cell were maintained at 60 °C and 40 °C, respectively (Zheng et al., 2006). The conversion (%) was calculated using Eq. (3).

$$\text{Conversion}(\%) = \frac{[\text{initial lactose}] - [\text{final lactose}]}{[\text{initial lactose}]} \times 100 \quad (3)$$

Yield (Y) of glucose, galactose and GOS which represents the fraction with respect to total concentration of initial lactose, was calculated using Eqs. (4–6).

$$Y_{\text{glucose}}(\%) = \frac{[\text{glucose}]}{[\text{Initial Lactose}]} \times 100\% \quad (4)$$

$$Y_{\text{galactose}}(\%) = \frac{[\text{galactose}]}{[\text{Initial Lactose}]} \times 100\% \quad (5)$$

$$Y_{\text{gos}}(\%) = \%\text{Concersion} - \%Y_{\text{glucose}} - \%Y_{\text{galactose}} \quad (6)$$

2.7. Statistical analysis

Sample collection and analysis were conducted in triplicates. Results were analysed using the statistical tool in MS Excel 2010. Each value corresponds to the mean of independent experiments.

3. Results and discussion

3.1. Fabrication and functionalization of polystyrene nanofibers

Structures and the local nanoenvironment of nanocarriers can significantly influence enzyme activity and stability upon immobilization and its bioconversion performance in industrial applications. Large surface areas and minimal defects are two essential criteria for the nanofibers used for β-galactosidase immobilization. Nanofibers with a large surface area are vital to host a high load of enzymes. The presence of defects on the nanomaterial surface could possibly reduce its adsorption capacity. High quality nanofibers are required to be fabricated from an electrospinning process. During the electrospinning process, an electric field charges the polymer solution to create a repulsive force which overcomes the surface tension and leads to a polymer jet eruption from the spinneret tip, thus fiber mats are produced at the collector (Feng et al., 2013). A range of operating variables, which could affect the quality and localized physiochemical properties of PS nanofiber, was optimized to obtain high quality nanofibers. The variables comprise of polymer concentration (10–30%, w/v), electric voltage (20–30 kV) and the distance between needle tips and collector (10–25 cm).

A total of 36 trials were carried out based on different combinations of the synthesis conditions as summarized in Table S1. The electrospun homogeneity, fiber alignment and lack of macroscopic defects are normally employed to describe the quality of final products. Good quality nanofibers were obtained from the trials using 20% (w/v) polymer concentration, basing on homogeneous and droplet-free fiber mats spread on the collector surface by visual inspection. The uniform size and ordered alignment of fibrous mats are further confirmed from microscopic images (Fig. 1a). It was found that polymer concentration strongly influenced the nanofiber quality. Desirable PSNFs can be obtained using 20% (w/v) PS regardless of the applied voltage or distance. These findings were in agreement with the data reported by An et al. (2015). At the lowest polymer concentration (10%, w/v), liquid droplets were produced instead of fibers, probably due to a high surface tension which is associated with a low viscosity of the liquid (Deitzel et al., 2001). In this case, the process is called electrospraying which is used in many industries to obtain aerosols with narrow distributions. In contrast, condensed fibers with major defects were produced using the PS solution at a high concentration (30%, w/v). The defect formation is due to a high viscosity of the PS solution. The resultant PS fibers fused together into a network rather than individual fibers and generated rough and thick mats. This fiber morphology at a high polymer concentration was also demonstrated by Deitzel et al. (2001) due to its low surface tension. It showed formation of beads on their surface which was observed as black dots under microscopic image (Fig. 1b), heterogeneous fibers diameters (Fig. 1c) and disordered alignments (Fig. 1d), and all these represent a certain level of defects.

The fabricated electrospun mats with high quality were then modified by soaking in HNO_3 solution. Oxidation using HNO_3 has shown a favourable surface modification for protein adsorption (Kaur and Suri, 2007). In a previous study, different ratios of HNO_3/H_2SO_4 for modifying polystyrene nanofiber surface were reported (An et al., 2015) and an acid mixing ratio of 4:1 (HNO_3/H_2SO_4) was found to significantly improve the enzyme loading. However, the acidic solution containing sulphuric acid resulted in fiber aggregation. Therefore, surface modification with HNO_3 solution was selected for nanofiber surface treatment. Fig. 1e and f shows the SEM images of unmodified and HNO_3-treated nanofibers. The acidic oxidation of the fiber surface changes the morphology of the PS fibers. The electrsopun mats becomes shorter fibers as a consequence of the HNO_3 treatment. Such modifications have been proven to create oxygen-containing reactive groups, such as carboxyl (COOH) and hydroxyl (OH), which are able to establish stable binding with biomolecules (Ros et al., 2002). As demonstrated by An et al. (2015), the presence of COOH group on the PS nanofibers facilitated to assemble dehydrogenase on the nanofiber surface as a functional biocatalyst. The wettability and hydrophobicity have been improved for the modified nanofibers in comparison to the as-spun fibers. Our previous results (An et al., 2015) show that the as-spun fibers are hydrophobic and they float on the water surface. After acidic treatment, the nanofibers are well-dispersed in water.

3.2. Immobilization of BSA and β-galactosidase

Two proteins, BSA and β-galactosidase at a concentration range of 0–10 mg/ml, were used in order to evaluate the protein immobilization performance on the nanofibers before and after HNO_3 treatment (Fig. 2). BSA and β-galactosidase generally exhibited similar adsorption performance on the nanofibers at all tested concentrations. The maximum adsorption was achieved at protein concentrations around 2 mg/ml and 4 mg/ml for the enzyme and BSA, respectively. Fig. 2a and b shows that a smaller amount of the bound protein was observed in the case of using unmodified nanofibers. For the PS fibers without surface modification, the proteins may adsorb onto the fiber surface through weak binding such as hydrophobic interactions or van der Waals forces (Fernandez et al., 2013). Thus the hydrophobic nature of the nanofibers drives enzyme deposition. In addition, the enzyme itself contains approximately 28–33% of hydrophobic amino acids which are favourable for hydrophobic binding (Tudorache et al., 2012). Such protein adsorption through hydrophobic interactions has been reported for lipases by Palomo et al. (2002) and Chen et al. (2008).

It is notable that the surface modification leads to a substantial increase in the adsorption yield. Approximately 80% of BSA and β-galactosidase were adsorbed on the modified carrier, which was approximately four times that of the unmodified counterpart (20%). It has been recognized that surface oxidation of carbon nanofibers can create more active sites with a large number of carboxylic acid groups, epoxy and hydroxyl groups, which act as anchoring sites for binding protein molecules (Stavyiannoudaki et al., 2009). A redox enzyme has been successfully employed on electrospun nonwoven poly(acrylonitrile-co-acrylic acid) nanofiber meshes, carrying carboxylic functional groups (Wang et al., 2009). In the present work, the binding forces for interfacial reactions might come from hydrogen bonding, electrostatic force and some hydrophobic interactions (Secundo, 2013). As such, functional groups introduced through the HNO_3 treatment favour and stabilize enzyme adsorption (Stavyiannoudaki et al., 2009).

High adsorption capacity is one of important criteria for enzyme nanocarriers. Adsorption capacity is defined as the amount of adsorbed enzyme (mg) per gram of enzyme support. The experimental data presented in Fig. 2c and d shows the effect of acidic treatment of the PS nanofiber surface on the adsorption capacity of BSA and β-galactosidase. It is noted that the nanofibers after treatment by HNO_3 have the similar adsorption capacity for both BSA and β-galactosidase. The maximum adsorption capacity was found to be around 4000 mg/g and 3100 mg/g for BSA and β-galactosidase, respectively. The protein adsorption capacity on the treated surface is about 2-fold for BSA and 3-fold for β-galactosidase in comparison

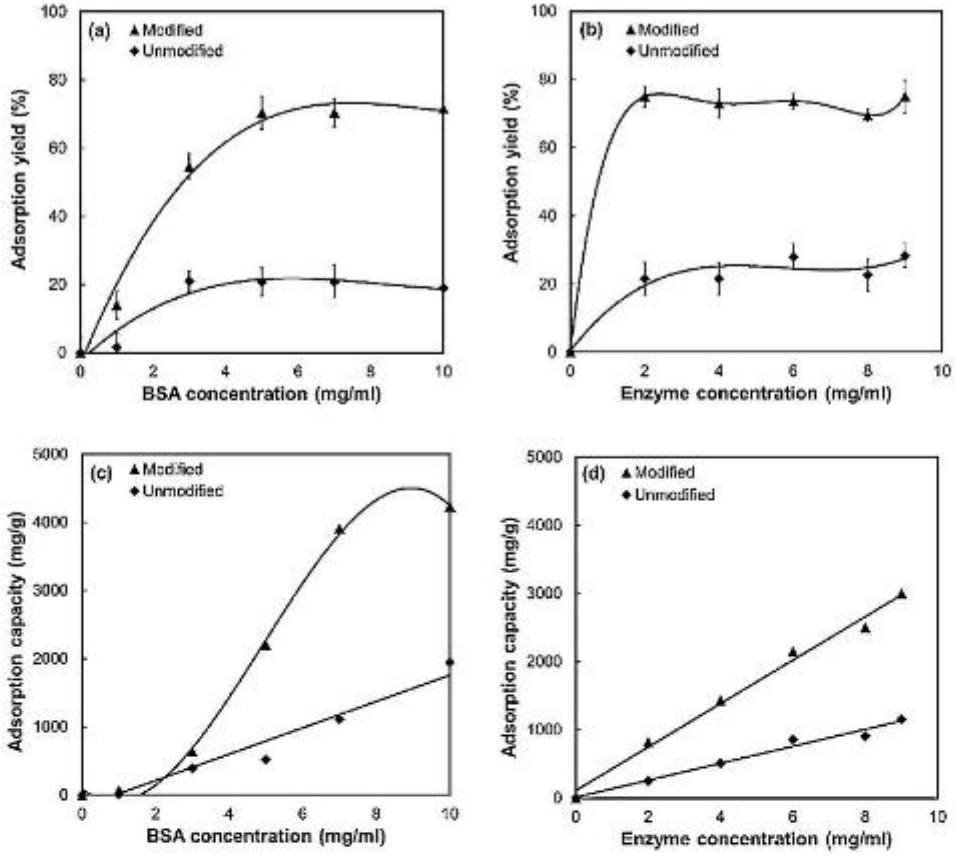

Fig. 2. Adsorption yield and adsorption capacity for (a,c) BSA and (b,d) PSNF-Gal on acid-modified and unmodified nanofiber surface.

with the untreated surface. The enhancement of adsorption could be ascribed to the protein binding through hydrogen bonding and electrostatic force.

The success in the development of the nanobiocatalysts towards bioprocess applications relies on their excellent performance, especially on enhancing or preserving their catalytic activity and stability upon immobilization. Fig. 3 presents the specific enzymatic activity of free and immobilized β-galactosidase at different concentrations. The activity of the enzyme immobilized on the nanofiber surface after acidic treatment was found to be comparable with the original activity of the free enzyme. Meanwhile, the decrease in enzyme activity for the unmodified carrier might be associated with the less availability of enzyme as evidenced by a lower adsorption yield as illustrated in Fig. 2b. In our previous study (Misson et al., 2015a), the PSNF-Gal has shown a promising recyclability. The nanobiocatalyst was demonstrated to retain 30% of its initial activity after nine operation cycles.

3.3. *Production of galacto-oligosaccharides*

The performance of PSNF-Gal was further evaluated for bioconversion of lactose into GOS. The reaction product stream from biocatalysis by PSNF-Gal includes glucose, galactose, GOS and the remaining lactose. The saccharides were analysed using HPLC with an Aminex HPX-87H column. GOS are eluted first in the chromatogram, followed by lactose, glucose and galactose (Zheng et al., 2006). Lactose, glucose and galactose are quantified using chemical standards. The amount of GOS is calculated based on the mass difference between the initial mass of lactose prior to the reaction and summation of the mass of glucose, galactose, and lactose after the reaction.

Fig. 4a and b shows the production profiles of lactose bioconversion using free β-galactosidase and PSNF-Gal. Free enzyme demonstrated a rapid lactose conversion during the first hour reaction (Fig. 4a). The major product was glucose (177 g/l), followed by galactose (80 g/l) and GOS at around 37 g/l. After extending the reaction time from 1 to 5 h, glucose leveled off while lactose decreased at a relatively small order. It is interesting to note that biocoversion using PSNF-Gal has a different reaction profile (Fig. 4b). The concentrations of glucose and galactose are remarkably lower than those produced by the free β-galactosidase. There is a sharp reduction in lactose concentration and a rapid increase in GOS production during the first hour, resulting in the highest conversion rate of 165 g/l/h, and the production rate of 110 g/l/h, respectively. GOS concentration reduces slightly beyond 2 h, while lactose concentation gradually increases. Lactose and isomers can be possibly re-synthesized through revesible reaction between the galactosyl-enzyme complex and the glucose molecules (Kim et al., 2004). Interestingly, the GOS concentration is much higher than that of glucose or galactose using PSNF-Gal up to a reaction time of 5 h. The amount of GOS produced was about 3-fold and 8-fold higher than glucose and galactose, respectively. The PSNF-Gal has the highest GOS production rate of 110 g/l/h in contrast with 37 g/l/h for the free counterpart.

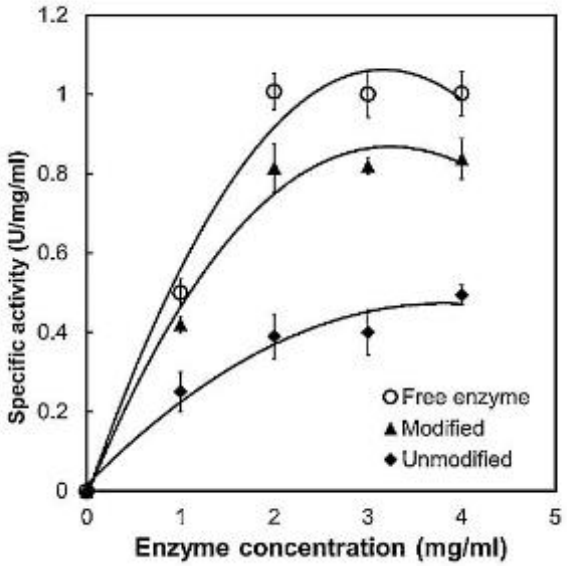

Fig. 3. Specific enzymatic activity for free β-galactosidase and PSNF-Gal on acid-modified and unmodified nanofiber surface.

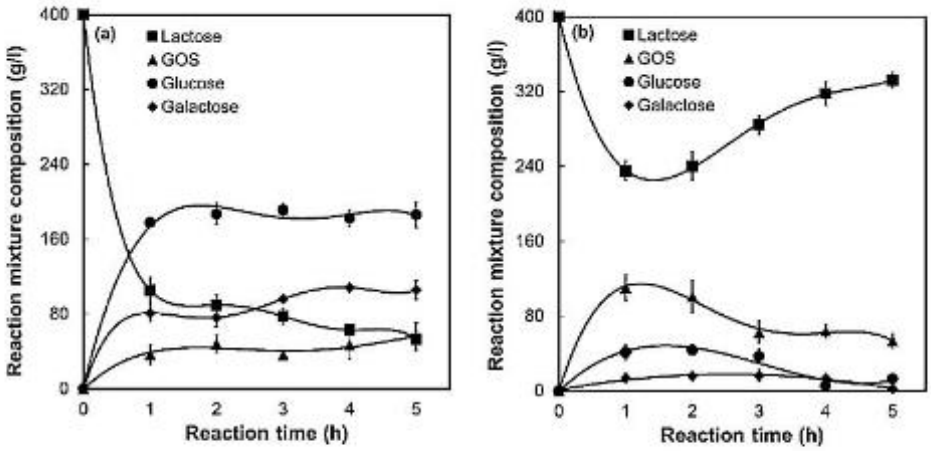

Fig. 4. Component concentration changes in the product stream at different reaction time for (a) free β-galactosidase and (b) PSNF-Gal. (Operation conditions: incubated at 37 °C using 400 g/l of initial lactose concentration).

Table 1
Comparison of various types of immobilized β-galactosidases for lactose conversion and GOS production yield.

Enzyme source	Support material	Initial lactose (g/L)	Conversion (%)	GOS (g/L)	Reference
Kluyveromyces lactis	Polystyrene nanofibers	400	41	110	This work
Bacillus circulans	Magnetic polysiloxane-polyvinyl alcohol	400	73	198	Rodriguez-Colinas et al. (2012)
Aspergillus oryzae	polyvinyl alcohol	400	75	120	Jovanovic-Malinovska et al. (2012)
Aspergillusoryzae	Magnetic polysiloxane-polyvinyl alcohol	400	50	104	Neri et al. (2009)
Aspergillus candidus	Alginate	400	–	87	Zhong et al. (2006)
Bacillus circulans	Membrane surface	200	–	40	Palai and Bhattacharya (2013)
Kluyveromyces lactis	Chitosan macroparticles	400	58	26	Klein et al. (2013)

The lactose conversion and the GOS yield are presented in Fig. 5 for both free β-galactosidase and the PSNF-Gal. Free β-galactosidase offers the advantage for lactose conversion (Fig. 5a). The amount of converted lactose by free β-galactosidase (86%) is higher than that by PSNF-Gal (41%). The PSNF-Gal, however, appears to have better catalytic capability for synthesizing GOS (Fig. 5b). A GOS yield of 28% is obtained in the first hour for the PNSF-Gal preparation in comparison with less than 9% for the free enzyme at the same reaction time. The GOS yield can also be calculated based on the consumed lactose, and this yield is estimated to be 67%. The difference in the GOS yield between the immobilized enzyme and its free counterpart is distinctive, increasing from

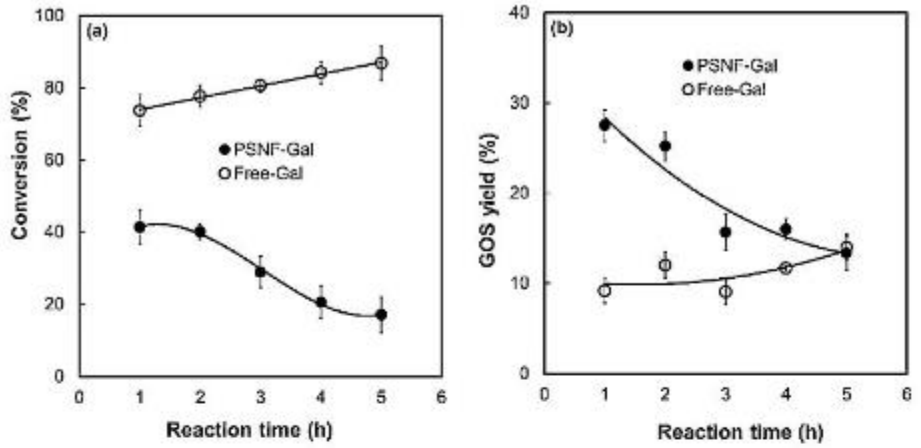

Fig. 5. (a) Lactose conversion and (b) GOS yield using free β-galactosidase (free-Gal) and PSNF-Gal. (Operation conditions; incubated at 37 °C within 5 h reaction time using 400 g/l of initial lactose concentration).

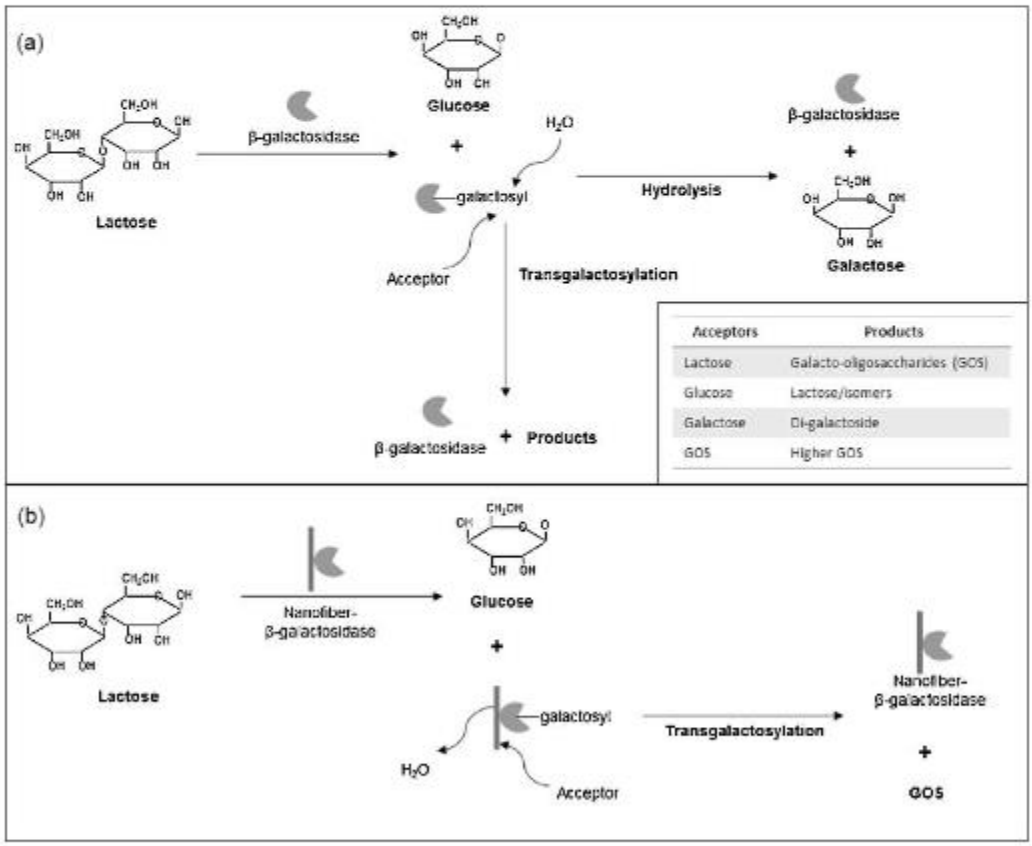

Fig. 6. (a) The reaction pathway of lactose hydrolysis and transgalactosylation using free β-galactosidase (Shen et al., 2012). (b) Proposed reaction pathway of lactose bioconversion using the PSNF-Gal due to localized nanoenvironment.

12% to 67%. The functionalized polystyrene nanofibers-based β-galactosidase has shown comparable bioconversion performance to some of reported immobilized enzyme on various supports for GOS production (Table 1) (Jovanovic-Malinovska et al., 2012; Klein et al., 2013; Neri et al., 2009; Palai and Bhattacharya, 2013; Rodriguez-Colinas et al., 2012; Zheng et al., 2006). This present study used a similar source of enzyme (*K. lactis*) as employed by Klein et al. (2013) but a different type of enzyme immobilization matrix was selected: polystyrene nanofibers in this work while chitosan macroparticles in Klein et al. (2013). The matrix difference can

be ascribed to morphology, size, functional groups on the matrix, hydrophobicity, surface charge and others. The local hydrophilic nanoenvironment of chitosan macroparticles could be the key factor for the low GOS yield as water molecules are preferable in the enzyme's active sites. In addition, a packed bed reactor was used by Klein et al. and a low yield of GOS from a continuous operation can be expected. Lactose conversion catalyzed by β-galactosidase has two different reaction pathways: hydrolysis to glucose and galactose and transgalactosylation to GOS (Gaur et al., 2006; Shen et al., 2012), which are sketched in Fig. 6a. According to the proposed pathways, enzyme-galactose complex is formed before entering either hydrolysis or transgalactosylation. Hydrolysis takes place when water acts a galactosyl acceptor, while transgalactosylation occurs when saccharides molecules succeed competing with the water activity (Jovanovic-Malinovska et al., 2012; Rodriguez-Colinas et al., 2012). In the free enzyme reaction system, both water and nucleophilic molecules have the equivalent opportunity to enter the enzyme's active site and react with the galactosyl-enzyme complex. Therefore, in the first hour, concentrations for both products from hydrolysis and transgalactosylation increase. After the first hour, the product glucose concentration keeps a constant value, while GOS fluctuates because GOS may be synthesized or hydrolyzed in the system. The increase or decrease of the GOS concentration depends on which reaction becomes preferable in the system.

In order to promote transgalactosylation catalyzed by β-galactosidase, the local nanoenvironment of the nanofibers is tuned with the hydrophobicity so that acceptors such as lactose or smaller units of GOS are preferable at the enzyme catalytic sites. This hydrophobic property of the nanofiber surface also reduces the water-driven hydrolysis activity. Therefore, the hydrophobic nature of PS nanofibers could be a key factor for GOS formation as presented in Figs. 4 and 5, particularly during the first hour of reaction. Another contributing factor in GOS synthesis may be associated with the reduced diffusion path for biomolecules. Galactose forms a galactosyl–enzyme complex at the enzyme's active sites, and this complex reacts with the acceptors which are produced from the enzymatic reactions and do not immediately diffuse out of the nanofiber surfaces, leading to a preference towards transgalactosylation reaction. This factor could be used to explain the reduced gap in GOS formation between PSNF-Gal and its free counterpart after 3–5 h reaction as presented in Fig. 5. After the nanofibers are exposed to aqueous solution for a few hours, water molecules start to penetrate into the enzymatic catalytic sites as the galactosyl acceptor, and hydrolysis competes with transgalactosylation. When the dynamic balance between both reactions is reached, enzyme on the nanofibers shares the similar performance as free enzyme.

Since PSNF-Gal is able to produce a high GOS yield during the first hour, residence time in the system can be reduced to meet the requiremets of continuous operations in large scale processes. Optimization of the catalytic process in a bioreactor system for continuous operation will be carried out to maximize the GOS yield, which will be expected to be much higher than the initial reported value (110 g/l).

4. Conclusion

Polystyrene nanofibers (PSNF) with excellent quality as enzyme carriers were successfully fabricated using electrospinning process. The PSNF surface was modified through chemical oxidation to improve enzyme loading and maintain a high enzyme activity. The lactose conversion by PSNF-Gal catalysis results in a high GOS yield as well as a high production rate. PSNF-Gal may beneficially promote transgalactosylation due to the hydrophobic nature of the polysterene surface. Another contributing factor could be the reduced diffusion path of nuclephilic molecules to facilitate transgalactosylation because these molecules could easily bind to the galactosyl-enzyme complex in such a nanoenvironment. This simple but effective nanobiocatalyst-assisted process may be economically viable for large scale GOS production.

Acknowledgements

MM gratefully acknowledges the financial support from the Universiti Malaysia Sabah and Malaysian Government. HZ thanks for the support from 111 Project (B12034). BHC appreciates the support by the State Key Program of National Natural Science Foundation of China (No. 21336009). SEM characterization by Masoumeh Zargar, HPLC facility support from Paul Grbin's research group and sugar analysis assistance by Nick Van Holst are highly appreciated.

Appendix A. Supplementary data

Supplementary data associated with this article can be found, in the online version, at http://dx.doi.org/10.1016/j.jbiotec.2016.02.014.

References

An, H., Jin, B., Dai, S., 2015. Fabricating polystyrene fiber-dehydrogenase assemble as a functional biocatalyst. Enzyme Microb. Technol. 68, 15–22.
Ansari, S.A., Husain, Q., 2012. Lactose hydrolysis from milk/whey in batch and continuous processes by concanavalin A-Celite 545 immobilized *Aspergillus oryzae* β-galactosidase. Food Bioprod. Process. 90, 351–359.
Bergamasco, J., de Araujo, M.V., de Vasconcellos, A., Luizon Filho, R.A., Hatanaka, R.R., Giotto, M.V., Aranda, D.A.G., Nery, J.G., 2013. Enzymatic transesterification of soybean oil with ethanol using lipases immobilized on highly crystalline PVA microspheres. Biomass Bioenergy 59, 218–233.
Bradford, M.M., 1976. A rapid and sensitive method for the quantification of microgram quantities of protein utilizing the principle of protein-dye binding. Anal. Biochem. 72, 248–254.
Bryjak, J., Aniulyte, J., Liesiene, J., 2007. Evaluation of man-tailored cellulose-based carriers in glucoamylase immobilization. Carbohydr. Res. 342, 1105–1109.
Chang, Y.K., Chu, L., 2007. A simple method for cell disruption by immobilization of lysozyme on the extrudate-shaped NaY zeolite. Biochem. Eng. J. 35, 37–47.
Chen, H., Yuan, L., Song, W., Wu, Z., Li, D., 2008. Biocompatible polymer materials: role of protein–surface interactions. Prog. Polym. Sci. 33, 1059–1087.
Cho, E.J., Jung, S., Kim, H.J., Lee, Y.G., Nam, K.C., Lee, H.J., Bae, H.J., 2012. Co-immobilization of three cellulases on Au-doped magnetic silica nanoparticles for the degradation of cellulose. Chem. Commun. Cambridge 48, 886–888.
Crespilho, F.N., Iost, R.M., Travain, S.A., Oliveira, O.N., Zucolotto, V., 2009. Enzyme immobilization on Ag nanoparticles/polyaniline nanocomposites. Biosens. Bioelectron. 24, 3073–3077.
Deitzel, J.M., Kleinmeyer, J., Harris, D., Beck Tan, N.C., 2001. The effect of processing variables on the morphology of electrospun nanofibers and textiles. Polymer 42, 261–272.
El-Aassar, M.R., 2013. Functionalized electrospun nanofibers from poly (AN-co-MMA) for enzyme immobilization. J. Mol. Catal. B: Enzym. 85–86, 140–148.
Feng, W., Ji, P., 2011. Enzymes immobilized on carbon nanotubes. Biotechnol. Adv. 29, 889–895.
Feng, C., Khulbe, K.C., Matsuura, T., Tabe, S., Ismail, A.F., 2013. Preparation and characterization of electro-spun nanofiber membranes and their possible applications in water treatment. Sep. Purif. Technol. 102, 118–135.
Fernandez, M.F., Sanroman, M.A., Moldes, D., 2013. Recent developments and applications of immobilized laccase. Biotechnol. Adv. 31, 1808–1825.
Ganzle, M.G., 2012. Enzymatic synthesis of galacto-oligosaccharides and other lactose derivatives (hetero-oligosaccharides) from lactose. Int. Dairy J. 22, 116–122.
Gaur, R., Pant, H., Jain, R., Khare, S.K., 2006. Galacto-oligosaccharide synthesis by immobilized *Aspergillus oryzae* β-galactosidase. Food Chem. 97, 426–430.
Grba, S., Stehlik-Tomas, V., Stanzer, D., Vahčić, N., Škrlin, A., 2002. Selection of yeast strain Kluyveromyces marxianus for alcohol and biomass production on whey. Chem. Biochem. Eng. Q. 16, 13–16.
Guidini, C.Z., Fischer, J., Resende M.M. d. Cardoso, V.L., Ribeiro, E.J., 2011. β-galactosidase of *Aspergillus oryzae* immobilized in an ion exchange resin combining the ionic-binding and crosslinking methods: kinetics and stability during the hydrolysis of lactose. J. Mol. Catal. B: Enzym. 71, 139–145.
Illanes, A., Cauerhff, A., Wilson, L., Castro, G.R., 2012. Recent trends in biocatalysis engineering. Bioresour. Technol. 115, 48–57.

Jovanovic-Malinovska, R., Fernandes, P., Winkelhausen, E., Fonseca, L., 2012. Galacto-oligosaccharides synthesis from lactose and whey by beta-Galactosidase immobilized in PVA. Appl. Biochem. Biotechnol. 168, 1197–1211.

Kaur, J., Suri, C.R., 2007. Direct hapten coated ELISA for immunosensing of low molecular weight analytes. Protoc. Exch., http://dx.doi.org/10.1038/nprot.2007.508.

Kim, C., ES, J., DK, O., 2004. A new kinetic model of recombinant betagalactosidase from *Kluyveromyces lactis* for both hydrolysis and transgalactosylation reactions. Biochem. Biophys. Res. Commun. 316, 738–743.

Kim, H., Kwon, H.-S., Ahn, J., Lee, C.-H., Ahn, I.-S., 2009. Evaluation of a silica-coated magnetic nanoparticle for the immobilization of a His-tagged lipase. Biocatal. Biotransform. 27, 246–253.

Klein, M.P., Fallavena, L.P., Schöffer J. d.N. Ayub, M.A.Z., Rodrigues, R.C., Ninow, J.L., Hertz, P.F., 2013. High stability of immobilized β-D-galactosidase for lactose hydrolysis and galactooligosaccharides synthesis. Carbohydr. Polym. 95, 465–470.

Liu, L., Xu, S., Zhao, R., Zhang, D., Li, Z., Li, Y., Xiao, M., 2012. Synthesis of galactooligosaccharides by CBD fusion beta-galactosidase immobilized on cellulose. Bioresour. Technol. 116, 327–333.

Matto, M., Husain, Q., 2009. Calcium alginate–starch hybrid support for both surface immobilization and entrapment of bitter gourd (Momordica charantia) peroxidase. J. Mol. Catal. B: Enzym. 57, 164–170.

Misson, M., Jin, B., Chen, B., Zhang, H., 2015a. Enhancing enzyme stability and metabolic functional ability of β-galactosidase through functionalized polymer nanofiber immobilization. Bioprocess Biosyst. Eng. 38, 1915–1923.

Misson, M., Zhang, H., Jin, B., 2015b. Nanobiocatalyst advancements and bioprocessing applications. J. R. Soc. Interface 12, 1–8.

Nahavi Zadeh, P.S., Mallak, K.A., Carlsson, N., Åkerman, B., 2015. A fluorescence spectroscopy assay for real-time monitoring of enzyme immobilization into mesoporous silica particles. Anal. Biochem. 476, 51–58.

Neri, D.F.M., Balcao, V.M., Costa, R.S., Rocha, I.C.A.P., Ferreira, E.M.F.C., Torres, D.P.M., Rodrigues, L.R.M., Jr, L.B.C., Teixeira, J.A., 2009. Galacto-oligosaccharides production during lactose hydrolysis by free Aspergillus oryzae β-galactosidase and immobilized on magnetic polysiloxane-polyvinyl alcohol. Food Chem 115, 92–99, 128.

Palai, T., Bhattacharya, P.K., 2013. Kinetics of lactose conversion to galacto-oligosaccharides by β-galactosidase immobilized on PVDF membrane. J. Biosci. Bioeng. 115, 668–673.

Palomo, J.M., Muñoz, G., Fernández-Lorente, G., Mateo, C., Fernández-Lafuente, R., Guisán, J.M., 2002. Interfacial adsorption of lipases on very hydrophobic support (octadecyl–Sepabeads): immobilization, hyperactivation and stabilization of the open form of lipases. J. Mol. Catal. B: Enzym. 19–20, 279–286.

Rodriguez-Colinas, B., Poveda, A., Jimenez-Barbero, J., Ballesteros, A.O., Plou, F.J., 2012. Galacto-oligosaccharide synthesis from lactose solution or skim milk using the β-galactosidase from *Bacillus circulans*. J. Agric. Food Chem. 60, 6391–6398.

Rodriguez-Colinas, B., Fernandez-Arrojo, L., Ballesteros, A.O., Plou, F.J., 2014. Galactooligosaccharides formation during enzymatic hydrolysis of lactose: towards a prebiotic-enriched milk. Food Chem. 145, 388–394.

Ros, T.G., van Dillen, A.J., Geus, J.W., Koningsberger, D.C., 2002. Surface oxidation of carbon nanofibres. Chem. Eur. J. 8, 1151–1162.

Secundo, F., 2013. Conformational changes of enzymes upon immobilisation. Chem. Soc. Rev. 42, 6250–6261.

Sheldon, R.A., van Pelt, S., 2013. Enzyme immobilisation in biocatalysis: why, what and how. Chem. Soc. Rev. 42, 6223–6235.

Shen, Q., Yang, R., Hua, X., Ye, F., Wang, H., Zhao, W., Wang, K., 2012. Enzymatic synthesis and identification of oligosaccharides obtained by transgalactosylation of lactose in the presence of fructose using beta-galactosidase from *Kluyveromyces lactis*. Food Chem. 135, 1547–1554.

Stavyiannoudaki, V., Vamvakaki, V., Chaniotakis, N., 2009. Comparison of protein immobilisation methods onto oxidised and native carbon nanofibres for optimum biosensor development. Anal. Bioanal. Chem. 395, 429–435.

Talbert, J., Goddard, J., 2012. Enzymes on material surfaces. Colloids and surfaces. B, Biointerfaces 93, 8–19.

Tran, D.N., Balkus, K.J., 2011. Perspective of recent progress in immobilization of enzymes. ACS Catal. 1, 956–968.

Tudorache, M., Protesescu, L., Negoi, A., Parvulescu, V.I., 2012. Recyclable biocatalytic composites of lipase-linked magnetic macro-/nano-particles for glycerol carbonate synthesis. Appl. Catal. A: Gen. 437–438, 90–95.

Verma, M.L., Barrow, C.J., Kennedy, J.F., Puri, M., 2012. Immobilization of beta-d-galactosidase from *Kluyveromyces lactis* on functionalized silicon dioxide nanoparticles: characterization and lactose hydrolysis. Int. J. Biol. Macromol. 50, 432–437.

Wang, Z.G., Wan, L.S., Liu, Z.M., Huang, X.J., Xu, Z.K., 2009. Enzyme immobilization on electrospun polymer nanofibers: an overview. J. Mol. Catal. B: Enzym. 56, 189–195.

Watanabe, T., Shinozaki, Y., Suzuki, K., Koitabashi, M., Yoshida, S., Sameshima-Yamashita, Y., Kuze Kitamoto, H., 2014. Production of a biodegradable plastic-degrading enzyme from cheese whey by the phyllosphere yeast Pseudozyma antarctica GB-4(1)W. J. Biosci. Bioeng. 118, 183–187.

Zheng, P., Yu, H., Sun, Z., Ni, Y., Zhang, W., Fan, Y., Xu, Y., 2006. Production of galacto-oligosaccharides by immobilized recombinant beta-galactosidase from *Aspergillus candidus*. Biotechnol. J. 1, 1464–1470.

Appendix 4

Enhancing Enzyme Stability and Metabolic Functional Ability of β-Galactosidase through Functionalized Polymer Nanofiber Immobilization

Bioprocess and Biosystem Engineering 2015; 38:1915–1923
DOI 10.1007/s00449-015-1432-5

Misson, M., Jin, B., Chen, B. & Zhang, H. (2015). Enhancing enzyme stability and metabolic functional ability of β-galactosidase through functionalized polymer nanofiber immobilization.
Bioprocess and Biosystem Engineering, 38(10), 1915-1923

Appendix 5

Immobilized β-Galactosidase on Functionalized Nanoparticles and Nanofibers: A Comparative Study

International Proceedings of Chemical, Biological and Environmental Engineering 2015; 90:1-7
DOI: 10.7763/IPCBEE. 2015. V90. 1

International Proceedings of Chemical, Biological and Environmental Engineering, V0l. 90 (2015)
DOI: 10.7763/IPCBEE. 2015. V90. 1

Immobilized β-Galactosidase on Functionalized Nanoparticles and Nanofibers: A Comparative Study

Mailin Misson [1, 2], Bo Jin [1], and Hu Zhang [1+]

[1] School of Chemical Engineering, University of Adelaide, Adelaide, SA 5000, Australia
[2] Biotechnology Research Institute, Universiti Malaysia Sabah, Jalan UMS, 88400, KK, Sabah, Malaysia

Abstract. In this study, two β-galactosidase nanocarriers made from nanofibers and nanoparticles were fabricated for bioconversion of lactose to galacto-oligosaccharides (GOS). Polystyrene nanofibers (PSNF) were synthesized using electrospinning and functionalized through chemical oxidation. Amino-carrying dendrimer-like silica nanoparticles with hierarchical pores (HPSNs) were fabricated through a one-pot sol-gel approach. PSNF-β-galactosidase (PSNF-Gal) and HPSNs-β-galactosidase (HPSNs-Gal) nanobiocatalyst assembly promises excellent biocatalyst activity, stability and functionality. The findings demonstrated PSNF and HPSNs possess great potential as enzyme nanocarriers. It is evident by 80 % adsorption yield in both cases. PSNF-Gal was found 8-fold greater adsorption capacity than HPSNs-Gal. In comparison to free β-galactosidase, PSNF-Gal also exhibited exceptional catalytic ability by favouring transgalactosylation over hydrolysis. As a result, the GOS formation increased from 19 % to 28 % and reduced undesirable products in lactose bioconversion. HPSNs, on the other hand, yielded 25 % GOS with a significant amount of hydrolysis by-products at similar operating conditions.

Keywords: Nanoparticles, nanofibers, nanobicocatalyst, enzyme immobilization.

1. Introduction

The nanobiocatalyst has become prominent research interests in assembling enzyme onto nanomaterial carriers. It is an emerging innovation that combines nanotechnology and biotechnology advances, aiming to improve enzyme stability, capability, and engineering performances [1]. Nanomaterial supports provide a large surface area and a modifiable surface to tailor the biotechnological requirements. To date, functional nanomaterials, such as nanofiber scaffolds, nanotubes, nanoparticles, nanocomposites and nanosheets, have been used as enzyme carriers. Despite the constant efforts in optimizing the immobilization protocol, enzyme poor stability such as leakage and deactivation in a reactor system remain as the major challenges in nanobiocatalyst development. Therefore, it leads to the need of exploring new technology for nanobiocatalysts.

Among the nanostructured materials examined for the nanobiocatalyst assembly, nanostructured fiber promises high enzyme loading and homogenous dispersion in a liquid phase. Their low hindrance in mass transfer due to high porosity and interconnectivity suits for bioprocesses using bioreactor systems [2]. On the other hand, porous materials like nanoparticles offer a number of outstanding characteristics, including excellent mechanical strength and uniform nanopores. In addition, nanoparticles possess tuneable periodic nanostructures which favourable for hosting large and small biomolecules [3]. The success of nanobiocatalyst technology is determined by catalytic stability, recyclability, high throughput, and productivity for a large-scale process.

In this work, we fabricated two enzyme carriers, polystyrene nanofibers (PSNF) and dendrimer-like silica nanoparticles with hierarchical pores (HPSNs). The PSNF was fabricated using electrospinning and

[+]Corresponding author. Tel.: + 61 88313 3810
E-mail address: hu.zhang@adelaide.edu.au.

functionalized through chemical oxidation. The dendrimer-like silica nanoparticles with hierarchical pores (HPSNs) was synthesized using sol-gel method and functionalized with amino groups. The functional groups are important as anchoring sites for enzyme binding. The potential of the nanocarriers in immobilizing enzyme were evaluated and compared. Next, their bioengineering performance in lactose bioconversion was assessed and benchmarked with free enzyme as comparative study. Lactose is abundantly present in dairy wastewater which has been regarded as high organic loading wastewater, causing significant eutrophication and toxicity in water streams [4]. Their bioconversion into valuable products such as galacto-oligosaccharide (GOS) endows a promising solution. GOS possess demonstrable health benefits such as prebiotic function, low caloric sugar alternatives, and low cariogenicity [5]. Therefore, this study is not only beneficial for sustainable green waste management, but also for the production of value-added products. The nanofiber and nanoparticle-based nanobiocatalysts also may be potentially viable for a range of enzyme-catalysed processes.

2. Materials and Methods

2.1. Preparation and functionalization of nanomaterials

Polystyrene (20 w/v) was dissolved in *N, N*-dimethylformamide (DMF) with gentle stirring for overnight to form a homogenous solution. The resultant solution was placed inside a 1-mm inner diameter needle tip of 5-mL syringe which was connected to a 25 kV voltage power supply. The flow rate was fixed at 2.5 ml/h while the electrospun polystyrene nanofibers (PSNF) were cast onto a metal-surface collector with a distance of about 10 cm from the needle tip. Approximately 1 cm x 2.5 cm piece of polystyrene nanofibers (PSNF) were immersed in nitric acid (HNO_3) (69%) for 2 h at room temperature [7]. The treated support was rinsed with water and PBS (pH 7.2) for three times to remove excess acids.

The preparation and functionalization of HPSNs were conducted using the methods developed by Du *et al.* [6]. The emulsion system comprised of 0.5 g of Cetyl trimethylammonium bromide (CTAB), 70 mL of H_2O, 0.8 mL of aqueous ammonia, 15 mL of ethyl ether and 5 mL of ethanol. The solution mixtures were vigorously stirred at 1000 rpm for 0.5 h at room temperature and stirred continuously for 4 h after addition of tetraethoxysilane (TEOS) (2.5 mL) and 3-aminopropyltriethoxysilane (APES) (0.1 mL). The reaction was stopped by adding a total of 1 mL of hydrochloric acid (HCl) (37%) and centrifuged for 12 min at 4200 rpm. The resultant white precipitate of HPSNs was washed with ethanol and water. The CTAB removal was conducted with ethanolic HCl (15 ml of concentrated HCl in 120 ml ethanol) at 70°C for 24h.

2.2. Immobilization of β-galactosidase

Approximately 10 mg pre-treated PSNF were submerged into β-galactosidase (0-8 mg/ml) containing the PBS solution overnight at 4 °C. It was thoroughly rinsed with water to remove free β-galactosidase. The supernatant and washing solution were collected to measure the concentration of non-adsorbed proteins. HPSNs (10 mg) were dispersed in 1 ml potassium phosphate buffer (pH 7.2) and sonicated for 30 min. The mixtures were submerged into β-galactosidase (0-8 mg/ml) and gently mixed overnight at 4 °C. The particles were collected through centrifugation and washed with water to remove free BSA or enzyme.

2.3. Bioconversion of lactose into galacto-oligosaccharide

Lactose (400 g/l) solution was prepared by dissolving lactose into PBS solution (pH 7.2) at 60 °C. Free or immobilized enzymes were added after the solution cooled down to 37 °C. The mixtures were incubated at 37 °C in an orbital shaker at 200 rpm. Samples were drawn after 2 h reaction and then immediately heated in boiling water for 5 min to deactivate enzyme activity [9].

2.4. Chemical analysis

The protein content was assayed by Bradford reagent method, by mixing 100 µl sample with 5 ml of Bradford reagent which was composed of 100 mg Coomassie Brilliant Blue G-250 in 50 ml of 95% ethanol, 100 ml of 85% phosphoric acid and then diluting to a final volume of 1 litre [8]. The sample was measured using a UV spectrophotometer (Shimadzu, Japan) at 595 nm. The protein concentration was determined from a calibration curve using BSA as a standard.

The enzyme activity were assayed in a reaction mixture containing 0.1 ml of enzyme solution, 1.7 ml of phosphate buffer saline (PBS) (pH 7.2) and 0.2 ml of 20 mM O-nitrophenyl-β-d-glactopyranoside (ONPG) at 37 °C for 10 mim. The reaction was stopped by adding 2 ml of 1M sodium carbonate. The liberated product was measured spectrophotometrically at 405 nm and the concentration was calculated from the O-nitrophenol standard curve.

Saccharides (lactose, glucose, galactose, GOS) were determined by high performance liquid chromatography (HPLC) (Agilent, Germany) using an Aminex HPX-87H column (300 x 7.8 mm). The flow rate of a pre-degassed 8 mmol/L-H_2SO_4 mobile phase was set at 0.5 ml min^{-1}. A total of 5 µl samples were injected and the saccharides were detected with a refractive index detector. The column and the detector cell were maintained at 60 °C and 40 °C, respectively.

2.5. Statistical analysis

Experimental works were carried out in triplicates and data were presented as a mean value with an average standard deviation of <5%.

3. Results and Discussion

3.1. Immobilization of β-galactosidase

Integration of a biological entity on a nanomaterial carrier is becoming of biotechnological interest. Owing to their exquisite properties as enzyme carriers, two potential materials, nanofibers and nanoparticles, were fabricated and evaluated in this study. The polystyrene nanofibers (PSNF) were fabricated using electrospinning system. Their surface was oxidised using HNO_3 which has been proven to create oxygen-containing reactive groups, such as carboxyl (COOH) and hydroxyl (OH), for protein adsorption [10]. Meanwhile, the dendrimer-like silica nanoparticles with hierarchical pores (HPSNs) were synthesized through a one-pot sol gel approach using CTAB as a template. The nanocarrier was functionalized with amino group to facilitate enzyme binding. Their performance in immobilizing enzyme is presented in Figure 1. Adsorption yield was determined by dividing the amount of adsorbed protein on the nanocarriers with the total protein for immobilization. The highest adsorption yield was determined to be 80 % at 2 mg/ml enzyme concentration for both nanocarriers. Increasing the enzyme concentration caused a slight decrease to PSNF-Gal while a sharp reduction trend shown by HPSNs-Gal. It indicates the PSNF provides a larger surface area to accommodate higher concentrations of enzyme.

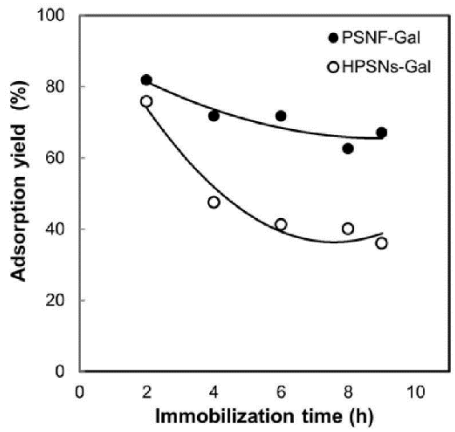

Fig. 1: The effect of enzyme concentration on the adsorption yield of HPSNs-Gal and PSNF-Gal.

Development of enzyme carriers with a high adsorption capacity is highly pursued. Adsorption capacity is defined as the amount of adsorbed enzyme (mg) per gram of enzyme support. Figure 2 compares the adsorption capacity between HPSNs-Gal and PSNF-Gal at different enzyme concentrations. It can be seen that the maximum adsorption capacity was 2500 mg/g and 320 mg/g for the PSNF-Gal and HPSNs-Gal, respectively. It indicates the PSNF carrier demonstrated nearly 8-fold higher capacity than the HPSNs. The

porosity of PSNF might have beneficially enhanced the penetration of biomolecules into all available surfaces. In addition, the surface modification through a specially determined chemical oxidation also probably has favoured the enzyme adsorption [7]. Nevertheless, it is also noticeable that HPSNs were promising to carry lower concentration of enzyme as indicated by the 80 % yield at 2 mg/ml (Figure 1). In previous study, the HPSNs have been proven as a remarkable carrier for small molecules like anticancer drugs and nucleic acids [6]. Their small particle size with open pores and uniform mesopores act as nanocontainers which may only suit for loading of small amount but potent biomolecules.

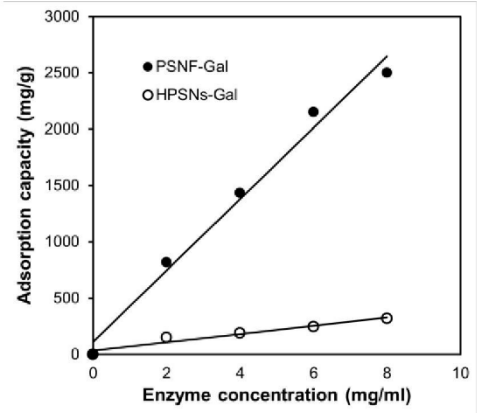

Fig. 2: The comparison of adsorption capacity between HPSNs-Gal and PSNF-Gal at different enzyme concentrations.

3.2. Production of galacto-oligosaccharide

After evaluating the immobilization capability, the performance of both PSNF and HPSNs nanobiocatalysts in lactose bioconversion into GOS was investigated. The findings were benchmarked with free β-galactosidase as a comparative study (Fig. 3). Free β-galactosidase was found to yield the highest bioconversion determined at 74 %. It was followed by the HPSNs-Gal and PSNF-Gal with respective yield of 59 % and 41 %. While free β-galactosidase could freely diffuse inside reaction medium to have greater interactions with substrates, both nanobiocatalysts might encounter mass transfer resistance thus resulted in lower bioconversion as shown in Fig. 3. Wu *et al.* [11] also has reported such unfavourable diffusion resistance created by enzyme carriers that were made from nanofibrous polyvinyl alcohol.

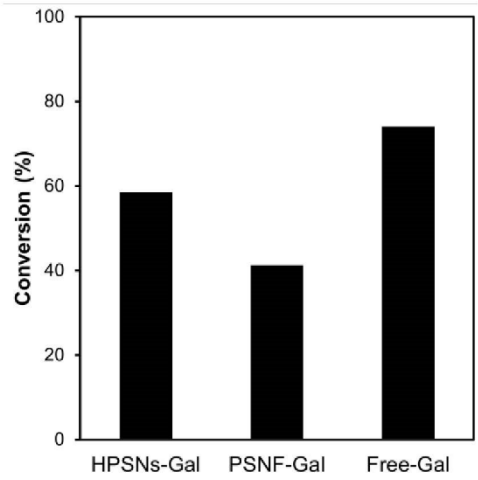

Fig. 3: The lactose bioconversion by HPSNs-Gal, PSNF-Gal and free-Gal at 400 g/l initial lactose concentration. (Enzyme concentration: 2 mg/ml in pH 7 phosphate buffer solution, incubated at 37 °C).

The profiles of product distribution in lactose bioconversion using β-galactosidase are illustrated in Fig. 4. The products comprise a mixture of glucose, galactose, galacto-oligosaccharide (GOS) and the remaining

lactose. Hydrolysis and transgalactosylation are the two possible pathways in β-galactosidase reactions [12]. Glucose and galactose are yielded in hydrolysis when water acts as a galactosyl acceptor, while transgalactosylation occurs for synthesis of GOS when nucleophilic molecules succeed to compete with the water activity [13]. Transgalactosylation is preferable because the GOS product is a beneficial functional food ingredient. It is noticeable that the highest hydrolysis products, glucose (44 %) and galactose (10%), was produced by the free β-galactosidase. It indicates the free enzyme favoured the hydrolysis pathway. This also further explains why the GOS yield by the free β-galactosidase was lower than the immobilized enzyme.

Meanwhile, the HPSNs-Gal exhibited an equal production of GOS and glucose determined about 25 %. Interestingly, the lactose biocoversion using PSNF-Gal showed very prominent reaction profiles (Fig 4). Firstly, the concentration of glucose and galactose were remarkably lower than 10 %. Secondly, the GOS yield was significantly higher than glucose (3-fold) and galactose (8-fold), signifying a preferance towards transgalactosylation over hydrolysis. The PSNF surface possesses hydrophobic properties [14] that could potentially repel water from the PSNF-Gal surface. As a result, it might reduce the water-driven hydrolysis activity and ultimately lead to the catalytic pathway of transgalactosylation. Thirdly, the highest GOS was obtained when using PSNF-Gal (28%) comparing with the HPSNs-Gal (25 %) and the free enzyme (19 %). In fact, the production of GOS was higher than employing β-galactosidase on other reported carriers such as polymeric membrane surfaces (13 %) and polysiloxane-polyvinyl alcohol (26 %) [15, 16].

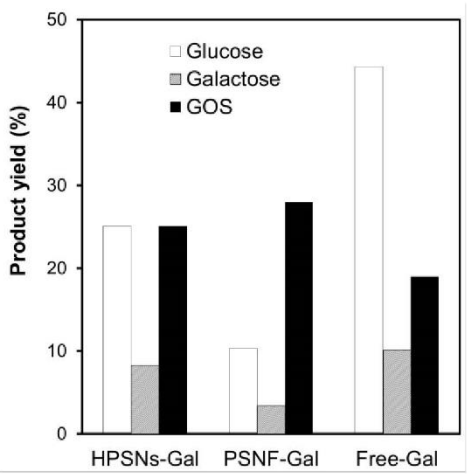

Fig. 4: The profile of product distributions by HPSNs-Gal, PSNF-Gal and free-Gal at 400 g/l initial lactose concentration. (Enzyme concentration: 2 mg/ml in pH 7 phosphate buffer solution, incubated at 37 °C).

3.3. Assessment of nanocarriers for bioprocessing application

Selection of nanomaterials to assemble enzyme forming nanobiocatalyst largely depends on many factors including adsorption capability, enzyme stability and productivity. Moreover, nanobiocatalyst with significant recyclability is a biotechnological interest. Besides of the recyclability of the enzyme-carrier assembly, developing recyclable support materials has gained increasing attention. HPSNs can be easily separated through sedimentation or centrifugation due to their high density. Nevertheless, their small size might cause the downstream process for biocatalyst recovery highly complex [17]. The particles tend to aggregate and may create a significant pressure drop in packed bed reactor system. It has become a major concern for industries besides the uneconomical cost for bulk materials synthesis. Meanwhile, a continuous fabrication of PSNF can be easily carried out using electrospinning device. The abundance of polymer resources in nature making the synthesis is considerably cheap. Importantly, enzyme-carrying PSNF can be readily located in a scalable reactor and promote easy separation. Hence, it endows potential translation of these bench-scale technologies into commercial practices. With regard to its bioengineering performance and its potential for scaling-up and reutilization, we propose the nanofiber-based nanobiocatalyst may beneficial for large scale enzyme-catalysed applications.

4. Conclusion

Surface-oxidized polystyrene nanofibers (PSNF) and amino-carrying dendrimer-like silica nanoparticles with hierarchical pores (HPSNs) exhibited great potential as enzyme nanocarriers. The employment of β-galactosidase on PSNF and HPSNs carriers as nanobiocatalysts assembly was beneficial not only for sustainable green waste management, but also for production of valuable products. PSNF was found to be relatively superior to HPSNs in hosting high enzyme loads. PSNF-Gal also exhibited distinguished reaction profiles by favouring transgalactosylation over hydrolysis, thus enhancing the GOS yield and reducing undesirable by-products in lactose bioconversion. The HPSNs-Gal, however, had an equal preference between the two reactions. Our research findings from experimental data exemplified a great potential of a nanofiber-based enzyme carrier for bioprocessing applications.

5. Acknowledgement

MM gratefully acknowledges the financial support from the Universiti Malaysia Sabah and the Malaysian Government. HZ thanks for the support from 111 Project (B12034). HPLC facility support from Paul Grbin's research group with sugar analysis assistance by Nick Van Holst, and technical supports by Jason Peak, Jeffrey Hiorns and Michael Jung from workshop department at School of Chemical Engineering are highly appreciated.

6. References

[1] M. Wang, Advances in carrier-bound and carrier-free immobilized nanobiocatalysts. *Chemical Engineering Science*. In Press (0):

[2] M. Misson, Nanobiocatalyst advancements and bioprocessing applications. *Journal of Royal Society Interface*. 2015, 12 (102):

[3] J. Liu, Magnetic nanocomposites with mesoporous structures: Synthesis and applications. *Small*. 2011, **7** (4): 425-443.

[4] T. Watanabe, Production of a biodegradable plastic-degrading enzyme from cheese whey by the phyllosphere yeast Pseudozyma antarctica GB-4(1)W. *Journal of Bioscience and Bioengineering*. 2014, 118 (2): 183-187.

[5] M. G. Ganzle, Enzymatic synthesis of galacto-oligosaccharides and other lactose derivatives (hetero-oligosaccharides) from lactose. *International Dairy Journal 22 (2012)*. 2012, 22: 116-122.

[6] X. Du, Developing functionalized dendrimer-like silica nanoparticles with hierarchical pores as advanced delivery nanocarriers. *Advanced Materials*. 2013, 25 (41): 5981–5985.

[7] H. An, Fabricating polystyrene fiber-dehydrogenase assemble as a functional biocatalyst. *Enzyme and Microbial Technology*. 2015, 68 (0): 15-22.

[8] M. M. Bradford, A rapid and sensitive method for the quantification of microgram quantities of protein utilizing the principle of protein-dye binding. *Anal Biochem*. 1976, 72: 248-254.

[9] L. Lu, Synthesis of galactooligosaccharides by CBD fusion beta-galactosidase immobilized on cellulose. *Bioresour Technol*. 2012, 116: 327-33.

[10] T. G. Ros, Surface Oxidation of Carbon Nanofibres. *Chemistry – A European Journal*. 2002, 8 (5): 1151-1162.

[11] Wu, L. *et al.*, Immobilization of cellulase in nanofibrous PVA membranes by electrospinning. *Journal of Membrane Science*. 2005, 250: 167-173.

[12] A. Gosling, Recent advances refining galactooligosaccharide production from lactose. *Food Chemistry 121*. 2010, 121: 307-318.

[13] B. Rodriguez-Colinas, Galacto-oligosaccharide Synthesis from Lactose Solution or Skim Milk Using the β-Galactosidase from Bacillus circulans. *Journal of Agricultural and Food Chemistry*. 2012, 60 (25): 6391-6398.

[14] J. Liu, Hydrophobic Electrospun Polyimide Nanofibers for Self-cleaning Materials. *Macromolecular Materials and Engineering*. 2015, 300 (3): 358-368.

[15] D. F. M. Neri, Galacto-oligosaccharides production during lactose hydrolysis by free Aspergillus oryzae b-galactosidase and immobilized on magnetic polysiloxane-polyvinyl alcohol. *Food Chemistry 128*. 2009, 115: 92-